Uppsala University
Department of Materials Science
Systems and Control Group

CONTROL AND ESTIMATION STRATEGIES APPLIED TO THE ACTIVATED SLUDGE PROCESS

Carl-Fredrik Lindberg

UPPSALA UNIVERSITY 1997

Dissertation for the Degree of Doctor of Philosophy in Automatic Control presented at Uppsala University in 1997.

ABSTRACT
Lindberg, C-F. 1997. Control and Estimation Strategies Applied to the Activated Sludge Process, 214pp. Uppsala. ISBN 91-506-1202-6.

Requirements for treated wastewater are becoming increasingly more stringent. This, in combination with increasing loads, and limited availability of land, calls for more efficient procedures for wastewater treatment plants. In this thesis, control and estimation strategies are developed in order to improve the efficiency of the activated sludge process.

Four different controllers for control of the external carbon flow rate are evaluated in a simulation study, and in pilot plant experiments. All controllers utilize feedforward from measurable disturbances.

On-line methods for estimating the time-varying respiration rate and the nonlinear oxygen transfer function from measurements of the dissolved oxygen concentration and the airflow rate are presented. The approaches are successfully applied to real data.

Two strategies for designing a DO controller are developed and practically evaluated. The basic idea is to explicitly take the nonlinear oxygen transfer function into account in the controller design. A supervision controller for the DO process is developed. Practical experiments in a pilot plant show that it is possible with this control strategy to keep the ammonium concentration at a constant and low level, and at the same time reduce the energy consumption and the effluent nitrate concentration.

Finally, multivariable controllers have been designed and evaluated in a simulation study. The key objective is to keep effluent ammonium and nitrate at low levels. The controllers are based on a linear state-space model, estimated by a subspace system identification method. The main advantage of these controllers, compared to SISO controllers, is that interactions in the process model are taken into account.

Key-words: Activated sludge, dissolved oxygen control, estimation, filtering, multivariable control, nonlinear control, oxygen transfer rate, recursive identification, respiration rate, smoothing, supervision control.

Carl-Fredrik Lindberg, Systems and Control Group, Uppsala University, Box 27, SE-751 03 Uppsala, Sweden

ISBN 91-506-1202-6
Printed in Sweden by Graphic Systems AB, Stockholm 1997

Preface

The thesis consists of seven chapters. In the first chapter an introduction to wastewater treatment and control of an activated sludge process is given. The second chapter gives a description of the pilot plant in Uppsala, and a simulation model of the pilot plant. The simulation model mimics a complete activated sludge process. Most simulation examples in the thesis are based on this model. The findings reported in the chapters have either been published or been accepted to various scientific journals or conferences.

Chapter 2, is based on

Carlsson, B., S. Hasselblad, E. Plaza, S. Mårtensson and C-F. Lindberg (1997). Design and operation of a pilot-scale activated sludge plant. *Vatten* **53**(1), 27–32.

Carlsson, B. and C-F. Lindberg (1995). A control and supervision system for an activated sludge pilot plant. Ninth Forum for Applied Biotechnology, 27–29 Sept. pp 2491–2494.

Carlsson, B., J. Latomaa and C-F. Lindberg (1994*b*). A control and supervision system for an activated sludge process (ett styr- och övervakningssytem för en aktivslamprocess. Reglermöte '94, 25–26 Oct., Västerås, Sweden (in Swedish).

Chapter 3, has partly been published in

Hallin, S., C-F. Lindberg, M. Pell, E. Plaza and B. Carlsson (1996). Microbial adaptation, process performance and a suggested control strategy in a pre-dentrifying system with ethanol dosage. *Water Science and Technology* **34**(1–2), 91–99.

Lindberg, C-F. and B. Carlsson (1996*a*). Adaptive control of external carbon flow rate in an activated sludge process. *Water Science and Technology* **34**(3–4), 173–180.

Lindberg, C-F. and B. Carlsson (1996*b*). Control strategies for the activated sludge process (styrstrategier för en aktivslambassäng i reningsverk). Reglermöte '96, 6–7 June, Luleå, Sweden (in Swedish).

Chapter 4, is partly based on:

Lindberg, C-F. and B. Carlsson (1996*d*). Estimation of the respiration rate and oxygen transfer function utilizing a slow DO sensor. *Water Science and Technology* **33**(1), 325–333.

Carlsson, B., C-F. Lindberg, S. Hasselblad and S. Xu (1994*a*). On-line estimation of the respiration rate and the oxygen transfer rate at Kungsängen wastewater plant in Uppsala. *Water Science and Technology.* **30**(4), 255–263.

Lindberg, C-F. and B. Carlsson (1993). Evaluation of some methods for identifying the oxygen transfer rate and the respiration rate in an activated sludge process. Technical Report UPTEC 93032R. Systems and Control Group, Uppsala University. Uppsala, Sweden.

Chapter 5, is partly presented in:

Lindberg, C-F. and B. Carlsson (1996*b*). Control strategies for the activated sludge process (styrstrategier för en aktivslambassäng i reningsverk). Reglermöte '96, 6–7 June, Luleå, Sweden (in Swedish).

Lindberg, C-F. and B. Carlsson (1996*c*). Efficient control of the DO in an activated sludge process. *Vatten* **52**(3), 209–212. (in Swedish).

Lindberg, C-F. and B. Carlsson (1996*e*). Nonlinear and set-point control of the dissolved oxygen dynamic in an activated sludge process. *Water Science and Technology* **34**(3–4), 135–142.

Lindberg, C-F. and B. Carlsson (1994*a*). Nonlinear control of the dissolved oxygen in an activated sludge process. (Olinjär reglering av syrehalten i en aktivslam bassäng). Reglermöte '94, 25–26 Oct. Västerås, Sweden (in Swedish).

Lindberg, C-F. and B. Carlsson (1994*b*). Nonlinear control of the dissolved oxygen in an activated sludge process. Technical Report UPTEC 94076R. Systems and Control Group, Uppsala University. Uppsala, Sweden.

Chapter 6, will partly be presented in

Lindberg, C-F. (1997). Multivariable modeling and control of an activated sludge process. Accepted for the 7th IAWQ Workshop on Instrumentation, Control & Automation of Water & Wastewater Treatment & Transportation Systems, Brighton UK, 6–11 July 1997.

Chapter 7, gives a conclusion, and some topics for future research.

Several of the results and findings in the thesis appear also in a more preliminary form in

Lindberg, C-F. (1995). Control of wastewater treatment plants. Licentiate thesis. UPTEC 95071R. Systems and Control Group, Uppsala University, Sweden

This work has been carried out in the STAMP project. STAMP is an abbreviation in Swedish for control of wastewater treatment plants, new methods and new process technology. The project was initiated and financed by the Swedish Board for Technical Development. One of the purposes of STAMP is to combine the different competence in a project on wastewater treatment. The project is hence interdisciplinary. It involves research in automatic control, microbiology, environmental technology, and work science. The research is also organized in four different consortia, which are located in Uppsala, Stockholm, Gothenburg and Lund/Malmö.

During my studies I have also been a co-supervisor for the following Master thesis projects:

Latomaa, J. (1994). A control and supervision system for an activated sludge pilot plant. Master's thesis. Systems and Control Group, Uppsala University. UPTEC 94077E.

Luttmer, J. (1995). Design of a simulator for an activated sludge process. Master's thesis. Systems and Control Group, Uppsala University. UPTEC 95149E.

Nakajima, S. (1996). On-line estimation of the respiration rate and the oxygen transfer function using an extended kalman filter. Master's thesis. Department of Signals, Sensors and Systems: Royal Institute of Technology, Sweden.

Acknowledgment

I would like to express my gratitude to my supervisor, Associate Prof. Bengt Carlsson for his encouragement, support and constructive criticism of my ideas and all work. I would also like to thank the head of the group Prof. Torsten Söderström, for providing a well organized PhD programme and for giving many valuable comments on the manuscript. I thank Associate Prof. Mikael Sternad who has been available for many discussions concerning various control problems.

I want to thank all members of the Systems and Control Group, and the Signals and Systems Group who have contributed by creating pleasant and stimulating working conditions. It has also been a pleasure to be a member at the STAMP research consortium in Uppsala and I wish to thank my colleges of the "STAMP-group". The support from the personnel at Kungsängsverket sewage treatment plant and Uppsala Municipal Service Department is gratefully acknowledged. A special thank to Jan Söderlund and Stefan Mårtensson for their special concern of the pilot plant.

I also want to thank following persons for reading and improving various parts of the manuscript: Serena Hasselblad, Claes Tidestav and Dr. Torbjörn Wigren.

I thank Jouko Latomaa for his programming of the computerized control and supervision system for the pilot plant and Ove Ewerlid for sharing his expert knowledge in C++ and Linux.

This work has been financially supported by the Swedish National Board for Technical Development (Nutek), contract 93-04185P, which is gratefully acknowledged. The pilot plant and its equipment were financed by the Public Works and Real Estate Department, Uppsala.

The experiment with surface active agents and their influence on the oxygen transfer rate, presented in Section 4.7, was financially supported by Örebro, Karlstad, Gävle and Borlänge wastewater treatment plant, Naturvårdsverket, Cellpa teknik and VA-ingenjörerna.

Contents

Chapter 1

Wastewater treatment — An introduction

Water is something special. Every living thing on earth – microorganisms, plants, animals, humans and even our brain – consists mostly of water. The earth also contains a lot of water. More than 70% of the earth's surface is covered by water, only a small part of which is suitable for either human consumption or agricultural use (approximately 0.5% of all water in the world). This small fraction is diminishing as agriculture, industry and housekeeping pollute and consume more and more of the drinkable water supply. Natural water cycles must be allowed to continue and human impact on water resources must be limited if disasters is to be avoided.

Central to this is proper treatment of wastewater whereby the nutrients trapped in sludge from wastewater treatment processes can be transferred back to soil.

This thesis considers different applications of control and estimation methods that aim to improve the operation of the activated sludge process in wastewater treatment plants. The suggested methods reduce the effluent nutrient concentrations, save energy, and reduce the need for external chemicals if such are used. The methods are verified both in simulations and in pilot plant experiments.

In Section 1.1 of this chapter a short historical review of the development of wastewater treatment in Sweden is presented. Section 1.2 contains a brief description of how a wastewater treatment plant works. The activated sludge process, an important step in wastewater treatment plant operations, is explained in Section 1.3. The different control strategies are applied to

this process. Section 1.4 gives some ideas on how advanced control theory can be applied using new on-line sensors and biological models. Finally, an outline of the other chapters is given in Section 1.5.

1.1 A short historical review of Swedish wastewater treatment

Much of the material in this section is taken from Lundgren (1994) and Finnson (1994).

Up until the nineteenth century the majority of the Swedish population lived in the countryside. Cities and towns were small and water closets were rare. Wastewater posed only minor problems. In the end of the 1800's the urban areas expanded rapidly, causing a variety of sanitary problems and epidemics. Suitable drinking water became increasingly harder to find while waste accumulated. The traditional method of garbage disposal, throwing it over the doorstep became untenable.

The introduction of water closets, in the beginning of the nineteenth century, solved many of these problems. Disease decreased and the urban population avoided many problems associated with latrines; emptying latrine-barrels (see Figure 1.1) and bad smell. The water closet was at the first sight a great technical simplification – waste just disappeared!

Figure 1.1: Latrine carrying in Stockholm, drawing from 1828 (Kommunförbundet 1988).

As an interesting sidenote, the toilet makes use of control technology. (Coury 1996). When you flush, the valve at the bottom of the tank opens and remains open because the valve floats, but when the tank is empty it closes. Another valve then opens and water starts to fill the tank again. As the water level rises a float is carried upward which closes the float valve when the tank is full. This system depends on two control loops where the water level is used for feedback. To avoid flooding at a failure there is also

a flush valve tube inside the tank.

The use of water closets, however, soon started to affect the recipients[1]. First to be detected were the visual problems, caused by untreated wastewater. These were partly solved by constructing long pipes to the sea, which in those days was believed to be capable of absorbing infinite amounts of wastewater. The risk of pollution and loss of fertilizer were considered a reasonable price to pay compared to the positive effects. The positive effects were also seen immediately, while the negative consequences took longer to detect. Almost 50 years went by before the associated pollution problems began to receive serious attention in Sweden.

Sedimentation tanks were introduced in the 1930's to deal with the visual problems with wastewater. By the 1950's biological treatment was initiated after problems began to show up with oxygen depletion in the recipients. Combined biological-chemical treatment was introduced in the 1970's, due to the eutrophication of lakes from phosphorus and nitrogen in wastewater. Developments in wastewater treatment technologies between 1965 and 1990 in Sweden are shown in Figure 1.2.

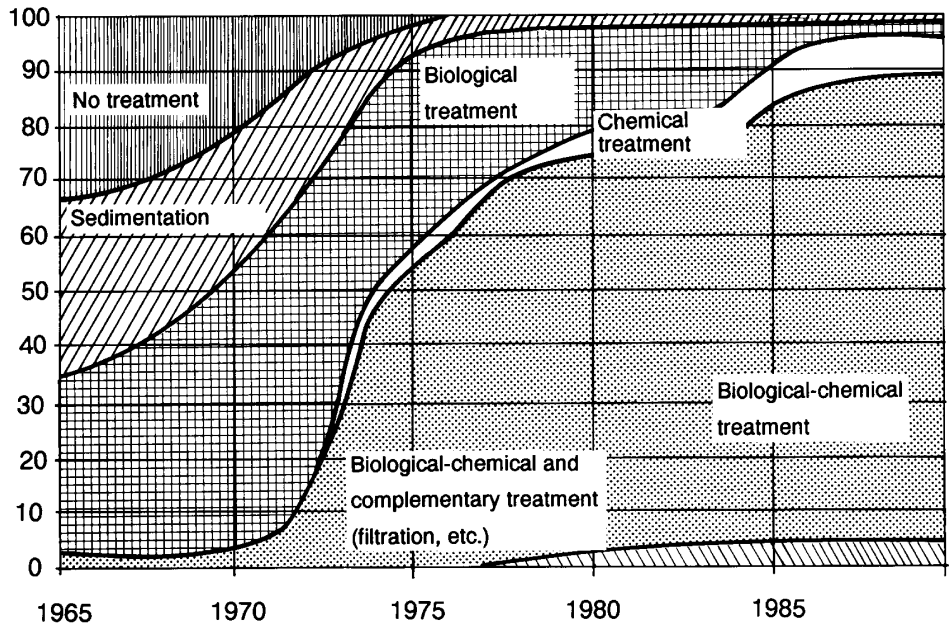

Figure 1.2: The development of wastewater treatment 1965–1990 in Sweden (Hultman 1992).

[1]The river, lake or other watercourse where the treated wastewater is let out into.

In 1992 a European Community directive required all member states to improve their wastewater treatment by the turn of the century. Sweden has decided to decrease of the nitrogen discharges by approximately 50% for larger wastewater treatment plants located on the coast from Norway to Stockholm. Phosphorus removal should also be increased for these plants. Further reduction of nitrogen demands more efficient control and operation of the wastewater treatment plants. This is one of the major motivations behind this thesis.

1.2 A wastewater treatment plant

In a modern wastewater treatment plant the wastewater is generally processed in several steps before it is released to the recipient. Tchobanoglous and Schroeder (1985) and Kommunförbundet (1988) give a survey of common practice. A schematic picture of a typical plant is presented in Figure 1.3. The four blocks represent different stages of the wastewater treatment processes.

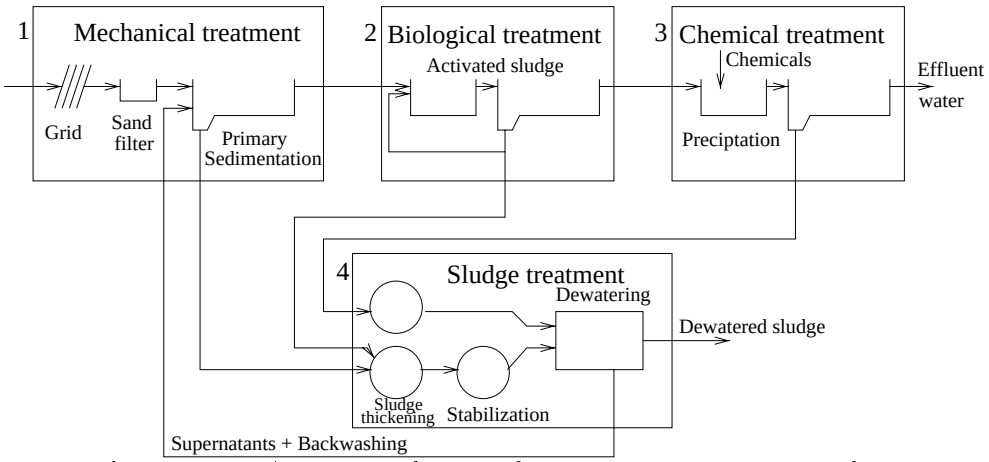

Figure 1.3: A common layout of a wastewater treatment plant (Kommunförbundet 1988).

First *mechanical treatment* is applied. Large objects like rags are first collected on a grid. Then heavy particles like sand are removed in a sand trap[2]. Lighter particles are removed in a primary settler.

The second block is often *biological*. In this part of the wastewater treatment plant microorganisms degrade organic matter and in some con-

[2]The sand trap works like a settler but with a higher water flow.

figurations nutrients are also removed. Different biological processes exist, but most larger wastewater treatment plants make use of the *activated sludge process*. In its basic configuration the activated sludge process consists of an aerated tank and a settler. The microorganisms grow slowly in the aerated tank. In order to maintain their population sizes, sludge from the settler which contains microorganisms is recirculated back to the aerated tank. Excess sludge is removed to both avoid sludge in effluent water and to maintain a reasonable suspended solids concentration. Further information is to be found in Section 1.3. Other types of biological treatment are also available. An *oxidation pond*, for example, is a pond where the wastewater is retained for 20–40 days. During this period the wastewater is treated by microorganisms, algae, and the influence of sunlight. The *trickling filter* is another kind of biological treatment. It is a construction filled with rocks or plastic objects to which the microorganisms attach and grow. The wastewater becomes treated while it trickles through the filter. Air is also blown through the filter to increase the oxygen concentration and hence improve treatment. *Wetlands* are yet a further biological alternative. In a wetland, wastewater is spread out over a large area with a water depth of around 0.5 meters. Plants and microorganisms treat the wastewater. Wetlands are usually used as a final polishing step and not as a replacement for an activated sludge process. In this thesis only the activated sludge process will be considered.

Phosphorus is often removed from the wastewater by *chemical treatment* as shown in the third block of Figure 1.3. But it is also common to have this step in the beginning – pre-precipitation. A precipitation chemical is added which turns phosphate into insoluble fractions. Precipitation chemicals also stimulate the creation of flocks. The insoluble phosphates as well as organically bounded phosphate then absorb or adhere to the flocks. The flocks are separated by either sedimentation or flotation. Instead of using chemicals, enhanced phosphorus removal can be applied in the activated sludge process by biological treatment. A special configuration of the activated sludge process makes this possible. Henze *et al.* (1995*b*), Balmér and Hultman (1988) and Isaacs and Henze (1995) discuss this further.

As a final step sometimes chlorination for disinfection and removal of bad smell is included before the water is released in the recipient.

Sludge from the different blocks is processed in the *sludge treatment*. The sludge consists of organic material which has to be stabilized to avoid odor and reduce the pathogenic content. The stabilization is commonly done in anaerobic digesters. In the digesters organic matter is degraded, and most pathogenic bacteria and microorganisms die due to the high tem-

perature. Bio-gas, methane and carbon dioxide are produced during digestion. Before sludge is transported away it is dewatered, either mechanically by centrifuging, filtering, and pressing, or by drying. This is done to reduce transportation costs since the sludge contains about 95% water. After treatment, sludge may be dumped or used as a fertilizer and soil conditioner. If the content of heavy metals or other poisonous matter in the sludge is too high, it is of course not suitable to use in agricultural practice. It may also be used as fuel or in construction materials (Bradley *et al.* 1992). Lue-Hing *et al.* (1992) gives a more detailed description on municipal sewage sludge management. The waste gathered in the grid and sand filter, in the mechanical treatment, is usually not treated. It is instead directly transported to a garbage dump.

1.3 The activated sludge process

A basic description of the activated sludge process is presented. How the activated sludge process can be extended for nitrogen removal is also explained. Finally, a simple mathematical model is given.

1.3.1 Basic description

In Figure 1.4 the basic layout of an activated sludge process is shown. The

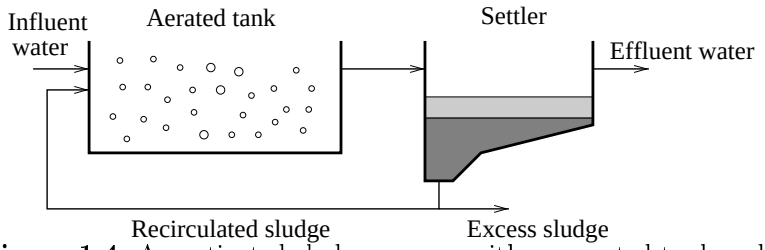

Figure 1.4: An activated sludge process with an aerated tank and a sedimentation tank.

activated sludge process is a biological process in which microorganisms oxidize and mineralize organic matter. All microorganisms enter the system with the influent wastewater. The composition of the species depends not only on the influent wastewater but also on the design and operation of the wastewater treatment plant. Microorganisms are kept suspended either by blowing air into the tank or by the use of agitators. Oxygen is used by the microorganisms to oxidize organic matter. To maintain the microbiological population, sludge from the settler is recirculated to the aerated tank.

The growth of the microorganisms and influent particulate inert matter is removed from the process as *excess sludge*. Microorganism concentration is controlled by the excess sludge flow rate.

A basic model of the biological renewal process in an activated sludge process is illustrated in Figure 1.5. Organic matter enters the plant in several different forms and is converted to other forms by biological processes. *Hydrolysis* transforms larger organic molecules in the initial fraction

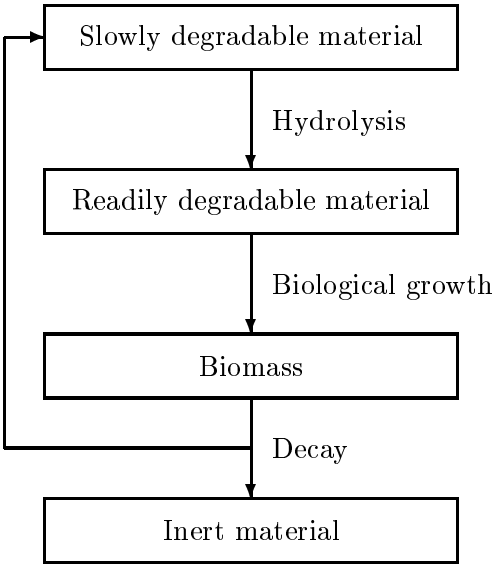

Figure 1.5: The biological renewal process (Henze *et al.* 1995*a*).

of slowly degradable matter into smaller, more easily accessible molecules (readily degradable matter). The speed of hydrolysis may be a constraint in a wastewater treatment plant if the influent wastewater mainly consists of slowly biodegradable matter, since the hydrolysis process is relatively slower than the growth rate of the microorganisms (biomass). The biomass growth rate depends on many variables such as the amount of biomass, the substrate, temperature, pH, and the presence of toxins. During bioreduction (decay of microorganisms), biologically inert (non-biodegradable) matter is produced. Incoming wastewater will contain some inert matter as well. This matter flows unaffected through the process and is collected and removed in the settler.

1.3.2 Biological nitrogen removal

Nitrogen is present in several forms in wastewater, e.g. as ammonium (NH_4^+), nitrate (NO_3^-), nitrite (NO_2^-) and as organic compounds. Nitrogen is an essential nutrient for biological growth and is one of the main constituents in all living organisms. The presence of nitrogen in effluent wastewater, however, presents many problems (Barnes and Bliss 1983).

- Ammonia (NH_3) is toxic to aquatic organisms, especially for higher life forms such as fish.
- When ammonium is oxidized to nitrate, a significant oxygen demand in the receiving water may give rise to a severe depletion of the dissolved oxygen concentration.
- Nitrite in drinking water is toxic, especially for human infants.
- Nitrogen is a nutrient stimulating growth of aquatic plants. When the plants die, oxygen is consumed by organisms degrading the litter.
- The presence of ammonium in the drinking water supply requires an increased chlorine dosages.

When untreated wastewater arrives to the wastewater treatment plant most nitrogen is present in the form of ammonium. Nitrogen can be removed by a two-step procedure. In the first step, ammonium is oxidized to nitrate in aerated zones. This process is called *nitrification* and can basically be described by the following two chemical formulas:

$$\begin{aligned} NH_4^+ + 1.5O_2 &\rightarrow NO_2^- + H_2O + 2H^+ \\ NO_2^- + 0.5O_2 &\rightarrow NO_3^- \end{aligned}$$

As seen above ammonium is not directly oxidized to nitrate. It must be first oxidized to nitrite and then to nitrate.

In the second step, the nitrate produced under aerobic conditions is transformed to nitrogen gas by a process called *denitrification*. The denitrification reaction takes place in an anaerobic environment where the bacteria responsible for denitrification respire with nitrate instead of oxygen. This environment is called anoxic. The process can be summarized by the following chemical formula:

$$4NO_3^- + 5\text{“}CH_2O\text{”} + 4H^+ \rightarrow 2N_2 + 5CO_2 + 7H_2O$$

where “CH_2O” stands for diverse the organic matter.

By using these two bacterial processes, nitrification and denitrification, nitrogen is removed from wastewater biologically. Anoxic zones in the activated sludge process are necessary for denitrification. Anoxic zones can be placed either in the beginning of the tank (pre-denitrification), see Figure 1.6, or in the end of the tank (post-denitrification). In a pre-denitrifying

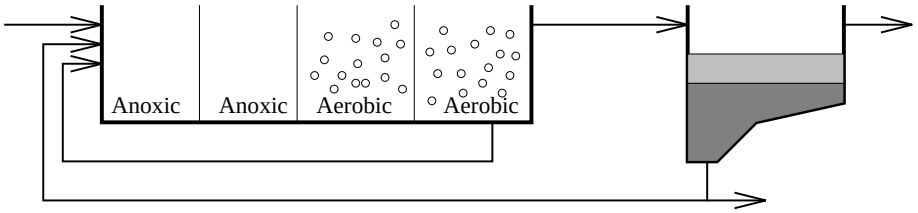

Figure 1.6: An activated sludge process with pre-denitrification.

system, an extra recirculation flow is usually introduced to transport the nitrate rich water back to the anoxic zone. Recirculated flow rate is typically higher than the influent flow rate. The presence of oxygen in the anoxic zone makes denitrification less efficient, and thus more carbon is required. To reduce the oxygen concentration caused by the recirculated water, an additional anoxic zone in the end of the bioreactor can be included.

Efficient biological nitrogen removal in activated sludge processes depends on sufficient supplies of carbon for the denitrifying bacterial population. If the influent wastewater lacks sufficient energy to support denitrification, an external carbon source can be added to make better use of the total nitrogen removal capacity, see also Chapter 3. Methanol, ethanol, acetate, primary sludge and various industrial waste products are possible carbon sources. The carbon content in the influent wastewater is used for denitrification if the anoxic zones are placed at the beginning of the activated sludge process (pre-denitrification). When the anoxic zones are placed after the aerobic zones (post-denitrification), a supplemental carbon source have to be added.

1.3.3 Mathematical models

There are several models of the biological processes in an activated sludge process. Of these, the most widely used is IAWQ's[3] Activated Sludge Model No. 1 (Henze *et al.* 1987). That model describes the three following biological processes: removal of organic matter, nitrification, and denitrification. To illustrate a biological process the following example from Henze *et al.*

[3]International Association for Water Quality. This association was formerly called International Association on Water Pollution Research and Control (IAWPRC).

(1987) is given. The process is a completely mixed bioreactor with the three components. In Figure 1.7 the bioreactor is illustrated.

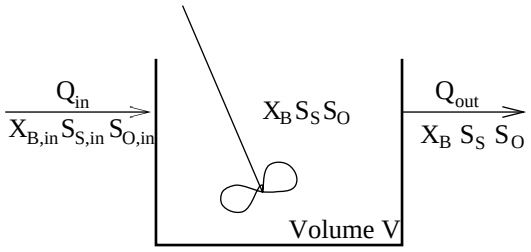

Figure 1.7: A completely mixed bioreactor.

To find the differential equations for each component in the process, the following basic balance equation can always be used.

$$\textit{Accumulation} = \textit{Input} - \textit{Output} + \textit{Reaction}$$

The reaction rate may, however, be more difficult to determine, but the following differential equations are proposed

$$\begin{aligned}
\frac{dX_B}{dt} &= \frac{Q_{in}}{V}X_{B,in} - \frac{Q_{out}}{V}X_B + \frac{\mu S_S}{K_S + S_S}X_B - bX_B \\
\frac{dS_S}{dt} &= \frac{Q_{in}}{V}S_{S,in} - \frac{Q_{out}}{V}S_S - \frac{1}{Y}\frac{\mu S_S}{K_S + S_S}X_B \\
\frac{dS_O}{dt} &= \frac{Q_{in}}{V}S_{O,in} - \frac{Q_{out}}{V}S_S - \frac{1-Y}{Y}\frac{\mu S_S}{K_S + S_S}X_B - bX_B
\end{aligned}$$

where X_B is biomass, S_S soluble substrate and S_O dissolved oxygen. $X_{B,in}$, $S_{S,in}$ and $S_{O,in}$ are the influent concentrations of biomass, soluble substrate and dissolved oxygen. The tank volume is denoted V, and the influent and the effluent flows are Q_{in} and Q_{out}, respectively. The growth yield is Y, μ is the maximum specific growth rate, K_S is the half-velocity constant and b is the decay rate. Note that the differential equations are coupled in a complicated nonlinear way.

We see that accumulation of the different components depends on several things: the flow rates, influent concentrations, parameter values, and the actual concentration of the different components. Nonlinear functions are also involved. If, for example, the soluble substrate concentration becomes very high, the growth rate of the biomass is still limited to less than the maximum specific growth rate μ. A description of the complete IAWQ model is given in Section 2.3.

1.4 Control of wastewater treatment plants

The allowed levels of pollutants in treated wastewater have become increasingly stringent with time. Taking into account current environmental problems, it is not unrealistic to believe that the this trend will continue. At the same time loads on existing plants plants are expected to increase due to growth of urban areas. This situation demands more efficient treatment procedures for wastewater.

One way to improve efficiency could be to construct new and larger basins, but this is expensive and often impossible since the land required is just not available. Another way would be the introduction of more advanced control and operating systems. This is expected to reduce the need for larger volumes, improve the effluent water quality, decrease the use of chemicals, and save energy and operational costs. Sustainable solutions to the problems of wastewater treatment will require the development of adequate information systems for control and supervision of the process.

Today many wastewater treatment plants use very simple control technologies or no automatic control at all. Control techniques in current use include simple PLC-techniques, time control, manual control, rules of thumb, or simple proportional control. Advanced models of the processes in a wastewater plant such as the IAWQ's Activated Sludge Model No. 1 have been developed over the years, but have not been used to any extent for practical control design. It is difficult to design a sensible controller based on the IAWQ model, which is nevertheless a very useful model to evaluate different control strategies. Several advanced control strategies have previously been suggested, see e.g. Bastin and Dochain (1990), Van Impe *et al.* (1992), Dochain and Perrier (1993), Nielsen and Lynggaard (1993), and Youssef *et al.* (1995).

The following reasons may explain why advanced control have not been extensively used. (See Olsson (1993*a*) for a more throughly treatment of the subject.)

- The effluent standards have not been tight enough. Economic penalties for exceeding the regulations along with stricter effluent regulations which are not based solely on long average values could encourage implementation of better control.
- Wastewater treatment is often considered as a non-productive process. Since control systems are expensive it may be difficult to convince a manager to introduce a more advanced system, especially when profit can not be guaranteed.

- On-line sensors have been unreliable and require a lot of maintenance.
- Many pumps, valves, and other actuators are not controllable; often they can only be switched on or off.
- The process is very complex and it is not obvious how to control and optimize the plant.
- Few control engineers have devoted their attention to wastewater treatment plants.

Interest for applying more sophisticated control is, however, growing. The reasons for this are most economical:

- Cost effective solutions are becoming more and more important. As the loads on existing plants increase, control and optimization may be able to handle the increasing loads with the same volumes.
- Stiffer requirements on treated wastewater.
- Fees and taxes related to the effluent water quality are making it more expensive to release pollutions.
- The general public's awareness of environmental issues is increasing and more and more focused on issues of sustainability and energy consumption.
- Improved on-line sensors and actuators are being continuously developed.
- More complex process alternatives, which are difficult to control manually.

Application of modern control theory in combination with new on-line sensors and the appropriate parts of advanced models has great potential to improve the effluent water quality, decrease the use of chemicals and to save energy and money, see Van Impe *et al.* (1992), Carlsson (1995), and Carlsson (1997) for more discussions. Nielsen and Önnerth (1995) suggest an expert system which use on-line sensors to control and optimize the plant performance. They also give a short overview of the development of on-line sensors over the last 25 years. The use of on-line sensors has increased rapidly in the last years, see Figure 1.8. This trend is expected to continue due to the large potential for reducing costs when used in combination with automatic control. Vanrolleghem and Verstraete (1993) surveyed new

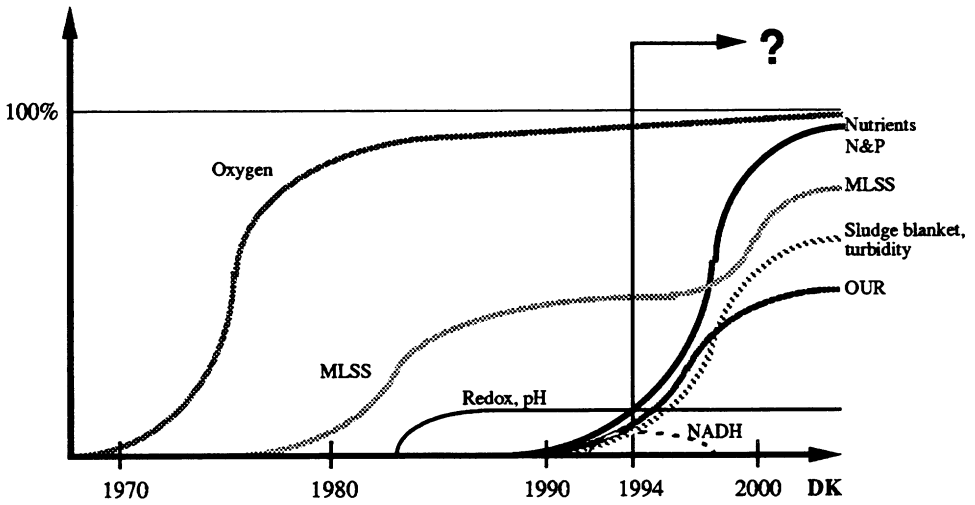

Figure 1.8: Use of sensors in full-scale control in Denmark (Nielsen and Önnerth 1995).

and existing technologies for monitoring wastewater treatment plants. The importance of integrating control and process design to obtain best overall performance has been illustrated by Andrews (1994). Cause-effects for relationships in an activated sludge plant have been established by Olsson and Jeppson (1994). These can be of help when designing controllers for new purposes, e.g. controlling the various flows.

The following are some examples of automatic control applied to the activated sludge process.

- Control of the dissolved oxygen concentration (DO) has been practiced for many years. This is due to:
  - The energy consumption can be reduced by controlling DO, since it requires much energy to blow air to several meter deep basins.
  - The effluent water quality depends to a great extent on a sufficiently high DO.
  - On-line sensors for DO measurements have been available for several years, see also Figure 1.8.

  See also Chapter 5 for DO control and DO set-point control.

- Pressure drop over the air valves can be minimized. A common strategy is to control the air pressure so that the most opened valve is almost completely opened, see Rundqwist (1986).

- The nitrate concentration can be kept low by adding an external carbon source. Using on-line measurements of the nitrate concentration, a proper flow rate of the external carbon source can be given, see Hellström and Bosander (1990), and Isaacs *et al.* (1993). By using feedforward control from influent total organic carbon (TOC) and recirculated nitrate, disturbances in influent water can be better rejected, Chapter 3 discuss this.

- It is important to control the chemical dosage in a wastewater plant. Phosphorus, for example, is removed by chemical precipitation. A combination of feedback and feedforward control from on-line sensors, flow rates and an experience data base may be useful to maintain appropriate chemical dosages.

- The ammonium concentration can be controlled by the DO set-point and/or the number of aerated zones. This is an alternative to using a fixed DO set-point, see Nielsen and Lynggaard (1993), and Chapter 3.

- Optimizing the different flow rates in the plant is an interesting field of research, see e.g. Nielsen and Lynggaard (1993), and Vanrolleghem (1994). Some of the flows determine the amount of biomass in the system. Maintaining a high concentration of biomass is a tempting strategy to improve plant performance, since a large biomass can degrade more organic material. Unfortunately, the sedimentation properties can be affected detrimentally and foam can also be created. Other forms of microorganisms may also adapt to the high concentration of biomass, which in turn makes the activated sludge process less efficient. At present it is, however, difficult to predict how an increased sludge concentration will influence sludge sedimentation properties.

- Influent flow can to some extent be controlled by constructing additional tanks or using the large wastewater tunnels as reservoirs. The large variations in the influent wastewater flow can then be significantly reduced. Variations in influent flow are mainly caused by rain water leaking into the pipes, or by drainage water. This type of variation forces plants to work with higher flows during short periods which is less efficient compared to a constant flow. Sometimes one also has to do by-pass actions to avoid sludge loss from the secondary clarifier. There have been experiments in Göteborg where the wastewater tunnels were used as reservoirs (Gustafsson *et al.* 1993). Also, outside Malmö (Nyberg *et al.* 1996) and in Denmark (Nielsen *et al.* 1996), similar trials have been done to avoid problems during high influent flow rates.

- The clarifier has the dual task of clarifying and thickening the sludge. Its function is crucial to the operation of the activated sludge process. Hence modeling, diagnostics, and control of the sedimentation process are also important topics, see e.g. Jeppsson (1996), and Bergh (1996).

- The activated sludge process is a multivariable process, i.e. it has several inputs (control handles) and several outputs. There are also many cross couplings. If, for example, the DO set-point is changed, both the ammonium and nitrate concentrations are affected. If the internal recirculation is varied, this affects several parameters in the process. Hence a multivariable controller which can use cross couplings efficiently, may be useful to optimize the plant performance. Dochain and Perrier (1993), and Chapter 6 take this up.

- A key goal in wastewater treatment is to maintain effluent quality standards at a minimum cost. Obviously, it is not enough to have an effective control of various subprocesses. One must also consider various types of supervision control based on some cost function. Such strategies have been discussed by Vanrolleghem *et al.* (1996).

- Control theories may also be used to design software sensors for estimating the respiration rate from measurements of the dissolved oxygen concentration and airflow rate, see Chapter 4.

The above list of control strategies for wastewater treatment is by no means complete. More ideas, examples and motivations can, for instance, be found in the IAWQ proceedings of the workshops in Instrumentation, Control and Automation of Water and Wastewater Treatment and Transportation Systems.

New control strategies may involve the use of simplified biological/physical models, feedforward control from measurable disturbances, simple estimation models, supervision control, and real-time estimation.

For a control engineer the activated sludge process in a wastewater treatment plant is a challenging topic for several reasons.

- The process is time-varying. It is a biological process where temperature, composition of influent water, amount of biomass, flows, etc, vary in time.

- The process is non-linear and time-varying. Several things make the process (model) nonlinear, e.g. the Monod functions ($\frac{\mu S_S}{K_S+S_S}$), and

multiplication of states (bilinearity). The pump flows, which varies in time, make the dynamic time-varying.

- The process has stiff dynamics. It has time constants which range from seconds to months. This may not have to be a major problem since cascade control may be applied. Cascade control means that a fast controller controls a fast sub-process and a slower controls the set-point of the fast controller.

- The process is multivariable. The process has several inputs and outputs. What should be considered as inputs and outputs are not obvious. An input could, for example, be a set-point for a fast controller, and an output does not necessarily have to be a concentration in the effluent, it could be a concentration in a zone. There are also large cross-couplings, e.g. if a flow is changed, many other variables are affected.

- Many sensors are still not reliable. Much progress has been made in sensor development in recent years. Common problems are that the sensors are fairly noisy, have long response times, require frequent maintenance, and that they drift.

- Large disturbances affect the process. Especially influent flow and influent concentrations are subject to large variation.

1.5 Outline of the thesis

In this section a brief summary of the main contributions in the thesis is presented. Note that each chapter contains a review of previous research.

In chapter 2 the pilot plant is presented. The pilot plant was designed to study new methods for efficient nutrient removal using advanced process technology, applied microbiology and automatic control. It is controlled by an advanced control and supervision system (CSS), where the user can via a graphical interface operate the plant, control data acquisition, save and plot data, respond to alarms and tune controllers. The CSS was developed as a Masters project (Latomaa 1994), where I have been co-supervisor. A simulator based on the control and supervision system has been the subject of another Masters project (Luttmer 1995), where I also have been co-supervisor. The simulator's main function is to run simulations on an activated sludge process. As such, the simulator is an effective teaching aid.

A simulation model is also presented in Chapter 2. This model is used in most simulations in this thesis. It is an approximation of the pilot plant, and the same volumes and flows are also used. The parameters in the model are, however, not calibrated to the real process. Prior experiments with the pilot plant, simulations are very useful to evaluate control strategies, or test different controllers.

An external carbon source can increase the denitrification rate and compensate for deficiencies in the influent carbon/nitrogen ratio. In Chapter 3 the problem of controlling the flow rate of an external carbon source is considered. The control strategy for the carbon dosage is based on keeping the nitrate level in the anoxic zone at a constant and low level. To better reject disturbances, feedforward from the mass flow of influent TOC and recirculated nitrate are used. Four different types of feedforward controllers are evaluated: a PID-controller, a direct adaptive controller, an indirect adaptive controller, and a model-based adaptive PID controller. The controllers are compared in a simulation study, and the direct adaptive controller is further tested in the pilot plant. Additionally a number of problems and their solutions concerning adaptive control are discussed in this chapter.

In Chapter 4, methods for estimating two essential parameters which characterize the dissolved oxygen concentration (DO) dynamics in an activated sludge process are presented. The two variables are the respiration rate $R(t)$, and the oxygen transfer function K_La. The respiration rate is a key variable that characterizes the DO process and the associated removal and degradation of biodegradable matter. The oxygen transfer function K_La describes the rate with which oxygen is transferred to the activated sludge by the aeration system. The K_La function is expected to be a nonlinear function of the airflow rate. The estimation algorithm is based on a Kalman filter which uses measurements of the dissolved oxygen concentration and airflow rate. To improve estimation, different models of the time-varying respiration rate and nonlinear oxygen transfer function have been developed, and evaluated in a simulation study and on real data. If the DO sensor has dynamic, this must be taken into account, otherwise the estimates will be biased. A filter which compensates for the DO sensor dynamic has been designed. This filter is not only useful for DO measurements, it can be applied to any sensor where there is need for compensation of the sensor dynamic. In a Masters project (Nakajima 1996), where I have been a co-supervisor, an extended Kalman filter was utilized, instead of the suggested filter to compensate for the sensor dynamic. Surfactants may reduce the oxygen transfer function K_La. The suggested estimation algorithm has been used to study the effect surfactants has on K_La. Both K_La and the respiration rate were found to be reduced by the addition

of a surfactant. An improvement over previous methods, this estimation algorithm is capable of both estimating a nonlinear K_La function and a time-varying respiration rate. Further, the filter which compensates for the sensor dynamics has tuning knobs for both smoothing lag and noise sensitivity.

The estimated nonlinear oxygen transfer function is used to design a nonlinear controller of the dissolved oxygen concentration in Chapter 5. The DO in the aerobic part of an activated sludge process should be sufficiently high in order for microorganisms to degrade organic matter and convert ammonium to nitrate. On the other hand, an excessively high DO, which requires a high airflow rate, results in high energy consumption and may even deteriorate sludge quality. Control of the DO is therefore important. Since the K_La function is nonlinear, the gain of the process will vary with varying airflow rate. By designing a nonlinear controller, a compensation for the nonlinearity can be made and high control performance may be obtained under all operating conditions. Simulations and practical experiments confirm these results. An outline for DO set-point control are given. Its purpose is to control the ammonium concentration in the aerated zone by the DO set-point. An experiment in the pilot plant with the set-point controller showed that it was not only possible to save energy due to a lower DO set-point, the effluent nitrate concentration was also significantly reduced. Possible disadvantages may be that sludge properties deteriorate due to the low DO, and nitrous oxide (N_2O) can be formed when the DO is low. These problems should, however, be compared to the achieved improvements. Spatial DO set-point control may also reduce this problem by switching off aeration in some zones when the DO set-point becomes too low. The DO set-point can then be increased in the remaining zones. A pressure controller is finally presented in this chapter. The idea, which is well known, is to control air pressure so that the most open air valve becomes almost completely open. This was later confirmed in the pilot plant.

Multivariable linear quadratic (LQ) controllers are designed in Chapter 6. The controllers are based on a linear state-space model estimated by a subspace system identification method. The main advantage of these controllers, compared to SISO controllers, are that they take all interactions in the process model into account. This allows for a sensible trade off between the different control handles and outputs. The following inputs are used: external carbon, internal recirculation rate, and DO set-point. Ammonium and nitrate in the last aerated zone are used as outputs. The controllers outlined also use feedforward from the measurable disturbances: influent flow rate, influent ammonium and influent carbon. The two different mul-

tivariable controllers have been evaluated in a simulation study. One of the controllers is based on differentiating the states, and the other has additional integration states. Both controllers have shown good performance in simulations. It was, however, found that the modeling part was crucial for the control performance.

Conclusions and some topics for future research are summarized in Chapter 7. Means of optimizing the activated sludge process using economic cost functions discussed are discussed. By setting prices on the effluent discharges, and on the control variables, i.e. blowing air, dosing external carbon, running pumps, etc., the most economically way to run the plant can be determined. Parts of this strategy could also be implemented in an extremum controller. Further discussions involves how wastewater treatment plants can be divided in different sub-processes, where each subprocess then are optimized separately.

Chapter 2

Pilot plant and simulation model

This chapter describes the pilot-scale activated sludge plant at the main municipal wastewater treatment plant in Uppsala, Sweden, and a simulation model of the pilot plant.

The pilot plant consists of two separate lines for pre-denitrification. The main purpose of the plant has been to study new methods for efficient nutrient removal using advanced process technology, applied microbiology and automatic control. Both lines are extensively monitored by on-line instruments and sampling programs. The plant is controlled by an advanced control and supervision system, where the user can via a graphical interface operate the plant, control data acquisition, save and plot data, respond to alarms and tune controllers.

To numerically evaluate different controllers and control strategies it is important to use a model which realistically simulates a true plant. A simulation model of the pilot plant has therefore been designed. The IAWQ's Activated Sludge Model No. 1. (Henze *et al.* 1987) has been used to model each zone of the bioreactor and the clarification-thickening model in Takács *et al.* (1991) has been used to model the settler.

This chapter is organized as follows. In the next section, a general description of the pilot plant and its instrumentation is given. The plant is controlled by a control and supervision system which is presented in Section 2.1.2. A simulator, based on the control and supervision system has been designed, and is outlined in Section 2.1.3. The different conducted experiment are presented in Section 2.2. A model of the pilot plant is

presented in Section 2.3.1, and the bioreactor model of each zone in the pilot plant is given in Section 2.3.2. The differential equations and parameter values for the activated sludge process are presented in Section 2.3.3. The settler model, simulation tool, and conclusions are given in Sections 2.3.4, 2.3.5 and 2.3.6, respectively.

2.1 The pilot plant

2.1.1 General layout of the pilot plant

The design and construction of the activated sludge pilot plant was initiated in 1993 and in June 1994 the plant was taken into operation. The basic process design including choice of instrumentation was developed by researchers from the Uppsala STAMP consortium and personnel from Uppsala Public Works Office. The tanks and sedimentation units were built by personnel from the wastewater plant in Uppsala. The tanks are made in stainless steel. The pilot plant which consists of two separate lines is placed indoors in an existing building at the Uppsala wastewater treatment plant. Line P1 is equipped with more on-line instruments than line P2, which mainly is used as a reference line. Both lines are primarily designed for nitrogen removal using pre-denitrification with the possibility to add an external carbon source. A schematic layout of line P1 is shown in Figure 2.1. Each line consists of an aeration tank (2.35 m^3) with a variable anoxic

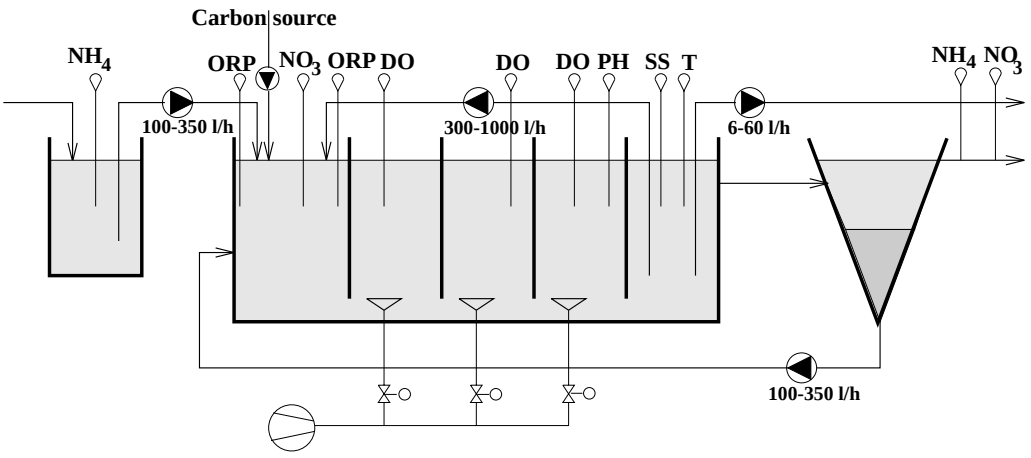

Figure 2.1: Layout of line P1 in the pilot-scale activated sludge plant.

to aerobic ratio and a settling tank (0.55 m^3). The configuration of the aeration tank is given in Table 2.1.

Cell no.	Volume of cell (m^3)	Operation
1	0.46	Anoxic
2	0.63	Aerated
3	0.44	Aerated
4	0.44	Aerated
5	0.38	Non-aerated

Table 2.1: The aeration tank consists of 5 cells, cell 1 and 5 have mixers (fixed, horizontal) and cells 2-4 are aerated.

Pre-precipitated and pre-sedimented wastewater from the full-scale plant is used as influent water to the pilot plant. A small equalization tank is installed before the pilot plant, see Figure 2.1. Peristaltic pumps are chosen in order to achieve well defined flow rates. The capacities of the pumps are given in Table 2.2.

Pump (number of pumps)	Capacity [l/h]
Influent (2)	100-500
Excess sludge (2)	5-60
Return sludge (2)	100-350
Internal recirculation (2)	300-1000

Table 2.2: Pumps in the pilot plant, line P1 and P2. All pumps listed in the table are peristaltic pumps, manufactured by Bredel and delivered by AKA pump. The pumps are controlled by the control system via frequency converters.

Excess sludge is removed from the aeration tank instead of from the sedimentation unit. This gives a higher flow rate which is easier to govern. The plant is equipped with on-line sensors for nitrate, ammonium, dissolved oxygen concentration, pH, redox, suspended solids and temperature, see Table 2.3.

Three vacuum samplers are used to collect water samples for laboratory analysis. The samplers take water from the influent (same to both plants) and the effluent from P1 and P2, respectively.

Membrane bottom aerators (Trelleborgs gummi) are used in the aerated zones. The air flow rate is controlled by electro-pneumatic valves (PMW

Sensor (No. of sensors)	Principle	Location
DO (6)		Cell 2-4 in P1 and P2
Ammonium (1)	Ion selective	Effluent or influent
Nitrate (2)	Ion selective	Cell 1 in P1 and effluent of P1 and P2
Susp. solids (2)	IR-light	Cell 3 in P1 and P2
PH (2)		Cell 1 and 4 in P1
Redox (4)		Cell 1 and 2 in P1 and P2
Temp (1)		Cell 5 in P1

Table 2.3: On-line sensors used in the pilot plant. All sensors are manufactured by Contronic, except for the suspended solids sensors which are manufactured by Cerlic.

Palmstiernas). The air to the tanks is provided by two side channel blowers (Ventur) with a maximum capacity of 39 m^3/h.

An important use of the pilot plant has been to evaluate different experiments with external carbon sources. External carbon can be added to both P1 and P2. The flow rate of external carbon is controlled by membrane pumps (LMI Milton Roy) with a maximum capacity of 8 l/h.

2.1.2 The control and supervision system

A novel control and supervision system (CSS) for the pilot scale plant was designed. The CSS consists of a PC equipped with measurement cards. The communication with the process is made via a switch cabinet. The switch cabinet, designed by Huddinge El, contains frequency converters, power supplies, relays and amplifiers. It also contains devices for running the plant manually. The following hardware is used for the CSS:

- A standard PC (486DX-66MHz with 16 Mb RAM)
- Two 16 channels 4-20 mA D/A cards, 12 bits resolution (Computer Boards)
- One 24 channels 4-20 mA A/D card, 12 bits resolution (Computer Boards)
- Two 48 channels binary cards (Computer Boards)

Linux, a public domain UNIX dialect was chosen as operating system. Most of the programming was made as a Master thesis work, see Latomaa (1994). The CSS was implemented in C++ and separated into two different processes which communicate through a common memory area. One process handles the actual control of the plant, i.e. start and stop of pumps, calculation of control signals, collection of data, checking alarms, etc. The other process manages the graphical user interface (GUI). The GUI was programmed by using Motif. Special attention was made to create a user-friendly interface which should be easy to interpret and effectively present the status of the plant, see Carlsson and Lindberg (1995) and Carlsson *et al.* (1994*b*). The user can via the GUI operate the plant and perform other tasks such as control data acquisition, plot data, respond to alarms, tune controllers, etc. Data from the on-line sensors are stored every 10th minute (averaged values are computed if the process is sampled faster than 10 min).

The plant is schematically drawn in the GUI, see Figure 2.2. The flow rate of a pump is changed by clicking on the pump symbol and then entering the flow rate. The pump symbol also indicates if the pump is switched off, is in auto or manual mode, or if there is a pump failure. The DO is controlled by varying the position of the air valves. The valve opening is usually controlled by PID controllers, but more advanced control schemes were evaluated in the experiments.

One interesting feature in the GUI is that the width of the pipes in the drawing is proportional to the actual flow rate in the plant, see also Olsson (1993*b*). To further improve the presentation of the status of the plant, staples, "pie-charts" and color coding are used.

For more information about the pilot plant, see Carlsson *et al.* (1997).

2.1.3 A simulator based on the control and supervision system

A simulator for an activated sludge process has been designed. What is special with this simulator compared to other simulators, is that the previous outlined control and supervision system is used. This means that the same user friendly GUI is used. It is hence very easy to, for example, change pump flow rates, DO set-points or carbon dosage. It is also easy to plot the different concentrations and vary the composition of the influent wastewater. The only difference to the GUI in the CSS is that a simulated process is controlled instead of the pilot scale plant, and the simulation runs of course much faster than the processes in the pilot scale plant.

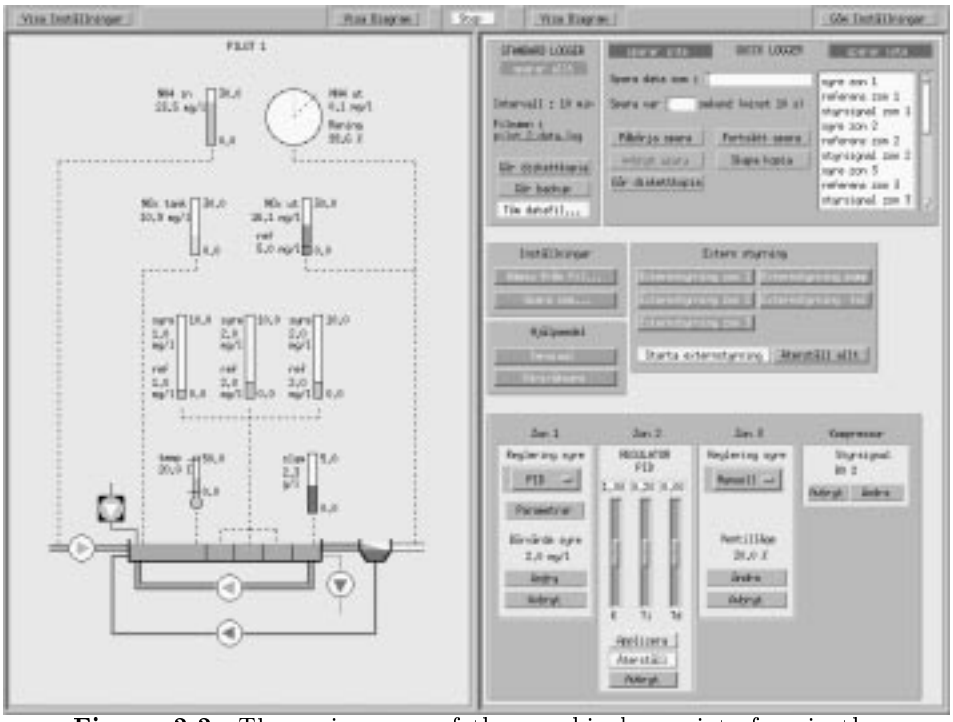

Figure 2.2: The main menu of the graphical user interface in the control and supervision system.

A simulator can, for example, be used for:

- Process understanding. Using the simulator better understanding of the complex activated sludge process can be gained.
- Education. This simulator has already been used in one course in wastewater treatment at Uppsala University and by personnel at the municipal wastewater treatment plant in Uppsala.
- Process control. Efficient control strategies are often model based. Also a good dynamic model can be used to test and evaluate different control strategies.
- Forecasting. Models can be used to predict future plant performance.

Each zone of the simulated activated sludge process is based on the IAWQ model. The Euler, the Heun and the Runge-Kutta methods are implemented in order to solve the differential equations numerically. A

number of parameters can be varied in the simulator model during runtime, for example, influent wastewater composition, zone volumes, flows, controller parameters, etc., but the number of zones is fixed, as well as the sensor configuration and placement of pumps. The programming work was made as a Master thesis work, see Luttmer (1995). For more information about the simulator see Carlsson and Hasselblad (1996), and Carlsson and Lindberg (1995).

2.2 Conducted experiments in the pilot plant

A pilot plant has been constructed. It is located at the main municipal wastewater treatment plant in Uppsala, Sweden. The main purpose of the plant has been to study new methods for efficient nutrient removal using advanced process technology, applied microbiology and automatic control.

During the period June 1994 to July 1996 a number of experiments have been conducted in the pilot plant. Many of the results have been published in leading journals and conference proceedings. For a quick reference, a short summary of all the experiments are given below. Detailed descriptions can be found in the cited references. The control related experiments discussed in this thesis are: 2, 4, 5, 6, and 8, see also Section 1.5.

1. Improved sedimentation by addition of weighting agents was studied by Andersson and Lundberg (1995). Experiments in the pilot plant were performed to evaluate the role of weighting agents on the limiting solids flux. It was found that the addition of calcium carbonate increased the limiting solids flux from by a factor of 2 and calculated on the volatile suspended solids by a factor of 1.5.

2. Addition of an external carbon source may be needed to improve the denitrification in an activated sludge process. Process performance and microbial adaption with ethanol in pre-denitrifying system were studied in Behse (1995) and Hallin *et al.* (1996). It was found that despite a rapid (30-40 h) response to ethanol on the nitrogen removal efficiency, it took around 12 days before the bacteria were fully adapted. Denitrification rate measured as mg N_2O-N/gVSS h was about 5 times higher in the ethanol line (P1) than in reference line (P2) after the adaptation period was completed. It was found that ethanol addition causes enzyme induction rather than alterations in species composition. Moreover, a control strategy for a carbon source dosage, based on measurements of nitrate-nitrogen was proposed. The objective was to control the flow rate of external car-

bon so that the nitrate level in the last anoxic zone is kept at a low value despite load changes. Practical tests showed that the control strategy worked well despite a rather noisy nitrate sensor, see further Lindberg and Carlsson (1996*a*) and Chapter 3.

3. A study how intermittent addition of ethanol to a pre-denitrification system affects the process performance and biological denitrifying capacity is reported in Hasselblad and Hallin (1996). The studied procedure mimics a possible operation strategy with addition of ethanol only at certain periods, e.g. weekends. The results show that in order to maintain process stability with intermittent dosage, the denitrifying bacteria have to sustain at a high capacity at each intermission. The rapid response to ethanol allows the use of advanced regulation strategies.

4. A nonlinear dissolved oxygen concentration (DO) controller has been implemented in the control and supervision system. The controller uses an estimate of the nonlinear oxygen transfer rate (see Carlsson *et al.* (1994*a*)) in order to linearize the DO process. By practical experiments in the pilot plant it was shown that this nonlinear controller outperform a standard linear controller, see further Lindberg and Carlsson (1996*d*) and Chapter 5.

5. A supervision DO controller has been suggested and evaluated in the pilot plant, see Lindberg and Carlsson (1996*d*), Lindberg and Carlsson (1996*b*) and Chapter 5. The main idea is to determine the DO so that a low effluent ammonium concentration is obtained. A desired ammonium level is compared with the actual level. If the effluent ammonium is too high the DO is increased and vice versa. This can lead to significant energy savings. In the experiment the air flow rate could be lowered considerable but also the nitrate level in the effluent decreased .

6. The problem to estimate the respiration rate and oxygen transfer rate from measurements of the DO and air flow rate (or valve positioning) has been studied in the pilot plant. The estimated respiration rate was close to values obtained from batch samples analysis. The estimated oxygen transfer function was nonlinear with respect to the air valve position. The estimation methods and result evaluation are reported in Lindberg and Carlsson (1996*c*), Carlsson *et al.* (1994*a*) and Chapter 4.

7. Seeding technology was studied to improve the nitrification process in order to obtain a high efficiency of the nitrogen removal during

winter time at low temperatures, and to decrease the volume needs, see Hultman *et al.* (1997). In this operational mode, excess activated sludge with high fraction of nitrifying bacteria (line P2) is seeded into the other activated sludge tank (line P1) to facilitate the nitrification process there. Line P1 was operated as a non-nitrifying system during the seeding test and with pre-sedimented wastewater as influent, while line P2 was operated with supernatant water (water from the sludge dewatering) as influent. The experiments indicated that the seeding effect of nitrifiers grown in activated sludge tank, allows nitrification at sludge ages that would otherwise preclude nitrification (tests were performed with aerobic sludge ages of 2.6, 1.4 and 0.9 days, respectively). The seeding was supplied with primary settled wastewater, and reject water which pass into the activated sludge tank. The maximum value of the growth rate for nitrification bacteria in the supernatant was about 0.24 days^{-1}. The developed model for seeding effects to an activated sludge process could reasonably well predict the obtained experiment data for the wastewater treatment line.

8. The pilot plant has been used in to evaluate how surfactants, which are important ingredients in modern washing agents, affect the oxygen transfer rate. External surfactants were added to the influent water in the pilot plant and K_La (oxygen transfer function) was both measured in laboratory batch experiments and estimated by the method suggested in Chapter 4. It was found that the external surfactant clearly reduced the K_La. Principal investigator was "Institutet för vatten- och luftvårdsforskning" (IVL).

2.3 The simulation model

To evaluate different controllers and control strategies it is important to use a model which realistically simulates a true plant. Here IAWQ's Activated Sludge Model No. 1 (from now on only referred as the IAWQ model) by Henze *et al.* (1987) has been used to model each zone of the bioreactor, and the clarification-thickening model by Takács *et al.* (1991) has been used to model the settler.

2.3.1 Model of the pilot plant

The practical experiments are performed in the pilot plant. Hence, it may be a good idea to design a simulation model which approximately models

the pilot plant for a prior evaluation of the controllers and control strategies.

All volumes and flows are approximately the same in the simulation model and in the pilot plant. The bioreactor and settler model are, however, not calibrated to the real plant. Instead default values for the models are used. The reason for not calibrating the models is that the suggested controllers and control strategies should be possible to apply to a large variety of plant configurations. The particular values of the controller parameters are not important. What is interesting is to study if a controller manages to control such a complex process as the activated sludge process. Further, it is also difficult, and time consuming to calibrate the physical models.

The pilot plant has the layout as presented in Figure 2.3, and zone fractions as given in Table 2.4. The total volume of the bioreactor is 2.35 m^3.

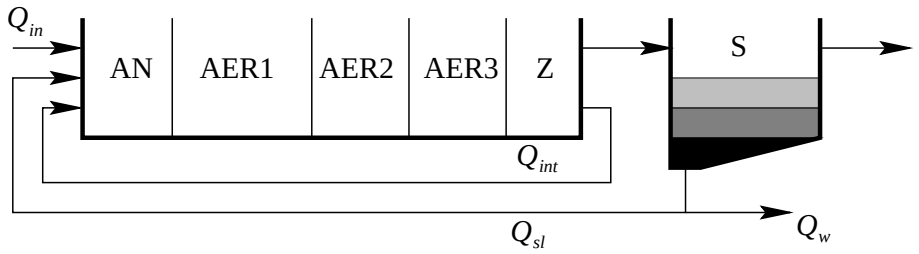

Figure 2.3: Layout of the the pilot plant.

Zone	AN	AER1	AER2	AER3	Z	S
Type	Anoxic	Aerated	Aerated	Aerated	Non-aerated	Settler
Volume [l]	460	630	440	440	380	550
Volume [%]	19	27	19	19	16	

Table 2.4: Volume of different parts of the pilot plant

The default flows in the simulation model are given in Table 2.5.

Flow	Q_{in}	Q_{int}	Q_{sl}	Q_w
[l/h]	200	600	200	4

Table 2.5: Default flows in the simulation model

2.3.2 The bioreactor model

The bioreactor model describes removal of organic matter, nitrification, and denitrification. The bioreactor model is simulated with IAWQ model presented by Henze *et al.* (1987) with the following exceptions:

- S_I (inert soluble organic matter) and S_{ALK} (total alkalinity) are not included, since they are not needed in this study.
- The inert ($X_{I,IAWQ}$) and particulate ($X_{P,IAWQ}$) matter are combined into one variable since their different fractions are not interesting in this study. Hence let $X_I = X_{I,IAWQ} + X_{P,IAWQ}$.
- A term to describe the oxygen transfer has been added in the equation for the dissolved oxygen (S_O). It is $K_La(u)(S_{O,sat} - S_O)$, where K_La is the oxygen transfer function, u is the airflow rate, and $S_{O,sat}$ is the saturated dissolved oxygen concentration.

This is the same model as is implemented in *Simnon* (Elmqvist *et al.* 1986) by Wikström (1993), but is slightly modified for the use in *Regsim* (Gustafsson 1988). Another settler model is also implemented, see Section 2.3.4.

2.3.3 Differential equations and parameter values

The reaction rates for the states are in Table 2.6 are presented here.

$S_{NH}(t)$	soluble ammonium nitrogen
$S_{NO}(t)$	soluble nitrate nitrogen
$S_{ND}(t)$	soluble biodegradable organic nitrogen
$S_O(t)$	dissolved oxygen
$S_S(t)$	soluble substrate
$X_{B,A}(t)$	autotrophic biomass
$X_{B,H}(t)$	heterotrophic biomass
$X_{ND}(t)$	particulate biodegradable organic nitrogen
$X_S(t)$	slowly biodegradable substrate
$X_I(t)$	particulate matter & products

Table 2.6: States included in the model.

The states starting with an X are particulate and the ones with a S are soluble.

The default influent concentrations in the simulation model are given in Table 2.7.

State	S_S	X_I	X_S	$X_{B,H}$	$X_{B,A}$	S_O	S_{NO}	S_{NH}	S_{ND}	X_{ND}
[mg/l]	60	50	100	25	0	0	1	25	2	6

Table 2.7: Default influent concentrations in the simulation model

According to the IAWQ model, except for the oxygen transfer $K_L a(S_{O,sat} - S_O)$, the reaction rates for the states are:

$$
\begin{aligned}
\frac{dS_S}{dt} &= -\frac{1}{Y_H}\hat{\mu}_H\left(\frac{S_S}{K_S+S_S}\right)\left(\frac{S_O}{K_{O,H}+S_O}\right)X_{B,H} \\
&- \frac{1}{Y_H}\hat{\mu}_H\left(\frac{S_S}{K_S+S_S}\right)\left(\frac{K_{O,H}}{K_{O,H}+S_O}\right)\left(\frac{S_{NO}}{K_{NO}+S_{NO}}\right)\eta_g X_{B,H} \\
&+ k_h \frac{\frac{X_S}{X_{B,H}}}{K_X+\frac{X_S}{X_{B,H}}}\left(\left(\frac{S_O}{K_{O,H}+S_O}\right)+\eta_h\left(\frac{K_{O,H}}{K_{O,H}+S_O}\right)\left(\frac{S_{NO}}{K_{NO}+S_{NO}}\right)\right)X_{B,H} \\
\frac{dX_I}{dt} &= f_P(b_H X_{B,H} + b_A X_{B,A}) \\
\frac{dX_S}{dt} &= (1-f_P)(b_H X_{B,H} + b_A X_{B,A}) \\
&- k_h \frac{\frac{X_S}{X_{B,H}}}{K_X+\frac{X_S}{X_{B,H}}}\left(\left(\frac{S_O}{K_{O,H}+S_O}\right)+\eta_h\left(\frac{K_{O,H}}{K_{O,H}+S_O}\right)\left(\frac{S_{NO}}{K_{NO}+S_{NO}}\right)\right)X_{B,H} \\
\frac{dX_{B,H}}{dt} &= \hat{\mu}_H\left(\frac{S_S}{K_S+S_S}\right)\left(\frac{S_O}{K_{O,H}+S_O}\right)X_{B,H} \\
&+ \hat{\mu}_H\left(\frac{S_S}{K_S+S_S}\right)\left(\frac{K_{O,H}}{K_{O,H}+S_O}\right)\left(\frac{S_{NO}}{K_{NO}+S_{NO}}\right)\eta_g X_{B,H} - b_H X_{B,H} \\
\frac{dX_{B,A}}{dt} &= \hat{\mu}_A\left(\frac{S_{NH}}{K_{NH}+S_{NH}}\right)\left(\frac{S_O}{K_{O,A}+S_O}\right)X_{B,A} - b_A X_{B,A} \\
\frac{dS_O}{dt} &= -\frac{1-Y_H}{Y_H}\hat{\mu}_H\left(\frac{S_S}{K_S+S_S}\right)\left(\frac{S_O}{K_{O,H}+S_O}\right)X_{B,H} \\
&- \frac{4.57-Y_A}{Y_A}\hat{\mu}_A\left(\frac{S_{NH}}{K_{NH}+S_{NH}}\right)\left(\frac{S_O}{K_{O,A}+S_O}\right)X_{B,A} + K_L a(S_{O,sat}-S_O) \\
\frac{dS_{NO}}{dt} &= -\frac{1-Y_H}{2.86Y_H}\hat{\mu}_H\left(\frac{S_S}{K_S+S_S}\right)\left(\frac{K_{O,H}}{K_{O,H}+S_O}\right)\left(\frac{S_{NO}}{K_{NO}+S_{NO}}\right)\eta_g X_{B,H} \\
&+ \frac{1}{Y_A}\hat{\mu}_A\left(\frac{S_{NH}}{K_{NH}+S_{NH}}\right)\left(\frac{S_O}{K_{O,A}+S_O}\right)X_{B,A} \\
\frac{dS_{NH}}{dt} &= -i_{XB}\hat{\mu}_H\left(\frac{S_S}{K_S+S_S}\right)\left(\frac{S_O}{K_{O,H}+S_O}\right)X_{B,H} \\
&- i_{XB}\hat{\mu}_H\left(\frac{S_S}{K_S+S_S}\right)\left(\frac{K_{O,H}}{K_{O,H}+S_O}\right)\left(\frac{S_{NO}}{K_{NO}+S_{NO}}\right)\eta_g X_{B,H} \\
&- \left(i_{XB}+\frac{1}{Y_A}\right)\hat{\mu}_A\left(\frac{S_{NH}}{K_{NH}+S_{NH}}\right)\left(\frac{S_O}{K_{O,A}+S_O}\right)X_{B,A} + k_a S_{ND} X_{B,H} \\
\frac{dS_{ND}}{dt} &= -k_a S_{ND} X_{B,H}
\end{aligned}
$$

$$+ \quad \frac{X_{ND}}{X_S} k_h \frac{\frac{X_S}{X_{B,H}}}{K_X + \frac{X_S}{X_{B,H}}} \left((\frac{S_O}{K_{O,H} + S_O}) + \eta_h (\frac{K_{O,H}}{K_{O,H} + S_O})(\frac{S_{NO}}{K_{NO} + S_{NO}}) \right) X_{B,H}$$

$$\frac{dX_{ND}}{dt} = (i_{XB} - f_P i_{XP})(b_H X_{B,H} + b_A X_{B,A})$$

$$- \quad \frac{X_{ND}}{X_S} k_h \frac{\frac{X_S}{X_{B,H}}}{K_X + \frac{X_S}{X_{B,H}}} \left((\frac{S_O}{K_{O,H} + S_O}) + \eta_h (\frac{K_{O,H}}{K_{O,H} + S_O})(\frac{S_{NO}}{K_{NO} + S_{NO}}) \right) X_{B,H}$$

where the parameter values are given in Table 2.8, which are the default values reported in Henze *et al.* (1987) for a temperature of 20°C. Some of these parameters show little variation from wastewater to wastewater and may be considered as constants, but others have larger variations. The values given in Table 2.8 are considered typical for neutral pH and domestic wastewater, but many paramters are strongly influenced by environmental conditions, see Henze *et al.* (1987).

To obtain the complete differential equations for the different states, the previously given reaction rates have to be complemented with the terms for the mass balance:

$$D(t)Z_{in} - D(t)Z$$

where $Z_{in}(t)$ is the influent concentration, $Z(t)$ is the effluent concentration which is equal to the concentration in the zone if the zone is completely mixed, $D(t)$ is the dilution rate (flow/volume).

To give more understanding of the different differential equations which describes the reaction rates for the states, some comments for a couple of the equations are given (taken from Jeppsson (1996)).

- The change in heterotrophic biomass ($X_{B,H}$) depends on three processes: Aerobic growth (the term which is multiplied by S_O), anoxic growth (the term which is multiplied by S_{NO}), and decay.
- The change in autotrophic biomass ($X_{B,A}$) is similar to the change in $X_{B,H}$, but there is no growth in an anoxic environment.
- The soluble substrate (S_S) concentration is reduced by the growth of heterotrophic bacteria ($X_{B,H}$) and increased by hydrolysis.
- The ammonium concentration (S_{NH}) is affected by the growth of both $X_{B,H}$ and $X_{B,A}$, since ammonium is used as a nitrogen source in the cell mass. The nitrification process also reduce the ammonium concentration.

Symbol	Value	Explanation
Y_A	0.24	yield for autotrophic biomass
Y_H	0.67	yield for heterotrophic biomass
i_{XB}	0.086 g N(g COD)$^{-1}$	mass of nitrogen per mass of COD in biomass
i_{XP}	0.06 g N(g COD)$^{-1}$	mass of nitrogen per mass of COD in products from biomass in endogenous mass
f_P	0.08	fraction of biomass yielding particulate products
$\hat{\mu}_A$	0.8 day^{-1}	maximum specific growth rate for autotrophic biomass
$\hat{\mu}_H$	6 day^{-1}	maximum specific growth rate for heterotrophic biomass
K_S	20 g COD m^{-3}	half saturation coefficient for heterotrophic biomass
$K_{O,H}$	0.2 g O_2 m^{-3}	oxygen half saturation coefficient for heterotrophic biomass
K_{NO}	0.5 g NO_3-N m^{-3}	nitrate half saturation coefficient for denitrifying heterotrophic biomass
K_{NH}	1.0 g NH_3-N m^{-3}	ammonium half saturation coefficient for autotrophic biomass
$K_{O,A}$	0.4 g O_2 m^{-3}	oxygen half saturation coefficient for autotrophic biomass
b_A	0.2 day^{-1}	decay rate coefficient for autotrophic biomass.
b_H	0.62 day^{-1}	decay rate coefficient for heterotrophic biomass
η_g	0.8	correction factor for μ_H under anoxic conditions
η_h	0.4	correction factor for hydrolysis under anoxic conditions
k_a	0.08 m^3 COD (g day)$^{-1}$	ammonification rate
k_h	3.0 g COD (g COD day)$^{-1}$	maximum specific hydrolysis rate
K_X	0.03 g COD (g COD)$^{-1}$	half saturation coefficient for hydrolysis of slowly biodegradable substrate
K_La		oxygen transfer function, see Chapter 4
$S_{O,sat}$	10 mg/l	saturated oxygen concentration

Table 2.8: The parameter values for the IAWQ model at a 20°C.

- The nitrate concentration (S_{NO}) is increased by nitrification, and decreased by denitrification.

2.3.4 The settler model

The settler is an important part of the activated sludge process. It is used for two purposes: clarification and thickening. In a settler, particulate matter in the water from the bioreactor sink to the bottom of the settler (thickening), and clear water is produced (clarification) and removed in the top of the settler. The particulate matter at the bottom of the settler (the activated sludge) contains necessary microorganisms for the biological reactions. The sludge is recirculated to the bioreactor to maintain a desired solids level.

There exist many different settler models in the literature. Grijspeerdt *et al.* (1995) have, however, made a comparative study where they found that the model by Takács *et al.* (1991) gave the most reliable results.

Jeppsson (1996) points out that in the traditional layer models, the fluxes are defined by empirical reasoning and sometimes contain *ad hoc* assumptions. The solution will then depend on the number of layers and there is no guarantee that the model produces physically relevant solutions satisfying the continuity equation. Despite the important fact as Jeppsson (1996) points out, the model by Takács *et al.* (1991) will be used since it still provides a good description of the real behavior.

The settler model by Takács *et al.* (1991) is used with two extensions:

- Soluble matters are included, and described by the following model:

$$\frac{dS}{dt} = \frac{Q}{V}(S_{in} - S)$$

  where S represent any soluble state in Table 2.6.

- The composition of the suspended material is considered, and is hence not treated as a whole MLVSS (mixed liquor volatile suspended solids). That is, X_I, X_S, X_{BA}, X_{BH}, and X_{ND} are calculated in each layer. Example: X_I is calculated in the bottom layer according to

$$\frac{dX_{I,n}}{dt} = \frac{1}{h}\left(\frac{(Q_s + Q_w)}{A}(X_{I,n-1} - X_{I,n}) + \min(v_{s,n-1}X_{I,n-1}, v_{s,n}X_{I,n})\right)$$

The settler is modeled as a tank with several horizontal layers where each layer is assumed to be completely mixed, see Figure 2.4.

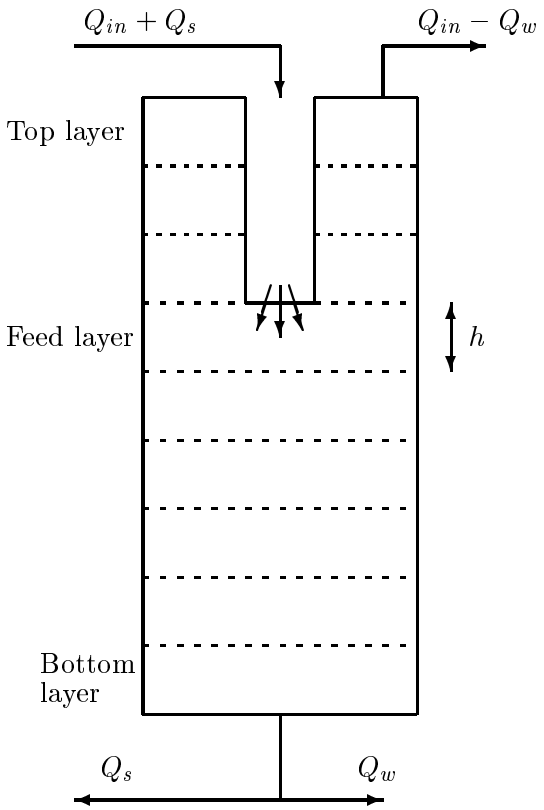

Figure 2.4: Layered settler model, where the different flows are defined in Figure 2.3.

The settler model is based on the solids mass balance around each layer. In Figure 2.5 this is shown across the settler layers. The solids flux is called J and depends on settling velocity v_s and sludge concentration X according to

$$J = v_s(X)X \tag{2.1}$$

The concentration in a layer is then found from

$$\frac{dX}{dt} = \frac{1}{h}\Delta J \tag{2.2}$$

where ΔJ is the difference in flux in the layer. Studying Figure 2.5 the difference in flux in each layer is obtained. Then using (2.2) the following equations for the sludge concentration where h is the height of each layer

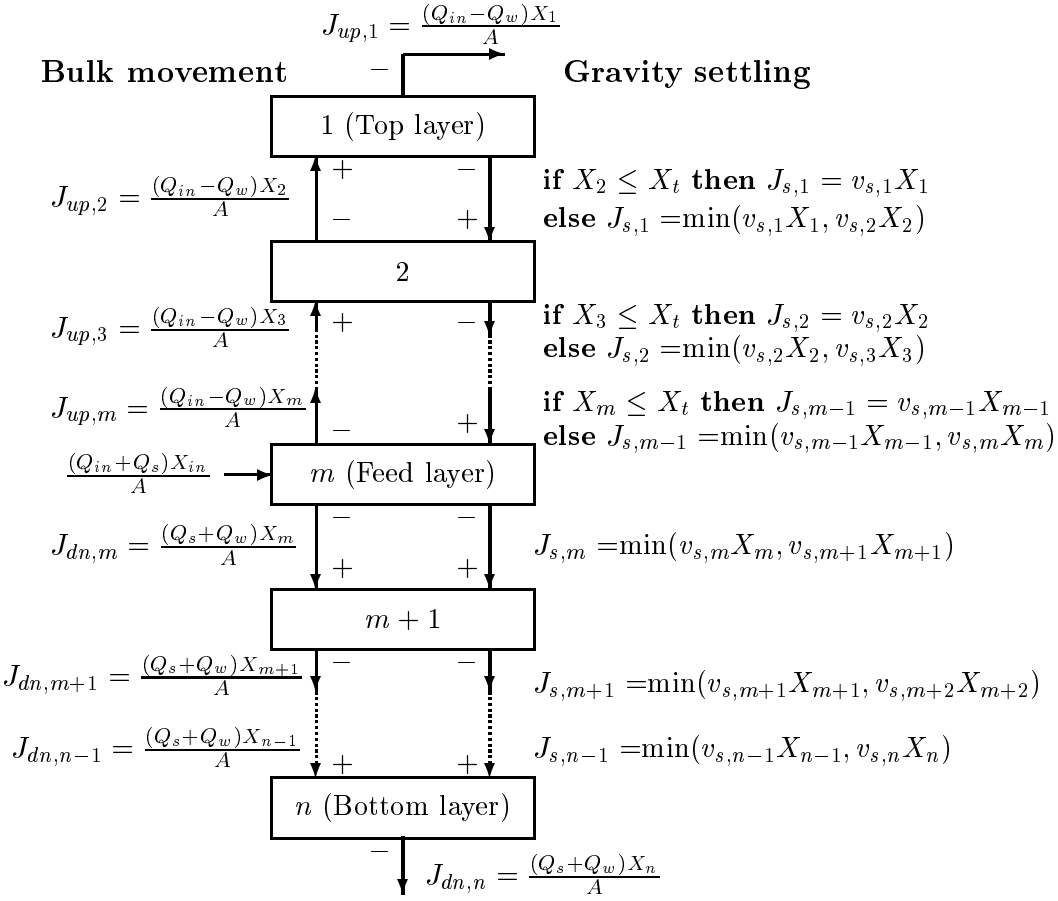

Figure 2.5: Solids balance across settler layers (Takács *et al.* 1991).

is found.

$$
\begin{aligned}
\frac{dX_1}{dt} &= \frac{1}{h}(J_{up,2} - J_{up,1} - J_{s,1}) \\
\frac{dX_i}{dt} &= \frac{1}{h}(J_{up,i+1} - J_{up,i} + J_{s,i-1} - J_{s,i}) \qquad 2 \leq i < m \\
\frac{dX_m}{dt} &= \frac{1}{h}(\frac{(Q_{in}+Q_s)X_{in}}{A} - J_{up,m} - J_{dn,m} + J_{s,m-1} - J_{s,m}) \\
\frac{dX_j}{dt} &= \frac{1}{h}(J_{dn,j-1} - J_{dn,j} + J_{s,j-1} - J_{s,j}) \qquad m+1 \leq j < n \\
\frac{dX_n}{dt} &= \frac{1}{h}(J_{dn,n-1} - J_{dn,n} + J_{s,n-1})
\end{aligned}
$$

The settling velocity from Takács *et al.* (1991) is given by

$$
\begin{aligned}
v_{s,i} &= v_0 e^{-r_h(X_i - X_{min})} - v_0 e^{-r_p(X_i - X_{min})} \qquad 1 \leq i \leq n \\
0 &\leq v_{s,i} \leq v_0'
\end{aligned}
$$

This gives a velocity profile as in Figure 2.6.

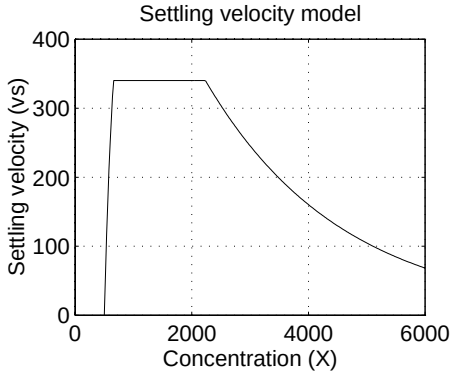

Figure 2.6: Settling velocity model.

The parameters in the settler model are chosen as in Table 2.9. The parameters in Table 2.9 which are connected with the settling velocity are chosen equal to the parameters for the pilot plant in Takács *et al.* (1991).

Remark: When referring to X this means $X = X_I + X_S + X_{BA} + X_{BH} + X_{ND}$ (=MLVSS).

2.3.5 Simulation tool

To simulate the previous described process a simulation program called *Regsim*, see Gustafsson (1988), has been used. The basic implementation of the computer code for the IAWQ model has been written by Wikström (1993) and Wikström (1994) for both *Simnon*, see Elmqvist *et al.* (1986) and *Simulink*, see MathWorks (1992). Minor changes of the computer code for the IAWQ model has been done to be able to run it in Regsim. The original simulation code has also been extended by some additional zones and various controllers. The main programming work of the settler model (for Simulink) has been done by Dr. Zhiguo Yuan at Department of Applied Mathematics, Biometrics and Process Control, University of Gent, Belgium. The basic reasons for using Regsim, instead of Simulink, in the simulations are that it is faster and it is easier to implement models and controllers than in Simulink.

2.3.6 Conclusions

The pilot plant has been a very fruitful tool in studying various aspects of the activated sludge process, ranging from innovative operating modes,

Symbol	Value	Explanation
v_0	712 m/d	maximum theoretical settling velocity.
v_0'	340 m/d	maximum practical settling velocity.
r_h	4.26 10^{-4} m^3/g	settling parameter associated with the hindered settling component of settling velocity equation.
r_p	5.0 10^{-3} m^3/g	settling parameter associated with the low concentration and slowly settling component of the suspension.
f_{ns}	5.0 10^{-4}	non-settleable fraction of the influent suspended solids.
A	0.55 m^2	surface area of clarifier.
X_{min}	$f_{ns}X_{in}$ g/m^3	minimum attainable suspended solids conc. in the effluent.
X_t	3000 g/m^3	threshold suspended solids concentration.
n	10	number of layers.
m	7	the feedlayer.
h	0.1 m	height of each layer.

Table 2.9: The parameters in the settler model.

microbiological studies to advanced control and estimation schemes. New methods have been easy and inexpensive to test. It is, however, important to observe that the operation of a pilot plant with an extensive instrumentation is quite demanding in terms of maintenance.

The results from the pilot plant studies have given important guidelines for full scale plant design and operation. One example is the seeding strategy which will be considered when the main wastewater treatment plant in Uppsala will be expanded. Also the developed control strategies show that an increased automation can lead to energy savings and reduced consumption of chemicals. Microbiological studies have given important insights for the choice of external carbon source.

The developed CSS has been an important part in the the operation of the pilot plant. Further, advanced control and estimation algorithms have been easy to implement.

The simulation model has been a very useful tool for evaluation of all the different controllers and control strategies. Much time and work have been saved by first doing simulations prior to practical tests in the pilot plant.

Chapter 3

Control of external carbon flow rate in a pre-denitrifying activated sludge process

Biological nitrogen removal in activated sludge processes is dependent on sufficient supplies of easily metabolized carbon compounds for the denitrifying bacterial population. An external carbon source can increase denitrification rates and compensate for deficiencies in the influent carbon/nitrogen ratio. This works, however, only if the denitrification process is carbon constrained. Possible carbon sources include methanol, ethanol, acetate, primary sludge and various industrial waste products. In this chapter some different controllers and control strategies for the external carbon source dosage in a pre-denitrifying activated sludge process are suggested.

It is important to control the flow rate of the external carbon source. A too low dosage will leave the denitrification process carbon constrained and the full capacity for nitrogen removal is not used. A too high carbon dosage is expensive, may cause carbon spill and increases the sludge production which affects the nitrification capacity, see Aspegren *et al.* (1992) and Hellström and Bosander (1990). Another problem with overdosing, discussed in Hallin and Pell (1996), is that the microorganisms may lose their capacity to use natural existing carbon sources.

When adding an external carbon source one should be aware that a very selected microbial system may be induced, and it may take weeks for

the microorganisms to adapt to the external carbon. It has been argued by Nyberg *et al.* (1993) and Andersson *et al.* (1995) that the flow rate of external carbon source should not be controlled automatically, due to the obtained sensitive microbial system, reliability problems with on-line sensors, and because the effluent standard of nitrate is based on average values. To sustain the adapted microbial system, which can metabolize external carbon, the external carbon flow rate should never be switched off. It is easy to design a controller which never give a carbon flow rate below a pre-specified minimum flow rate. Note also that it is possible to switch off some carbon sources for several days (e.g. ethanol) without losing denitrification capacity, see Hasselblad and Hallin (1996). Further, the reliability problems with the on-line sensors can be reduced by maintaining these frequently. It is also likely that on-line nitrate sensors will be more reliable in the future. According to e.g. Lynggaard-Jensen *et al.* (1996) reliable sensors already exist.

A constant flow rate of carbon is only advantageous when the influent variations of the carbon/nitrogen ratio are small. When the variations are large, a constant carbon dosage will be too low during some hours and too high during other periods. The average nitrate concentration will then not be reduced as much with a constant dosage as it would with a controlled dosage. In a typical plant the load often varies by a factor of 6 or more, see Van Impe *et al.* (1992). If external carbon is added in the last step of a wastewater treatment plant, it is very important to give a correct dosage, since there are no later steps in the plant where an excessive dosage can be degraded. An example is control of the nitrate concentration in a sand filter, see Hultman *et al.* (1994).

A reasonable control strategy for the carbon dosage is to keep the nitrate level in the anoxic zone (just before the aerobic zone in a pre-denitrifying plant) at a constant low level. That strategy has been discussed in Hellström and Bosander (1990). An approach where the controller design is based on the IAWQ model has been done by Yuan *et al.* (1996). Another strategy where the carbon dosage is based on presence or no presence of nitrate in the effluent has been suggested by Vanrolleghem *et al.* (1993). The carbon dosage has been controlled by considering the oxygen demand in Linde (1993). Brenner (1991) presented a simulation study with an external carbon source and found that the aerobic volume fraction and recirculation rate should be increased when carbon is added, but the aerobic volume fraction could be decreased if the biomass instead is increased. Londong (1992) has also controlled the nitrate level, but the interest was mainly focused on the recirculation rate instead of the carbon dosage. The recirculation rate has also been considered in Andersson *et al.* (1995). The

carbon dosage control in an alternating nitrification-denitrification process is different compared to the continuous activated sludge plant. In that process, the nitrate level is not used for control. Instead a model of the denitrification rate is estimated, which is then used to determine the carbon dosage, so that the denitrification is completed within the current operation cycle, see e.g. Isaacs *et al.* (1993).

The carbon dosage controllers presented here can all use feedforward from influent mass flow of Total Organic Carbon (TOC) and mass flow of nitrate in recirculated water. Instead of using feedforward from recirculated nitrate, influent ammonium may be used, but the recirculated nitrate more directly influences the nitrate level in the anoxic zone. Flow changes in the internal recirculation will also make that feedforward more unreliable, hence feedforward from the nitrate concentration is preferred.

The outline of the chapter is as follows. In Section 3.1 the model of the nitrate process is discussed. The differential equation for the nitrate concentration is studied further and an ARX approximation is presented. The control strategy is outlined in Section 3.2. Signals suitable for feedforward, and different types of controllers are also discussed. The following four different controllers are evaluated: a PID-controller with fixed parameters in Section 3.3, a model-based adaptive PID controller in Section 3.4, a direct adaptive controller in Section 3.5, and an indirect adaptive controller in Section 3.6. Some practical aspect for adaptive control are considered in Section 3.7. Simulations using the four different controllers are presented in Section 3.8. The direct adaptive controller is also evaluated at the pilot plant; the experiment is presented in Section 3.9. Finally, conclusions are given in Section 3.10.

3.1 Modeling the nitrate process

To design a controller with high performance, some kind of process model is usually needed. The IAWQ model is rather complex, since it involves 13 nonlinear coupled differential equations, and several more or less unknown parameters, which are difficult to estimate on-line, see e.g., Jeppsson (1993). The complete IAWQ model is not suitable for controller design, parts of it may, however, be useful. This has been used in the design by Yuan *et al.* (1996) together with the assumption that there are only small variations in the parameters of the IAWQ. To illustrate some of the problems in the dynamics of the nitrate concentration, its differential equation based on the IAWQ model is studied. Assuming zero dissolved oxygen concentration, which is reasonable for an anoxic zone, the following differential equation

for the soluble nitrate $S_{NO}(t)$ is obtained.

$$\frac{dS_{NO}}{dt} = D_{in}S_{NOin} - D_{out}S_{NO} - \frac{1-Y_H}{2.86Y_H}\hat{\mu}_H\left(\frac{S_S}{K_S+S_S}\right)\left(\frac{S_{NO}}{K_{NO}+S_{NO}}\right)\eta_g X_{B,H} \tag{3.1}$$

where

$S_{NO}(t)$	is the soluble nitrate
$S_{NOin}(t)$	is the influent soluble nitrate
$S_S(t)$	is the soluble substrate. The external carbon is included in S_S
$X_{B,H}(t)$	is the heterotrophic biomass
$D_{in}(t)$	is the influent dilution rate (flow/volume)
$D_{out}(t)$	is the effluent dilution rate
Y_H	is the yield for heterotrophic biomass = 0.67
$\hat{\mu}_H$	is the maximum specific growth rate for heterotrophic biomass = 0.25 (=6/24) h^{-1} at 20^o C
K_S	is the half saturation coefficient for heterotrophic biomass = 20 g COD m^{-3}
K_{NO}	is the nitrate half saturation coefficient for denitrifying heterotrophic biomass = 0.5 g NO_3- N m^{-3}
η_g	is the correction factor for μ_H under anoxic conditions = 0.8

The parameters in (3.1) are not constant. They vary with, e.g., wastewater composition, temperature, and heterotrophic biomass which usually is not measurable. The values given above are the default values at 20^o C in Henze *et al.* (1987).

As can be seen in equation (3.1) the gain of the process varies with the S_S, S_{NO}, and $X_{B,H}$. It also depends on time varying parameters as K_S and K_{NO}, and flow rates. Since there are so many uncertainties in the process, we prefer to estimate an ARX model, which is easier to estimate than all the model parameters in (3.1). An ARX model is also easier to use in a controller design. An approach to estimate a model where some of the physical knowlegde in (3.1) is used will, however, also be utilized. By using real-time estimation (estimation for time-varying systems) the linear model can be adapted to time-varying operating points. If the parameter variations in the estimated linear model are large it may be suitable to use an adaptive controller, but if the estimated model is almost time-invariant it is better to use a non-adaptive controller.

The following ARX model will be used to model the nitrate process

$$A(q^{-1})y(t) = B(q^{-1})q^{-k}u(t) + D_1(q^{-1})q^{-d_1}w_1(t) + D_2(q^{-1})q^{-d_2}w_2(t) + n(t) \tag{3.2}$$

This model is used for design of the indirect adaptive controller as well as the PID controller. In the direct adaptive controller, the controller parameters are estimated directly, but the underlying model is assumed to be of the same type as (3.2). In (3.2), k, d_1, and d_2 are time delays, and $A(q^{-1})$, $B(q^{-1})$, $D_1(q^{-1})$, and $D_2(q^{-1})$ are polynomials in the backward shift operator q^{-1}. The nitrate concentration in the anoxic zone is denoted by $y(t)$, and the external carbon flow rate by $u(t)$. The signal $w_1(t)$ is influent mass flow of the TOC (or soluble substrate) and $w_2(t)$ is recirculated mass flow of nitrate ($Q_{int}S_{NO,int} + Q_{sl}S_{NO,sl}$), where the index $_{int}$ stands for internal recirculation flow, and $_{sl}$ for sludge return flow. A drifting disturbance $n(t)$ has also been included to model unmeasurable load disturbances. It is given by

$$n(t) = \frac{1}{\Delta(q^{-1})}e(t) \tag{3.3}$$

where $e(t)$ is zero mean white noise and $\Delta(q^{-1}) = 1 - q^{-1}$.

The carbon/nitrogen (w_1/w_2) ratio can be used instead of the two separate signals if the flow rates (Q_{int}, Q_{sl} and Q_{in}) are constant, see Lindberg (1995). This is advantageous since less parameters then have to be estimated. Simulations have also shown that separating the carbon and nitrate signals does not improve the model (and control). For the direct adaptive controller the performance has even improved when the w_1/w_2 ratio was used in the simulations. Note though, that this is only valid when the flow rates are constant. If the flow rates are time-varying it could perhaps be expected that the ratio between the mass flow rates would work equally well, but is does not. This may depend on that the changes in flow rates have large impact of the time constants in the process.

An alternative to the unstructured estimation of the parameters in the ARX model is to use some of the model structure in (3.1). The following approximation

$$\begin{aligned}\frac{S_{NO}(t+1) - S_{NO}(t)}{h} = &\frac{Q_{int}(t)S_{NOint}(t) + Q_{sl}(t)S_{NOsl}(t)}{V} \\ &- \frac{Q_{in}(t) + Q_{int}(t) + Q_{sl}(t)}{V}S_{NO}(t) \\ &- K_{ext}(t)\frac{S_{S,ext}}{V}u(t) - K_{SS}(t)\frac{Q_{in}(t)}{V}TOC_{in}(t)\end{aligned} \tag{3.4}$$

could be reasonable when the influent nitrate concentration (to the bioreactor) is low, the nitrate concentration ($S_{NO}(t)$) is controlled at a constant value, and the substrate concentration ($S_S(t)$) does not vary too much. If S_{NO} and S_S are constant the nonlinearities related to these concentrations in (3.1) do not have to be considered. In (3.4) only the parameters $K_{ext}(t)$

and $K_{SS}(t)$ have to be estimated. The other parameters are either known or measured. The parameter $S_{S,ext}$ is the substrate concentration of the external carbon source which is added with the flow rate $u(t)$, and $TOC_{in}(t)$ is influent total organic carbon.

3.2 Control strategy

The main control objective is to control the external carbon dosage so that the nitrate concentration in the anoxic zone is kept at constant and low level. Feedforward is used from the influent TOC and the internally recirculated nitrate concentration, see Figure 3.1. Feedforward is useful when there is a possibility to measure disturbances before or at the same time as they affect the process. A measurable disturbance can then be rejected simultaneously as it enters the process. In some cases it can be completely rejected, i.e. its effect is not detected at the output. A non-measurable disturbance can not be rejected until the disturbance is detected on the output, at this time the controller can start to compensate by feedback.

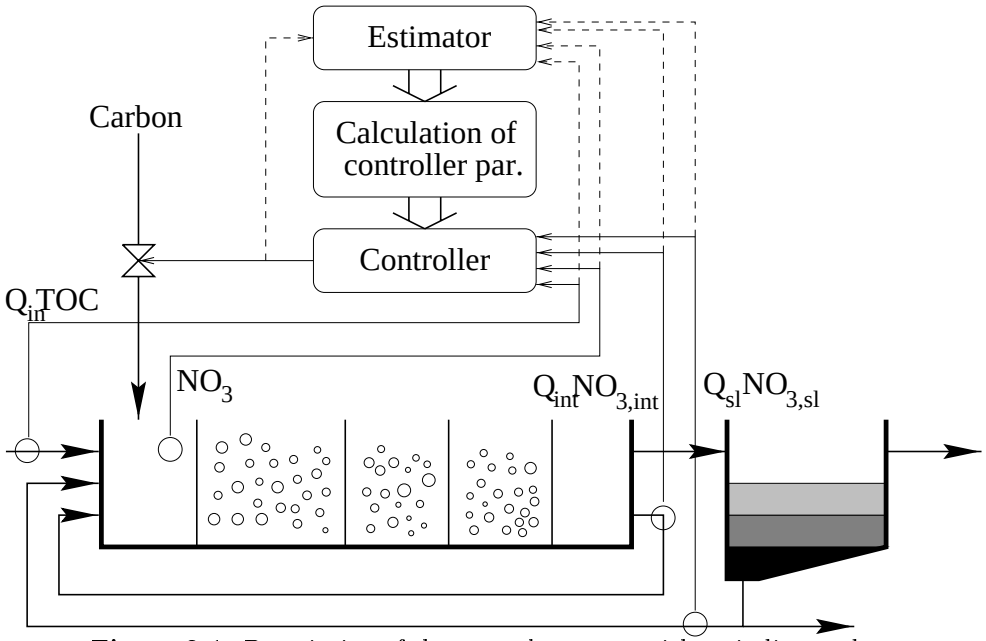

Figure 3.1: Description of the control strategy with an indirect adaptive controller. The nitrate concentration in the anoxic zone of the activated sludge process is controlled by the external carbon flow rate. To better reject disturbances, feedforward from the mass flow of influent TOC and mass flow of recirculated nitrate is included.

In the controller design, it is assumed that the measured TOC level in the influent water is correlated with the influent soluble substrate (S_S). The external carbon source is also treated as soluble substrate. Note that this assumption makes the model valid only for a process where the sludge has adapted to the external carbon source. When using a carbon source where the microorganisms need long time to adapt, e.g. methanol, it is probably necessary to extend the IAWQ model with an extra substrate state to be able to model the slow adaptation phase of the external carbon to the process. This is a topic for future research.

When no sensors for feedforward measurements are available, one could consider the possibility to model the daily variations in influent concentrations and use the predicted disturbances in a feedforward controller. This type of feedforward from a knowledge database is also a topic for future research.

Four different carbon dosage controllers will be presented. A PID-controller, a direct adaptive, an indirect adaptive controller, and a model-based adaptive PID controller are studied. In the direct adaptive controller the controller parameters are estimated directly, the block *calculation of controller parameters* in Figure 3.1 is hence not needed for this controller. The indirect adaptive controller is based on a recursively estimated process model, which is used for controller design, see Figure 3.1. The four controllers are evaluated on the simulation model of the activated sludge process which was presented in Section 2.3. The direct adaptive controller has also been tested at the pilot plant at Kungsängsverket, Uppsala.

The configuration of the activated sludge process and sensor placement used in all simulations is shown in Figure 3.1. The activated sludge process hence consists of five zones and a settler. The external carbon is added in the first zone, which is anoxic. The nitrate concentration is also measured in that zone. The following three zones are aerobic, where the dissolved oxygen is controlled at a certain prespecified level. The last zone is non-aerated, in order to reduce the dissolved oxygen (DO) concentration in the recirculated water to improve denitrification. In all the recirculated water (internal rec. and sludge rec.) the nitrate concentration is measured. The nitrate concentration in the influent water is so small that it is no point to use feedforward from that flow. The TOC concentration in the influent wastewater is, however, measured. If the mass flow variations of nitrate in the recirculated sludge are small, feedforward from this variation does not give any performance improvement, and this sensor is hence not necessary.

3.3 A PID-controller

The PID controller is probably the most widely used controller. Well tuned it can give reasonable performance for many processes. It is, however, difficult to tune a PID controller manually, especially if the process dynamics is slow. There exist different ways to tune a PID controller. For example, the classical Ziegler-Nichols rules can be used, but they give fairly low damping. Often, a better choice is auto-tuning which is based on the relay method, see Åström and Hägglund (1984). Auto-tuning works as follows, the controller is disconnected and replaced by a relay, which induces a limit cycle oscillation. The period and the amplitude of the oscillations give a point on the Nyquist curve, which is used to choose the controller parameters. This method of tuning can also be applied to other controller structures than PID-controllers.

Another way to obtain the controller parameters is to identify a model of the system using a system identification algorithm, for example, a least squares method or a prediction error method, see e.g. Söderström and Stoica (1989). The identified model is then used to derive the controller parameters for a desired closed loop response. A problem with this method is that the closed loop poles can only be chosen arbitrary for a limited set of model structures.

An approach to derive the feedforward is to estimate a model of the process and use it together with the feedback (the PID-controller) to derive an optimal (in LQ sense) feedforward. Another simpler approach is just to apply a static gain from the feedforward measurements. In the simulations in Section 3.8 such an approach is used.

The PID-controller with feedforward has the following structure.

$$\begin{aligned}
\Delta u(t) &= K[(e(t)-e(t-1)) + \frac{h}{T_i}e(t) - \frac{T_D}{h}(y_f(t)-2y_f(t-1)+y_f(t-2))] \\
&+ K_{f1}\Delta w_1(t) + K_{f2}\Delta w_2(t) \qquad (3.5)\\
u(t) &= u(t-1)+\Delta u(t) \qquad (3.6)\\
e(t) &= y_{ref}(t)-y(t) \qquad (3.7)\\
y_f(t) &= py_f(t-1)+(1-p)y(t) \qquad (3.8)
\end{aligned}$$

where K, T_i T_D are the usual PID parameters, h is the sampling interval, K_{f1} and K_{f2} are the feedforward gains, $y_f(t)$ is $y(t)$ low-pass filtered and $\Delta w_1(t)$ and $\Delta w_2(t)$ are the differentiated ($\Delta w_1(t) = w_1(t) - w_1(t-1)$) feedforward signals, i.e. influent mass flow of the TOC, and recirculated mass flow of nitrate. In (3.5), the derivative of the error $e(t)$ is not used, instead only the derivative of $y_f(t)$ is used to avoid large changes in the

control signal when there is a step change in the reference signal $y_{ref}(t)$. Using the low-pass filtered output $y_f(t)$ also make the controller less noise sensitive. The low-pass filter parameter p should be chosen faster than the dominant dynamics.

Here a least squares method is used to identify a model with the following structure

$$(1 + aq^{-1})y(t) = bu(t-1) + d_1 w_1(t-1) + d_2 w_2(t-1) \tag{3.9}$$

A PI controller is then sufficient to place the poles arbitrary. Applying the PI controller to the model (3.9) and placing the closed loop poles at p (a double pole) gives the controller parameters

$$K = -\frac{a + p^2}{b} \tag{3.10}$$

$$T_i = \frac{bKh}{1 - a - bK - 2p} \tag{3.11}$$

For a more detailed description of how the PI parameters were obtained, see also Section 5.2.1. The feedforward parameters are not so difficult to chose by hand. Here they are chosen to $K_{f1} = 0.05$ and $K_{f2} = 0.7$. Alternatively (3.9) could be used to determine the feedforward gains. The deadbeat feedforward is given by

$$K_{f1} = -\frac{d_1}{b} \qquad K_{f2} = -\frac{d_2}{b} \tag{3.12}$$

If a deadbeat feedforward is not desirable one could scale the feedforward gain to make it smaller.

Remark: The model structure (3.9) is not the same as used in the indirect adaptive controller, where the $B(q^{-1})$ polynomial has two coefficients. The different structure depends on that a PID controller can not place the closed loop poles arbitrary for such a model. Using only one coefficient in the $B(q^{-1})$ polynomial works also reasonable well when the controller operates in the range where it was tuned.

3.4 A model-based adaptive PI controller

Using the model (3.4), i.e.

$$\frac{S_{NO}(t+1) - S_{NO}(t)}{h} = \frac{Q_{int}(t)S_{NOint}(t) + Q_{sl}(t)S_{NOsl}(t)}{V}$$
$$-DS_{NO}(t) - K_{ext}(t)\frac{S_{S,ext}}{V}u(t) - K_{SS}(t)\frac{Q_{in}(t)}{V}TOC_{in}(t) \tag{3.13}$$

a model-based adaptive PI controller can be designed. In (3.13), $D = (Q_{int} + Q_{sl} + Q_{in})/V$, $u(t)$ is the external carbon flow rate, and K_{ext} and K_{SS} are recursively estimated parameters. Using (3.13) the parameters for the PI controller are given by

$$K = \frac{p^2 + Dh - 1}{hK_{ext}\frac{S_{S,ext}}{V}} \tag{3.14}$$

$$T_i = \frac{h}{\frac{2p-2+Dh}{hK_{ext}\frac{S_{S,ext}}{V}K} - 1} \tag{3.15}$$

for a double pole at $z = p$.

The parameters K_{ext} and K_{SS} can be estimated with, for example, a recursive least squares method. A predictor for an RLS method is given by

$$\hat{y}(t+1|t) = y(t) + h[\frac{Q_{int}(t)S_{NOint}(t) + Q_{sl}(t)S_{NOsl}(t)}{V} - Dy(t) - \varphi^T(t)\theta(t)]$$

$$\varphi^T(t) = [\ \frac{S_{S,ext}u(t)}{V} \quad \frac{TOC_{in}(t)Q_{in}(t)}{V}\ ] \tag{3.16}$$

$$\theta^T(t) = [\ K_{ext}(t) \quad K_{SS}(t)\ ] \tag{3.17}$$

The parameter estimates are then updated by using (3.57).

3.4.1 Extention of the model-based adaptive PI controller

Instead of using (3.13), more physical knowledge could be included by considering the S_S concentration and take the nonlinear monod relation for S_S into account. The following models are then used

$$\frac{S_{NO}(t+1) - S_{NO}(t)}{h} = \frac{Q_{int}(t)S_{NOint}(t) + Q_{sl}(t)S_{NOsl}(t)}{V} - DS_{NO}(t) - K(t)\frac{S_S(t)}{K_S + S_S(t)} \tag{3.18}$$

$$\frac{S_S(t+1) - S_S(t)}{h} = \frac{Q_{in}(t)S_{S,in}(t)}{V} - DS_S(t) + \frac{S_{S,ext}}{V}u(t) \tag{3.19}$$

where $K(t)$ is estimated and it is assumed that K_S is known and S_S is measurable. Since the S_S concentration needs to be measured in the anoxic zone, a possibility to reduce the number of sensors could be to move the TOC sensor, which measure in the influent water, to the anoxic zone. The feedforward of S_S is then lost, but since the S_S concentration is measured in the anoxic zone instead, not so much performace is lost anyway. If TOC is measured instead of S_S, the parameter K_S probably have to be updated.

The PI controller designed here uses the temporal control signal $x(t)$, instead of the flow rate $u(t)$. The signal $x(t)$ is defined by

$$x(t) = \frac{S_S(t)}{K_S + S_S(t)} \tag{3.20}$$

The flow rate $u(t)$ is determined from (3.19) and becomes

$$u(t) = \frac{V}{S_{S,ext}} \left[\frac{S_S(t+1) - S_S(t)}{h} - \frac{Q_{in}(t) S_{S,in}(t)}{V} + D S_S(t) \right] \tag{3.21}$$

where S_S is measured, $S_{S,in}$ is either measured or neglected if no feedforward sensor is available, and $S_S(t+1)$ is the future desired S_S concentration, which is computed from $x(t)$ in (3.20) as

$$S_S(t+1) = \frac{x(t)}{1 - x(t)} K_S \tag{3.22}$$

The controller design is similar to the adaptive model-based PI controller, K and T_i are given by (3.14) and (3.15) with the difference K_{ext} is replaced by $K(t)$.

The same estimator as for the adaptive model-based PI controller is used, except that $\varphi(t)$ in (3.16) is changed to $\varphi(t) = x(t)$ and $\theta(t)$ in (3.17) is changed to $\theta(t) = K(t)$.

3.5 A direct adaptive controller

A direct adaptive control strategy is appealing since the controller parameters are estimated directly from data, which among other things makes the controller easy to implement. The resulting controller has also often shown to be robust, see e.g. Åström and Wittenmark (1989). Problems may, however, arise if the true system is non-minimum phase, and a minimum-variance or generalized minimum-variance controller is used, see e.g. Åström and Wittenmark (1989). There exist other controllers that overcome this problem, for example, the MUSMAR (MultiStep Multivariable Adaptive Regulator) method, see Mosca *et al.* (1984).

Here, only the *generalized minimum-variance* (GMV) controller, introduced by Clarke and Gawthrop (1975) is considered. The reason is that the GMV controller works well in both the simulation studies and in the pilot plant, and that it is also less complex.

The generalized minimum-variance (or Clarke-Gawthrop) controller is derived from input output data Y_t, and designed to minimize the k-step ahead sliding horizon criterion

$$J = \frac{1}{2}\mathrm{E}[y^2(t+k) + \rho(\Delta u(t))^2 | Y_t] \tag{3.23}$$

In the derivation of the controller, $y(t+k)$ is found from the k step predictor of (3.2). The predictor is determined by using the identity

$$C = \Delta A\frac{R}{B} + q^{-k}S \tag{3.24}$$

The controller is then found by setting the derivative of J with respect to Δu to zero. This gives the control law which minimizes (3.23) for the system (3.2). Implemented as an integrating controller with feedforward the control law becomes

$$(R(q^{-1})+\frac{\rho}{r_0}C(q^{-1}))\Delta u(t) = -S(q^{-1})y(t)-Q_1(q^{-1})\Delta w_1(t)-Q_2(q^{-1})\Delta w_2(t) \tag{3.25}$$

$$u(t) = u(t-1) + \Delta u(t) \tag{3.26}$$

where $R(q^{-1})$, $S(q^{-1})$, $Q_1(q^{-1})$ and $Q_2(q^{-1})$ are the controller polynomials, and $C(q^{-1})$ could be considered as an observer polynomial and used as a used parameter. The derivation of (3.25) is well known, see e.g. Åström and Wittenmark (1990), but for completeness a derivation is given in Appendix A. In the derivation, the prediction horizon k in the controller is set equal to the time delay in the process k. The time delays of the measurable disturbances are also set equal to k.

To make the controller robust to low-frequency modeling errors and to make it possible to remove drifting disturbances and disturbances of random step type, integration (Δu) has been included. By deriving the incremental control signal (Δu) in (3.25) and then calculate $u(t)$ as in (3.26), integration is obtained.

The closed-loop poles of the generalized minimum-variance controller are given by the roots of

$$(B + \frac{\rho}{r_o}A\Delta)C = 0 \tag{3.27}$$

The poles will hence move between the roots of B and the roots of $A\Delta$ depending on ρ. This explains why there are problems when the open-loop system is unstable and/or non-minimum phase. It can be difficult (or impossible) to find a suitable input penalty ρ if the open loop system is of this type.

The generalized minimum-variance controller is usually easy to tune. If the observer polynomial, the degree of the controller polynomials and the sampling rate are fixed, then there is only one tuning parameter (ρ). The tuning parameter ρ trades off output variance to input variance. A small ρ makes the controller faster but also more sensitive to noise and modeling errors. The best choice of ρ has to be tried out. Usually ρ has to be changed by a factor of ten to get a significant change in the controlled system.

When determining the degree of the controller polynomials, it is a good idea to try to keep the number of estimated parameters as low as possible. It is often reasonable to start with few controller parameters and then increase the number of estimated parameters until the controller gives acceptable performance. If the number of estimated parameters is too high the parameters may start to drift, although the real process has not changed.

Here the following controller structure has been selected

$$(r_0 + \frac{\rho}{r_0})\Delta u(t) = t_0 y_{ref}(t) - (s_0 + s_1 q^{-1}) y(t) + q_1 \Delta w_1(t) + q_2 \Delta w_2(t) \quad (3.28)$$

where the controller parameters r_0, s_0, s_1, q_1 and q_2 are estimated. The $C(q^{-1})$ polynomial in (3.25) is, as seen in (3.28), chosen to

$$C(q^{-1}) = 1 \quad (3.29)$$

which is the same choice as in Clarke and Gawthrop (1975).

The reference signal $y_{ref}(t)$ is also included in (3.28). To get the static gain equal to 1, $y_{ref}(t)$ is multiplied by t_0, which should be chosen to

$$t_0 = S(1) = 1 \quad (3.30)$$

For a further explanation of the choice of T-polynomial see Section 3.7.6.

3.5.1 Parameter estimation

The controller parameters in (3.28) can be estimated directly by, for example, a RLS algorithm, see e.g. Ljung and Söderström (1983).

In Appendix A, a predictor for the system (3.2) is derived. The predictor, for directly estimating the controller parameters in (3.25) is given by

$$\begin{aligned} \hat{y}(t+k|t) &= R\frac{\Delta u(t)}{A_o} + S\frac{y(t)}{A_o} + Q_1\frac{\Delta w_1(t)}{A_o} + Q_2\frac{\Delta w_2(t)}{A_o} \\ &= R\Delta u_f(t) + S y_f(t) + Q_1 \Delta w_{f1}(t) + Q_2 \Delta w_{f2}(t) \end{aligned} \quad (3.31)$$

where the filtered signals $u_f(t)$, $y_f(t)$ and $\Delta u_f(t)$ are defined by

$$u_f(t) = \frac{1}{A_o}u(t) \qquad \Delta w_{f1}(t) = \frac{1}{A_o}\Delta w_1(t) \tag{3.32}$$

$$y_f(t) = \frac{1}{A_o}y(t) \qquad \Delta w_{f2}(t) = \frac{1}{A_o}\Delta w_2(t) \tag{3.33}$$

In the derivation in Appendix A, A_o should be equal to the true C polynomial, where $C(q^{-1})$ is the color of the unmeasurable noise. It is, however, not necessary that $A_o = C$ to obtain consistent estimates because the controller parameters surprisingly converg to consistent estimates also when the A_o-polynomial differs from the true one, see Åström and Wittenmark (1989). This is not valid for all adaptive controllers, but it applies for the adaptive (generalized) minimum-variance controller. The A_o polynomial can hence be considered as a filter chosen by the designer. To improve the estimates one should choose $1/A_o$ as a low-pass filter, to remove undesired high frequency dynamics. Here A_o is chosen as

$$A_o = 1 - 0.7q^{-1} \tag{3.34}$$

The predictor in (3.31) can be rewritten to

$$\hat{y}(t|t-1) = \varphi^T(t-1)\theta \tag{3.35}$$

where

$$\varphi^T(t-1) = [\Delta u_f(t-1) \quad y_f(t-1) \quad y_f(t-2) \quad \Delta w_{f1}(t-1) \quad \Delta w_{f2}(t-1)]$$

$$\theta = [r_0 \quad s_0 \quad s_1 \quad q_1 \quad q_2]^T$$

The parameter vector θ is updated by

$$\hat{\theta}(t) = \hat{\theta}(t-1) + P(t)\varphi(t)\varepsilon(t) \tag{3.36}$$

In (3.36), $\hat{\theta}(t)$ denotes the estimated parameter vector, $P(t)$ is the covariance matrix which is updated recursively, see (3.51) – (3.56) for a numerically sound way of calculating $P(t)$, $\varphi(t)$ is the regression vector and

$$\varepsilon(t) = y(t) - \hat{y}(t|t-1) \tag{3.37}$$

is the prediction error.

Numerical problems may occur when estimating many parameters. One way to obtain better estimates is to fix r_0, for example, at $r_0 = -1$. This works when b_0 is in the approximate range $-3 < b_0 < -0.3$. Another possibility is to estimate r_0 only during an initial period of high excitation and keep it fixed after the high excitation. Note that setting r_0 to a fixed value does not constrain the controller to time invariant systems, since the other controller parameters may still be able to compensate for a fixed r_0.

3.6 An indirect adaptive controller

In an *indirect* adaptive controller, the controller design is based on a recursively estimated model of the system. The advantage of this design method compared to a direct adaptive controller, is that a much wider range of controller design methods can be applied. Non-minimum phase systems, for example, will not cause any particular problems. Some possible drawbacks with the indirect method are that it requires more computations than a direct adaptive controller, and that the derived controller also may be less robust than a direct adaptive controller, see Åström and Wittenmark (1989).

The model (3.2) used for controller design can, for example, be estimated by a recursive least squares method, see e.g. Söderström and Stoica (1989).

The selected controller is an LQ controller with feedforward. A frequently used criterion in LQ design, see e.g. Åström and Wittenmark (1990), is the following

$$J = \lim_{N\to\infty} \frac{1}{N} \sum_{t=0}^{N} [\mathrm{E}y^2(t) + \rho \mathrm{E}u^2(t)] \tag{3.38}$$

In Lindberg (1995), an extended version was derived where it is possible to partition the control signal into two separate parts, one which originates from the feedforward and one from the feedback. These parts can then be penalized differently. In Appendix B the control algorithm is given. The criterion for this LQ controller is

$$J = \lim_{N\to\infty} \frac{1}{N} \sum_{t=0}^{N} \mathrm{E}y^2(t) + \mathrm{E}(\sqrt{\rho_e}\Delta u_e(t) + \sqrt{\rho_v}\Delta u_v(t))^2 \tag{3.39}$$

where u_e is the control signal which originates from the unmeasurable disturbance and u_v is the control signal which is computed from the measurable disturbance.

The advantage of using separate penalties is that slow (robust) feedback can be used in combination with fast feedforward which rejects the measurable disturbances quickly. The controller structure which minimizes (3.39) and where a reference signal also is included is

$$R(q^{-1})\Delta u(t) = T(q^{-1})y_{ref}(t) - S(q^{-1})y(t) - \frac{Q_1(q^{-1})}{P_1(q^{-1})}w_1(t) - \frac{Q_2(q^{-1})}{P_2(q^{-1})}w_2(t) \tag{3.40}$$

A block diagram of the control strategy in (3.40) is presented in Figure 3.2, but with only one measurable disturbance. The LQ controller uses all available information to find the optimal controller. If a model of the measureable disturbance exist ($w(t) = \frac{G}{H}v(t)$) this information is used to improve the control.

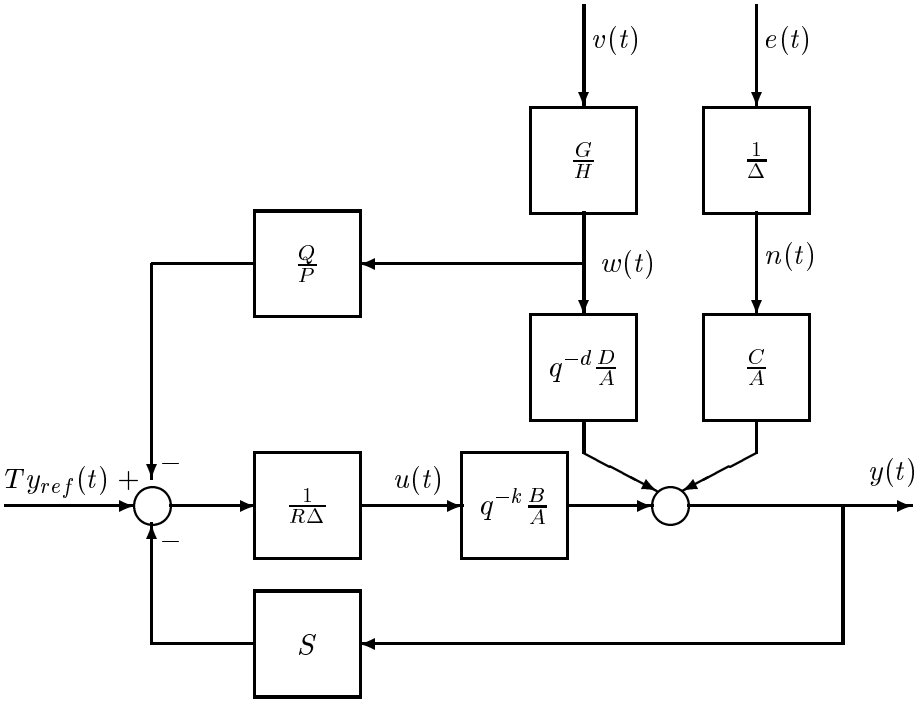

Figure 3.2: The process with the controller. Feedforward is utilized from the measurable disturbance $w(t)$, which is modelled as filtered white noise ($\frac{G}{H}v(t)$).

Remark: The *optimal LQ feedforward* depends on the feedback, but the *optimal LQ feedback* does not depend on the feedforward, see Kwakernaak and Sivan (1972).

3.6.1 Identification of the process

The following ARX model is identified

$$\begin{aligned} A(q^{-1})y(t) &= B(q^{-1})q^{-k}u(t) + D_1(q^{-1})q^{-d_1}w_1(t) \\ &+ D_2(q^{-1})q^{-d_2}w_2(t) + n(t) \end{aligned} \tag{3.41}$$

which is the same model as (3.2). The G and H polynomials, see Figure 3.2, are used to model the measurable disturbance and are not estimated. Instead $G/H = 1/\Delta$ is set to a random walk process in the controller design. Knowledge of G/H would make it possible to better reject measurable disturbances. The C polynomial, see Figure 3.2, can be considered as a observer polynomial and be used as a design parameter.

To determine the model structure, data was generated by exciting the carbon flow rate in the simulated activated sludge process with a PRBS (Pseudo Random Binary Sequence) control signal in 30 hours. The mean values of the signals were removed before use in the identification. The degrees of the polynomials could be chosen by Akaike's information criterion, see Akaike (1981), which penalizes high-order models. Here the degrees of the polynomials were chosen as low as possible, but still with a reasonable fit between the simulated output of the identified model and the "real" output. The selected structure is

$$(1 + aq^{-1})y(t) = (b_1 + b_2q^{-1})q^{-1}u(t) + d_1q^{-1}w_1(t) + d_2q^{-1}w_2(t) \quad (3.42)$$

The predictor in the algorithm for estimating the parameters in (3.42) can be written as

$$\hat{y}(t|t-1) = \varphi^T(t-1)\theta \quad (3.43)$$

where

$$\begin{aligned} \varphi(t-1) &= [-y_f(t-1) \quad u_f(t-1) \quad u_f(t-2) \quad w_{f1}(t-1) \quad w_{f2}(t-1)]^T \\ \theta &= [a \quad b_1 \quad b_2 \quad d_1 \quad d_2]^T \end{aligned}$$

and

$$\begin{aligned} y_f(t) &= F(q^{-1})y(t) \qquad u_f(t) = F(q^{-1})u(t) \\ w_{f1}(t) &= F(q^{-1})w_1(t) \qquad w_{f2}(t) = F(q^{-1})w_2(t) \end{aligned}$$

In (3.44) the signals in the regressor vector $\varphi(t)$ have been filtered by $F(q^{-1})$, because the mean value of the signals are not zero. To identify a system with non-zero mean, one can, for example, remove the average value of the signals before they are used in the estimator to obtain a correct model. In recursive methods it is, difficult to remove average values. An approach which works for signals with non-zero mean and drifting signals, is to differentiate the signals i.e. multiply the regressor with Δ. As differentiated signals are quite noisy, it is a good idea to low-pass filter the differentiated signals. Low-pass filtering also remove undesired high frequency dynamics. A suitable filter is then

$$F(q^{-1}) = \frac{\Delta(1-f)}{(z-f)} \quad (3.44)$$

Such a filter has been used in the simulations in Section 3.8 with the filter pole in $f = 0.7$. Another possible filter suggested in Åström and Wittenmark (1989) is

$$F(q^{-1}) = \frac{\Delta(1-f)^2}{(z-f)^2} \tag{3.45}$$

where f also is a filter pole, chosen by the designer. It could, however, be difficult to choose the pole for the low pass filter. A too slow filter removes interesting dynamics and a too fast filter does not remove the undesired high frequency dynamics. An appropriate filter choice for the regressor, has been given by Åström and Nilsson (1994), which is especially suitable for estimation in closed-loop and is related to the sensitivity function of the closed-loop system. Their suggested filter is

$$F(q^{-1}) = \frac{\Delta R}{A\Delta R + z^{-k}BS} \tag{3.46}$$

where $A(q^{-1})$ and $B(q^{-1})$ are the system polynomials, and $R(q^{-1})$ and $S(q^{-1})$ are the controller polynomials.

3.6.2 Observer polynomials

The previous LQ design implies pole placement at the zeros of

$$\alpha(q^{-1}) = \beta_e(q^{-1})C(q^{-1}) \tag{3.47}$$

where $\beta_e(q^{-1})$ is defined by the spectral factorization

$$r_e\beta_e\beta_e^* = BB^* + \rho_e A\Delta\Delta^* A^* \tag{3.48}$$

The C-polynomial is usually not known, and may be hard to estimate. To control the sensitivity to measurement noise in the feedback loop, the $C(q^{-1})$ polynomial could be selected freely and considered as an observer polynomial, see Sternad (1991). An appropriate choice of $C(q^{-1})$ will reduce the high frequency gain of the controller. Preferably C is chosen so that $1/C$ becomes a low pass filter. The best value depends, for example, on the actual noise level and sampling period.

The G polynomial, which is included in the model of the measurable disturbance $w(t) = \frac{G}{H}v(t)$, may be considered as a design variable in the same way as the C polynomial. Hence, when the feedforward measurements are corrupted by noise it may be advantageous to select $1/G$ as a low-pass filter.

There exists an optimal solution when measurement noise affects the feedforward measurements, see Sternad (1989). The idea is to use a spectral factorization which gradually "switches off" the feedforward when the variance of the measurement noise increases. A very similar effect can be obtained by increasing the penalty ρ_v.

3.6.3 Calculation of the controller

From (3.42) we have a system with the following parameters

$$A = 1 + aq^{-1} \quad B = b_1 + b_2 q^{-1} \quad D = d_0 \quad k = 1 \quad d = 1$$

The procedure for deriving the feedforward compensation is identical for the two different measurable disturbances, because D_1 and D_2 are assumed to have the same structure. For simplicity, a case with only one measurable disturbance is studied.

Since no model of the measurable disturbances are assumed, a random walk may be an appropriate choice.

$$G = 1 \quad H = \Delta \quad C = 1 + cq^{-1}$$

The C polynomial is considered as a user parameter where $1/C$ is chosen as a low-pass filter. The choice of C is discussed in Section 3.6.2.

The degrees of the controller polynomials are given in Appendix B.1.1

$$\begin{array}{lll} R = 1 + r_1 q^{-1} & S = s_0 + s_1 q^{-1} & P = G\beta_v \\ Q = \Delta Q_1 & Q_1 = k_0 + k_1 q^{-1} + k_2 q^{-2} & L = l_0 + l_1 q^{-1} \end{array}$$

Note that as $H = \Delta$, (B.23) then have to be used instead of (B.15). The L-polynomial is not a controller polynomial. It is only an auxiliary polynomial.

Solving the spectral factorization (3.48) gives the coefficients in $\beta_e = 1 + \beta_{e1} q^{-1} + \beta_{e2} q^{-2}$. Then the feedback polynomials R and S are found by using equation (B.11), which gives

$$\begin{aligned} 1 \quad &+ \quad q^{-1}(r_1 - 1 + a + b_1 s_0) + q^{-2}(-r_1 + a r_1 - a + b_1 s_1 + b_2 s_0) \\ &+ \quad q^{-3}(b_2 s_1 - a r_1) \equiv 1 + q^{-1}(c + \beta_{e1}) + q^{-2}(\beta_{e1} c + \beta_{e2}) + \beta_{e2} c q^{-3} \end{aligned}$$

Considering the terms with equal powers in q^{-1} gives a linear system of equations:

$$\begin{bmatrix} 1 & b_1 & 0 \\ a-1 & b_2 & b_1 \\ -a & 0 & b_2 \end{bmatrix} \begin{bmatrix} r_1 \\ s_0 \\ s_1 \end{bmatrix} = \begin{bmatrix} 1 - a + c + \beta_{e1} \\ a + c\beta_{e1} + \beta_{e2} \\ c\beta_{e2} \end{bmatrix}$$

The feedforward filter denominator P is determined from (B.13) i.e.

$$P = G\beta_v \tag{3.49}$$

and the feedforward numerator Q is obtained by solving (B.23), since $w(t)$ is a drifting disturbance. Entering the polynomials into (B.23) gives

$$\begin{aligned}
- \quad & q^{-2}d_0g_0\rho_v s_1 + q^{-1}d_0g_0(b_1r_1 + \rho_v(s_1 - s_0 - as_1)) \\
+ \quad & d_0g_0(b_1 + r_1b_2 + \rho_v(s_0 + as_1 - as_0)) + qd_0g_0(\rho_v as_0 + b_2) \\
= \quad & q^{-2}(r_vk_2 + l_0\alpha_3) + q^{-1}(r_vk_1 + r_v\beta_{v1}k_2 + l_0\alpha_2 + l_1\alpha_3) + r_vk_0 \\
+ \quad & r_v\beta_{v1}k_1 + r_v\beta_{v2}k_2 + l_0\alpha_1 + l_1\alpha_2 + q(r_v\beta_{v1}k_0 + r_v\beta_{v2}k_1 + l_0 + l_1\alpha_1) \\
+ \quad & q^2(r_v\beta_{v2}k_0 + l_1)
\end{aligned}$$

which in matrix form can be written as

$$\begin{bmatrix} 0 & 0 & r_v & \alpha_3 & 0 \\ 0 & r_v & r_v\beta_{v1} & \alpha_2 & \alpha_3 \\ r_v & r_v\beta_{v1} & r_v\beta_{v2} & \alpha_1 & \alpha_2 \\ r_v\beta_{v1} & r_v\beta_{v2} & 0 & 1 & \alpha_1 \\ r_v\beta_{v2} & 0 & 0 & 0 & 1 \end{bmatrix} \begin{bmatrix} k_0 \\ k_1 \\ k_2 \\ l_0 \\ l_1 \end{bmatrix} = \begin{bmatrix} -d_0g_0\rho_v s_1 \\ d_0g_0(b_1r_1 + \rho_v(s_1 - s_0 - as_1)) \\ d_0g_0(b_1 + r_1b_2 + \rho_v(s_0 + as_1 - as_0)) \\ d_0g_0(\rho_v as_0 + b_2) \\ 0 \end{bmatrix}$$

where r_v and $\beta_v = 1 + \beta_{v1}q^{-1} + \beta_{v2}q^{-2}$ are found by solving the spectral factorization (B.14).

For spectral factorizations of order two, like in this example, there exists an explicit solution, see Peterka (1984). The solution is based on the equation for the roots of a third order polynomial, and is presented below. Set

$$m_2q^2 + m_1q + m_0 + m_1q^{-1} + m_2q^{-2} = r(1 + \beta_1q^{-1} + \beta_2q^{-2})(1 + \beta_1q + \beta_2q^2) \tag{3.50}$$

and define

$$\lambda = \frac{m_0}{2} - m_2 + \sqrt{(\frac{m_0}{2} + m_2)^2 - m_1^2}$$

then

$$\begin{aligned}
r &= \frac{\lambda + \sqrt{\lambda^2 - 4m_2^2}}{2} \\
\beta_1 &= \frac{m_1}{r + m_2} \\
\beta_2 &= \frac{m_2}{r}
\end{aligned}$$

Spectral factorizations of orders higher than two have to be solved by numerical methods, for which there exist efficient methods, see e.g. Ježek and Kučera (1985).

Remark: When deriving the control signal, one may instead of multiplying Q_1 with Δ and then obtaining $(Q_1\Delta)w(t) = Qw(t)$, differentiate $w(t)$ and then let Q_1 operate on $\Delta w(t)$.

3.7 Practical aspects for the adaptive controllers

Some important problems in adaptive control and their (possible) solutions will considered in this section.

3.7.1 Potter's square root algorithm

When updating the parameters in a recursive algorithm, the covariance matrix $P(t)$ is used. To avoid numerical problems with accumulating rounding errors and which leads to $P(t)$ becoming indefinite, Potter's square root algorithm can be used, see e.g. Ljung and Söderström (1983).

Define the matrix $S(t)$ through

$$P(t) = S(t)S^T(t) \tag{3.51}$$

and update $S(t)$ instead of $P(t)$ as

$$\begin{aligned} f(t) &= S^T(t-1)\varphi(t) && (3.52)\\ \beta(t) &= \lambda + f^T(t)f(t) && (3.53)\\ \alpha(t) &= \frac{1}{\beta(t) + \sqrt{\beta(t)\lambda}} && (3.54)\\ L(t) &= S(t-1)f(t) && (3.55)\\ S(t) &= \frac{S(t-1) - \alpha(t)L(t)f^T(t)}{\sqrt{\lambda}} && (3.56) \end{aligned}$$

The parameter estimates are then updated as

$$\hat{\theta}(t) = \hat{\theta}(t-1) + L(t)\frac{\varepsilon(t)}{\beta(t)} \tag{3.57}$$

Note that there will be less computations in (3.57) if $\varepsilon(t)$ is divided by $\beta(t)$ before it is multiplied by $L(t)$.

If Potter's algorithm is not used, the diagonal elements of $P(t)$ could be checked instead. The matrix $P(t)$ should always be positive definite, which means that all diagonal elements of $P(t)$ always must be larger than zero. If they are not, $P(t)$ can be set to an identity matrix times a small constant. Note that positive diagonal elements does not guarantee that $P(t)$ is positive definite, but this test is at least better than no checking at all.

3.7.2 Choice of initial covariance matrix and initial regressor

The initial covariance matrix $P(0)$ should reflect the uncertainty of the parameter vector. Usually the uncertainty is large and $P(0)$ could be chosen as $P(0) = \sigma^2 I$, where σ is a large value which in is related to the variance of the elements in the φ vector, and the parameter vector is set to $\hat{\theta}(0) = 0$. Note that the regressor $\varphi(t)$ has to be filled with "real signal values" before the estimation algorithm can be started. Otherwise the parameters take huge steps in wrong directions, and it may then be hard or impossible for the parameters to recover to reasonable values.

It is also a good idea to disconnect the controller and replace the control signal with a PRBS signal, for example, and then only run the estimator during the first 30-50 samples. This gives the system a high excitation and the parameters can better converge. Note that this is only possible if the open loop system is stable.

3.7.3 The forgetting factor λ

The forgetting factor λ should reflect the parameter variations in the real process. To determine λ one could use the relation for the memory length, which is approximately equal to $2/(1-\lambda)$. A value of λ between 0.95 and 0.998 is often suitable. When there is little noise and few parameters are estimated a smaller λ can be selected. In the simulations $\lambda = 0.95$ was used.

3.7.4 Estimator windup

A common problem when using a forgetting factor $\lambda < 1$ is estimator windup, which makes the covariance matrix $P(t)$ grow exponentially during periods with low excitation. An example of estimator windup is shown in Figure 3.3. It is the indirect adaptive controller with feedforward, applied to control the nitrate concentration. Note that the scale in Figure 3.3 for the trace of the covariance matrix is logarithmic. As seen, the trace of $P(t)$ grows exponentially, during low excitation, and when the system is excited again the estimated parameters take a too large step. The system controlled by this controller (not shown) has very bad performance.

There exist different methods to avoid estimator windup. One feasible strategy to reduce the problem, which is used here, is a combination of the algorithm suggested in Ahlén and Sternad (1988) and Åström and

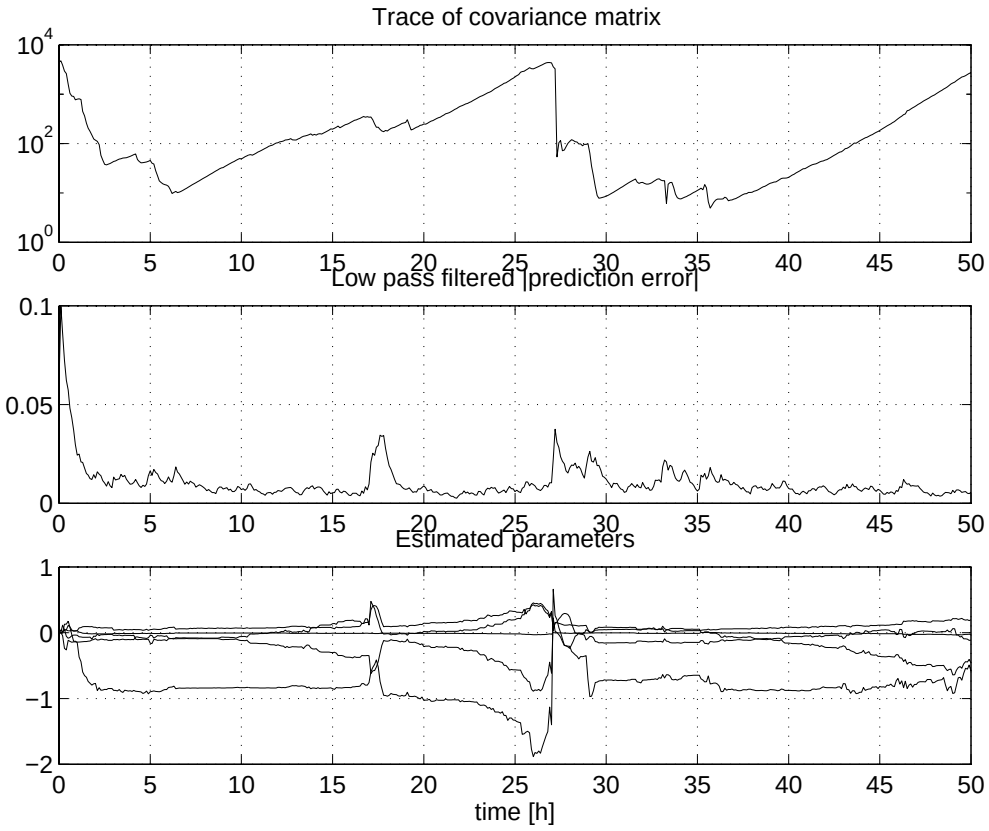

Figure 3.3: Illustration of estimator windup.

Wittenmark (1989). This strategy is as follows:

- Low-pass filter the absolute value of the prediction error i.e.

$$m(t) = 0.8m(t-1) + 0.2|\varepsilon(t)| \tag{3.58}$$

- IF $m(t) > \delta$ THEN update $\hat{\theta}(t)$ ELSE $\hat{\theta}(t) = \hat{\theta}(t-1)$
- IF $m(t) > \delta$ AND trace$(P(t)) <$, THEN update $P(t)$ ELSE $P(t) = P(t-1)$

The adaptation is hence switched off when the absolute value of the prediction error $|\varepsilon(t)|$ is small. It is switched on again when it is larger than δ. To prevent the $P(t)$ to grow too much, its trace is also checked. If the trace of $P(t)$ is too large it is not updated, even if the prediction error is large.

The boundaries δ and , in the algorithm have to be tested out for best performance. δ should be chosen so that $m(t)$ most of the time is smaller than δ, and , can be chosen to a rather large value, for example, trace$(P(0))$ or a bit smaller.

This method to avoid estimator windup is applied to the same process and controller as in Figure 3.3. The result is given in Figure 3.4. Comparing the result with previous one in Figure 3.3 we note that the covariance matrix stays small and the estimated parameters have much smoother movements. The low-pass filtered prediction error also stays smaller.

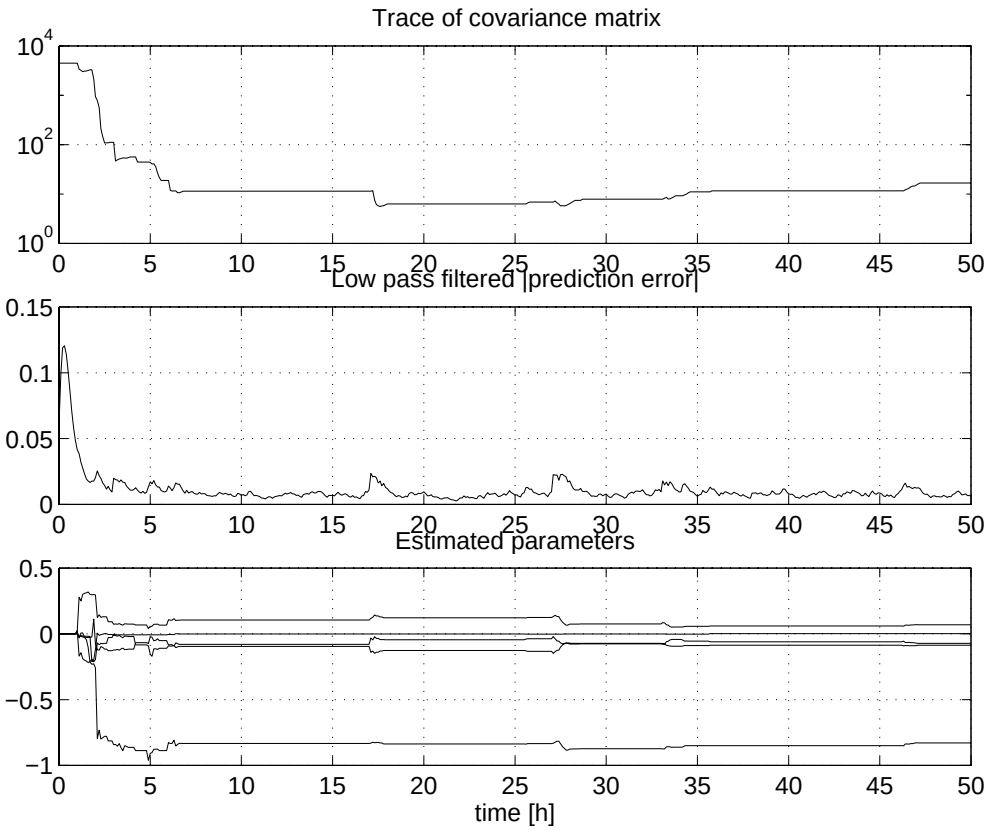

Figure 3.4: Illustration of *no* estimator windup. The same simulation as in Figure 3.3 is used, except for that the algorithm in Section 3.7.4 is applied to avoid windup.

3.7.5 Scaling the regressors

If the estimated parameters differs much in size, e.g. more than a factor 10, then the signal in the regressor can be scaled. This improves the numerical properties and the estimates, see also Åström and Wittenmark (1989).

3.7.6 Including the reference signal

The direct adaptive controller is extended with a reference signal $y_{ref}(t)$ in the following way

$$(R(q^{-1}) + \frac{\rho}{r_0}C(q^{-1}))\Delta u(t) = T(q^{-1})y_{ref}(t) - S(q^{-1})y(t) - Q(q^{-1})\Delta w(t) \tag{3.59}$$

and the indirect adaptive controller in this way

$$R(q^{-1})\Delta u(t) = T(q^{-1})y_{ref}(t) - S(q^{-1})y(t) - \frac{Q(q^{-1})}{P(q^{-1})}w(t) \tag{3.60}$$

The $T(q^{-1})$ polynomial filters the reference signal and may be chosen to

$$T(q^{-1}) = mC(q^{-1}) \tag{3.61}$$

where m is a constant which is selected to obtain the static gain equal to one. This is obtained by choosing

$$m = \frac{\beta_e(1)}{B(1)} = \frac{S(1)}{C(1)} \tag{3.62}$$

where β_e is defined in the spectral factorization (3.48). This choice of m is found by deriving the closed loop system from $y_{ref}(t)$ to $y(t)$, which is

$$y(t) = \frac{q^{-k}BT}{AR\Delta + q^{-k}BS}y_{ref}(t) \tag{3.63}$$

and by using $AR\Delta + q^{-k}BS = \beta_e C$, together with $\Delta(1) = 0$.

For the direct controller, the identity (3.24) can be used to determine the closed loop denominator $AR\Delta + q^{-k}BS$, which then becomes BC. Hence, if $C(q^{-1}) = 1$ then $T = S(1) = C(1) = 1$. It may, however, happen that $S(1) \neq 1$. It is then better to use $T = S(1)$, because this makes the static gain more safer equal to one.

3.7.7 A servo filter

If a faster servo response than provided by (3.61) is desired, there exist two possibilities. One option is to decrease the feedback penalty ρ_e. Alternatively, a servo filter can be included. The servo filter is often to prefer, since decreasing ρ_e will make the controller more sensitive to measurement noise.

The servo filter in (3.61) cancelles the observer poles. The poles placed in the zeros of β_e are, however, not cancelled. This can be obtained by replacing the $T(q^{-1})$ polynomial in (3.61) by the following rational transfer function

$$\frac{T(q^{-1})\beta_e(q^{-1})N(1)}{\beta_e(1)N(q^{-1})} \tag{3.64}$$

where $T(q^{-1})$ is defined in (3.61), and $\beta_e(q^{-1})$ contains the closed loop poles which are not included in $C(q^{-1})$. The polynomial $\beta_e(q^{-1})$ is canceled by the servo filter, and replaced by the new (faster) dynamic, given by $N(q^{-1})$ which is chosen by the user. The factors $\beta_e(1)$ and $N(1)$ are included to obtain unit static gain of the transfer function from the reference signal to the output. The $N(q^{-1})$ polynomial may e.g. be chosen as a second order polynomial with well damped complex conjugated roots.

Note that high pass filtering of the reference signal may require a large control signal, which may not be possible to achieve in a real plant. The performance robustness may also decrease with an increasing high pass filtering.

Remark: It is not necessary to cancel the complete β_e polynomial. Alternatively only parts of β_e could be canceled.

3.7.8 Choice of sampling rate

In a real system it is not always possible to select the sampling rate. If it is possible to choose it is suitable to sample around 10 times during a rise time of the closed-loop system, see also Åström and Wittenmark (1990).

3.8 Simulations

The previously outlined controllers are here evaluated in a simulation study. The aim of the control is to keep the nitrate concentration as close as possible to a desired set-point (here 1mg/l) by adding an external carbon source.

3.8.1 Simulation setup for the activated sludge process

In all simulations, the true process is simulated by the model presented in Chapter 2.3 with the following exceptions:

- *Measurement noise*: Zero mean white noise with standard deviation 0.1 is added to the nitrate measurements.
- *Flows and concentrations*: The flows and concentrations presented in Figure 3.5 are used, all other flows and concentrations are the default ones in Section 2.3.

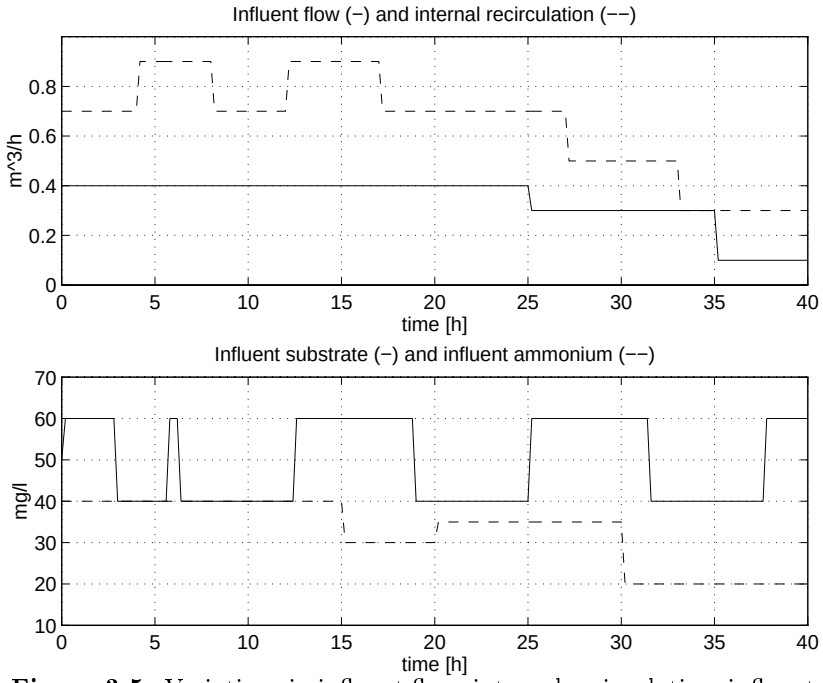

Figure 3.5: Variations in influent flow, internal recirculation, influent soluble substrate and influent ammonium during the simulation.

3.8.2 PI control

A PI-controller with feedforward is used here to control the nitrate level in the anoxic zone. The PI controller is tuned based on pole placement, using an estimated linear process model

$$(1 + aq^{-1})y(t) = bu(t-1) \tag{3.65}$$

The parameters (a and b) are only estimated during the first 7 hours. The parameters could be continuously estimated like in the indirect adaptive controller, but they are not. Instead it is illustrated how a well tuned controller at one operating point works at many operating points. The feedforward gains are chosen by manual tuning. The calculation of the PI parameters was outlined in Section 3.3.

A simulation using the PI controller is presented in Figure 3.6. The simulation indicates that a PI controller with feedforward can control the carbon dosage well at many operating points, but at some operating points the controlled system becomes rather oscillative. It should, however, be

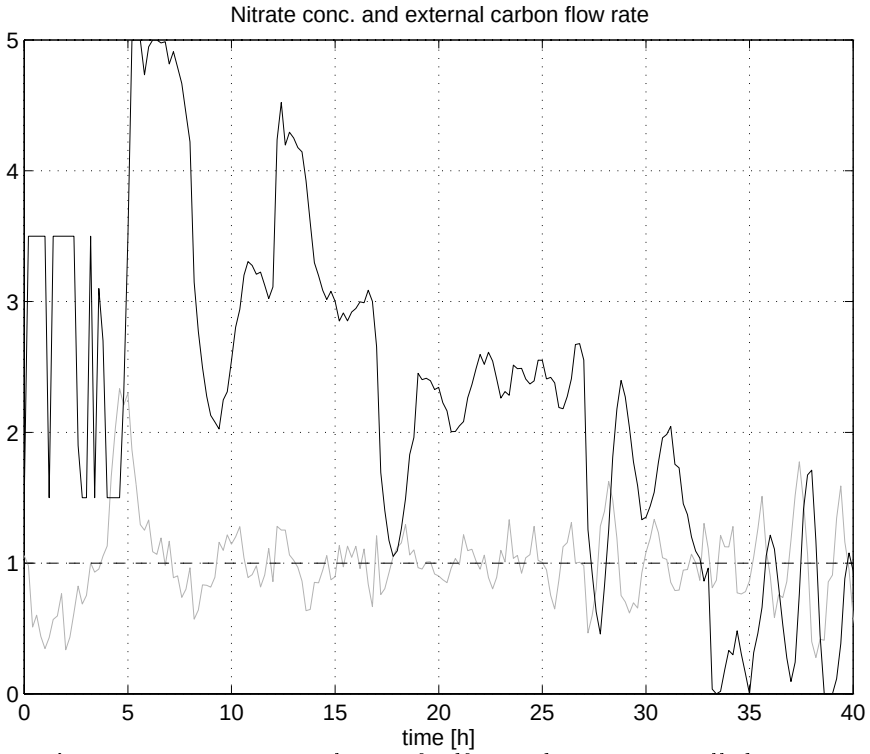

Figure 3.6: PID-control with feedforward. The controlled nitrate concentration in the anoxic zone (grey line), the set-point (dashed) and the corresponding external carbon flow rate (black line) are shown.

mentioned that it is possible to find a tuning which works reasonably well at all operating points in this simulation. In a real process there are, however, more parameters which vary, than what have been changed here. Several tunings may hence be necessary when, for example, temperature and biomass change to make the PI controller work reasonably well. For

an adaptive controller this is not necessary.

3.8.3 Direct adaptive control

A generalized minimum-variance controller will now be used to control the activated sludge process. The process is not controlled during the first 5 hours. Instead a PRBS control signal is used to excite the process to give a better estimated model. The controller parameter r_0 is not estimated it is fixed. The forgetting factor is chosen to $\lambda = 0.95$ and the penalty is chosen to $\rho = 2000$. The initial parameter is $\theta(0) = [\ -1 \quad 0 \quad 0 \quad 0 \quad 0\ ]^T$ and initial covariance matrix is $P(0) = S(0)S^T(0) = 90^2 I$, except for the P(1,1) element which is set to zero to make r_0 fixed. The control signal u is here divided by 1000 (the flow is in the unit m^3/h instead of litre/h) because the r_0 parameter will then have about the same size as the other estimated parameters. The result of the simulation with the direct adaptive

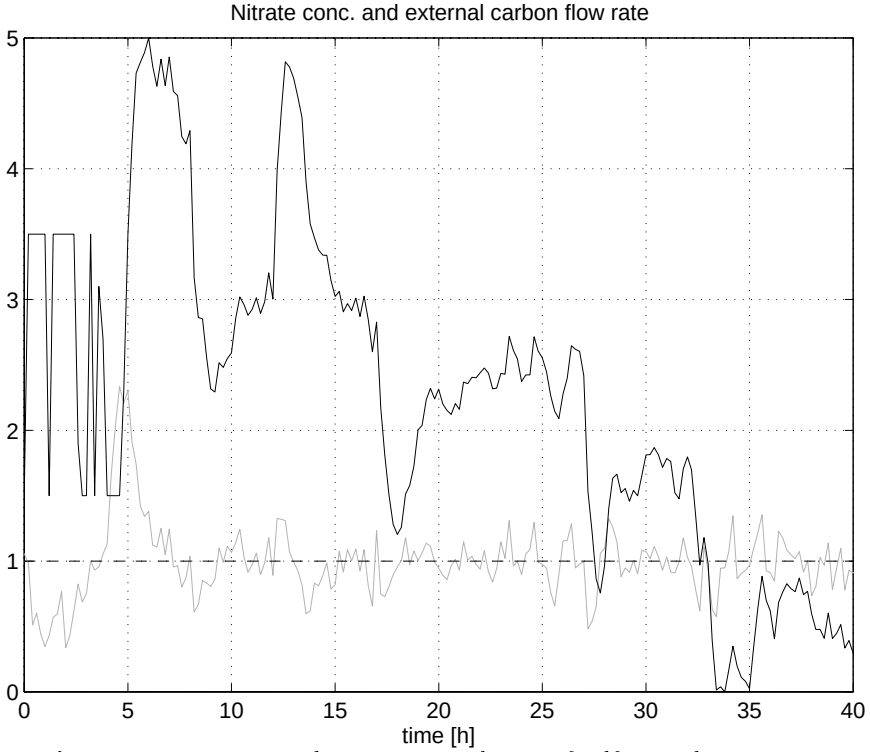

Figure 3.7: Direct adaptive control with feedforward. The controlled nitrate concentration in the anoxic zone (grey line), the set-point (dashed) and the corresponding external carbon flow rate (black line) are shown.

controller is illustrated in Figure 3.7. From the simulations it is seen that the controller manages to maintain the nitrate concentration quite well despite the disturbances.

3.8.4 Indirect adaptive control

Next, the indirect adaptive controller presented in Section 3.6 is evaluated. In the controller design the C-polynomial is chosen to $C(q^{-1}) = 1 - 0.9q^{-1}$, and the two penalties are chosen to $\rho_e = 0.05$ and $\rho_v = 0.01$. The forgetting factor is set to $\lambda = 0.95$. The initial parameter is $\theta(0) = 10^{-3}[\ 1 \quad 1 \quad 1 \quad 1 \quad 1\ ]^T$ and initial covariance matrix is $P(0) = 30^2 I$. The ideas in Section 3.7 to improve the estimation are applied.

In the simulation shown in Figure 3.8 it is seen that this type of controller also works very well.

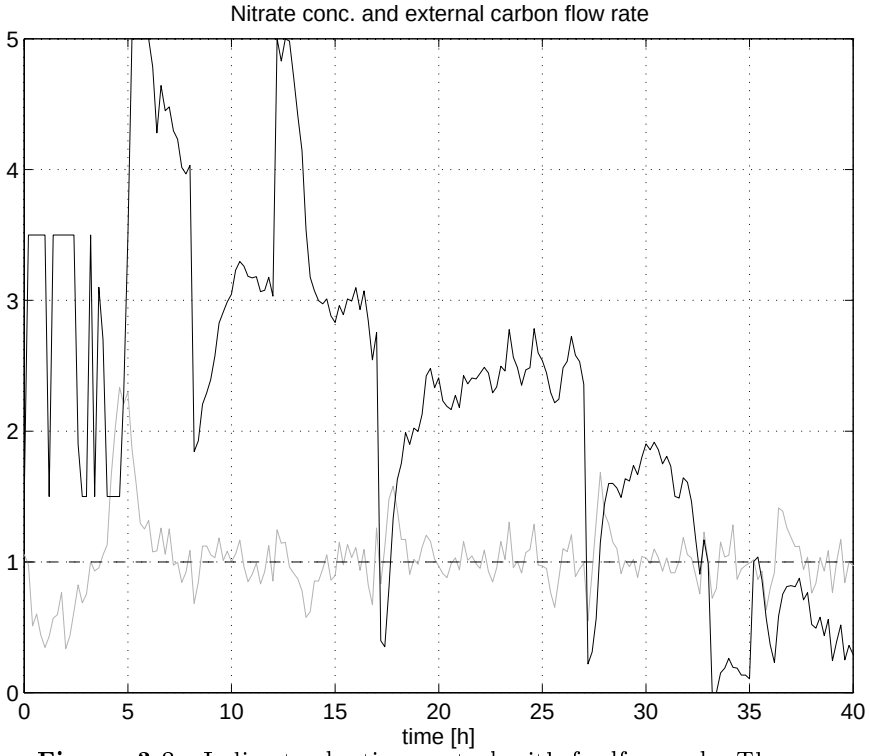

Figure 3.8: Indirect adaptive control with feedforward. The controlled nitrate concentration in the anoxic zone (grey line), the setpoint (dashed) and the corresponding external carbon flow rate (black line) are shown.

3.8.5 Model-based adaptive PI control

This controller uses physical information of the process which reduce the number of parameters to be estimated. The physical knowledge is used in the controller design. An advantage is when a flow rates, for example, are changed, then the controller parameters are immediately updated. In an adaptive (black-box) controller it takes some time before the controller parameters adapts to the new flow rates.

In the controller design the closed loop poles are set to a double pole in $z = 0.8$. The forgetting factor is set to $\lambda = 0.95$. The initial parameter vector is set to $\theta(0) = [\ 1 \quad 1\ ]^T$ and the initial covariance matrix is set to $P(0) = 30^2 I$. The feedforward gains are fixed, and tuned manually to $K_{f1} = 0.05$ and $K_{f2} = 0.7$. A simulation of the controller is shown in Figure 3.9.

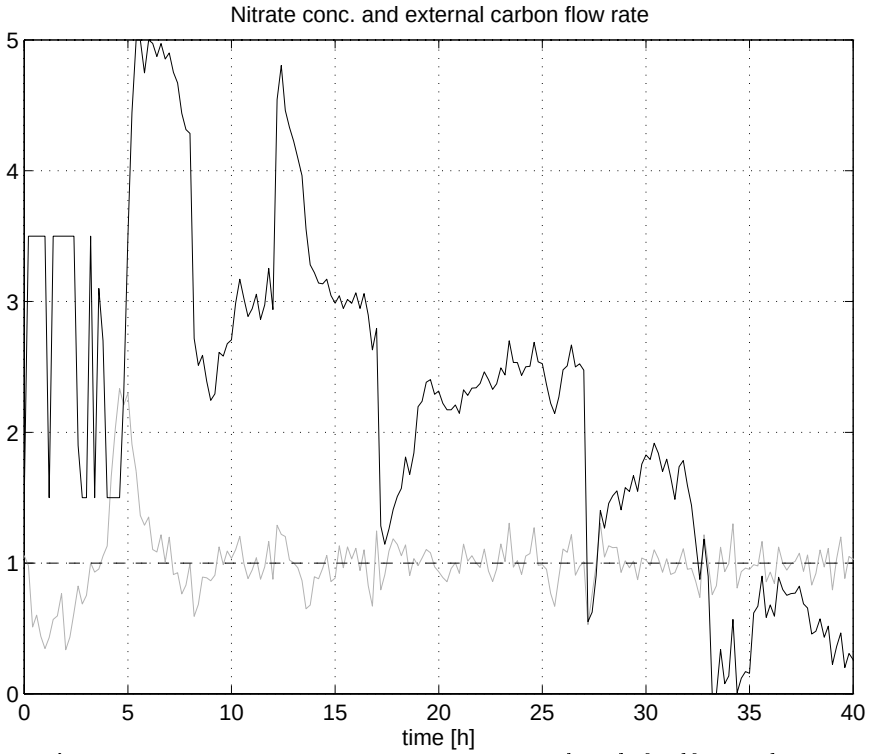

Figure 3.9: Model-based adaptive PI control with feedforward. The controlled nitrate concentration in the anoxic zone (grey line), the set-point (dashed line) and the corresponding external carbon flow rate (black line) are shown.

Remark 1: Using the same model, an LQ controller with feedforward could be also be designed, but this has not been considered here.

Remark 2: One idea to maintain the dynamic for the nitrate concentration model could be to vary the sampling rate when the flow rates changes. For a system with the following dynamic

$$y(t+1) = y(t) + \frac{Qh}{V}(u(t) - y(t))$$

the discrete-time transfer function is constant, if the variations in Q are compensated with variations in the sampling interval h, i.e. Qh is kept constant. A problem with this approach on the carbon dosage dynamics, is that a change in the sampling rate affects many parameters. It hence is not obvious if this approach could introduce a simplification.

3.8.6 Extended model-based adaptive PI control

This controller uses some extensions compared to the model-based adaptive PI control, and it was described in Section 3.4.1.

In the controller design the closed loop poles are set to a double pole in $z = 0.8$. The forgetting factor is set to $\lambda = 0.95$. The initial parameter is set to $\theta(0) = 0.1$ and the initial covariance matrix is set to $P(0) = 30^2$. The feedforward gain is fixed and tuned manually to $K_{f1} = 0.07$

The performance is similar to the model-based adaptive PI controller, but since this controller take the nonlinearity of the S_S concentration into account, the variations in the control signal becomes larger during disturbances in the flow rate, as seen in Figure 3.10. The higest peaks are not shown in this figure, but in Figure 3.11 it is shown that the maximum amplitude of the control signal is around 10 l/h.

This or the model-based adaptive PI controller has probably the best performance.

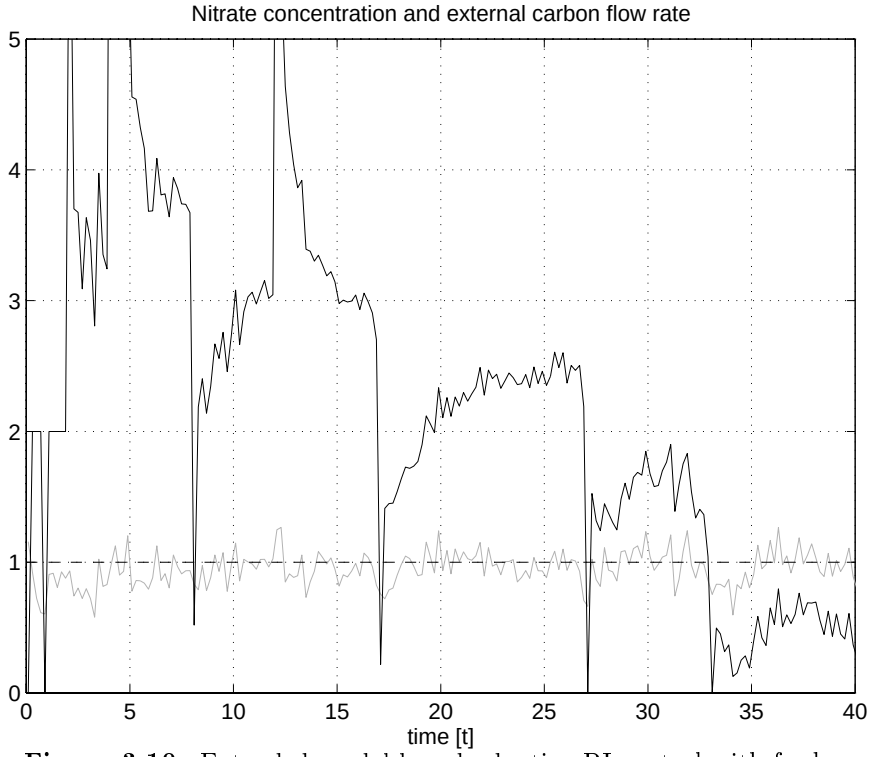

Figure 3.10: Extended model-based adaptive PI control with feed-forward. The controlled nitrate concentration in the anoxic zone (grey line), the set-point (dashed line) and the corresponding external carbon flow rate (black line) are shown.

3.8.7 Illustration of feedforward

Two comparisons with and without feedforward are simulated here. In the first comparison the model-based PI controller with and without feedforward is studied. In the second comparison an indirect adaptive LQ controller is studied.

The controllers use the same initialization as in Section 3.8.6 and Section 3.8.4, but measurement noise is set to zero to make the difference between the two strategies easier to see. Another difference is that the model-based PI controller is tuned slower, the closed loop poles in 0.85 instead of 0.8.

In Figure 3.11 a simulation with the model-based PI controller is shown.

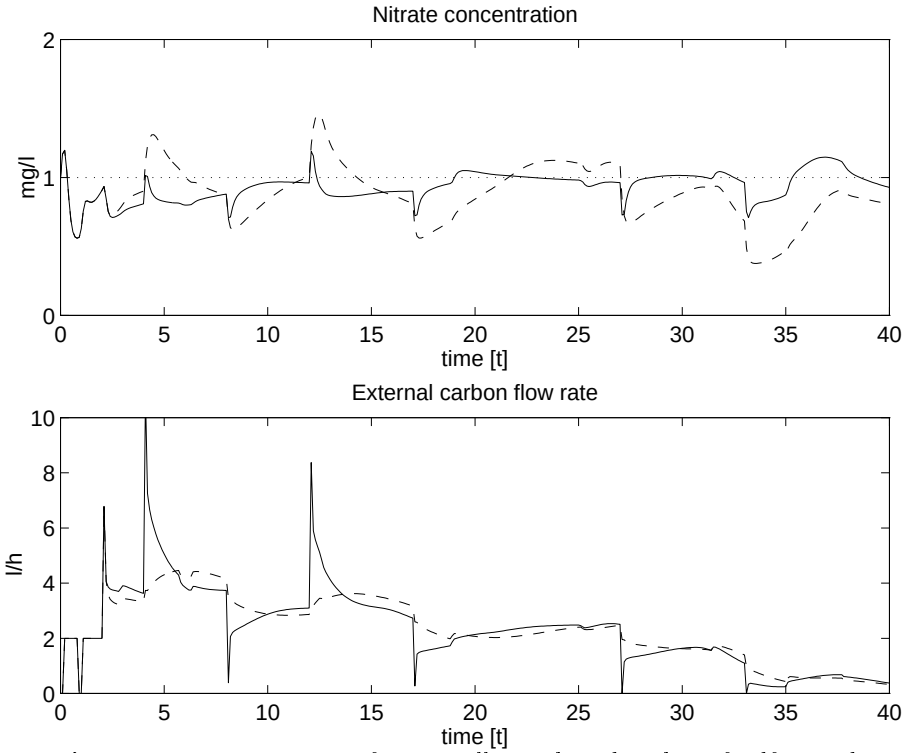

Figure 3.11: Illustration of a controller with and without feedforward for the model-based PI controller. The solid lines correspond to the controller with feedforward, and the dashed lines to the controller without feedforward. The set-point line is dotted.

The controller rejects, as expected, the disturbances faster with feedforward. The flow rate disturbances seem, however, very hard to reject. Despite large variations (notches) in control signal, these disturbances are not

completely rejected. The controller is tuned to be quite slow, this explains why the controller error takes time to eliminate.

A simulation with the indirect adaptive LQ controller is shown in Figure

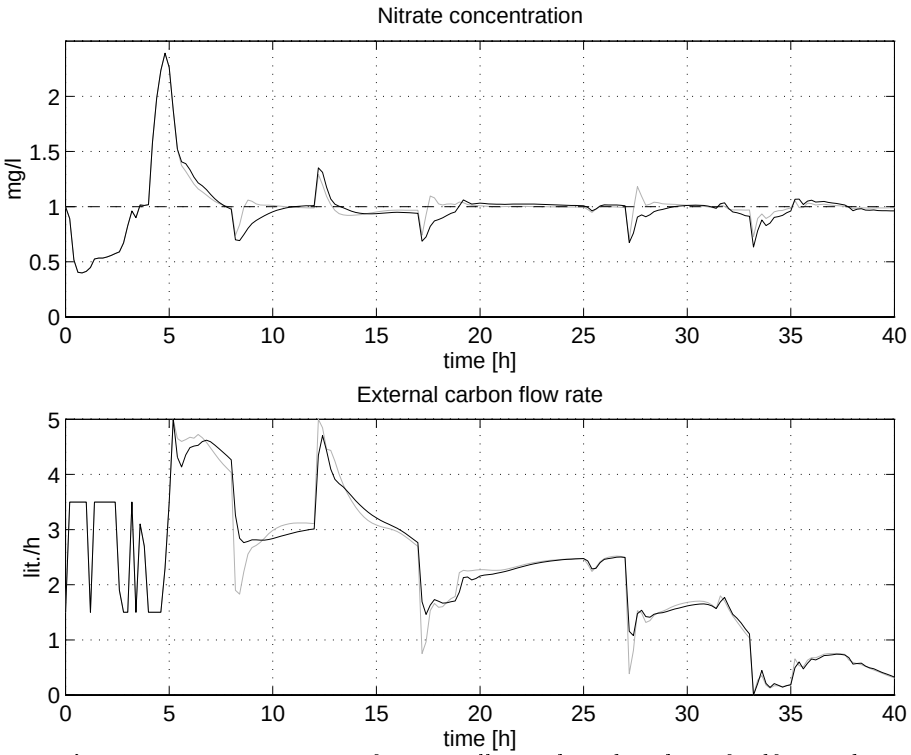

Figure 3.12: Illustration of a controller with and without feedforward for an indirect adaptive LQ controller. The black lines correspond to the controller without feedforward, and the grey lines to the controller with feedforward. The set-point line is dashed.

3.12. This controller is tuned to be faster than the controller in Figure 3.11. Feedforward does not seem to improve the performance so much here. Hence, if the nitrate sensor is reliable and not noisy, feedforward may not improve the control in a large extent. A reason for this is that changes in the nitrate concentration, caused by variations in the flow rates are very difficult to compensate for by an external carbon source. If the nitrate sensor is less reliable a slower controller, as in Figure 3.11, may be used, and then feedforward is more useful.

3.9 Evaluation in the pilot plant

The direct adaptive controller has also been evaluated in the pilot plant.

3.9.1 Conditions on the plant

The line P1 was used during the experiment, which was operated as a single sludge system with pre-denitrification and with ethanol as external carbon source with a concentration of 22000 mg COD/l. The influent flow was 220 l/h and the return sludge flow was 260 l/h. Internal recirculation was 300 l/h. The excess sludge pump rate was zero due to low mixed liquor suspended solids (MLSS). The temperature was 13.5^oC and the average MLSS was 3200 mg/l.

3.9.2 The controller

The direct adaptive controller was used, but without feedforward, since the pilot plant lacks sensors for measurements of nitrate and TOC. The controller has the following stucture:

$$\Delta u(t) = [(\hat{s}_0 + \hat{s}_1)y_{ref}(t) - (\hat{s}_0 y(t) + \hat{s}_1 y(t-1))]/(r_0 + \rho/r_0) \qquad (3.66)$$

where $\rho = 1$ and r_0 was fixed to $r_0 = 0.1$ during the whole experiment. Hence only s_0 and s_1 were estimated. The control signal was constrained and given by

$$u(t) = \begin{cases} u_{min} & \text{if } u(t-1) + \Delta u(t) < u_{min} \\ u(t) & \text{if } u_{min} < u(t-1) + \Delta u(t) < u_{max} \\ u_{max} & \text{if } u(t-1) + \Delta u(t) > u_{max} \end{cases} \qquad (3.67)$$

The parameters were estimated by the algorithm given in Section 3.5.1 with

$$\begin{aligned} \theta &= [s_0 \quad s_1]^T \\ \varphi(t) &= [y_f(t) \quad y_f(t-1)]^T \end{aligned}$$

where $y_f(t)$ was a low-pass filtered version of $y(t)$ where the low-pass filter $1/A_o$ has the pole in 0.80. The parameter vector was initialized with $\theta(0) = [0\ 0]^T$, and the covariance matrix $P(0) = 10I$. The forgetting factor was $\lambda = 0.95$, and the sampling interval was 20 minutes. The ideas in Section 3.7 to improve the estimation were applied. The carbon flow rate was not controlled during the first 20 samples. Instead the control signal was given by a PRBS in order to achieve good initial control parameters.

3.9.3 Results

The experiment with the adaptive controller is presented in Figure 3.13. The different events which occured during the test period (18 – 26 Jan 1996) is described in Table 3.1.

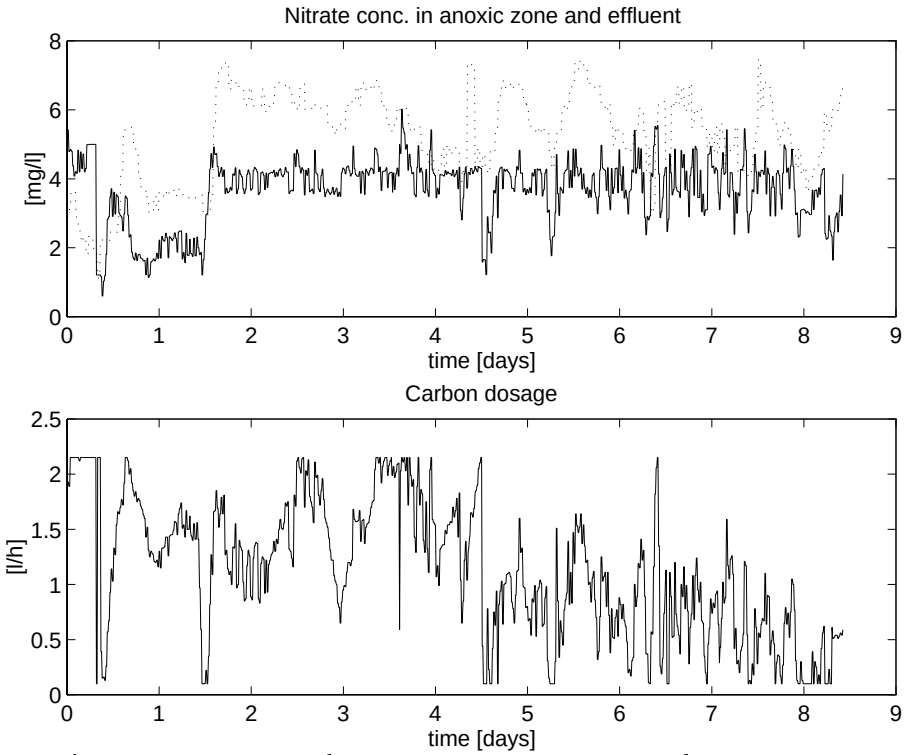

Figure 3.13: *Upper plot:* Nitrate concentration in the anoxic zone (solid line) and in effluent water (dotted line). *Lower plot:* The carbon flow rate. The carbon source has the conc. 22000 mg COD/l.

Due to a malfunction, starting around day 5, in the real plant, the COD concentration in the influent water to the pilot-scale plant increased from approximately 200 mg COD/l to 600 mg COD/l. This may explain the decreased carbon flow rate at the end of the experiment. This problem may also have masked the effect of the changes made in the inflow rate, see Table 3.1.

The controller performed quite well despite the rather noisy nitrate sensor, and it also rejected disturbances well. The latter can be seen by the behavior when the sensor is calibrated (the sensor output then goes abruptly down). It is also interesting to study the variations of carbon flow

Time	Event	Comment
0.3	Cleaning of sensor	The control experiment is started. After a short transient the nitrate conc. is kept close to the reference value = 2 mg/l.
1.5	Calibration	The calibration gives a small decrease in the nitrate conc.
1.5	Changed ref. value	The reference value is increased from 2 to 4 mg/l. When the set-point is changed, the controller decreases the carbon flow rate and the nitrate conc. quickly comes close to the new value at the set-point.
4.5	Calibration	This gives a decrease in the measured nitrate conc. which the controller compensates for.
5.5	Increased inflow	from 220 to 300 l/h, no visible effect
6.5	Decreased inflow	from 300 to 100 l/h, no visible effect
7.5	Increased inflow	from 100 to 220 l/h, no visible effect

Table 3.1: Events during the experimental period.

rate where one can see that a constant flow rate would not be optimal. Further, it could also be difficult to find a suitable level of a constant flow rate.

3.10 Conclusions

In this chapter four different types of controllers for the external carbon flow rate have been evaluated by means of simulation studies. One of the controllers was also tested in a practical experiment.

The evaluated controllers were a PID-controller, a generalized minimum-variance (direct adaptive) controller, an indirect adaptive controller, and a model-based PI controller. All controllers used feedforward from the recirculated nitrate mass flow and influent TOC mass flow. The control strategy was based on keeping the nitrate concentration in the anoxic zone at a constant and low level.

It can be concluded that all four controllers have similar performance for control of the nitrate concentration. Any of them may hence be a useful tool for a more pertinent control of the activated sludge process.

Some individual comments about the controllers could, however, be given:

- The PID-controller gave reasonably good control. It was easy to implement but it may be difficult to tune. It may also give poor control when the process is time-varying and may then even become unstable.
- The direct adaptive controller gave reasonably good performance and adapts well to changes in the process.
- The indirect adaptive controller also gave reasonably good performance and adapted well to changes in the process. The estimated process model can be be used for a wide range of controller designs. This means that unstable and non-minimum phase systems are of no particular problem. A drawback is that the suggested LQ controller is more complex and requires more computations than the other controllers.
- The model-based adaptive PI controller has high control performance. It used much physical information about the process and few parameters needed to be estimated. By using physical knowledge of the process in the controller design, the controller could, for example, immediately update the controller parameters when there is a change in a flow rate.

The adaptive controllers requires a safety net to work properly. The safety

net was described and simulations have shown that the adaptive controllers work well.

A practical experiment with the direct adaptive controller has also been performed. It showed that the direct adaptive controller managed well to control the nitrate concentration in the anoxic zone.

A possible extension could be to control the reference value of the nitrate concentration in the anoxic zone so that the effluent nitrate could be kept at a constant and low level.

Chapter 4

Estimation of the dissolved oxygen concentration dynamics

In this chapter methods for estimating two essential parameters which characterize the dissolved oxygen concentration (DO) dynamics in an activated sludge process are presented. The two variables are the respiration rate $R(t)$, and the oxygen transfer function K_La. The name oxygen transfer function is chosen to stress that it depends on several variables. Other common names in the literature are e.g. oxygen transfer rate and mass transfer coefficient. Knowledge of these two variables are of interest in both process diagnosis, Olsson and Andrews (1978), and process control including dissolved oxygen control, see, e.g., Spanjers (1993), Klapwijk *et al.* (1993), Spanjers *et al.* (1996) and Lindberg and Carlsson (1996*d*).

The respiration rate is the key variable that characterizes the DO process and the associated removal and degradation of biodegradable matter. It is the only true indicator of biologically degradable load, Holmberg *et al.* (1989). If toxic matter enters the plant, for example, this can be detected as a decrease in the respiration rate, since the microorganisms slow down their activity or some of them die. A rapid decrease in the respiration rate may hence be used as a warning that toxic matter has entered the plant and a by-pass action may be taken to save the microorganisms. The respiration rate can also be used for improved DO control, see Chapter 5. For more control applications using the respiration rate, see Spanjers *et al.* (1996).

The oxygen transfer function K_La (actually it is $K_La(u)(y_{set-y})$) de-

scribes the rate with which oxygen is transferred to the activated sludge by the aeration system. The K_La function can be expected to be nonlinear and it depends on several factors. Here, only its main time-varying dependence is considered, namely the airflow rate.

To find the respiration rate and the K_La function one could e.g. do batch tests, use a respirometer (the respirometer do not measure K_La) or apply an estimation algorithm (software sensor). The latter method is used here. The estimation algorithm is based on measurements of the dissolved oxygen concentration and the airflow rate which are used as inputs to a Kalman filter. Several estimation approaches have been suggested e.g. by Holmberg (1981), Ko *et al.* (1982), Holmberg and Olsson (1985), Holmberg *et al.* (1989), Bocken *et al.* (1989), Cook and Jowitt (1985), Carlsson and Wigren (1993), Carlsson *et al.* (1994*a*) and Lukasse *et al.* (1996). Many of these approaches have used simplified assumptions. For example, the respiration rate is assumed to be time invariant, or the oxygen transfer function is a linear function or a linear trend of the airflow rate. In Holmberg (1990) it was argued that a linear trend model of K_La leads to identifiability problems. Here a method is suggested which may avoid these problems. The simplified assumptions are not used, and also, the DO sensor dynamics is considered.

In the suggested estimation scheme, two models of the nonlinear K_La function are suggested, an exponential function and a cubic spline function. For other possible parameterizations of K_La, see Lindberg and Carlsson (1993). Different models of the time-varying respiration rate are studied. In particular, a filtered random walk model is considered, including two special cases: a random walk model and an integrated random walk model. These cases are obtained by specific choices of the filter pole in the model for describing the time variation. The K_La function and the respiration rate are tracked by a Kalman filter by using the measurements of airflow rate and DO, see also Holmberg and Olsson (1985) and Ljung and Söderström (1983).

When estimating the respiration rate and oxygen transfer function from measurements of DO and airflow rates, it is necessary that a high excitation in the airflow rate, both in frequency and amplitude, is used. A high excitation of the airflow rate, implies rapid changes in DO. If the DO sensor is not fast, the estimates will be biased. A filtering procedure developed by Ahlén and Sternad (1989) is applied to reduce the influence of the DO sensor dynamics. The filtered DO measurements can then be used for estimating the respiration rate and the oxygen transfer function. The suggested method is successfully illustrated both in simulations and on real data from the pilot

plant.

Furthermore, the effect of surface active agents is evaluated in the pilot plant. The suggested estimation approach to find K_La and the respiration rate was applied. The results show that both K_La and the respiration rate are significantly decreased by addition of surfactants[1].

The outline of this chapter is as follows. The oxygen transfer function K_La and the definition of the α and β parameters are discussed in Section 4.1. In Section 4.2 the model of the DO dynamics is outlined, and a discrete time model of the DO dynamics is derived. The estimator which is based on a Kalman filter is presented in Section 4.3. Two models of the nonlinear K_La function and three models of the time varying respiration rate are also presented. A slow DO sensor influences the estimates of K_La and respiration rate. In Section 4.4 a filter is derived which compensates for the slow sensor. The different approaches to model K_La and the respiration rate are evaluated in a simulation study in Section 4.5. In Section 4.6, the algorithm is applied to real data from the pilot plant. The influence of surfactants on K_La is studied in Section 4.7. Conclusions are given in Section 4.8.

4.1 The oxygen transfer function

When air is blown into the wastewater of an activated sludge process, oxygen is transferred to the water. The function which describes the oxygen transfer to the wastewater by the aeration system is called the K_La function. The most common way to describe the rate of change in DO, due to that air is blown into water, is by the following expression

$$\frac{dy}{dt} = K_La(u(t))(y_{sat} - y(t)) \qquad y_{sat} > y(t) \tag{4.1}$$

where $y(t)$ is the DO, y_{sat} is the saturated DO and $u(t)$ is the airflow rate. In (4.1), K_La depends only on the airflow rate $u(t)$. The oxygen transfer function in a real plant depends, however, on several other factors, for example, type of diffusers, wastewater composition, temperature, design of aeration tank, tank depth, placement of diffusers, etc, but the main *time-varying* dependence is the airflow rate.

The oxygen transfer function K_La can be considered to consist of two parts, K_L and a. The K_L part can be seen as an absorption coefficient and the a part as an *area/volume* ratio. The area and volume are easy to

[1]Surfactants are important ingredients in e.g. modern washing agents.

understand for an open tank without aeration devices. The volume is then the tank volume and the area is the contact area between water and air. When using aeration devices, the area depends on the bubble size which is affected by the aeration device and the airflow rate. The contact time between the bubbles and the wastewater is also important. Small bubbles are preferred, since they rise more slowly and have hence longer contact time. Many small bubbles are also better than a few large bubbles because the contact area with the wastewater becomes larger. Both K_L and a are, however, usually unknown so they are lumped into one parameter denoted K_La.

When discussing K_La at least two other parameters should be mentioned, the α and β parameters. They describe the relation between clean water and wastewater, see e.g. EPA (1989) and Harremoës *et al.* (1994). K_La for wastewater is found by multiplying K_La for clean water (K_La_{CW}) by the constant α, i.e. the constant α is defined as

$$\alpha = \frac{K_La}{K_La_{CW}} \tag{4.2}$$

In a similar way β compensates for the difference in saturated dissolved oxygen concentration between wastewater y_{sat} and clean water y_{satCW}

$$\beta = \frac{y_{sat}}{y_{satCW}} \tag{4.3}$$

There exist further extensions of (4.1), see e.g. Harremoës *et al.* (1994) and EPA (1989), but these are not considered. The extensions are also hard to make use of since they contain many unknown parameters.

4.2 The dissolved oxygen dynamics

In this section the dissolved oxygen dynamics will be outlined. Both a continuous-time model and its corresponding discrete-time model is treated.

4.2.1 A continuous time model

In an activated sludge process, biodegradable matter is degraded by microorganisms which consume oxygen. Studying a completely mixed tank gives the following dissolved oxygen mass balance, see e.g. Bastin and Dochain (1990)

$$\frac{dy(t)}{dt} = \frac{Q(t)}{V}(y_{in}(t) - y(t)) + K_La(u(t))(y_{sat} - y(t)) - R(t) \tag{4.4}$$

where

$y(t)$	is the DO in the zone
$y_{in}(t)$	is the DO of the input flow
y_{sat}	is the saturated value of the DO
$Q(t)$	is the wastewater flow rate
V	is the volume of the wastewater
$K_La(u)$	is the oxygen transfer function, see also Figure 4.2
$u(t)$	is the airflow rate into the zone from the air production system
$R(t)$	is the respiration rate

In general, it is assumed that $y(t)$, $y_{in}(t)$, $u(t)$ and $Q(t)$ are measured and that y_{sat} and V are known constants.

Equation (4.4) describes the rate of change in the dissolved oxygen concentration. The first term of the right hand side in (4.4) is a pure mass balance, influent oxygen – effluent oxygen times the dilution rate Q/V. The next term, $K_La(u(t))(y_{sat} - y(t))$, caused by aeration is the addition of oxygen, and the last term $R(t)$ describes the oxygen consumption. Figure 4.1 illustrates the DO process.

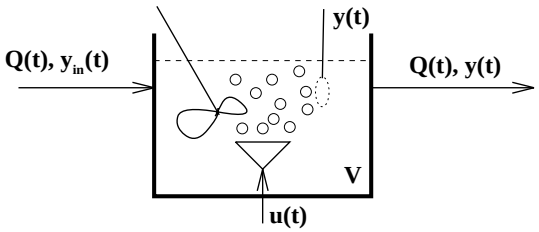

Figure 4.1: A completely mixed aerated tank.

The respiration rate $R(t)$ depends on the biomass concentration and describes the oxygen consumption by the microorganisms. It is usually regarded as consisting of two terms, oxygen needed for growth and oxygen needed for maintenance energy. The respiration rate is time-varying. Typically, it has a daily variation around a nonzero mean value, but it may change abruptly due to disturbances. The oxygen transfer function K_La is assumed to depend nonlinearly on the airflow rate. A typical K_La function is shown in Figure 4.2. Note that the slope of K_La (the gain) changes when the airflow rate changes.

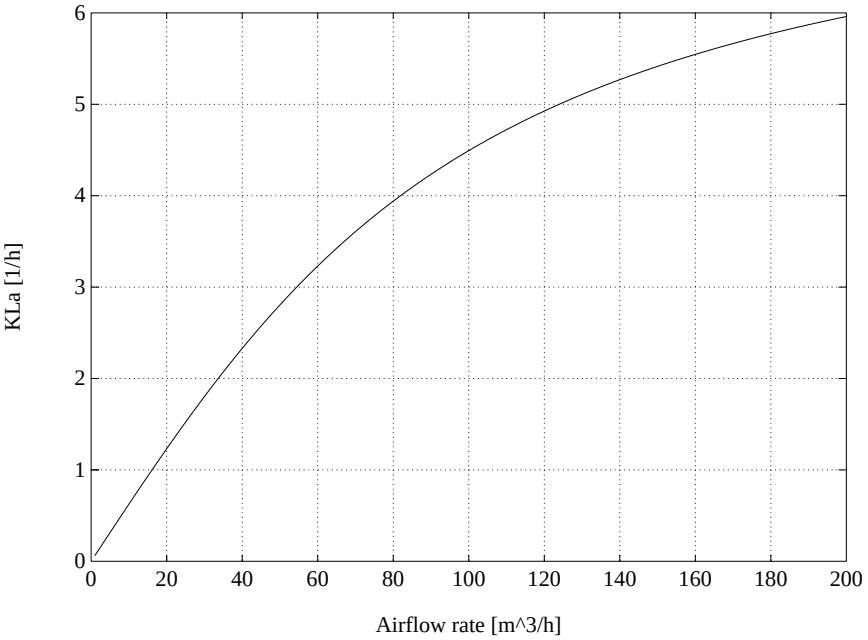

Figure 4.2: Typical shape of the oxygen transfer function ($K_L a(u)$) as a function of the airflow rate (u).

4.2.2 A discrete-time model

There exist several ways to obtain a discrete-time model from a continuous-time model like (4.4). One way is to use zero-order-hold sampling. This alternative is used here. Zero-order-hold sampling assumes that all signals except $y(t)$ are constant during the sampling interval. When that is true the discrete-time model describes exactly the continuous-time model at the sampling instants. This approximation is reasonable for sufficiently fast sampling.

Zero-order-hold sampling of the DO dynamics has previously been made by Holmberg (1990) and Cook and Jowitt (1985). For completeness, the derivation is repeated here. Rewrite (4.4) to

$$\frac{dy(t)}{dt} = A(t)y(t) + B(t) \tag{4.5}$$

where

$$A(t) \quad = \quad -(K_L a(u(t)) + \frac{Q(t)}{V})$$

$$B(t) \quad = \quad -R(t) + \frac{Q(t)}{V} y_{in}(t) + K_L a(u(t)) y_{sat}$$

Assuming that $A(t)$ and $B(t)$ are constant within each sampling period, model (4.5) is sampled by using theory in, for example, Åström and Wittenmark (1990) which gives

$$y(kh+h)) = e^{A(kh)h} y(kh) + \frac{B(kh)}{A(kh)} (e^{A(kh)h} - 1) \tag{4.6}$$

where h is the sampling interval and k is the discrete time. Now set

$$h^* = \frac{1}{A(kh)} (e^{A(kh)h} - 1) \tag{4.7}$$

and the sampled model becomes

$$\frac{y(kh+h)) - y(kh)}{h^*} = A(kh) y(kh) + B(kh) \tag{4.8}$$

In the following we will for notational simplicity replace kh with t. This gives together with A and B inserted in (4.8)

$$y(t+1) = y(t) + h^* [\frac{Q(t)}{V} (y_{in}(t) - y(t)) + K_L a(u(t)) (y_{sat} - y(t)) - R(t)] + w(t) \tag{4.9}$$

In (4.9), a term $w(t)$ has been added to describe measurement noise and model misfit.

4.3 The estimator

What makes it nontrivial to identify the dissolved oxygen dynamics is that

- The respiration rate $R(t)$ is time-varying.
- The oxygen transfer function $K_L a$ is nonlinear.
- The absolute levels of the respiration rate and $K_L a$ are hard to uniquely determine.
- The DO sensor may have a significant dynamics.

A possible remedy to the above problems is

- Use a Kalman filter approach to track the time-varying respiration rate.

- Use the three following assumptions regarding the K_La function:

  A1 The oxygen transfer function K_La can be sufficiently well described by a static nonlinearity of the airflow rate $u(t)$.

  A2 The parameters in the K_La model change slowly in comparison with the respiration rate.

  A3 The oxygen transfer function is zero when the airflow rate is zero, i.e. $K_La(0) = 0$, see Carlsson and Wigren (1993) and Carlsson *et al.* (1994*a*).

- Pre-filtering may reduce the influence of the DO sensor dynamics, see Section 4.4.

Assumption *A1* is reasonable in cases where not *very* fast sampling is used so that the dynamics of the air pipes etc. can be neglected. Assumption *A2* may not be valid for all wastewater plants but preliminary experiments from the municipal treatment plant in Uppsala do not indicate any fast changes in the K_La parameters apart from changes due to variations in the airflow rate. A more detailed evaluation of this point is, however, an interesting topic for further investigations. Assumption *A3* holds if the oxygen transfer function from the surrounding air is neglected. This is a reasonable approximation if K_La is small for zero airflow rate as compared to the average airflow rates. Assumption *A3* means that a "bias free" model structure can be used which improves the accuracy of the estimates.

Remark: Instead of estimating the respiration rate, other methods may be used. For example, the respiration rate can be measured by a respirometer, see e.g. Spanjers (1993). In a respirometer, water from the activated sludge process is pumped into a vessel, where the decay in oxygen concentration is used to determine the respiration rate. An off-gas method is another alternative to measure the respiration rate. It is based on measurements of O_2, the airflow rate, and CO_2 in the exhaust air. A problem with this method is to collect all the exhaust air. A third alternative to obtain the respiration rate, is to switch the aeration on and off, see Ryckaert *et al.* (1995). When the aeration is switched off, the decay in oxygen concentration is used to estimate the respiration rate. When the aeration is switched on again a fixed value of K_La may be estimated.

4.3.1 Different models of the nonlinear K_La function

That K_La not is linear has been discussed in e.g. Bennett (1980) who presents various physical models of K_La, Holmberg (1981) and Holmberg

(1990) approximate K_La with a linear trend model, Holmberg *et al.* (1989) used a linear model, but concluded that $K_La = \alpha\sqrt{u}$ could be a better approximation. Similarly Lukasse *et al.* (1996) used the following K_La model $K_La = \alpha u + \beta\sqrt{u} + \gamma$. In Lindberg and Carlsson (1993) several different K_La models have been evaluated, for example, piece wise linear models, polynomial, exponential and spline models.

To make it possible to use a nonlinear K_La in the Kalman filter, it has to be parameterized. In this section two different nonlinear models of the K_La function and their parameterization are presented.

An exponential model of K_La

An exponential K_La model may be a suitable choice, because it can be given a similar shape of the K_La function as in Figure 4.2, which is natural in a physical sense (the oxygen transfer deteriorates for high airflows). Further, only two parameters are necessary to estimate, and it is also easy to invert this K_La function. Inverting is useful in design of a nonlinear controller. The exponential K_La model is

$$K_La(u(t)) = k_1(1 - e^{-k_2 u(t)}) \tag{4.10}$$

The gradient of the K_La model, which is needed in the estimation algorithm in Section 4.3.4, is found by taking the partial derivative of K_La with respect to the unknown parameter vector $\theta_{K_La} = [k_1 \; k_2]^T$

$$\psi^T_{K_La}(t, \theta_{K_La}) = \frac{\partial K_La}{\partial \theta_{K_La}} \tag{4.11}$$

The gradient can be approximated by

$$\psi^T_{K_La}(t, \theta) = \begin{bmatrix} 1 - e^{-\hat{k}_2 u(t)} & \hat{k}_1 u(t) e^{-\hat{k}_2 u(t)} \end{bmatrix} \tag{4.12}$$

where $\hat{k}_1$ and $\hat{k}_2$ are the estimated values of k_1 and k_2, this common approach when the true values not are known, see also Ljung and Söderström (1983).

A cubic spline model of K_La

An alternative to the exponential model or the piecewise linear approximation in Carlsson and Wigren (1993) and Carlsson *et al.* (1994*a*), is a cubic spline. Such a model may give a good approximation of the nonlinear K_La function. It has an inherent smoothness which is natural from a physical

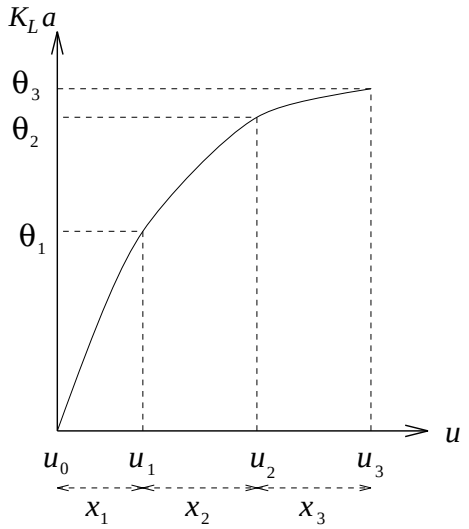

Figure 4.3: A spline approximation of $K_L a$.

point of view. In Figure 4.3 a cubic spline is shown, together with some of the parameter definitions.

From Dahlquist *et al.* (1974) it follows that a cubic spline polynomial can be written in the following form where u is in the interval $u_{i-1} \leq u < u_i$

$$\begin{aligned} K_L a(u)_i &= m_i\theta_i + (1-m_i)\theta_{i-1} \\ &+ x_i m_i(1-m_i)[(k_{i-1}-d_i)(1-m_i) - (k_i - d_i)m_i] \end{aligned} \quad (4.13)$$

where θ_i is defined in Figure 4.3 and

$$\begin{aligned} x_i &= u_i - u_{i-1} \\ d_i &= \frac{\theta_i - \theta_{i-1}}{x_i} \\ m_i &= \frac{u - u_{i-1}}{x_i}, \quad u \in [u_{i-1}, u_i] \\ i &= 1, 2, \ldots, n \qquad n = \text{number of grid points } - 1 \end{aligned}$$

The variables $k_0, k_1, ..., k_n$ are the derivatives of the spline in the grid points. Note that $K_L a(u_i)_i = \theta_i$.

The linear regression form for the spline model is

$$K_L a(u(t)) = \psi^T_{K_L a}(t)\theta_{K_L a} \quad (4.14)$$

$$\theta_{K_L a} = [\theta_0 \ \ldots \ \theta_n]^T \quad (4.15)$$

The derivation and definition of $\psi^T_{K_L a}(t)$ is given in Appendix C.

Note that θ_0 should not be estimated since we assumed in assumption *A3* that $K_L a(0) = 0$. It is, however, included here for generality. This implies in the algorithm that θ_0 is set to 0 and the term which corresponds to θ_0 in the covariance matrix (4.35) is set to zero.

4.3.2 Modeling the time-varying respiration rate

Here some approaches for modeling the respiration rate are suggested. A random walk model, a filtered random walk model and an integrated random walk model are considered.

A random walk model is given by

$$R(t) = \frac{1}{1 - q^{-1}} e_{rw}(t) \tag{4.16}$$

where $e_{rw}(t)$ is zero mean white noise.

An filtered random walk model is given by

$$R(t) = \frac{1}{(1 - fq^{-1})(1 - q^{-1})} e_{rw}(t) \tag{4.17}$$

where f is the filter pole. As a special case, the random walk model is obtained by setting $f = 0$, and as another special case the integrated random walk model is found by setting $f = 1$.

Equation (4.17) can be rewritten as

$$R(t) = (1 + f)R(t - 1) - fR(t - 2) + e_{rw}(t) \tag{4.18}$$

and then into a state space form, which is useful in the Kalman filter.

$$\begin{aligned} Z(t+1) &= AZ(t) + Be_{rw}(t) && (4.19) \\ R(t) &= CZ(t) && (4.20) \end{aligned}$$

where

$$\begin{aligned} Z(t) &= \begin{bmatrix} R(t) \\ R(t-1) \end{bmatrix} \qquad A = \begin{bmatrix} 1+f & -f \\ 1 & 0 \end{bmatrix} && (4.21) \\ B &= \begin{bmatrix} 1 \\ 0 \end{bmatrix} \qquad C = \begin{bmatrix} 1 & 0 \end{bmatrix} && (4.22) \end{aligned}$$

The random walk model (4.16) can also be written in the state space form (4.19) and (4.20) with

$$A = B = C = 1 \tag{4.23}$$

A filtered random walk model gives good tracking of the respiration rate, better than, for example, a random walk model, see also Lindbom (1995) and Ljung and Gunnarsson (1990) for a treatment of general tracking problems. Note that bad tracking of the respiration rate also deteriorates the estimated K_La function.

4.3.3 Putting the models together

In Section 4.3.1, two different K_La models were given and in Section 4.3.2 three respiration rate models were presented. These models are now put together into one model which will be used in a Kalman filter in Section 4.3.4.

If the K_La function varies in time, it may also be suitable to describe its variations by a random walk model

$$\theta_{K_La}(t) = \theta_{K_La}(t-1) + e_{K_La}(t) \tag{4.24}$$

where e_{K_La} is zero mean white noise. Normally, when K_La is assumed time invariant, $e_{K_La} = 0$. The respiration rate is modeled by (4.19) and (4.20). Collecting all parameters in one vector gives

$$\theta = \begin{bmatrix} \theta_{K_La} \\ Z \end{bmatrix} \tag{4.25}$$

$$\theta(t+1) = F\theta(t) + e_\theta(t) \tag{4.26}$$

where

$$F = \begin{bmatrix} I & 0 \\ 0 & A \end{bmatrix} \qquad e_\theta(t) = \begin{bmatrix} e_{K_La}(t) \\ Be_{rw}(t) \end{bmatrix} \tag{4.27}$$

and I is the identity matrix.

Derivation of the regressor

Since the exponential K_La model is not linear in its parameters, the regressor $\psi^T_{K_La}$ is derived from the gradient of the prediction error, as

$$\psi^T(t,\theta) = -\left(\frac{\partial \varepsilon(t,\theta)}{\partial \theta}\right) \tag{4.28}$$

where the prediction error $\varepsilon(t,\theta)$ is determined by

$$\varepsilon(t) = y(t) - \hat{y}(t|t-1) \tag{4.29}$$

Inserting the predictor $\hat{y}(t|t-1)$, which is based on equation (4.9) gives

$$\begin{aligned}\varepsilon(t) &= y(t) - \Bigg(y(t-1) + h^*[\frac{Q(t-1)}{V}(y_{in}(t-1) - y(t-1)) \\ &+ \widehat{K_L a}(u(t-1))(y_{sat} - y(t-1)) - \hat{R}(t-1)]\Bigg) \end{aligned} \tag{4.30}$$

Applying (4.28) with the prediction error in (4.30) gives

$$\psi^T(t,\theta) = h^*[(y_{sat} - y(t))\frac{\partial \widehat{K_L a}}{\partial \theta} \quad -\frac{\partial \hat{R}}{\partial \theta} \ ] \tag{4.31}$$

which can be written as

$$\psi^T(t,\theta) = h^*[(y_{sat} - y(t))\psi^T_{K_L a}(t) \quad -C \ ] \tag{4.32}$$

where $\psi^T_{K_L a}$ is given by (4.11) for the exponential model and (C.21) for the spline model. The C-vector is either given by (4.22) or (4.23) depending on the model of the respiration rate.

4.3.4 The Kalman filter

A Kalman filter interpretation is used to estimate the time-varying respiration rate and the nonlinear oxygen transfer function. This approach uses measurements of DO and airflow rate to estimate the oxygen transfer function $K_L a$ and the respiration rate by a Kalman filter. A schematic figure of the estimator is shown in Figure 4.4.

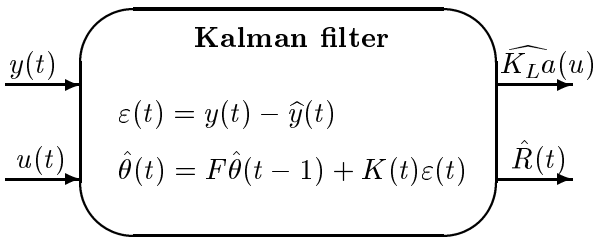

Figure 4.4: The estimator where $K_L a$ and $R(t)$ are estimated from measurements of DO and airflow rate, see also Carlsson *et al.* (1994*a*).

The Kalman filter equations can, for example, be found in Ljung and Söderström (1983). These equations together with the parameter modeling from Section 4.3.3 give

$$\hat{\theta}(t) = F\hat{\theta}(t-1) + K(t)\varepsilon(t) \tag{4.33}$$

$$K(t) = \frac{FP(t-1)\psi(t)}{r_2 + \psi^T(t)P(t-1)\psi(t)} \tag{4.34}$$

$$P(t) = FP(t-1)F^T - \frac{FP(t-1)\psi(t)\psi^T(t)P(t-1)F^T}{r_2 + \psi^T(t)P(t-1)\psi(t)} + R_1 \tag{4.35}$$

where $\varepsilon(t)$ is defined in (4.29), θ in (4.25), $\psi(t)$ in (4.32), and the choice of R_1 in (4.37) for a random walk and (4.38) for a filtered random walk, and $r_2 = 1$.

In the predictor, the parameters $y(t)$, $y_{in}(t)$, $u(t)$ and $Q(t)$ are measured, V and y_{sat} are assumed known and $R(t)$ and $\theta_{K_L a}$ are estimated. The parameter h^* is derived according to (4.7) with an estimated value of $K_L a(u)$.

Choice of R_1 and r_2

The covariance matrix R_1 is given by

$$R_1 = \mathrm{E}e_\theta(t)e_\theta(t)^T = \begin{bmatrix} \mathrm{E}e^2_{K_L a} & 0 \\ 0 & BB^T\mathrm{E}e^2_{rw} \end{bmatrix} \tag{4.36}$$

and describes how fast the different components in θ are expected to vary. Usually $\mathrm{E}e^2_{K_L a}$ and $\mathrm{E}e^2_{rw}$ are not known. The variance of the measurement noise $w(t)$ is denoted by r_2. It is possible to rewrite (4.35) so that R_1 is replaced by R_1/r_2 and r_2 by 1. Then only R_1 is used as a design parameter. This is reasonable, since in most cases neither R_1 nor r_2 are known.

Setting $R_1 = 0$ implies no tracking capability, since $K(t)$ then goes to zero when $t \to \infty$. Hence to be able to track time-varying parameters it is necessary to set $R_1 > 0$. The magnitude of R_1 should reflect the true variations of the time varying parameters and has in general to be tried out.

In the dissolved oxygen dynamics, the respiration rate is time-varying and the $K_L a$ function is assumed to be a very slowly changing (or time-invariant) nonlinearity of the airflow rate. The covariance matrix R_1 then becomes

$$R_1 = \begin{bmatrix} \gamma_1 & 0 & 0 \\ 0 & \gamma_1 & 0 \\ 0 & 0 & \gamma_2 \end{bmatrix} \tag{4.37}$$

for the random walk case, and

$$R_1 = \begin{bmatrix} \gamma_1 & 0 & 0 & 0 \\ 0 & \gamma_1 & 0 & 0 \\ 0 & 0 & \gamma_2 & 0 \\ 0 & 0 & 0 & 0 \end{bmatrix} \tag{4.38}$$

for the filtered random walk case. The parameter γ_1 should be a small number which reflects the slow variation in the K_La parameters. The much faster variation in the respiration rate is reflected in a larger γ_2. The choice of γ_2 also depends on the filter pole in the filtered random walk model. The closer f is to 1, the smaller γ_2 should be selected.

The covariance matrix R_1 should have appropriate values. A too small value of γ_2 may give (a larger) bias in the estimate, since the Kalman filter will not be able to the follow the variations in the true respiration rate. On the other hand, a too large value of γ_2 results in unnecessary large variations (due to measurement noise) of the estimated respiration rate.

Remark 1: In (4.37) and (4.38) only two K_La parameters are assumed to be estimated. The size of R_1 has to be changed if another number of parameters are estimated.

Remark 2: If K_La is assumed to be non time-varying, the estimation procedure can be divided into two steps. In the first step K_La and the respiration rate are estimated during high excitation of the airflow rate. In the second step, which occurs when the estimated parameters in the K_La function has settled, the high excitation of the airflow rate can be switched off. Normal operation of the DO can then again be applied. The respiration rate is then estimated by setting all elements in the covariance matrix (P) to zero, except for the elements which are only related to the respiration rate, see Carlsson (1993)

Choice of initial values to the Kalman filter

The Kalman filter needs initial values of $\hat{\theta}(0)$ and $P(0)$. The choice of $P(0)$ should reflect the uncertainty in the a priori guess of $\hat{\theta}(0)$. The relevant choice is, see Ljung and Söderström (1983),

$$P(0) = \frac{\mathrm{cov}(\hat{\theta}(0))}{\mathrm{E}||\varphi(t)||^2} \tag{4.39}$$

Often only a crude guess about $\mathrm{cov}(\hat{\theta}(0))$ is available. A typical choice is then to set

$$\hat{\theta}^T(0) = \begin{bmatrix} 0 & \dots & 0 \end{bmatrix} \text{ and } P(0) = \sigma^2 I \tag{4.40}$$

where I is the identity matrix, and σ^2 should be chosen large.

Remark: A *very* important practical issue when using any kind of recursive algorithm is the initialization. If one uses a large σ at $t = 0$ and the regressor is filled with zeros, it is very likely that the parameters take some large steps in a wrong direction which they often never recover from. A remedy is to wait with the updating until the regressor is filled with data.

4.3.5 An alternative approach of estimating K_La

A possible alternative approach to the Kalman filter approach discussed above is to first differentiate the model and treat the differentiated respiration rate as white noise. Differentiating is a well known method in system identification to be applied to systems with non-zero means, see, e.g., Söderström and Stoica (1989).

Since the differentiated respiration rate is treated as a white noise, fewer parameters have to be estimated than in the previously mentioned approaches where the respiration rate also was estimated. Estimating fewer parameters usually implies higher accuracy of the remaining parameters. The value of the respiration rate is not lost by the use of this approach, it can still be determined by using equation (4.9) together with the estimated K_La.

Using (4.9) (neglecting the noise $w(t)$) and calculating $y(t+1) - y(t)$ gives

$$\begin{aligned} y(t+1) - y(t) &= y(t) - y(t-1) + h^*[\frac{Q(t)}{V}(y_{in}(t) - y(t)) \\ -\frac{Q(t-1)}{V}&(y_{in}(t-1) - y(t-1)) + K_La(u(t))(y_{sat} - y(t)) \\ &-K_La(u(t-1))(y_{sat} - y(t-1)) - (R(t) - R(t-1))] \end{aligned} \tag{4.41}$$

Assuming that the respiration rate can be modeled by

$$R(t) = \frac{1}{1-q^{-1}}e_{rw}(t) \tag{4.42}$$

where the noise e_{rw} is assumed to be zero mean white noise, gives

$$R(t) - R(t-1) = e_{rw}(t) \tag{4.43}$$

Inserting (4.43) in (4.41) gives the predictor

$$\hat{y}(t+1|t) \quad = \quad 2y(t) - y(t-1) + h^*[\frac{Q(t)}{V}(y_{in}(t) - y(t))$$

$$- \quad \frac{Q(t-1)}{V}(y_{in}(t-1) - y(t-1)) + K_L a(u(t))(y_{sat} - y(t-1))$$
$$- \quad K_L a(u(t-1))(y_{sat} - y(t-1))] \tag{4.44}$$

The gradient of (4.44) becomes

$$\psi^T(t) = h[(y_{sat} - y(t-1))\psi^T_{K_L a}(t-1) - (y_{sat} - y(t-2))\psi^T_{K_L a}(t-2)] \tag{4.45}$$

where $\psi^T_{K_L a}(t)$ is defined in (4.11). Note that this predictor is different as compared to the previous one.

This method works very well when no measurement noise exists, even better than the other methods. Its performance deteriorates, however, fast (faster than it does for the other methods) when measurement noise is added. A possible explaination could be that differentiation amplifies noise.

4.4 Estimation utilizing a slow DO sensor

When estimating the respiration rate and oxygen transfer function from measurements of DO and airflow rates, it is necessary that a high excitation in the airflow rate is used. A high excitation in airflow rate implies rapid changes in DO. If the DO sensor is not fast, the estimates will be biased. In this section a filtering procedure, developed by Ahlén and Sternad (1989), is applied to reduce the influence of the DO sensor dynamics. The filtered DO measurements are then used for estimating the respiration rate and the oxygen transfer function.

4.4.1 Simple illustration of the problem

Assume for simplicity that $Q(t) = u(t) = 0$. Inserting this in (4.4) gives the respiration rate

$$R(t) = -\frac{dy}{dt} \tag{4.46}$$

The respiration rate can hence be estimated from the slope of the sensor output. If the DO sensor is slow, how will then the estimated respiration rate be affected, when using (4.46)? An example will illustrate this question.

Let the DO sensor have a step response as shown in Figure 4.5. The true DO is changed from zero to one mg/l at time $t = 0$.

If the DO is 2 mg/l at $t = 0$, applying the respiration rate in the lower plot of Figure 4.6 then gives the DO shown in the upper plot in the same

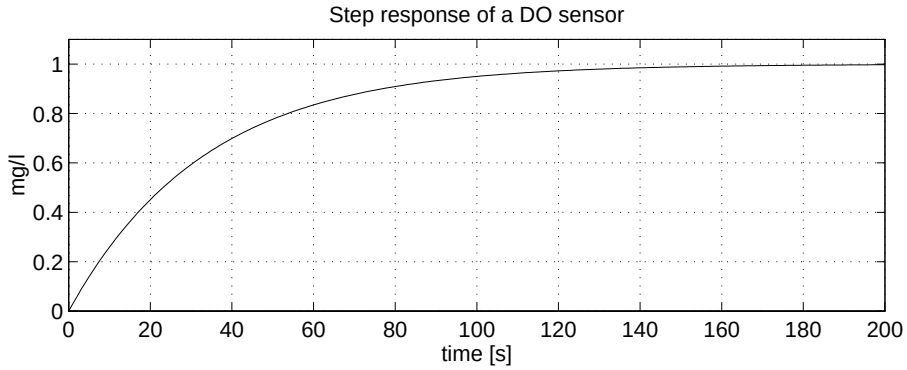

Figure 4.5: Step response of a DO sensor.

figure. We can see that DO sensor output is slower than the true DO. Using the derivative of the sensor output as an estimate of the respiration rate will hence not give a correct estimate. It takes time before a reliable estimate of the respiration rate is achieved. If there is a step change in the respiration rate, the settling-time to obtain a correct estimate will then be as long as the settling-time for the DO sensor. The estimate of the respiration rate is filtered by the sensor dynamics.

When the airflow rate is highly excited, which it should be to give good estimates of the respiration rate and $K_L a$, the DO sensor output will not follow the true DO and the estimates will be biased.

4.4.2 Filtering the DO measurements

Assume that the DO is measured by a sensor. Obviously, what is available for data processing is the output from the sensor (denoted $y_s(t)$ below). By filtering the DO measurements it is possible to reduce influence of the sensor dynamics. This is utilized by using a fixed lag smoother. A block diagram of the sensor, the input model and the filter is shown in Figure 4.7.

We would like to find a filter, which based on the measurements of the sensor output ($y_s(t)$) gives the actual DO in the activated sludge process. The problem is to find a filter which minimizes the mean square error between the true DO and the filtered DO, i.e. we want to minimize

$$\mathrm{E}(y(t) - \hat{y}(t|t-m))^2 \tag{4.47}$$

where $\hat{y}(t|t-m)$ denotes a prediction of $y(t)$ based on data up to time $t-m$. The user choice m determines whether we have a predictor ($m > 0$),

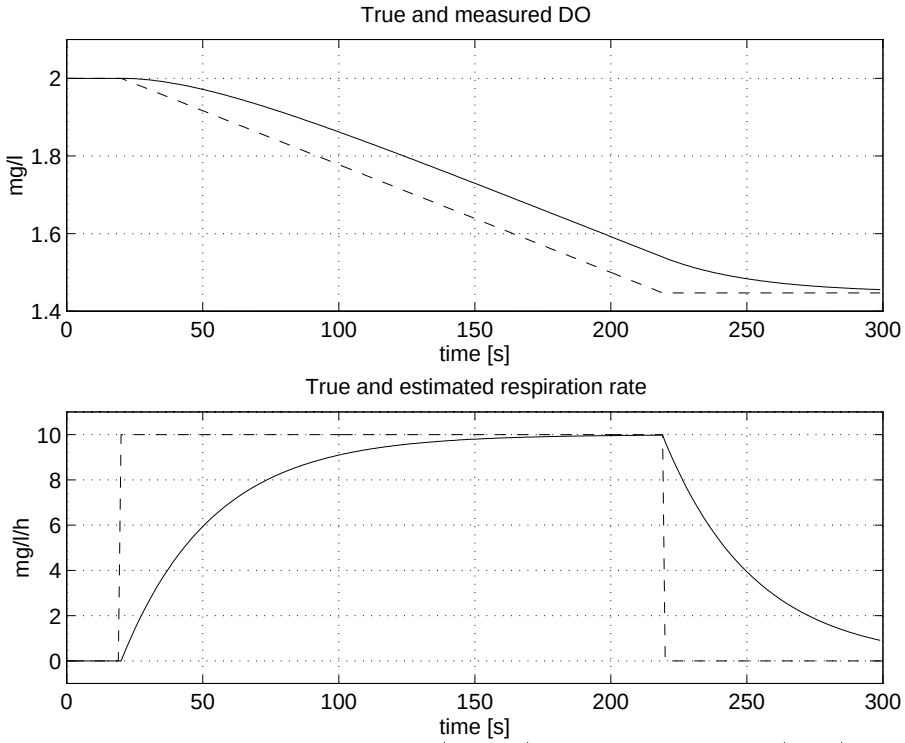

Figure 4.6: Upper plot: True (dashed) and measured DO (solid). Lower plot: True (dashed) and estimated respiration rate (solid).

filter ($m = 0$), or smoother ($m < 0$). It is advisable to use $m < 0$ since it gives a smaller error ($y(t) - \hat{y}(t|t-m)$). The more negative m is chosen, the smaller the error will be. No significant improvements is, however, found after some value of m. Note that choosing $m < 0$ gives a delay between the actual DO and the filtered DO.

For an optimal solution of the filter, a sensor model and an input model is required. A simple input model which generates a drifting signal is

$$y(t) = \frac{1}{\Delta(q^{-1})} e(t) \tag{4.48}$$

where $e(t)$ is zero mean white noise, and $\Delta(q^{-1}) = 1 - q^{-1}$ is a polynomial in the backward shift operator q^{-1}.

The sensor is modeled by

$$y_s(t) = q^{-k} \frac{B(q^{-1})}{A(q^{-1})} y(t) + w(t) \tag{4.49}$$

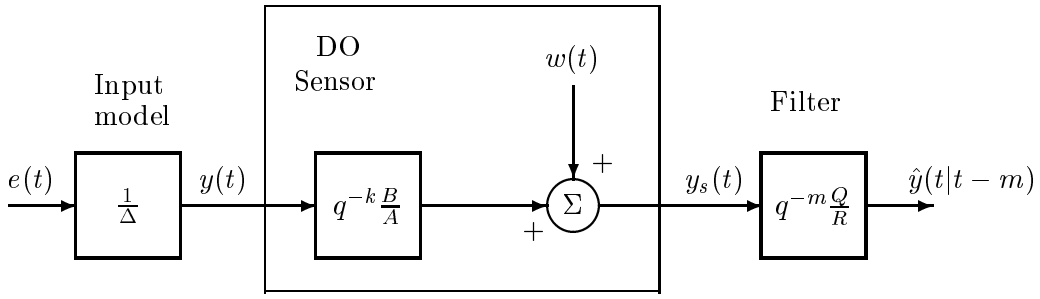

Figure 4.7: Block diagram of the input signal, the sensor model and the filter.

In (4.49) k is a time delay, $A(q^{-1})$ and $B(q^{-1})$ are polynomials and $w(t)$ is zero mean white measurement noise.

The problem of minimizing (4.47) is an LQ problem, which either could be solved by a Kalman filter approach or by a polynomial approach. The latter method is applied here.

The filter which minimizes (4.47) is given by

$$\hat{y}(t|t-m) = q^{-m}\frac{Q(q^{-1})}{R(q^{-1})}y_s(t) \tag{4.50}$$

where the $Q(q^{-1})$ and $R(q^{-1})$ polynomials are found by solving the following design equations, see Ahlén and Sternad (1989)

$$r\beta\beta_* = BB_* + \rho A\Delta A_*\Delta_* \tag{4.51}$$
$$z^{m+k}B_* = r\beta_* Q_1 + z\Delta L_* \tag{4.52}$$
$$Q = Q_1 A \tag{4.53}$$
$$R = \beta \tag{4.54}$$

In (4.51) – (4.54) and in the following the argument (q^{-1}) is left out for simplicity. Conjugate polynomials (denoted by $_*$) are used in (4.51) and (4.52). A conjugate polynomial is defined as follows. Consider a general polynomial $P = p_0 + p_1 q^{-1} + \cdots + p_{nP}q^{-nP}$. The conjugate polynomial is then defined by $P_* = p_0 + p_1 q + \cdots + p_{nP}q^{nP}$. The polynomial β is a stable (the roots of β are inside the unit circle) and monic (the first coefficient in the polynomial is 1) polynomial. The polynomial L is an auxiliary polynomial, and $\rho = \mathrm{E}w^2/\mathrm{E}e^2$ is the noise to signal ratio, which is normally used as user design parameter.

The degrees of the polynomials in the design equations (4.51)–(4.54) are given by:

$$n\beta = \begin{cases} nB & \text{if } \rho = 0 \\ \max\{nB, nA+1\} & \text{if } \rho > 0 \end{cases} \tag{4.55}$$

$$nQ_1 = \max\{-m-k, 0\} \tag{4.56}$$

$$nL = \max\{nB+m+k, n\beta\} - 1 \tag{4.57}$$

where nB denotes the degree of the B polynomial, etc.

Remark 1: The presented approach may, for example, also be of interest for DO sensors used in respirometers, see e.g. Spanjers and Olsson (1992).

Remark 2: Efficient numerical methods exist for solving the spectral factorization (4.51), which can only be solved analytically for degrees of β less than 3.

Remark 3: It is possible to derive a filter for a more general case where the measurement noise $w(t)$ is colored and the input model is more general, see further Ahlén and Sternad (1989).

4.4.3 Determination of A, B, k and ρ

The sensor model, i.e. the A and B polynomials and time delay k, can be determined by a least squares method, where suitable polynomial degrees and time delay have to be tried out, see e.g. Söderström and Stoica (1989). Necessary data for estimating the sensor dynamics can be achieved by moving the the DO sensor between waters with different DO and register the sensor response.

The parameter ρ is probably easiest to find by trial and error. A small ρ gives a noisy result and a large ρ gives a slow response to changes in DO. When estimating the respiration rate from the DO measurements, simulations have indicated that it is better to choose a too small than a too large ρ.

4.4.4 An example

To illustrate the procedure outlined above, an example is given. The dynamics of the sensor in this example corresponds to the model obtained for the DO sensor at the pilot plant in Uppsala. For a sampling interval of 10s the following parameters were identified from the data given in the experiment shown in Figure 4.8 using a least squares method (ARX model

structure)

$$A = 1 - 0.45q^{-1} \qquad B = 0.55 \qquad k = 2 \tag{4.58}$$

In Figure 4.8 the DO sensor is moved between different zones. The true DO is obtained by considering the DO constant in each zone and using the steady-state value from the DO sensor as the constant value. The time of moving the DO sensor is logged.

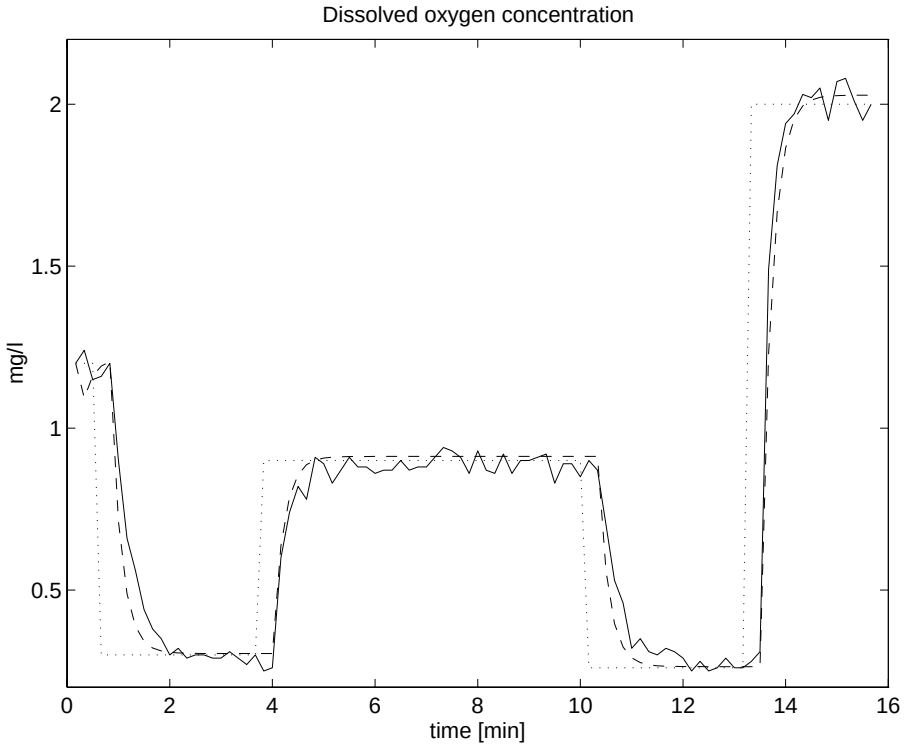

Figure 4.8: Experiment in the pilot plant for identifying the dynamics of the DO sensor. True DO (dotted line), measured DO (solid line) and true DO filtered by (4.58) (dashed line).

Using the polynomials (4.58) in the design equations (4.51) – (4.54) with a smoothing lag $m = -3$, and $\rho = 0.1$, gives the Q_1 and R polynomials:

$$Q_1 = 0.3553 + 0.9787q^{-1} \qquad R = 1 - 0.3464q^{-1} + 0.0801q^{-2} \tag{4.59}$$

The filter then becomes:

$$\hat{y}(t|t+3) = q^3 \frac{(0.3553 + 0.9787q^{-1})(1 - 0.4500q^{-1})}{1 - 0.3464q^{-1} + 0.0801q^{-2}} y_s(t) \tag{4.60}$$

In Figure 4.9 the filtering is illustrated for different ρ, and m, with and without measurement noise. As seen, when $k > -m$ there will be a delay in the filtered signal compared to the the true DO. A small ρ gives in the noise free case a smaller error between true and filtered DO, but for measurement noise a large ρ may be preferable.

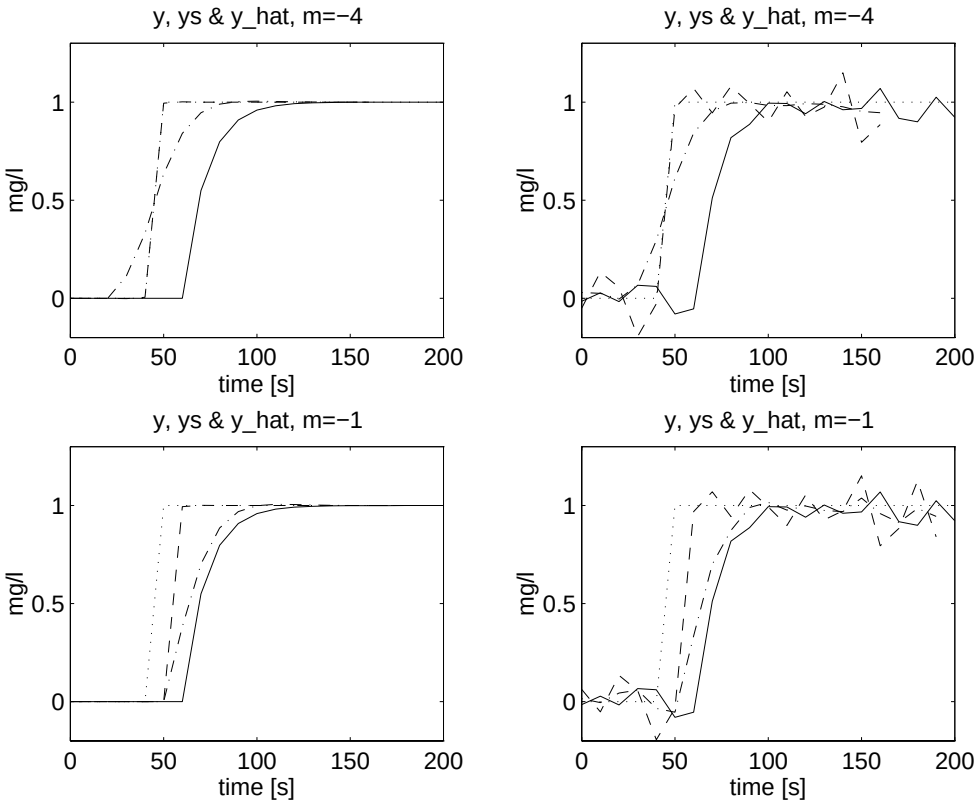

Figure 4.9: Example of smoothing. The shown signals are $y(t)$ (dotted line), $y_s(t)$ (solid line), $\hat{y}(t)$ with $\rho = 0.001$ (dashed line), and $\hat{y}(t)$ with $\rho = 1$ (dash-dotted line). *Left column:* No measurement noise ($w(t) = 0$). *Right column:* Measurement noise with $\mathrm{E}w(t)^2 = 0.05^2$.

When the DO signal is filtered (here the filtered DO is denoted $y_f(t) = \hat{y}(t|t-m)$) the previously presented estimation algorithm can be used.

4.5 Simulated examples

In this section some simulations are performed to illustrate how well the respiration rate and the K_La function can be estimated using different respiration rate and K_La models.

4.5.1 Simulation setup

In the simulations, a setup is used which approximately corresponds to the first aerobic zone in the pilot plant at Kungsängsverket. In the pilot plant the airflow rate can not be measured. Instead the valve opening is used, see Section 4.6.1 for more details. If the airflow rate or valve opening is used does not change the estimation algorithm, the general idea is the same.

The system used for generating the data is simulated by

$$y(t+1) = y(t)+h^*[\frac{Q(t)}{V}(y_{in}(t)-y(t))+K_La(u(t))(y_{sat}-y(t))-R(t)] \quad (4.61)$$

where

- The wastewater flow, $Q = 1000$ l/h
- The volume of the zone, $V = 630$ l
- The saturated DO, $y_{sat} = 10$ mg/l
- The influent DO, $y_{in}(t) = 0$ mg/l
- The oxygen transfer function $K_La(u) = 5 \arctan(\frac{20u}{1000})$ h^{-1}
- The respiration rate $R(t) = 20 + 15 \sin(6t)$ mg/l/h.
- $h^*(t) = \frac{1}{A(t)}(e^{A(t)h} - 1)$, $A(t) = -(K_La(u(t)) + \frac{Q(t)}{V})$
- The sampling period, $h = 1/360$ h, (10s)
- Zero mean white measurement noise with standard deviation 0.1 has been added to the output.

In the estimation algorithm the following setup is used:

- Correct values were used for Q/V, $y_{in}(t)$ and y_{sat}.
- In the covariance matrix R_1, γ_1 is set to 0, and γ_2 is given by:
  - $\gamma_2 = 100$ for the random walk model.
  - $\gamma_2 = 0.05$ for the integrated random walk model.
  - $\gamma_2 = 0.2$ for the filtered random walk model where $f = 0.97$.

- The airflow $u(t)$ (valve opening) is divided by 1000 in the estimation algorithm. This scaling makes the estimated K_La parameters to be in the same range. This is especially important when using the exponential model since it improves the numerical properties.
- $\hat{\theta}(0) = [10\ 10\ 10\ 10]^T$. For the random walk model there is one element less in the θ-vector.
- Note, the regressor first has to be filled with (real) data before $\hat{\theta}$ can be updated. Here the first 8 samples are used to fill the regressor with real data. The initial covariance matrix is then selected to:
  * $P(0) = 10^4 I$ for the random walk model.
  * $P(0) = \text{diag}(10^4, 10^4, 10, 10)$ for the integrated random walk model.
  * $P(0) = \text{diag}(10^4, 10^4, 10^2, 10^2)$ for the filtered random walk model where $f = 0.97$.
  * $P(0) = \text{diag}(0, 10^5, 10^5, 10^5, 10^2, 10^2)$ for the filtered random walk model where $f = 0.97$ and the spline approximation is used.
- The grid points for the spline approximation of K_La are equally spaced, i.e. $u_1 = 33.3$, $u_2 = 66.7$, and $u_3 = 100$.

It is *very important* that the input signal is sufficiently exciting, both in amplitude and in frequency to obtain good estimation result, especially when the data are corrupted by measurement noise, as it always is in a real plant.

The estimates may be improved by running the estimation algorithm twice. The final estimates of the K_La parameters and the corresponding elements in the covariance matrix from the first run are then used as initial parameters in the second run. This approach has, however, not been applied here, since the estimates were sufficiently good.

The highly excited airflow rate used for the identification is shown in Figure 4.10, where the corresponding dissolved oxygen concentration also is displayed.

4.5.2 Estimation results of the simulations

The different respiration rate models and K_La approximations are simulated in this section with the previously given parameters.

First an exponential K_La model combined with a random walk model of the respiration rate is simulated. The result is given in Figure 4.11.

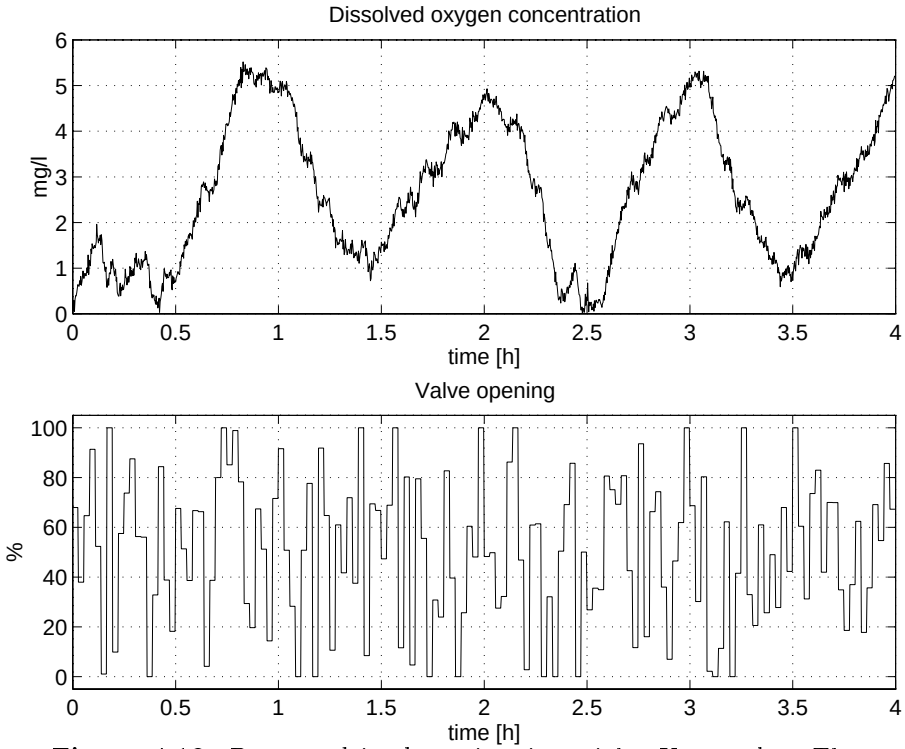

Figure 4.10: Data used in the estimation trials. Upper plot: The dissolved oxygen concentration (y) Lower plot: The valve opening. The DO is simulated from the input $u(t)$.

As can be seen, both the estimated K_La and the estimated time-varying respiration rate is quite close to their true values.

An exponential K_La model and integrated random walk model is applied in Figure 4.12. This method tracks the respiration rate slightly better during some periods, but slightly worse during other periods. It seems like the estimated respiration rate has problems to change to an upward direction.

The exponential K_La model and filtered random walk seem to give the best result, which can be seen in Figure 4.13. The estimated respiration rate has just a small time lag and the estimated K_La is very close to the true function.

Applying the cubic spline K_La model and filtered random walk to the same data gives the result in Figure 4.14, which is very similar to to the exponential K_La model with the filtered random walk model.

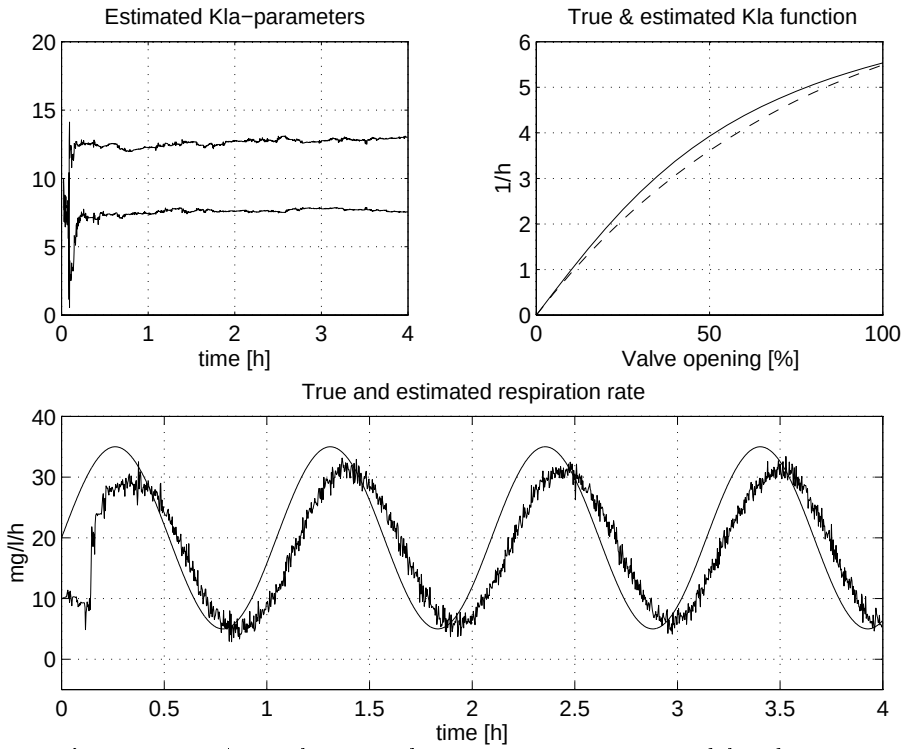

Figure 4.11: A simulation with an exponential K_La model and a random walk model of the respiration rate. Upper left plot: The settling of the parameters in the exponential K_La model. Upper right plot: True K_La (solid line) and estimated K_La (dashed line) at the final time. Lower plot: True (smooth line) and and estimated respiration rate.

As a conclusion one can say that the different suggested methods do not show any large differences. What is most important is the initialization of the covariance matrix P and choice of the R_1 matrix. A filtered random walk model seems, however, to be to prefer. A spline or exponential model give almost identical results. Since the exponential model is simpler we might as well use that one.

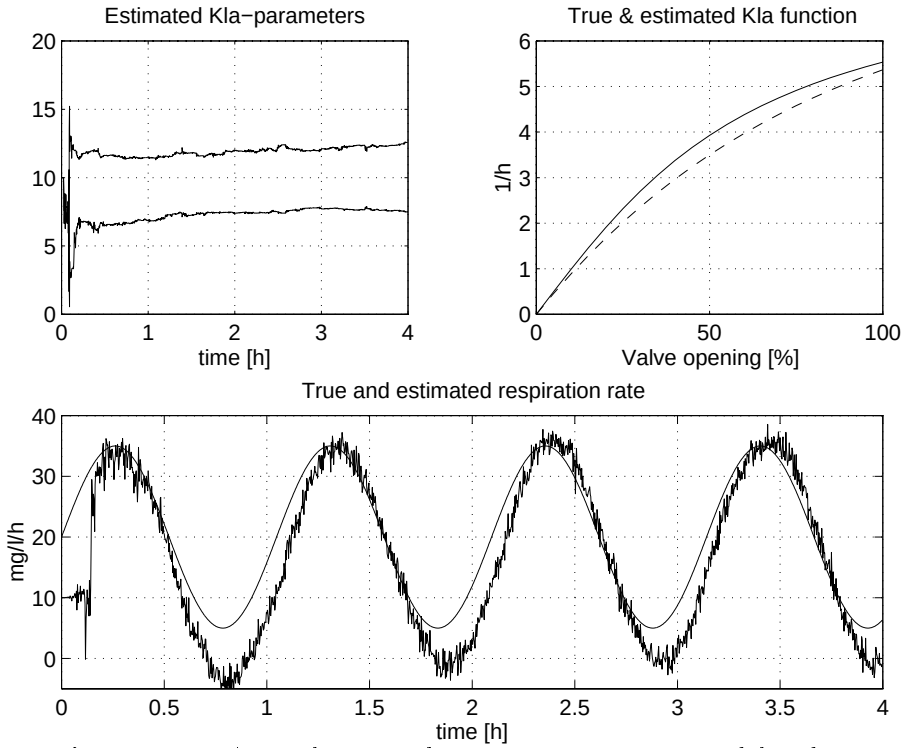

Figure 4.12: A simulation with an exponential K_La model and an integrated random walk model of the respiration rate. Upper left plot: The settling of the parameters in the exponential K_La model. Upper right plot: True K_La (solid line) and estimated K_La (dashed line) at final time. Lower plot: True (smooth line) and and estimated respiration rate.

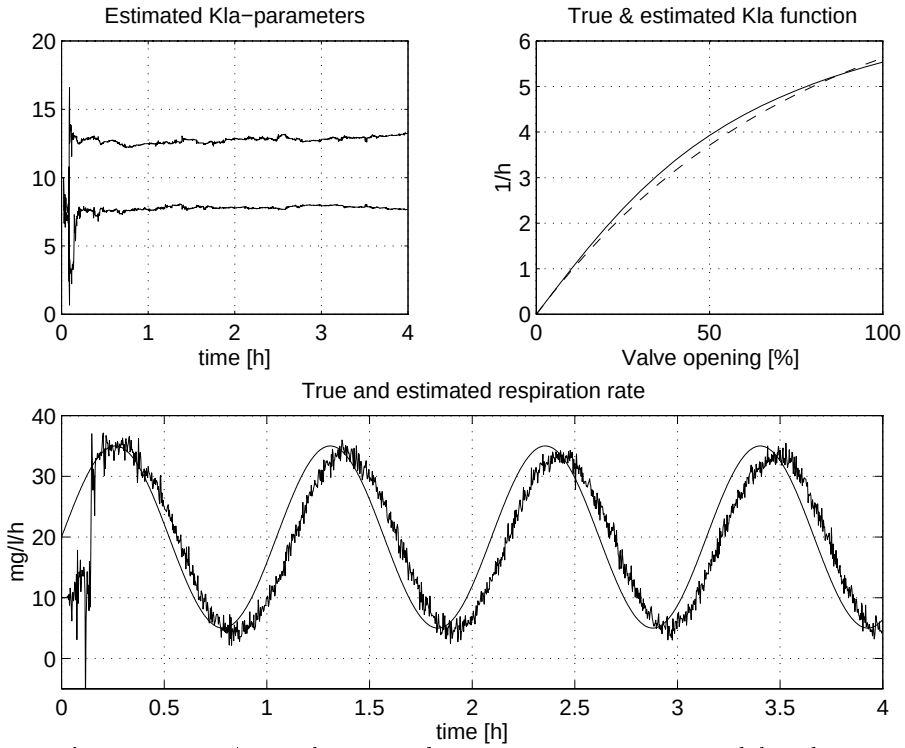

Figure 4.13: A simulation with an exponential K_La model and an filtered random walk model of the respiration rate. Upper left plot: The settling of the parameters in the exponential K_La model. Upper right plot: True K_La (solid line) and estimated K_La (dashed line) at final time. Lower plot: True (smooth line) and and estimated respiration rate.

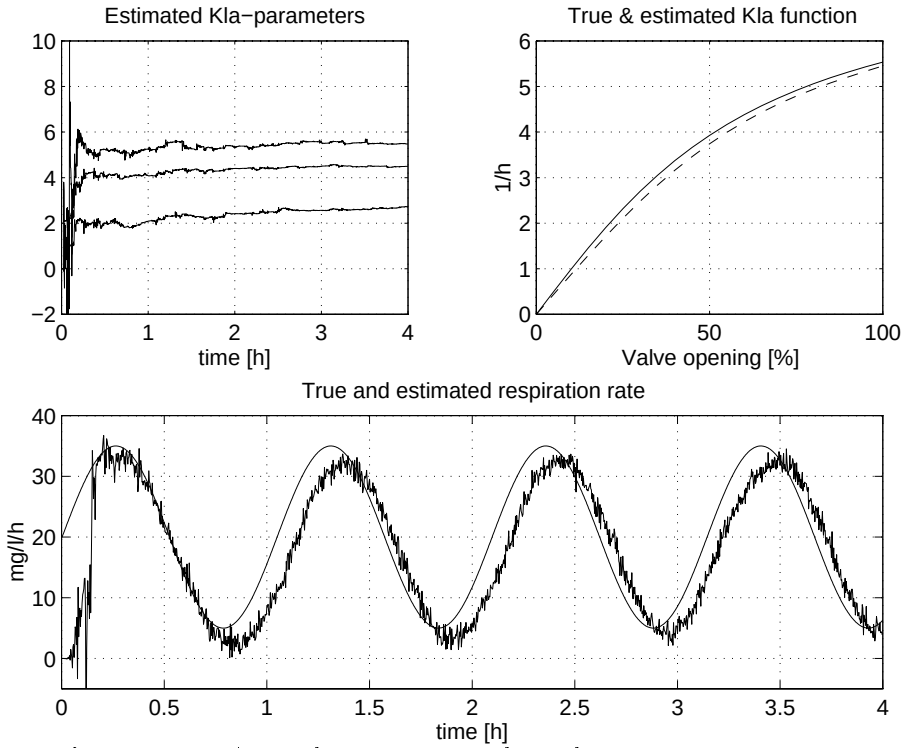

Figure 4.14: A simulation with a cubic spline K_La approximation and a filtered random walk model of the respiration rate. Upper left plot: The settling of the parameters in the spline K_La model. Upper right plot: True K_La (solid line) and estimated K_La (dashed line) at final time. Lower plot: True (smooth line) and and estimated respiration rate.

4.5.3 Simulation with time-varying K_La

A simulation has been made to study the effect of a time-varying K_La function. The same setup is used as before, but at $t = 1.5$h the true K_La function is increased by a factor 2. The parameter $\gamma_1 = 1$ during the whole simulation, this to allow variations in K_La. The result of the estimation experiment is shown in Figure 4.15, and the corresponding DO concentration is shown in Figure 4.16. The airflow rate is the same as before.

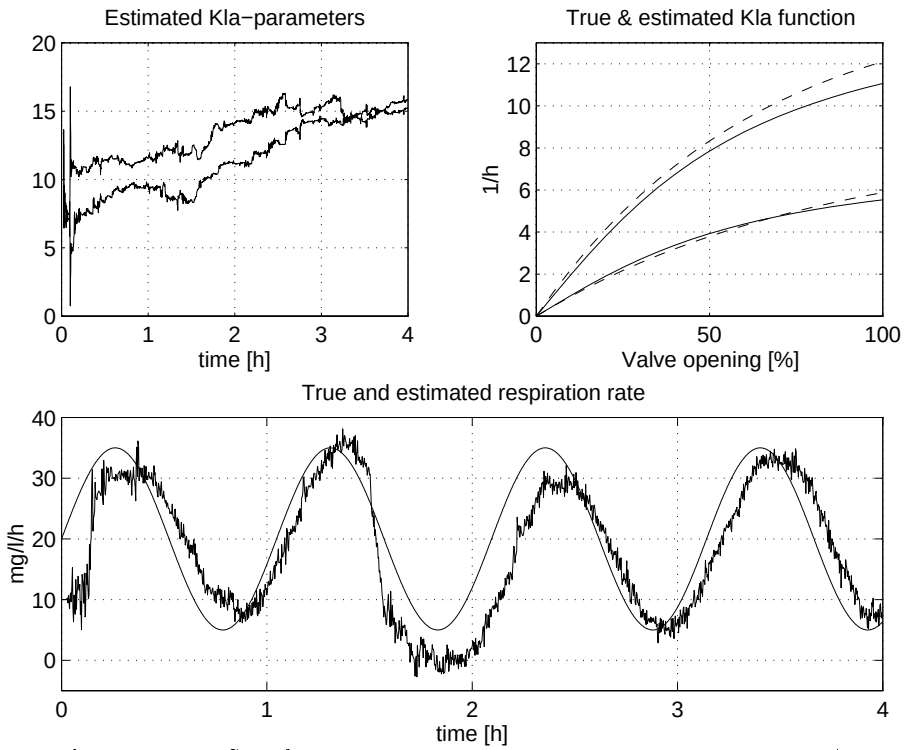

Figure 4.15: Simulation experiment with a time-varying K_La . At $t = 1.5$h the true K_La function is multiplied by 2. An exponential K_La function and a filtered random walk model of the respiration rate is used. Upper right plot: True K_La (solid line) and estimated K_La (dashed line) at 1.5h (lower curves) and at final time (upper curves). Lower plot: True (smooth line) and and estimated respiration rate.

It is interesting to see how fast the estimation algorithm recovers after the change in K_La. Studying the estimated respiration rate we find that one hour after the change in K_La, it is back on reasonable values again.

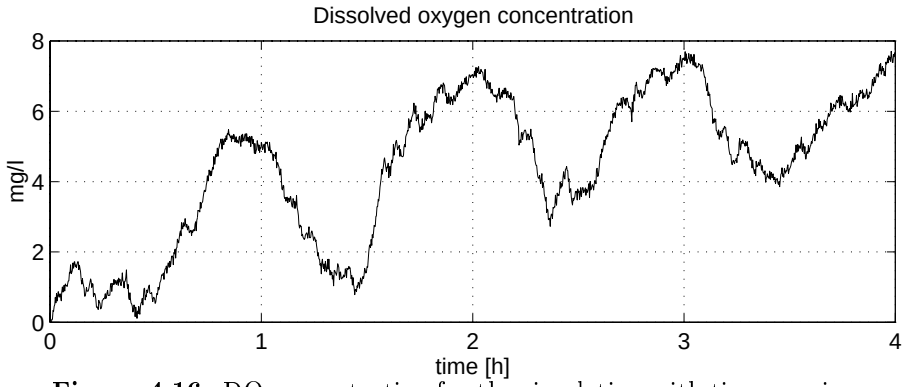

Figure 4.16: DO concentration for the simulation with time-varying K_La.

4.5.4 Simulation with a slow DO sensor

The influence of the sensor dynamics will here be illustrated by comparing two estimation experiments, one where the sensor dynamics has been taken into account and one where it has not.

The estimation result is presented in Figure 4.17 where estimates of K_La and respiration rate are compared with and without filtering of the DO measurements. The filter which filters the DO sensor signal is given in (4.60), and the sensor dynamics are given by (4.58). Note that the estimates based on no filtering of the DO sensor signal becomes more biased than the estimates obtained when the suggested filtering procedure is used.

Remark: The bias in the estimates becomes larger if the excitation (in frequency) of the airflow rate is increased, and smaller if the excitation is decreased. Note, however, that a high excitation is necessary for tracking of fast time variations of the respiration rate. A perhaps intuitive way to understand why there will be a bias in the estimates when using a highly excited airflow rate is the following. The DO sensor low pass filters the DO measurements. These measurements do then appear less excited than what they actually are. If u is highly excited, and y is not, the estimator gives a smaller value of the estimated K_La function than the true value, because a DO process with a smaller value of K_La gives the same effect on $y(t)$, as a slow DO sensor do. Since the expression $K_La(u)(y_{sat} - y) - R$ is used in the estimator, a smaller K_La also gives a smaller estimate of the respiration rate.

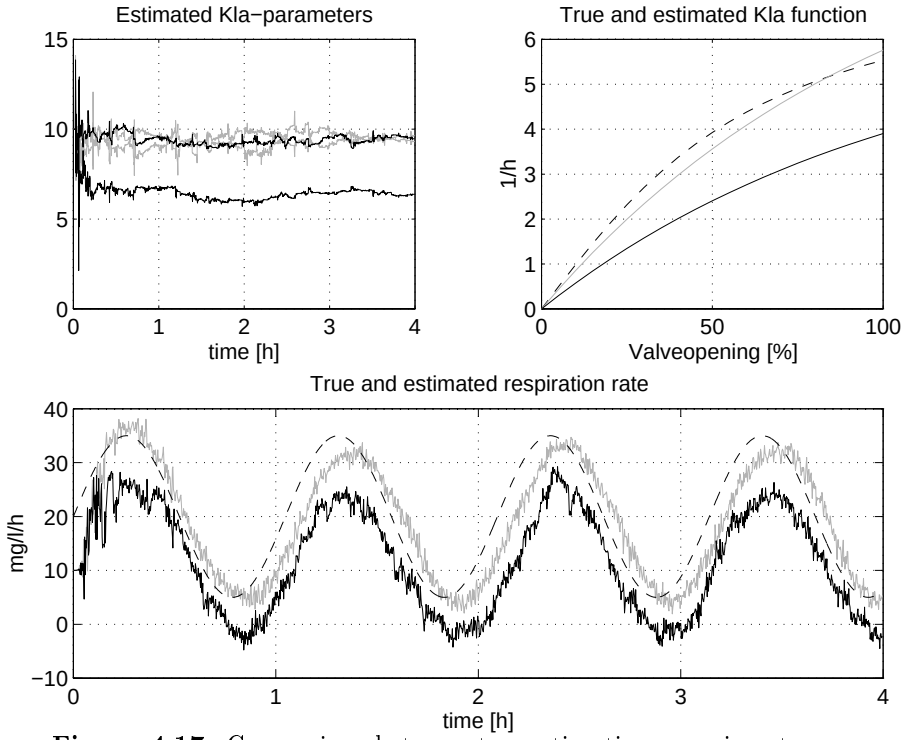

Figure 4.17: Comparison between two estimation experiments, one where the sensor dynamics has been taken into account and one where it has not. In all plots, dashed lines correspond to true values, grey lines to estimates with filtered DO measurements and black lines to estimates where no filtering has been applied.

4.6 Application to real data

In this section the exponential K_La model and filtered random walk model are used in the estimation algorithm. Laboratory batch experiments of the respiration rate have for comparison also been measured. How the nonlinear valve characteristics is included in K_La is also considered.

4.6.1 Including the valve characteristics in K_La

In the pilot plant, as well as in many other plants, no measurements of the airflow rates are available. A reasonable approach (for not very fast sampling) is then to neglect the valve dynamics and regard the valve as a nonlinear static function, i.e.

$$u(t) = g(\varphi(t)) \tag{4.62}$$

where $u(t)$ is the airflow rate, g is a static function and $\varphi(t)$ is the valve opening which is measurable.

Including (4.62) in the K_La model gives

$$y(t+1) = y(t)+h[\frac{Q(t)}{V}(y_{in}(t)-y(t))+K_La^g(\varphi(t))(y_{sat}-y(t))-R(t)]+w(t) \tag{4.63}$$

where

$$K_La^g(\varphi(t)) = K_La(g(\varphi(t))) \tag{4.64}$$

The approach presented in Section 4.3 can now be applied by replacing K_La with K_La^g.

4.6.2 A practical experiment

Several experiments have been performed to estimate K_La and the respiration rate, both in the pilot plant and in the full scale plant, see e.g. Carlsson and Wigren (1993), Carlsson (1993), Carlsson *et al.* (1994*a*) and Lindberg and Carlsson (1996*c*). Here, one of the experiment in the pilot plant at Uppsala wastewater treatment plant is presented.

In the experiment filtering of the DO measurement is applied. The setup of the DO filter and the estimator is identical to the setup used in the simulation study presented in Section 4.5.4. The respiration rate has for comparison also been measured in laboratory batch experiments, see Section 4.6.3 for a further explanation.

In Figure 4.18 the estimated and measured respiration rate are presented. Note that the different methods almost obtain the same values of the respiration rate.

Remark 1: If the DO measurement is not filtered, the estimated respiration rate became lower, here ≈ 3 mg/l/h.

Remark 2: Practical experiment have shown that the estimated respiration rate depends on the airflow rate and/or DO. This was detected in sequential experiments with identical excitation sequences where a correlation between the estimated respiration rates was detected. The true respiration rate probably depends on the DO since, for example, DO=0 gives $R(t) \approx 0$.

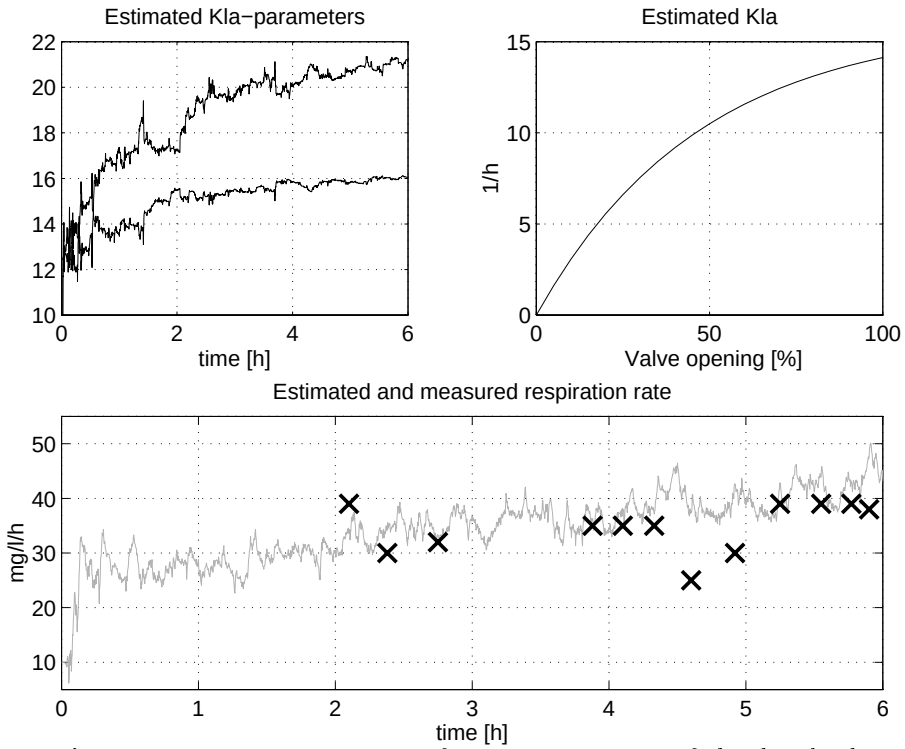

Figure 4.18: Estimation result from measurements of the dissolved oxygen concentration in the pilot plant. Measured respiration rate is marked by x.

4.6.3 Laboratory batch experiments

The laboratory batch experiments were done in the following manner. A sample from the sludge in the activated sludge process was taken when the DO was high. Immediately after the sample was taken a fast oxygen sensor was put into the sample for registering the decay of the DO. The respiration rate was then considered to be equivalent to the mean derivative of the DO slope during the first 100 s. The slope of the DO is time-varying. In the beginning the derivative is large and in the end it is small. During the first 100 s it is still quite large.

4.7 Experiments with surface active agents

The surfactants which are important ingredients in modern washing agents have been suspected to lower the K_La values at the WWTP. Investigations in Wagner and Pöpel (1996) have shown that surfactants do affect K_La.

Three different types of surfactants exists, nonionic, anionic, and kationic. The nonionic surfactants reduce the oxygen transfer more than the others, see Wagner and Pöpel (1996). A problem with a low K_La value is that it is harder to maintain a desired DO set-point and that it requires more energy to do so. The DO set-point is difficult to reach due to the fact that little oxygen is transfered to the wastewater.

To make further evaluation some experiments have been conducted in the pilot plant in cooperation with Jonas Röttorp at IVL who was principal investigator. An external nonionic surfactant (alcohol ethoxylate) was added to the influent water to the pilot plant. The flows and concentrations were varied during the experiment in the following manner:

1. Surfactant concentration 10 mg/l, influent flow 200 l/h, internal recirculation 400 l/h and return sludge flow 200 l/h.
2. The same surfactant concentration, but influent flow 400 l/h, internal recirculation 800 l/h and return sludge flow 350 l/h.
3. Surfactant concentration lowered to 5 mg/l, and the same flow rates.
4. Surfactant dosing switched off, and the same flow rates.

In the first phase of the experiment, when the flows were low, no influence of the surfactant was detected. Therefore the flow rates were increased. The surfactant dosing was also increased to maintain the same concentration in the influent flow. A significant decrease in the estimated K_La could then be seen, and it was not possible to maintain the desired DO, even though the airvalve was completely open. In the end of the experiment the dosage was lowered to 5 mg/l, but the K_La value was still at the same low level. When the external dosage of surfactants was switched off, the estimated K_La increased again. The DO was back at normal levels after a few days. The respiration rate and K_La was estimated with the previously outlined method.

At the pilot plant, where the experiment was conducted, one line was used as a reference line and the other was used for the experiments. In Figures 4.19, 4.20 and 4.21 some typical estimation results from the experiments are presented. Due to a mistake no data were saved from the experimental line before the experiment was conducted, so a comparison before and during dosage can not be made. The lines at the pilot plant were, however, not identical when the experiment started. Among other things the suspended solids concentration differed, but when comparing the different figures one can still see that

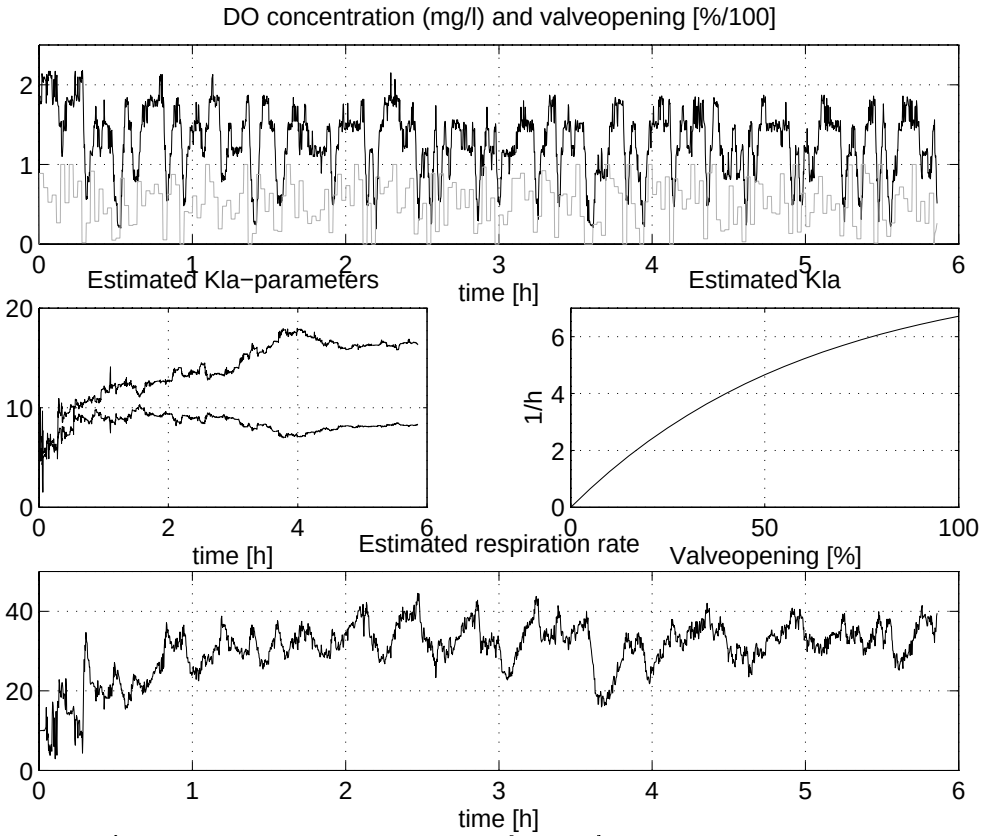

Figure 4.19: Estimation in the reference line. In the upper plot, is the DO the black line and the grey line is the valve opening/100.

- K_La and the respiration rate is significantly higher in the reference line. Note that from the definition in (4.2), $K_La = \alpha K_La_{CW}$. Hence the change of K_La is due to changes in the factor α.
- K_La and the respiration rate increases when the surfactant dosage is switched off.
- Both K_La and the respiration rate are affected by the surfactant dosage.
- Normally the DO varies quite much when the airflow rate is changed, but in Figure 4.20 where the surfactant is added, almost nothing happens in the DO (which also is very low). The reason is that both K_La and the respiration rate have become very low.

The suspended solids concentration decreased from about 3 g/l to 1 g/l

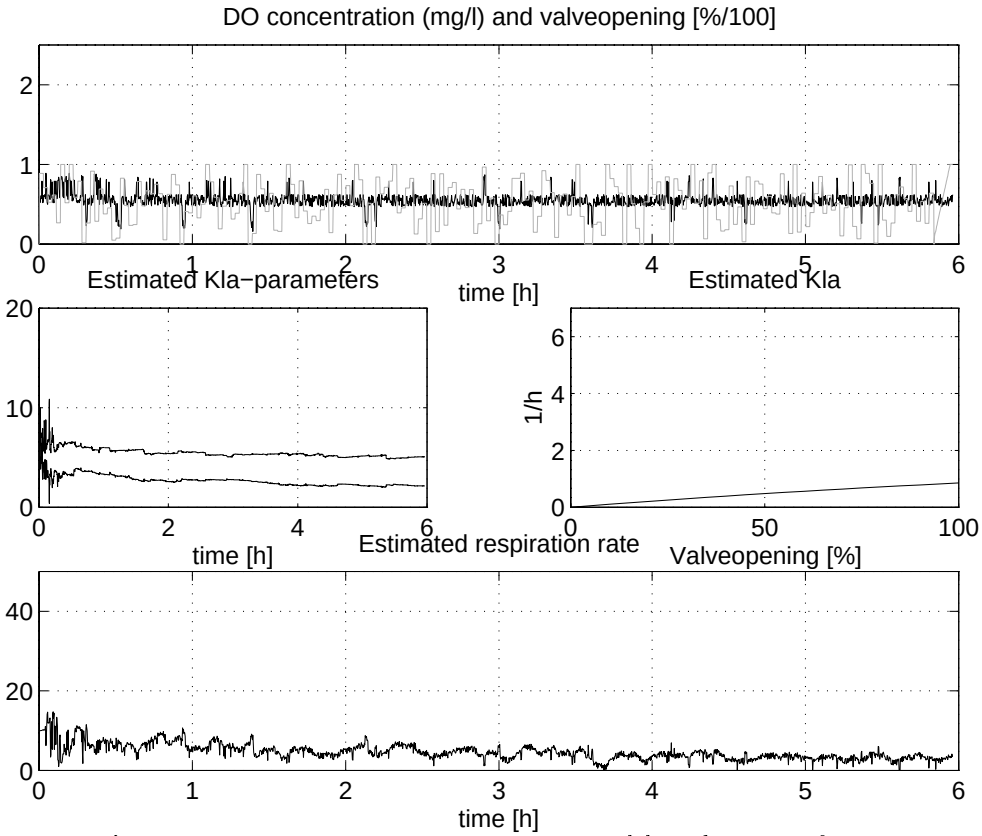

Figure 4.20: Estimation in the experimental line during surfactant dosage. In the upper plot is the DO the black line and the valve opening/100 is the grey line.

during the experiment in the experimental line. The suspended solids concentration was reasonable constant around 2.5 g/l in the reference line. The excess sludge pumping was switched off in both lines. Thus, the decrease of the sludge concentration in the experimental line is caused by bad settling properties. The results of the experiments therefore also indicates that the surfactant may have a bad effect on the settling properties. A lower suspended solids concentration also affect the estimated respiration rate which becomes lower, due to less biomass.

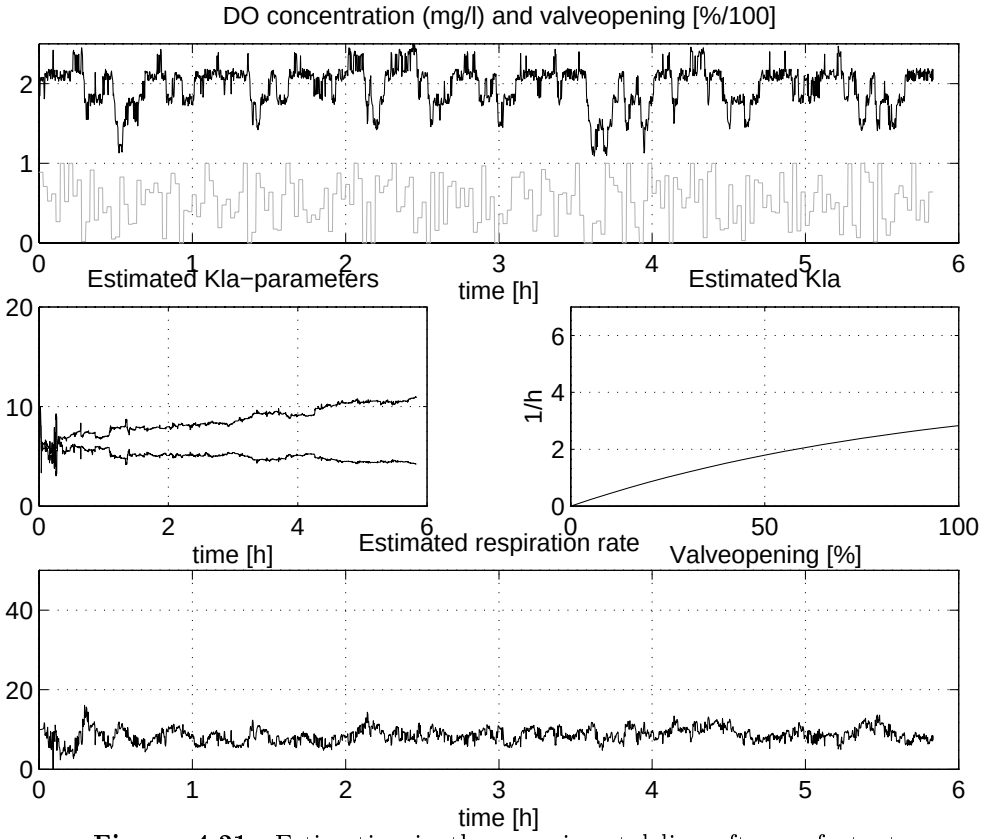

Figure 4.21: Estimation in the experimental line after surfactant dosage. In the upper plot is the DO the black line and the valve opening/100 is the grey line.

4.7.1 Laboratory batch experiments

Laboratory batch experiments for measuring K_La (for a fixed airflow rate, which also gives a fixed K_La) was made during the experiments. The method is based on studying an increase in DO as illustrated in Figure 4.22. Assuming $Q(t) = R(t) = 0$ and inserting this in (4.4) gives

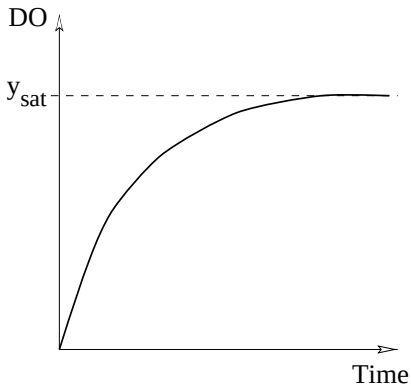

Figure 4.22: Example of an increase in DO during aeration in a batch experiment.

$$\frac{dy(t)}{dt} = K_La(y_{sat} - y(t)) \tag{4.65}$$

It is reasonable to assume $R(t) = 0$, since sedimented wastewater has been used. The solution of (4.65) is

$$y(t) = y_{sat} - Ke^{-K_La\ t} \tag{4.66}$$

where K is an arbitrary constant and t is the time. Reordering and logarithming (4.66) gives

$$\log(y_{sat} - y(t)) = \log(K) - K_La\ t \tag{4.67}$$

K_La (for a fixed airflow rate) is hence found as the slope of a curve generated by $\log(y_{sat} - y(t))$ but with opposite sign. The value of y_{sat} is found as steady-state value from the aeration. This K_La value is, however, not comparable with the one obtained in the estimation algorithm.

This method did, however, not detect any change in K_La, but the suggested estimation method in this chapter did. Since the process required more oxygen during the experiment, it is likely that the suggested method in this chapter gives a more correct answer.

4.8 Conclusions

Identification algorithms for estimating the time-varying respiration rate and the nonlinear K_La function have been presented. The estimation is based on measurements of the dissolved oxygen concentration and the airflow rate. Two different models of the nonlinear K_La function have been suggested: an exponential model and a cubic spline model. Three models for modeling the respiration rate have also been considered: a random walk model, a filtered random walk model, and an integrated random walk model. The exponential model and a cubic spline model were approximately equally good. The filtered random walk model was the best one of the different respiration rate models.

In order to track the time varying respiration rate and the nonlinear K_La function, a Kalman filter was used. To illustrate the estimation procedure simulation studies have been performed with good results. The results from the simulations were also confirmed on real data from a pilot activated sludge plant, where the estimated respiration rate was compared with batch laboratory measurements. Also, a nonlinear model of the oxygen transfer function was achieved.

When the DO sensor has dynamics it should not be neglected. By filtering the output from the DO sensor, the influence of the sensor dynamics can be reduced. The filtering procedure may also be useful in other applications where there is need for compensating the sensor dynamics, e.g. in respirometers.

An experiment with surface active agents was performed and the suggested estimation method was applied to detect changes in K_La and the respiration rate. Significant changes were detected in both K_La and the respiration rate which decreased to almost zero. An interesting observation is that when the DO is affected by surfactants, the DO is almost constant. The DO will not become lower due to the respiration rate is almost zero, and the DO will not increase by increased airflow rate due to K_La is almost zero.

Chapter 5

Control of the dissolved oxygen concentration

The dissolved oxygen concentration (DO) in the aerobic part of an activated sludge process should be sufficiently high to supply enough oxygen to the microorganisms in the sludge, so organic matter is degraded and ammonium is converted to nitrate. On the other hand, an excessively high DO, which requires a high airflow rate, leads to a high energy consumption and may also deteriorate the sludge quality. A high DO in the internally recirculated water also makes the denitrification less efficient, see Olsson and Jeppson (1994). Hence, both for economical and process reasons, it is of interest to control the DO. Several control strategies for the DO have been suggested in the past. Flanagan *et al.* (1977) presented a linear PI controller with feedforward from the respiration rate and the flow rate. In Wells (1979) different control strategies for the activated sludge process were applied, among others DO control. A dead-beat controller, based on a recursively estimated model with a linear $K_L a$ was designed in Ko *et al.* (1982). Holmberg *et al.* (1989) and Bocken *et al.* (1989) also base their design on a recursively estimated model with a linear $K_L a$, but the excitation of the process was improved by invoking a relay which increases the excitation. Pole placement was then used to design the controller. Rundqwist (1986) designed a self-tuning controller, and Carlsson *et al.* (1994*a*) have applied auto-tuning.

One problem with controlling the DO is that the process dynamics are nonlinear. This means that high control performance for all operating conditions may be hard to achieve with a linear controller. The objective of the work presented here is a design method which gives a high performance

controller for all operating conditions. The key idea is to explicitly take the nonlinear characteristics of the oxygen transfer function K_La into account in the control design. The design method consists of two separate parts: an estimation part described in Chapter 4 and a controller design part which is presented here.

The controller design is based on a linearization of the DO process, obtained by using the inverse of the estimated $K_La(u)$. Two different control design approaches are suggested for the linearized DO process:

- A pole-placement design with a PI controller
- A linear quadratic (LQ) controller which uses feedforward from the respiration rate upstream.

An advantage compared to auto-tuning of PID-regulators, see Åström and Hägglund (1984) or Åström and Wittenmark (1989), is that the suggested nonlinear controller requires only one single tuning (estimation) event, while auto-tuning of a gain scheduling regulator may require several tunings for this type of nonlinear process.

An important issue is the choice of set-point for the DO controller. In practice the DO set-point often is kept at some fixed level. A DO set-point controller is suggested, where the set-point is selected so that a prespecified ammonium concentration in the last aerated zone is obtained, see also Nielsen and Lynggaard (1993). Using the set-point controller in the pilot plant made it not only possible to save energy due to a lower DO set-point, the effluent nitrate concentration was also reduced significantly. The nitrate reduction probably depends on that the lower DO levels made denitrification in the aerated zones possible. The naturally existing carbon in the aerated zones is then in a larger extent used for denitrification instead of being oxidized. Less oxygen is also recirculated when using a low DO set-point, which improves denitrification in the anoxic zone. Possible disadvantages may be that the sludge properties deteriorate due to the low DO, and that nitrous oxide (N_2O) can be formed when the DO is low. These problems should, however, be compared to the achieved improvements.

To save energy the air pressure in the aeration system can be controlled. A strategy suggested in, for example Rundqwist (1986) and Robinson (1990) has been evaluated in the pilot plant with positive result.

The outline of the chapter is as follows. The control problem is presented in Section 5.1, where problems using linear control of a nonlinear process are discussed. The controller design of a nonlinear PI-controller

and a nonlinear LQ-controller with feedforward are is given in Section 5.2. The different control strategies are compared in some simulation studies in Section 5.3. The proposed controllers are compared at the pilot plant in Section 5.4. Section 5.5 presents a controller for controlling the set-point of the dissolved oxygen. It is based on control of the ammonium concentration. A practical experiment with the DO set-point controller has been made in the pilot plant. Section 5.6 gives a short review of a common pressure controller which minimizes the pressure drop over the throttle valves. Finally, the conclusions are given in Section 5.7.

5.1 The control problem

The gain of the DO process varies with respect to the airflow rate due to the nonlinear K_La function, see Figure 4.2 and Olsson and Piani (1992). The DO process also has a bilinear term ($K_La(u)y$), see further (5.1). This may cause problems when using a linear controller. In Figure 5.1 such a problem is illustrated, where a linear PI-controller is tuned for high performance during a high airflow rate but used for a low airflow rate. More examples are given in Section 5.3. A high airflow rate corresponds here to 80% open valve. When the load to the plant decreases, the process gain (the derivative of K_La) increases, and an oscillating system is obtained.

If the linear controller instead was tuned for high performance during a low load, a slow closed loop response would be obtained for a high load. A fair step response for all loads is however possible by taking the nonlinear K_La into account. This is utilized in the following sections.

5.2 The nonlinear DO controller

In the past there has been an extensive research in controller design for linear systems, and many high performance controllers for linear systems exist. The DO process is, however, not a linear system. From Chapter 4, the following discrete-time model of the dissolved oxygen dynamics was given.

$$y(t+1) = y(t)+h^*[\frac{Q(t)}{V}(y_{in}(t)-y(t))+K_La(u(t))(y_{sat}-y(t))-R(t)] \quad (5.1)$$

The DO dynamics in (5.1) can be linearized by introducing a variable $x(t)$, defined as

$$x(t) = K_La(u(t))(y_{sat} - y(t)) \quad (5.2)$$

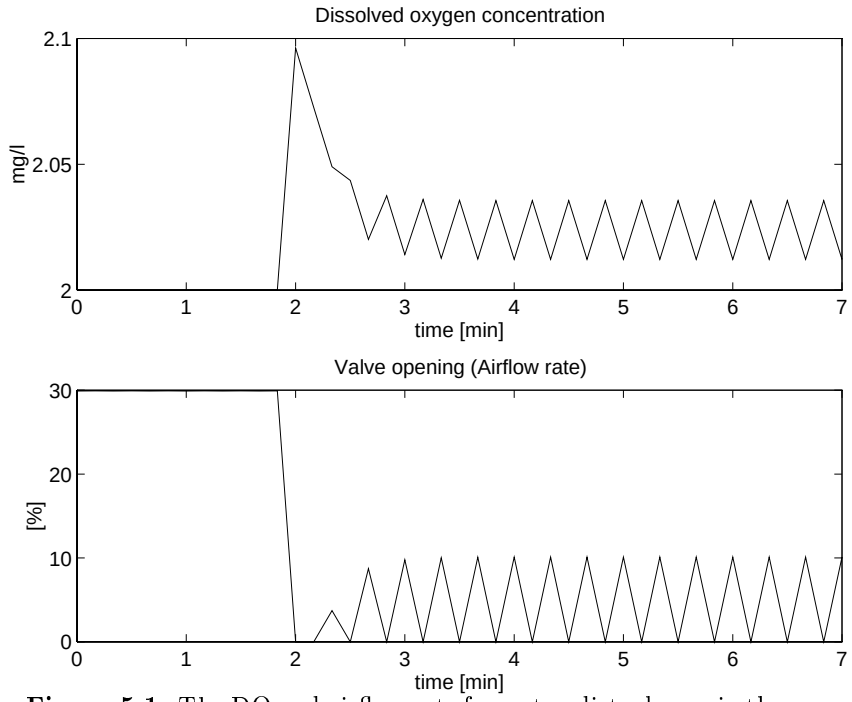

Figure 5.1: The DO and airflow rate for a step disturbance in the respiration rate during a low load (low respiration rate) when controlled by a linear PI-regulator which is tuned for a high load.

The control signal $u(t)$ is calculated by using the inverse of an estimated K_La function. This approach is sometimes referred to as *exact linearization*, see Khalil (1996). The linearization requires that the estimated K_La model is invertible. An exponential model can be a suitable choice. See further Chapter 4 for how an estimated K_La function can be obtained. The control signal $u(t)$ is determined by replacing K_La with its estimate, and using (5.2)

$$u(t) = \widehat{K_La}^{-1}(\frac{x(t)}{y_{sat} - y(t)}) \tag{5.3}$$

This procedure extends the idea used in Holmberg *et al.* (1989), where a linear K_La model was used.

For the case when an exponential model of K_La is used ($K_La(u) = k_1(1 - e^{-k_2 u})$), see (4.10) $u(t)$ is given by

$$u(t) = -\frac{1}{\hat{k}_2}\ln\left(1 - \frac{x(t)}{\hat{k}_1(y_{sat} - y(t))}\right) \tag{5.4}$$

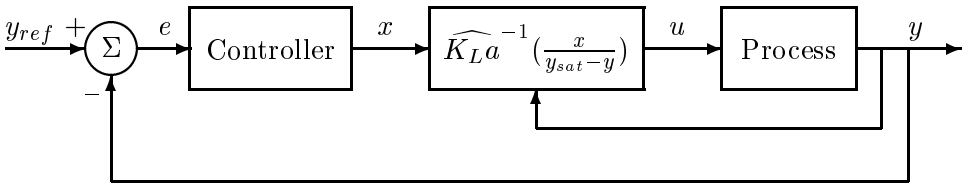

Figure 5.2: The basic idea with the nonlinear controller.

A block diagram of the linearized process is shown in Figure 5.2.

If the derivative of the estimated K_La is different from the derivative of the true K_La function, the gain of the process model (the derivative of K_La) will also be different. This may deteriorate the controller performance. If the estimated K_La is smaller than the true, the controller gain will be larger than expected. A too large controller gain may result in a noise and modeling error sensitive controller. If the estimated K_La becomes larger than the true K_La the resulting controller will instead be slower than expected.

Inserting (5.3) in the process model (5.1) and assuming a correctly estimated K_La gives the linearized process model

$$(q - 1 + \frac{Q}{V}h^*)y(t) = h^*x(t) + h^*\frac{Q}{V}y_{in}(t) - h^*R(t) \tag{5.5}$$

Note that the flow (Q) usually is time-varying. When using (5.5) for controller design the controller parameters will then also be time-varying.

Remark: In the above discussions we have neglected the valve characteristics. If the valve characteristic is nonlinear, two approaches are possible.

- Use cascade control, where a local controller controls the airflow rate, see Rundqwist (1986) and Robinson (1990). Obviously this approach requires the airflow rate to be measured.
- Use a model to compensate for the nonlinear valve characteristics. This can easily be incorporated in the K_La model, see further Section 4.6.1.

5.2.1 Pole-placement with a PI-controller

Pole-placement will here be used to choose suitable parameters of a PI-regulator. The controller design is performed in two steps. First the closed

loop transfer function is derived, then the controller parameters are determined from a user specified pole-placement, e.g. a double pole.

The transfer function for a continuous-time PI-regulator is

$$X(s) = K(1 + \frac{1}{T_I s})E(s) \tag{5.6}$$

where $X(s)$ and $E(s)$ are the Laplace transforms of the controller output and error signal, K is the proportional gain and T_I is the integration time. The error signal is defined as

$$e(t) = y_{ref}(t) - y(t) \tag{5.7}$$

Sampling the PI controller (5.6) with an Euler (backward difference) approximation gives

$$x(t) = K(1 + \frac{qh}{T_I(q-1)})e(t) \tag{5.8}$$

where h is the sampling period. By combing the transfer function from $x(t)$ to $y(t)$ in (5.5) with the controller (5.8), the closed loop transfer function from $y_{ref}(t)$ to $y(t)$ is found to be

$$H_{CL}(z) = \frac{Kh^*((1 + \frac{h}{T_I})z - 1)}{z^2 + z(h^*(\frac{Q}{V} + K + \frac{Kh}{T_I}) - 2) + 1 - h^*(\frac{Q}{V} + K)} \tag{5.9}$$

To calculate suitable parameter values for K and T_I, the closed loop poles are selected to be a double pole in $z = p$. Complex conjugated poles would of course also be possible, but will not be considered. Comparing the poles of (5.9) with the desired pole location

$$(z - p)^2 = z^2 - 2zp + p^2 \tag{5.10}$$

gives two equations, where K and T_I are found to be

$$K = \frac{1 - p^2}{h^*} - \frac{Q}{V} \tag{5.11}$$

$$T_I = \frac{h}{\frac{1}{K}(\frac{2-2p}{h^*} - \frac{Q}{V}) - 1} \tag{5.12}$$

This method is an easy way of tuning a PI-controller. The user has only to choose one parameter, the pole location p. The pole location approximately trades off control energy and speed. A double pole close to 1 gives a slow controller which is less sensitive to noise and modeling errors, while a pole location close to the origin gives a fast closed loop system that, however, is sensitive system to noise and modeling errors.

Remark 1: To calculate the controller parameters K and T_I, the parameter h^* is needed, see (4.7). Since it involves $K_La(u)$, which is not known, this might be difficult. Reasonable choices are to approximate $K_La(u)$ in h with a fixed value of $K_La(u)$, for example $K_La(u_{max})/2$, or to iterate twice to find a reasonable $u(t)$ which determines $K_La(u)$.

Remark 2: Feedforward from $y_{in}(t)$ may be used in combination with a PI-regulator. The feedforward can be derived from (B.23), where the PI-controller has to be expressed in the form of $R(q^{-1})$ and $S(q^{-1})$ polynomials. An alternative is to use a static feedforward compensator.

Remark 3: The zeros can not be controlled with this structure of the PI controller. Zeros slower than the poles may cause overshoot in the step response despite real valued poles. Unstable zeros cause a non-minimum phase system, where the step response first may go in the wrong direction. The zeros can be moved by scaling the reference signal.

Remark 4: The PI controller (5.8) can be implemented in differential form, i.e.

$$\begin{aligned} \Delta x(t) &= K(\Delta e(t) + \frac{h}{T_I}e(t)) && (5.13)\\ x(t) &= x(t-1) + \Delta x(t) && (5.14) \end{aligned}$$

which makes it easy to constrain the control signal when it has reached its limit.

5.2.2 Linear quadratic (LQ) control with feedforward

An LQ controller with feedforward can be applied to the linearized DO process (5.5). The controller design is started by rewriting the linearized DO process model (5.5) into q^{-1} notation

$$(1 + q^{-1}(\frac{Q}{V}h^* - 1))y(t) = q^{-1}h^*x(t) + q^{-1}h^*\frac{Q}{V}y_{in}(t) - q^{-1}h^*R(t) \quad (5.15)$$

Assume that the respiration rate and the DO of the input flow can be modeled as random walks, i.e.

$$y_{in}(t) = \frac{1}{\Delta}v_1(t) \qquad R(t) = \frac{1}{\Delta}v_2(t) \quad (5.16)$$

Adding a term $C(q^{-1})\frac{1}{\Delta}e(t)$ to describe unmodelled disturbances, the model (5.15) can be written as

$$\begin{aligned} A(q^{-1})y(t) &= q^{-k}B(q^{-1})x(t) + q^{-d_1}D_1(q^{-1})\frac{1}{\Delta}v_1(t)\\ &+ q^{-d_2}D_2(q^{-1})\frac{1}{\Delta}v_2(t) + C(q^{-1})\frac{1}{\Delta}e(t) \quad (5.17) \end{aligned}$$

where the noise sequences $v_1(t)$, $v_2(t)$ and $e(t)$ are all zero mean white noise, and the polynomials and parameters in are given by

$$\begin{array}{ll} A(q^{-1}) = 1 + q^{-1}(\frac{Q}{V}h^* - 1) & D_1(q^{-1}) = h^*\frac{Q}{V} \\ B(q^{-1}) = h^* & D_2(q^{-1}) = h^* \\ C(q^{-1}) = 1 + cq^{-1} & k = 1 \quad d_1 = 1 \quad d_2 = 1 \end{array}$$

The $C(q^{-1})$ polynomial can be considered as a user parameter and is chosen so that $1/C$ becomes low-pass, as suggested in Section 3.6.2. This choice makes the controller less noise sensitive since the high frequency gain is reduced.

The LQ-controller to be used has the following structure

$$R(q^{-1})\Delta u(t) = T(q^{-1})y_{ref}(t) - S(q^{-1})y(t) - \frac{Q_1(q^{-1})}{P_1(q^{-1})}y_{in}(t) - \frac{Q_2(q^{-1})}{P_2(q^{-1})}R(t) \tag{5.18}$$

The derivation of the controller polynomials in (5.18) are identical to the calculations in Section 3.6.3 with $b_2 = 0$. The $T(q^{-1})$ polynomial is given by (3.61) in Section 3.7.6.

This controller uses feedforward from both influent DO and influent respiration rate. If all aerated zones are controlled, the influent DO to a zone can then be expected to have small variations. Not much can then be gained by using feedforward from influent water.

The respiration rate can either be measured by a respirometer or estimated by the algorithm outlined in Chapter 4. Note that it is possible to fix K_La and only estimate the respiration rate by setting all elements in the covariance matrix to zero, except for the ones corresponding to the respiration rate. It is then not necessary to use a high excitation in the airflow rate to estimate the respiration rate.

Remark: For the DO process, it is possible to calculate the PI-controller parameters K and T_I from the pole location in β, see (B.12). The PI-controller will, however, not be identical to the LQ-controller, since the PI-controller moves the closed loop zeros, which the LQ-controller does not.

5.3 Simulations

In Section 5.1 a simulation example was given where the nonlinear K_La was not taken into account in the controller design. This resulted in oscillative control. Some additional examples are given here, where the advantage of

nonlinear control is illustrated. An example where feedforward from the respiration rate is applied, is also shown.

5.3.1 Simulation setup

In the simulations in this section the following setup has been used, which to some extent corresponds to the first aerated zone in the pilot plant at Kungsängsverket, see Section 2.1.

The true system has been simulated by (5.1), i.e.

$$y(t+1) = y(t)+h^*[\frac{Q(t)}{V}(y_{in}(t)-y(t))+K_La(u(t))(y_{sat}-y(t))-R(t)] \quad (5.19)$$

where

- The flow through the zone, $Q = 1000$ l/h
- The volume of zone, $V = 630$ l
- The saturated DO, $y_{sat} = 10$ mg/l
- The influent DO, $y_{in}(t) = 0$ mg/l
- The oxygen transfer function, $K_La(u) = 15(1 - e^{-15\frac{u(t)}{1000}})$ h^{-1}
- Two cases for variations of the respiration rate $R(t)$ are considered, a low load case and a high load case. In the low load case there is a step from 40 to 5 mg O_2/l/h, and in the high load case a step from 60 to 85 mg O_2/l/h.
- $h^*(t) = \frac{1}{A(t)}(e^{A(t)h} - 1)$, $A(t) = -(K_La(u(t)) + \frac{Q(t)}{V})$
- The sampling period, $h = 1/360$ h
- The K_La used for generating the data and the K_La used in the nonlinear controller design are identical.

To get a fair comparison between the linear and nonlinear controller, both controllers should be tuned for equal performance at a given operating point. This can be achieved by adjusting the gain of the controllers appropriately.

For the linear PI-controller, the controller gain is constant at all operating points. This gain is denoted by K_{PI}^{lin}. The gain of the nonlinear

PI-controller can be considered to consist of two parts. A linear part from the PI-controller, denoted K_{PI}^{nonlin} and the gain from the inverse of the estimated K_La function. The latter gain is denoted by K_{inv}^{nonlin}. At a given operating point (u_0), it is determined by

$$K_{inv}^{nonlin} = \frac{1}{\frac{dK_La(u)}{du}(y_{sat} - y(t))}|_{u=u_0} \tag{5.20}$$

The linear and the nonlinear controller becomes equal at a given operating point if

$$K_{PI}^{lin} = K_{inv}^{nonlin} K_{PI}^{nonlin} \tag{5.21}$$

This relation will be used in the comparisons.

Remark: The simulations here correspond to values of the pilot plant at Kungsängsverket, where the airflow rate cannot be measured. The airflow rate $u(t)$ is instead replaced by the valve opening in the simulations.

5.3.2 Examples

The following simulation examples are given here:

- Fast control of the DO, corresponding to pole placement in 0.5.
- Slower control of the DO, corresponding to pole placement in 0.9.
- LQ control with and without feedforward.

All examples are simulated both for a step change at low load where the respiration rate decreases from 40 to 5 mg O_2/l/h, and at a high load where the respiration rate increases from 60 to 85 mg O_2/l/h.

The parameters of the nonlinear PI-controller are determined by (5.11) and (5.12), and the gain of the linear controller is given by (5.21).

The fast control case is shown in Figure 5.3. The figure illustrates that a linear controller which works well for low loads becomes quite slow during high loads. If the linear controller instead is tuned for a high load it becomes oscillative for a low load. The nonlinear controller on the other hand keeps the system well damped at all loads. The reason is that the nonlinear controller change its gain to compensate for the gain changes in the system.

In the next example, a case is illustrated where the controllers are tuned to be slower than in Figure 5.3. What can be seen in Figure 5.4 is that

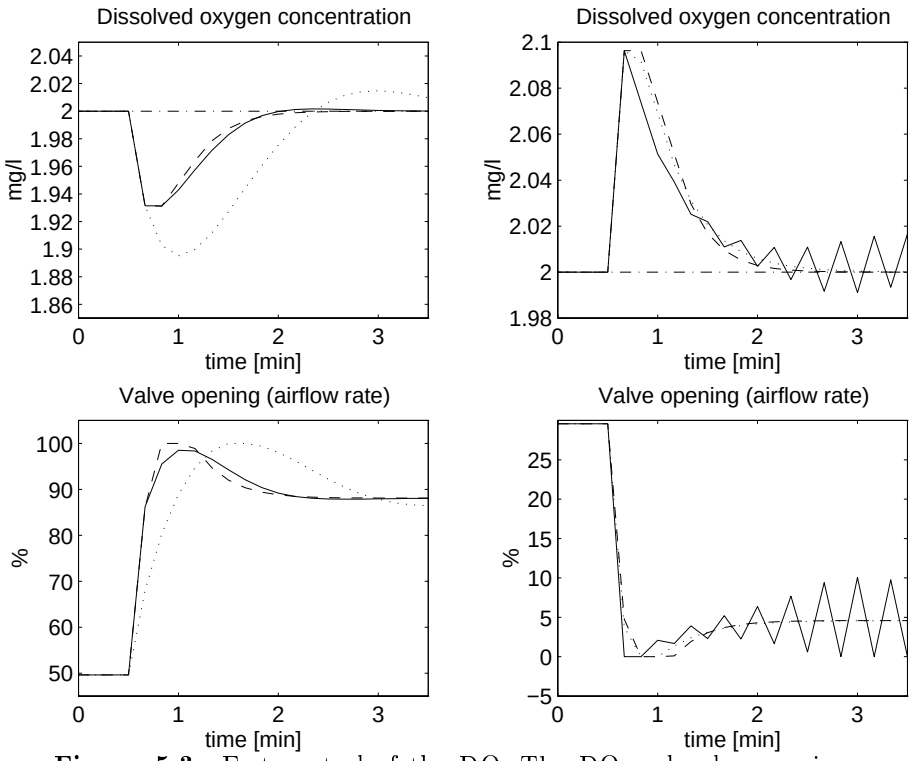

Figure 5.3: Fast control of the DO. The DO and valve openings are shown for a step disturbance in the respiration rate during a high load (left column) and a low load (right column). The reference value (dash-dotted) is 2 mg/l. Two linear PI controllers are used, one tuned at a high load (solid) and another tuned at a low load (dotted). The nonlinear PI-controller is also shown (dashed).

the disturbance at a high load is rejected considerably slower by the linear controller compared to the nonlinear, when they are tuned for equal performance at a low load. A linear controller tuned at a high load becomes instead faster at the load load, while the nonlinear controller maintain the same speed at all operating points.

Feedforward may be included to reject measurable disturbances. An example in Figure 5.5 shows the result of a nonlinear LQ controller with feedforward from the respiration rate. The same controller, but without feedforward, is for comparison also illustrated in the same figure. Zero mean white noise with standard deviation 0.02 has been added to the DO measurements, to illustrate the noise sensivity of the controller. As can be seen in Figure 5.5, the feedforward controller completely rejects the

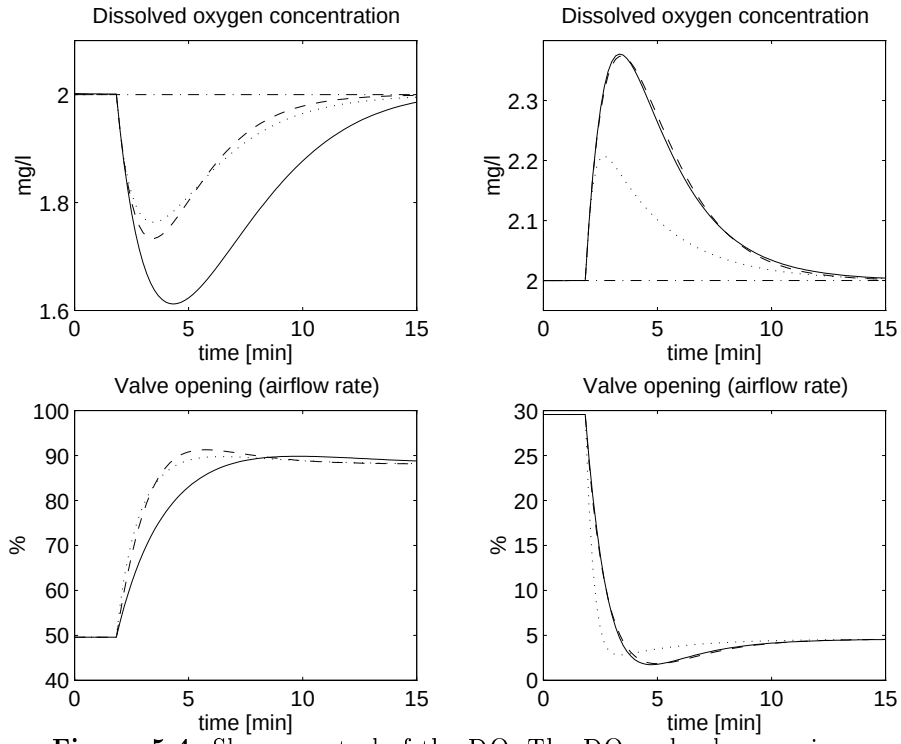

Figure 5.4: Slower control of the DO. The DO and valve openings are shown for a step disturbance in the respiration rate during a high load (left column) and a low load (right column). The reference value (dash-dotted) is 2 mg/l. Two linear PI controllers are used, one tuned at a high load (dotted) and another tuned at a low load (solid). The nonlinear PI-controller is also shown (dashed).

disturbance, while the output is disturbed quite much for the controller without feedforward.

The LQ controller in Figure 5.5 uses separate penalties on the measurable and unmeasurable disturbances, $\rho_e = 10^{-3}$ and $\rho_v = 10^{-4}$. The C-polynomial is set to $C(q^{-1}) = 1 - 0.9q^{-1}$. If the zero of the C-polynomial is chosen close to 1, the controller becomes less sensitive to measurement noise since the high frequency gain in the feedback loop then is reduced.

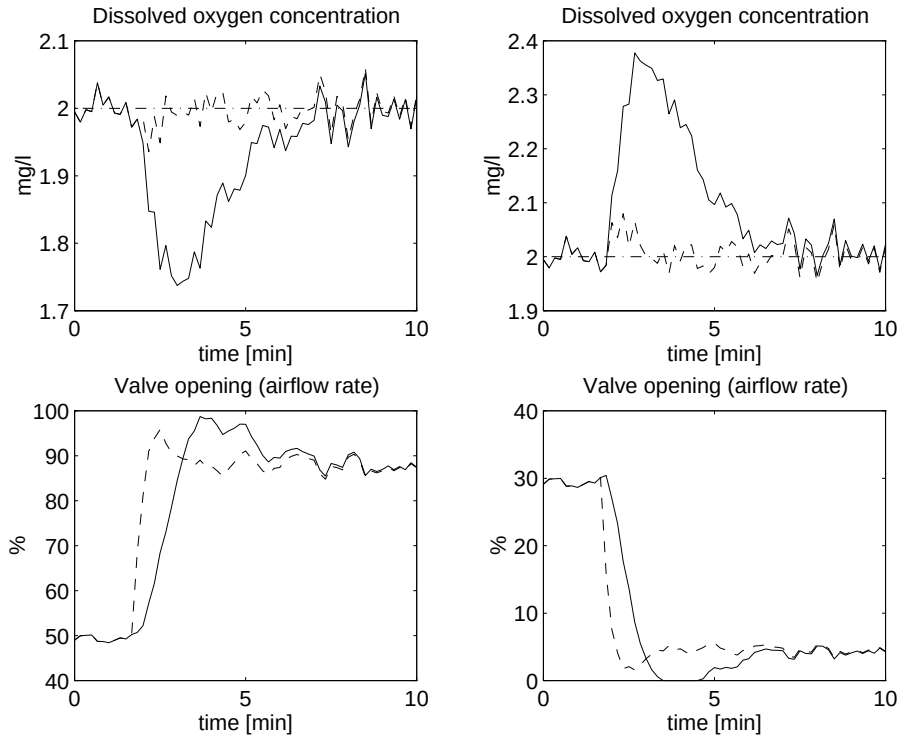

Figure 5.5: Nonlinear LQ control with (dashed) and without (solid) feedforward. The DO and valve openings are shown for a step disturbance in the respiration rate during a high load (left plots) and a low load (right plots). The reference value (dash-dotted) is 2 mg/l.

5.4 Practical experiment

The suggested nonlinear PI-controller was tested at the pilot plant in Uppsala and compared to a linear PI-controller.

The experiment was performed in the first aerobic zone in the pilot plant, where the load variations are expected to be largest and the nonlinear controller might be most useful.

The experiment was started by estimating the nonlinear K_La function. In the estimation scheme we used the estimation algorithm presented in Chapter 4 with an exponential K_La model. The estimated respiration rate was also compared with lab measurements to assess if the estimated respiration rate was reasonable. If the estimated and measured respiration rates do not differ too much, the estimated K_La is regarded as reasonable. The estimated K_La function is shown in Figure 5.6.

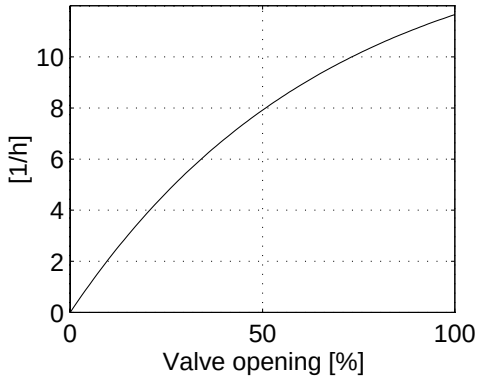

Figure 5.6: The estimated K_La to be used in the controller design.

In the experiment, changes in DO set-point was made instead of changes in respiration rate which is more difficult generate. To simulate a decrease in the respiration rate the DO set-point is lowered from approximately 4 mg/l to 1 mg/l at $t = 7$ min (the time t and initial DO set-point is slightly different in the two figures). First the performance of the linear controller is studied, this is shown in Figure 5.7. As seen the performance is acceptable at a high airflow rate, but at the low DO set-point, where the airflow rate is low the performance deteriorates significantly. The controlled process starts to oscillate for low airflow rates as predicted by the simulations. In particular this type of oscillations may deteriorate the control valve.

Next, the nonlinear controller which uses the estimated K_La was applied. Figure 5.8 illustrates the performance of the nonlinear controller. This controller gives a much better result for the low DO set-point, since

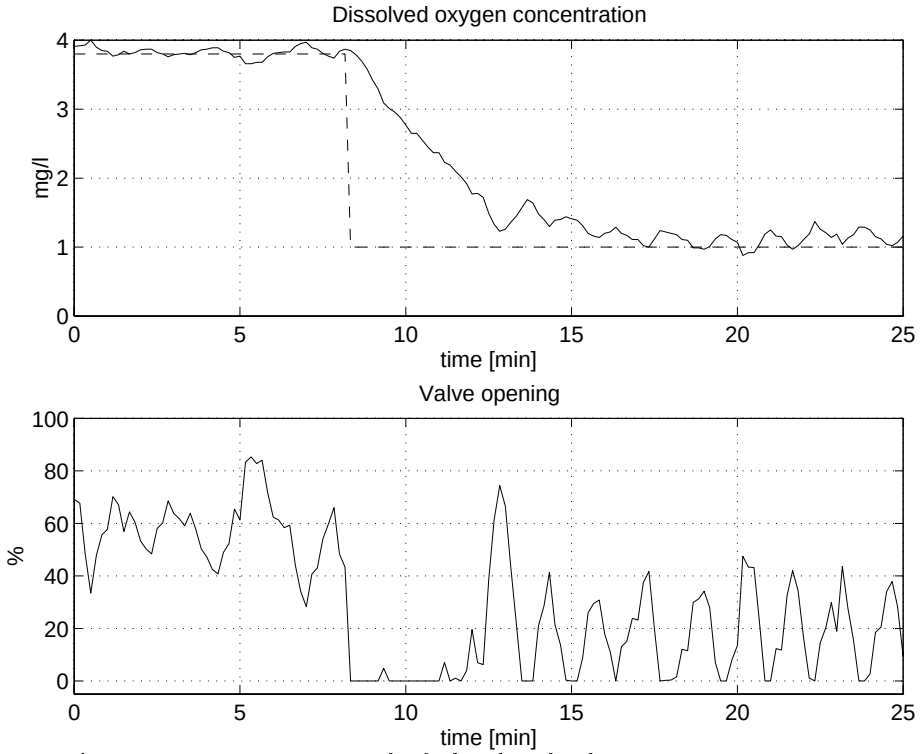

Figure 5.7: Linear control of the dissolved oxygen concentration. The DO set-point is dashed.

the nonlinear controller reduces its gain at the low airflow rate. The oscillations in the control signal for the high DO set-point probably depends on the large controller gain in combination with the neglected dynamics in the sensor.

The nonlinear controller hence has acceptable performance for all working conditions, while the linear controller starts to oscillate for low airflow rates. This result illustrates that the DO process actually is nonlinear, and a nonlinear controller, also in practice, can outperform a linear controller.

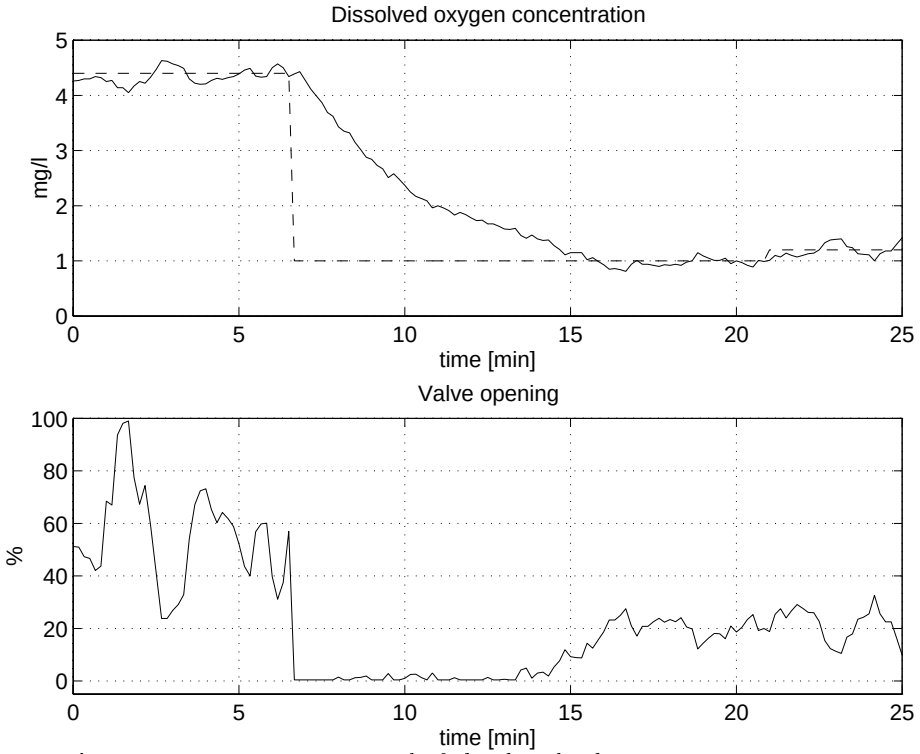

Figure 5.8: Nonlinear control of the dissolved oxygen concentration. The DO set-point is dashed.

5.5 Control of the dissolved oxygen set-point

In the aerobic part of an activated sludge process, ammonium is converted to nitrate by nitrification, see also Section 1.3. The nitrification process requires oxygen, which is obtained by blowing air into the tank. Normally a constant DO, controlled by varying the airflow rate guarantees that sufficient oxygen is supplied to the process. An alternative to a constant DO set-point is to use a *time-varying* DO set-point, which is determined by the ammonium concentration in the last aerobic zone, see also e.g. Nielsen and Lynggaard (1993), and Sorensen *et al.* (1994) for control of the DO set-point in a Bio-denitro^{TM} process.

The DO set-point control gives or may give the following advantages, depending on the existing plant performance:

- Better control of effluent ammonium.
- Lower average DO set-point which saves energy (due to a lower air consumption).
- Lower nitrate concentration in the effluent, because of improved denitrification due to a lower DO.
- Lower dosage of external carbon (if it is added).

Possible disadvantages may be that the sludge properties deteriorate due to the low DO, and that nitrous oxide (N_2O) can be formed when the DO is low. These problems should, however, be compared to the achieved improvements. Another variant of DO set-point control may reduce these problems. When there are several aerated zones, which often is the case, spatial DO control is possible. The idea is to switch on or off aeration in the first or last zone(s) when the DO set-point becomes too high or too low. This latter strategy avoids that the DO set-point becomes too low, and it is probably better than using the same DO set-point in all aerated zones. This strategy has, however, not been evaluated.

The basic idea is to control the DO set-point from on-line measurements of the ammonium concentration, this is illustrated in Figure 5.9. This structure is referred to as cascade control, where the inner DO loop is much faster than outer the ammonium loop. The controller tries to maintain a prespecified ammonium concentration by varying the DO set-point. To avoid the DO set-point becomes too high or too low, it should only be allowed to vary in an interval e.g. 0.5–4 mg O_2/l, which is easily implemented.

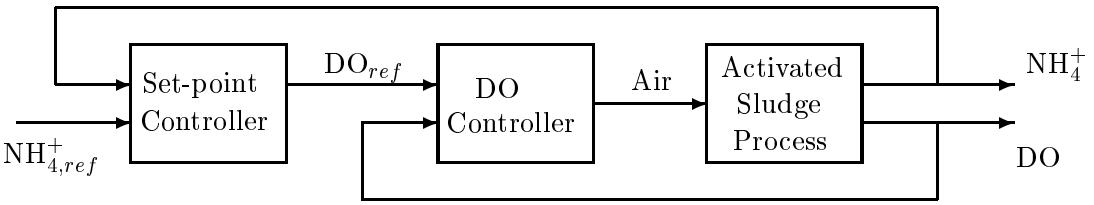

Figure 5.9: Block diagram of the DO set-point controller

The ammonium set-point should usually be chosen low, but if there are problems to maintain this low concentration one could increase the ammonium set-point, to reduce the DO set-point.

5.5.1 A practical experiment

A practical experiment with the DO set-point controller has been made in the pilot plant.

The same DO set-point was used in all three aerated zones. The ammonium concentration was measured in the last aerated zone where the highest ammonium concentration is expected to be found, see also Figure 5.10. The ammonium sensor gives a new value every 20th minute. The

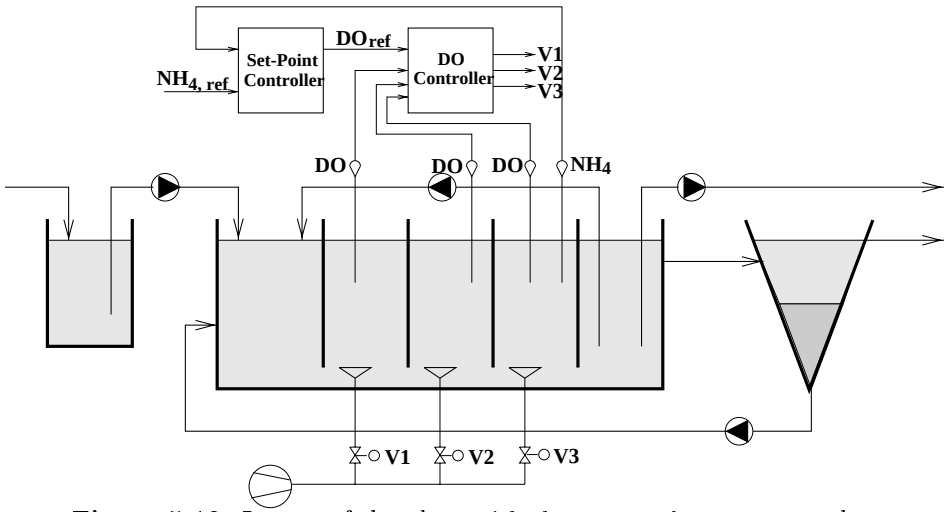

Figure 5.10: Layout of the plant with the sensor placement together with the controller.

flows were kept constant during the whole experiment, and they were: influent=220 l/h, internal rec.=660 l/h, return sludge=260 l/h and excess

sludge=0 l/h. The mean suspended solids concentration was 1.5 g/l (and increasing), and the water temperature was 7^{o}C.

The experiment is illustrated in Figure 5.11. The set-point controller

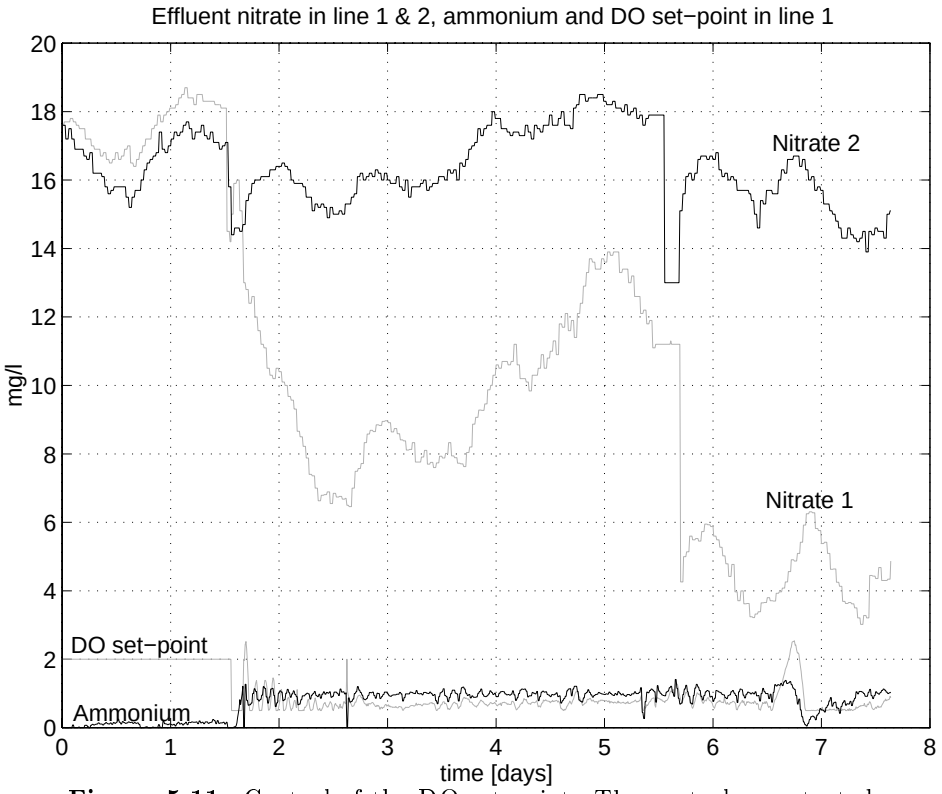

Figure 5.11: Control of the DO set-point. The control was started after 1.5 days with an ammonium set-point of 1 mg/l. The experiments were made in line 1, line 2 was used as a reference.

was started after approximately 1.5 days with a set-point of the ammonium concentration at 1 mg/l. Since the ammonium level was lower than the ammonium set-point, the DO set-point was decreased from 2 mg/l to below 1 mg/l. The experiments were made in line 1 while line 2 was used as reference. The large abrupt changes in the nitrate concentrations at $t = 1.5$ and $t = 5.5$ in Figure 5.11 are caused by calibrations of the nitrate sensor.

A positive effect of the lower DO level was that the effluent nitrate level was significantly decreased. Note that the total effluent nitrate level for the controlled line (1) is reduced to less than half. Effluent ammonium was increased from about zero to the set-point of 1 mg/l, but this minor increase should be compared with the large reduction in effluent nitrate.

The significant reduction in nitrate which was found in the pilot plant experiment is probably not possible to reach in a more optimized plant. In for example plants with a large anoxic zone, the nitrate reduction will probably not be that large. Also, the composition of the influent carbon may affect the results. The large potential in terms of energy savings and nitrogen reduction of this control strategy should however still be considered.

5.5.2 Tuning of the DO set-point controller

The controller used in Figure 5.11 was not accurately tuned. Both the DO set-point and ammonium concentration sometimes oscillated. A way to tune the controller could be to estimate a model between the DO set-point and the ammonium concentration, and use it for controller design.

Only very low DO levels (around 0.5 mg/l) were needed to remove all ammonium in this configuration of the pilot plant. These levels were hard to obtain, since a valve opening smaller than 10% is not suitable if the mixing in the zone should be sufficient. A model between actual DO (not set-point) and ammonium was hence estimated instead.

An excitation experiment of the DO set-point is shown in Figure 5.12. As can be seen, the valve saturated in its lower position during long periods. When this happen and the DO is high (higher than the set-point), the ammonium concentration did not increase. Therefore it is not suitable to use all the data in Figure 5.12 to identify a model. Instead, only the data between approximately 8 – 38 h is used.

After removing the mean value of the DO and ammonium, an estimation algorithm was applied to the data. Simulating the identified model gives the result shown in Figure 5.13, where the mean values have been added again after the simulation. As can be seen, the output error (OE) method gives a slightly better result than the LS method with an ARX model.

The ARX structure is

$$y(t) = \frac{B(q^{-1})}{A(q^{-1})} q^{-1} u(t) + \frac{1}{A(q^{-1})} e(t) \tag{5.22}$$

where $y(t)$ is the ammonium concentration and $u(t)$ is the dissolved oxygen concentration. The LS method gave $A(q^{-1}) = 1 - 0.9538q^{-1}$ and $B(q^{-1}) = -0.2217$.

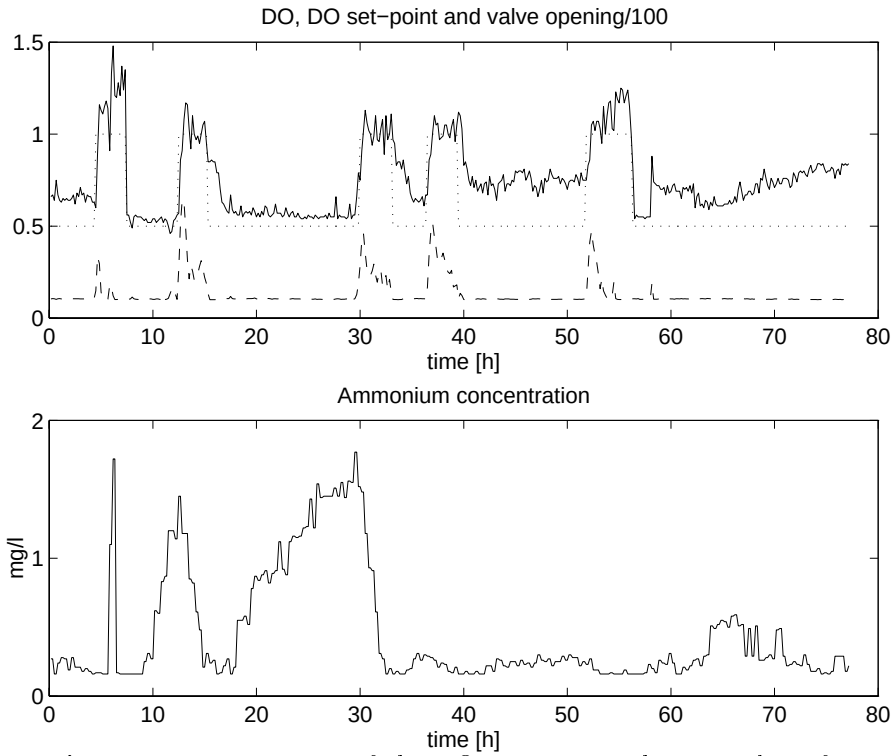

Figure 5.12: Excitation of the DO set-point in the pilot plant, for generating data to estimate the dynamics between DO set-point and ammonium concentration. In the upper plot are DO (solid) DO set-point (dotted) and valve opening/100 (dashed) shown. In the lower plot, the ammonium concentration is shown.

The output error structure is

$$y(t) = \frac{B(q^{-1})}{A(q^{-1})} q^{-1} u(t) + e(t) \tag{5.23}$$

Applying the OE method gave $A(q^{-1}) = 1 - 0.9675q^{-1}$ and $B(q^{-1}) = -0.2115$.

Some advantages with the OE method are given in Söderström (1996). They are:

- The estimates may be consistent even if the noise is colored.
- The number of parameters could be chosen low, because the noise is not modeled.

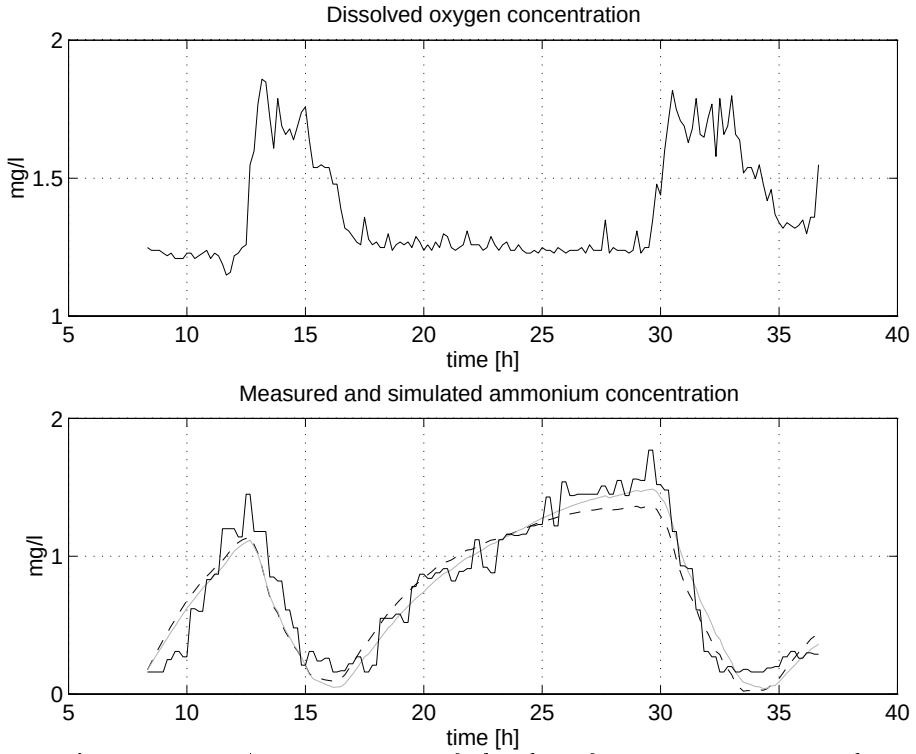

Figure 5.13: A suitable part of the data from Figure 5.12, used to identify a model between DO and ammonium. In the lower plot, measured NH_4 (solid black line), simulated NH_4 with OE-est. model (grey line), and simulated NH_4 with LS-est. model (dashed line).

- The OE model will be good in the frequency range where the input signal is strong. The LS method often emphasize the modeling in too high frequencies.

The identified model between DO and ammonium concentration has the same degrees of polynomials and time delay as the previous linearized DO model (5.5). The same approach for determining the controller parameters can hence be used in this controller design as was used for the DO linearized controller.

Remark: In this experiment all flows were kept constant. That is perhaps not the most common case for a normal WWTP. Since the flow rates were not considered in the previous outlined design, a possible solution could be to make the identification during 'normal flows, and then design a controller which is only slightly faster than the open loop system. The

biomass and other factors which affect the nitrification rate are not considered either. To maintain a high performance during the year a couple of tuning events may be necessary, or an adaptive controller could be implemented.

5.6 Pressure control

For completeness, a controller which controls the pressure in the air blowing system is also described. This strategy has been given before by, for example Rundqwist (1986) and Robinson (1990). The reasons for controlling the air pressure are to guarantee that sufficient air is generated, and to save energy.

The airflow rate in an activated sludge process is often controlled by throttle valves. To minimize the loss of energy, the most opened valve should be kept completely open. The standard solution to this problem is illustrated in the block diagram in Figure 5.14. The idea is to measure the valve openings and feed back the most open valve (φ_{max}) to the pressure controller. The controller increases the pressure if $\varphi_{max} > \varphi_{ref}$ and decreases it if $\varphi_{max} < \varphi_{ref}$. Note the signs at the summation point.

One would like to keep the most open valve 100% open, but there would then be no control authority in the positive direction, due to the pressure controller is tuned to be slow. The pressure controller should be made slow due the coupling effects between the valves and a complicated high frequency dynamics, see Rundqwist (1986).

In order to illustrate the approach, a practical experiment in the pilot plant has been performed. This is illustrated in Figure 5.15. The previous controller is implemented in line 1 and line 2 is used as a reference.

The pressure is controlled to make the most open valve equal to the set-point (90%). The controller manage to do this very well. The valve opening for the first zone lays almost perfect at 90%. The DO is also kept very close to its set-point at 2mg/l in zone 1. For the other zones the DO sometimes is above the set-point due to the valves are not allowed to have a smaller opening than 10%. In Figure 5.15 the pressure variation is also shown. It varies due to the changing load. In the other line (2) the pressure is hold constant during the experiment. To make sure the process always get sufficient oxygen the constant pressure has to be selected high. The largest valve opening in line 2 is most of the time around 30% open which means that an unnecessary high pressure is used which costs more energy than the time varying pressure.

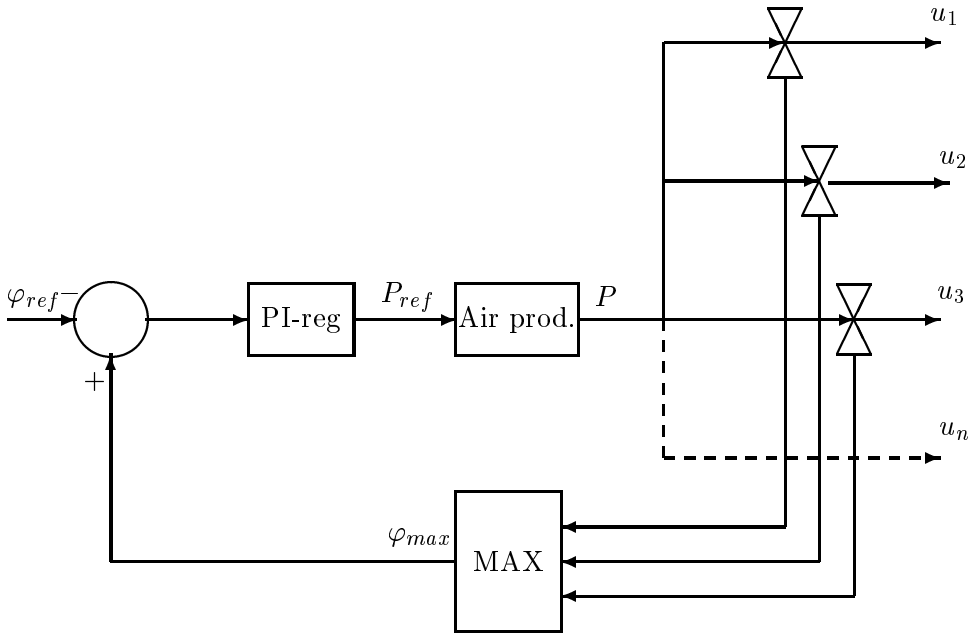

Figure 5.14: A pressure controller, whose goal is to keep the most open valve φ_{max} equal to the reference valve opening φ_{ref}.

The tuning of the pressure controller could either be done manually or be based on an estimated model.

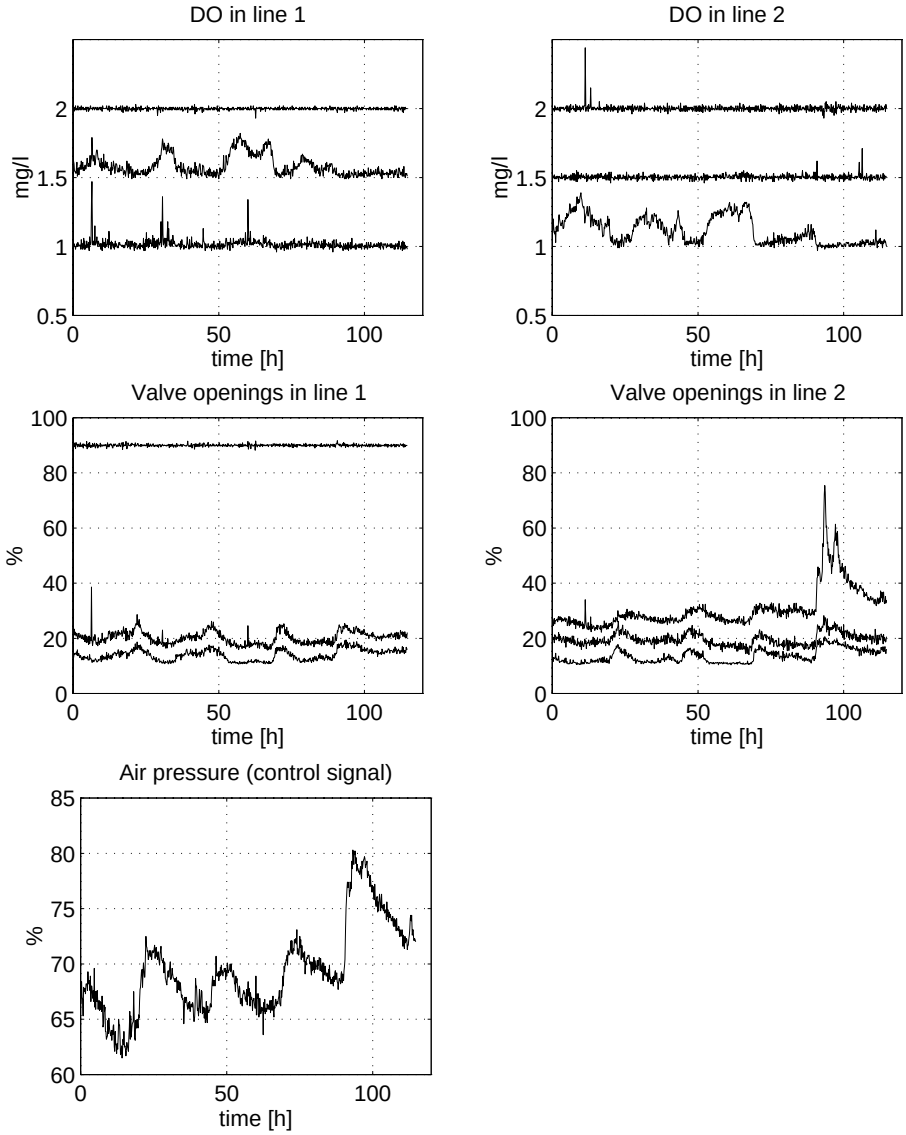

Figure 5.15: Experiment in the pilot plant with the pressure controller. The DO set-points for the three zones in both lines have been set to 2 mg/l, but the DO in zone 2 and 3 are shifted in the plot with 0.5 mg/l respectively 1.0 mg/l. The valve openings in the zones in both lines are also shown. The minimum allowed valve opening is 10 % to obtain sufficient mixing. This causes the controlled DO to become higher than the set-point in some zones.

5.7 Conclusions

The control of the DO in an activated sludge process is an important problem both for economical and process reasons. The basic idea has been to explicitly take the nonlinear oxygen transfer function $K_L a$ into account in the control design. The oxygen transfer function was found from an estimation experiment where a Kalman filter was used. Two design approaches were applied on the linearized process: pole-placement with a PI-regulator and linear quadratic control with feedforward.

In a simulation study, the performance of the controllers were illustrated. It was shown that the nonlinear DO controller outperforms a standard linear PI controller. The nonlinear controller has also been tested in a pilot plant. The tests confirmed the positive results from the simulations.

A set-point controller for the DO process was presented. The basic idea was to control the DO set-point so that the ammonium concentration in the last aerobic zone was kept low. An experiment in the pilot plant showed that, by using this controller not only energy could be saved due to a lower DO set-point, but also the effluent nitrate concentration becomes significantly lower. How the set-point controller could be tuned was also discussed.

Finally an experiment with a pressure controller in the pilot plant was made. It illustrated that it was possible to control the air pressure so that the most open valve was almost completely open.

Chapter 6

Multivariable modeling and control

The activated sludge process is a quite complex process where many states and nonlinear relations are involved. The process is multivariable, i.e. it has several inputs and outputs. This means among other things that one input affects several outputs. For example, a change in the airflow rate affect both the ammonium and nitrate concentrations. Another problem is that the activated sludge process is nonlinear, for example the dynamics depends on actual flow rates and concentrations.

In this chapter, a linear time-invariant multivariable model is estimated around an operating point. The model uses the external carbon flow rate, the internal recirculation rate, and the DO set-point as inputs (the DO set-point can be used as input instead of the airflow rate when cascade control is applied). Ammonium and nitrate in the last aerated zone are used as outputs. The model also includes influent flow rate, influent ammonium and influent carbon (substrate) as measurable disturbances. The estimated model is then used for controller design. Two different integrating LQ controllers are designed which uses feedforward from the measurable disturbances.

The main advantage of such a controller is that it takes the interactions in the process model into account and an optimal (in an LQ sense) trade-off between the different inputs and outputs can be utilized. In the past, mostly SISO (single input single output) control strategies have been suggested for control of the nitrate and ammonium concentration. For example, Londong (1992) controlled the nitrate level by varying the inter-

nal recirculation rate and Lindberg and Carlsson (1996*a*) by varying the dosage of an external carbon source. The ammonium concentration can be controlled by the DO. This has been demonstrated in e.g. Lindberg and Carlsson (1996*d*) and Sorensen *et al.* (1994). Few examples of multivariable control applied to wastewater treatment is found in the literature, and those who are found have not controlled the ammonium and nitrate level. For examples, Dochain and Perrier (1993), Bastin and Dochain (1990), and Youssef *et al.* (1995) have designed multivariable controllers, but only validated their control strategy on simplified models.

6.1 Modeling

As mentioned previously, the activated sludge process is a complex process where many components and nonlinear relations are involved. It is hence a delicate problem to find a model which sufficiently well describe this process. One way to find such a model is to use physical knowledge of the process. Several such models have been suggested, and the most widely used one is probably the IAWQ model, presented by Henze *et al.* (1987), see also Chapter 2. This model contains 13 coupled nonlinear differential equations and around 20 more or less unknown parameters. An activated sludge process also consists of several zones and a settler. The IAWQ model only describes one zone. Several IAWQ models therefore have to be connected to each other in order to model a bioreactor. Finally a settler model, about as complex as the IAWQ model, also has to be included. It is not easy to tune such a model or use it for controller design. Another approach to modeling is to use a black-box model, which is linear and time invariant. A system identification method can then be applied to estimate its parameters from input-output data. Such a model is suitable for controller design, which is the main purpose here. It will also be shown (by simulations) that the identified black-box model, describes the activated sludge process well, at least around an operating point. A drawback with this type of model is that the physical insight of the process is lost. For example, the states are artificial and it is not possible to understand how a process variable, which not is directly included in the model, affects the process. An advantage is that this model only needs input/output data to be estimated.

Since the activated sludge process is nonlinear we may need different sets of linear models to be able to approximate the process at different operating points. When the activated sludge process is controlled we try to stay around an operating point. This reduces the nonlinear effects, and it may be sufficient with only one linear model. It will also be shown (by

simulations) that the estimated model works well for large changes in both influent flows and influent concentrations. If, however, one linear model can not approximate the real process, a couple of models may be used at different operating points.

Grey-box modeling, where parts of the physical model structure is included, could be an alternative to black-box modeling. Since the structure is very complex in the connected IAWQ models and the settler model, such an approach has been abandoned.

6.1.1 What to model?

What to model is an interesting question. Often one knows what to model since the inputs and outputs are known, and the model establishes a relation between these signals. For an activated sludge process it is, however, not clear what should be considered as an input or an output. This depends among other things on the purpose of the model. *Where* to measure is not obvious either.

The purpose of the modeling is, as mentioned before, to use the derived model for controller design. In an activated sludge process it is desired to keep the effluent ammonium concentration and the effluent nitrate concentration at low levels. Our aim will therefore be to control these concentrations, and keep them close to the desired set-points.

The activated sludge process contains dynamics with time constants which range from seconds (e.g. pressure in air pipes) to weeks (e.g. sludge retention time). To cover all dynamics in one model is not suitable. A better solution is to divide the model into a couple of smaller models which approximately have the same time constants. The set-point of a fast process can then be controlled by a slower process (cascade control). In that way the fast dynamics may be neglected when considering the slower models. An example is a model of the dissolved oxygen concentration (DO), where only the relation between DO and airflow rate is included, the relation between valve position and the airflow rate is excluded. Here, the set-point of the DO is considered as an input instead of e.g. airflow rate.

From e.g. Olsson and Jeppson (1994) we find that the following control handles: external carbon dosage, internal recirculation rate, and DO set-point affect the ammonium and nitrate concentrations, and they also do it in approximately the same time scale (hours). Hence, these three control variables will therefore be used as inputs. As outputs we consider ammonium and nitrate. To improve the model, influent flow, influent carbon

and influent ammonium will be used as measurable disturbances. During identification the disturbances are, however, considered as normal inputs. Influent carbon can be approximated by measurements of, for example, TOC (Total Organic Carbon). TOC has usually not the same effect on the activated sludge process as the soluble substrate, but if the difference in effect only differs by a scaling factor, TOC will work equally well in the model. In Figure 6.1 all inputs and outputs used in the model are summarized.

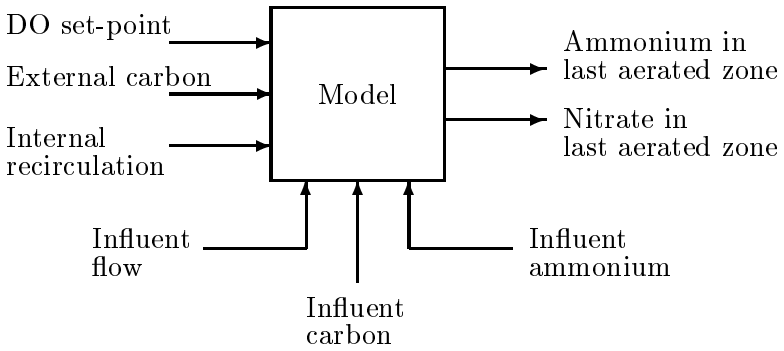

Figure 6.1: Input signals (DO set-point, external carbon and internal recirculation), measurable disturbances (influent flow, influent carbon and influent ammonium) and outputs (nitrate and ammonium in last aerated zone) which the model is based on

It would perhaps be natural to use *effluent* ammonium and *effluent* nitrate as model outputs, but if the model as in this case is aimed for controller design it is better to use measurements further upstream. This to reduce the time delay in the model. A shorter time delay makes it possible to design a faster controller with better disturbance rejection. Both the ammonium concentration and the nitrate concentration will therefore be measured in the last aerated zone. After this zone no more ammonium is converted to nitrate (assuming that no biological reactions occur in the settler), which means that the lowest ammonium concentration and highest nitrate concentration in the activated sludge process is measured (in a pre-denitrifying plant).

Remark: In Chapter 3 the nitrate concentration was measured in the anoxic zone. This was suitable in that situation because the internal recirculation flow was constant and the model should only describe the relation between external carbon dosage and nitrate concentration. Here, simulations have shown that a multivariable controller based on a model where

the nitrate concentration in the anoxic zone is an output will fail. Such a controller switch off the internal recirculation, probably due to the fact that the nitrification process is badly modeled. By switching off the internal recirculation, it is easy to maintain a low nitrate concentration in the anoxic zone for a pre-denitrifying activated sludge process, but the effluent nitrate concentration will be rather high.

6.1.2 Subspace identification

For SISO (Single Input Single Output) systems polynomial models like ARMAX models are convenient both for identification and controller design purposes. For MIMO (Multiple Input Multiple Output) systems, polynomial models are complex, since they become matrix fraction decompositions. In these models it is not obvious how to choose the polynomial degrees and the time delays. An alternative to polynomial models, is to use Subspace State Space System Identification (4SID). The advantages are that the user has relatively few design variables, the methods have robust numerical properties, and relatively low computational complexity (Viberg *et al.* 1995).

A short introduction to subspace identification

The problem formulation in subspace identification is as follows: Given input and output measurements, find an appropriate order n and system matrices (Van Overschee and De Moor 1996). This is a very general formulation and in system identification which could fit to many identification methods. The solution to the problem in the subspace based techniques is, however, quite different compared to the techniques based on an iterative search. The subspace methods uses projections and singular value decompositions to find the model. The following derivation is mostly taken from Viberg (1994) who gives an overview of existing subspace based techniques.

Assume that the true system can be described by

$$x(t+1) = Ax(t) + Bu(t) \tag{6.1}$$
$$y(t) = Cx(t) + Du(t) \tag{6.2}$$

and define

$$U = \begin{bmatrix} u(0) & u(1) & u(2) & \dots & u(j-1) \\ u(1) & u(2) & u(3) & \dots & u(j) \\ \vdots & \vdots & \vdots & & \vdots \\ u(i-1) & u(i) & u(i+1) & \dots & u(i+j-2) \\ u(i) & u(i+1) & u(i+2) & \dots & u(i+j-1) \\ \vdots & \vdots & \vdots & & \vdots \\ u(2i-1) & u(2i) & u(2i+1) & \dots & u(2i+j-2) \end{bmatrix} \tag{6.3}$$

where the number of columns j typically is chosen to $j = N - 2i + 1$ so that all data are used. Matrices for the output Y and the state X are generated in the same way as for the input U, replace all u with y respectively x. The parameter i is a user parameter, similar to the number of block rows in some algorithms, e.g. N4SID[1].

Introduce the extended observability matrix , and the lower block Toeplitz matrix H

$$, = \begin{bmatrix} C \\ CA \\ \vdots \\ CA^{2i-1} \end{bmatrix} \qquad H = \begin{bmatrix} D & 0 & \dots & 0 \\ CB & D & \dots & 0 \\ \vdots & \vdots & \ddots & \vdots \\ CA^{2i-2}B & CA^{2i-3}B & \dots & D \end{bmatrix} \tag{6.4}$$

The following matrix equation can then be derived

$$Y = , X + HU \tag{6.5}$$

and the orthogonal projection onto the null space of U, introduced as

$$\Pi_{U^T}^{\perp} = I - U^T(UU^T)^{-1}U \tag{6.6}$$

Multiplying (6.5) by $\Pi_{U^T}^{\perp}$ gives

$$Y\Pi_{U^T}^{\perp} = , X\Pi_{U^T}^{\perp} \tag{6.7}$$

since $U\Pi_{U^T}^{\perp} = 0$. Now, make a singular value composition of $Y\Pi_{U^T}^{\perp}$ and partition it as

$$Y\Pi_{U^T}^{\perp} = Q_s S_s V_s^T + Q_n S_n V_n^T \tag{6.8}$$

where the Q matrices contains the left singular vectors, the S matrices are diagonal matrices with the corresponding singular values, and the V matrices contains the right singular vectors. The product of the matrices with

[1] Numerical algorithms for Subspace State Space System Identification (Van Overschee and De Moor 1996).

the index $_s$ contains the signal subspace, and the product of the matrices with the index $_n$ contains the noise subspace. In absence of noise $S_n = 0$. Data from a real process always contains noise, hence $S_n \neq 0$. One then have to find the border between S_s and S_n. A common approach is then to set the border where the singular values drop to small values.

The observability matrix , is then estimated by

$$, = Q_s \tag{6.9}$$

In fact, , should be chosen so that $\mathcal{R}(,) = \mathcal{R}(Q_s)$. The particular choice (6.9) is simple and corresponds to a specific realization dependent choice of coordinates. The system matrix A is found from , through the relation

$$, _{2:n} = , _{1:n-1}A \tag{6.10}$$

where , $_{2:n}$ is , with the first block row deleted and , $_{1:n-1}$ is , with the last block row deleted. The system of equations (6.10) is over-determined in the unknown matrix A, and can be solved in several ways. The C matrix is given by the first row(s) of , , according to (6.4).

Multiplying (6.5) with Q_n^T yields

$$Q_n^T Y = Q_n^T HU \tag{6.11}$$

which gives an over-determined system of equations that can be solved in a least squares sense with respect to B and D. Note that Q_n^T, $= 0$ since , $= Q_s$, which is orthogonal to Q_n.

The presented algorithm is just one of many variants. There exists methods which are more efficient and take care of process and measurement noise, see e.g. Van Overschee and De Moor (1996).

6.1.3 Application of subspace identification to the activated sludge process

In Section 6.1.1 it was concluded that a model should be found which models the two outputs, nitrate and ammonium in the last aerated zone, based on the three inputs DO set-point, external carbon, internal recirculation, and the three measurable disturbances influent flow, influent carbon and influent ammonium.

A discrete-time model is estimated from the input-output data using subspace identification:

$$\begin{aligned} x(t+1) &= Fx(t) + Gu(t) + G_d d(t) && (6.12)\\ y(t) &= Cx(t) && (6.13) \end{aligned}$$

where $y(t)$ is the outputs, $u(t)$ the inputs, $d(t)$ the measurable disturbances, and $x(t)$ is a state vector. The state vector $x(t)$ is "artificial", created by the subspace algorithm, and it does usually not contain any measurable states. The other parameters in (6.12) and (6.13), i.e. F, G, G_d, and C are matrices.

The structure of (6.12) is not directly suitable for identification. It can be rewritten such that the measurable disturbances $d(t)$ are considered as inputs and included in the input vector as

$$x(t+1) = Fx(t) + \begin{bmatrix} G & G_d \end{bmatrix} \begin{bmatrix} u(t) \\ d(t) \end{bmatrix} \tag{6.14}$$

Generation of data

It is *very* important to excite the input signals in a sensible way to be able to estimate a linear black-box model from input-output data. The input signals should have a sufficient excitation in both amplitude and frequency. The output concentrations should not deviate too much from normal operating levels.

The activated sludge process is simulated by the model presented in Section 2.3 with the input signals given in Figure 6.2 and measurable disturbances in Figure 6.3. The return sludge flow in Figure 6.4 is also varied, but not included in the model. The internal recirculation, and return sludge, were generated by low pass filtering white noise. Values above the maximum limit or below the minimum limit have been set to the limit for each control signal. The gain and bandwidth of the low pass filters is different for the different signals, as well as the mean values. The excitation of the DO set-point was the most critical signal to generate. The activated sludge process is very nonlinear for DO values close to zero. To avoid that the ammonium concentration, which also depends on the DO, becomes large, a PID controller for the DO set-point is used, as outlined in Section 5.5. The DO set-point is hence generated by a PID controller during the simulation. The PID controller tries to follow a reference signal in the ammonium concentration by varying the DO set-point. The ammonium reference signal is excited by PRBS (Pseudo Random Binary Signals). This (usually) gives a control signal with reasonable excitation in both amplitude and frequency. The reason for that the ammonium concentration in Figure 6.5 does not look like a PRBS is that the PID controller constrains the DO set-point between 0.2 – 4 mg/l. The carbon flow rate was generated in a similar way as the DO set-point. The nitrate concentration in the anxoic zone was controlled by the controller outlined in Section 3.4. The

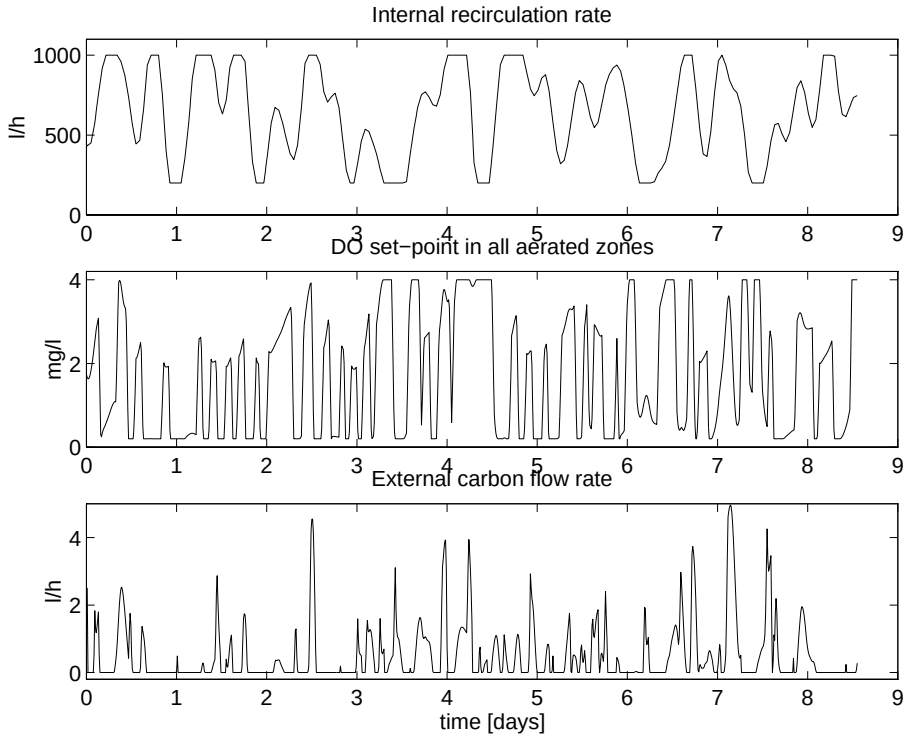

Figure 6.2: Input signals to the activated sludge process.

nitrate reference signal was varied as a PRBS between 0.5 and 2.5 mg/l. It is not necessary to generate this flow rate by a controller, but it may improve the estimated model, because the process appear less nonlinear if the carbon dosage does not saturate the nitrate concentration at very low levels.

The measurable disturbances could normally not be manipulated. Here they are generated by low pass filtering white noise.

Including the return sludge flow as a measurable disturbance in the model did not improve the estimated model. Therefore it is not included and only considered as an unmeasurable disturbance.

Applying the signals in Figure 6.2, 6.3 and 6.4 as inputs to the simulation model, gives the outputs in Figure 6.5. To make the output signals more realistic, noise has been added to the outputs. The noise was zero mean with standard deviation 0.1 on the ammonium output and 0.1 on the nitrate output. The sampling interval was chosen to 0.2 hours.

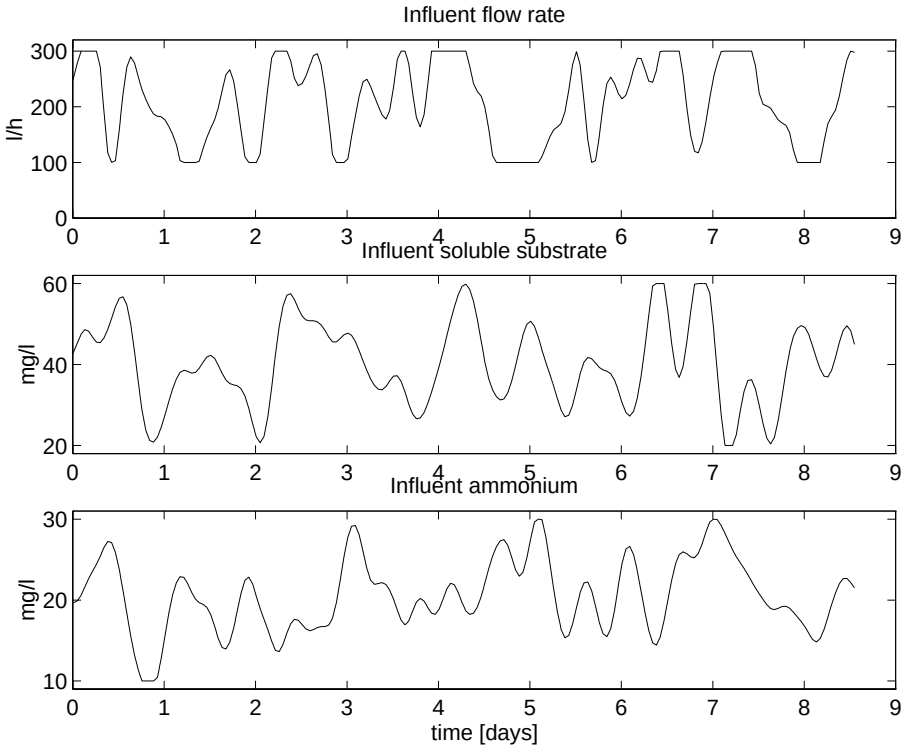

Figure 6.3: Measurable disturbances in the activated sludge process.

Using the data

Now we have all data for estimating a model. The N4SID (Numerical algorithms for Subspace State Space System Identification) algorithm in Van Overschee and De Moor (1996) is used to identify a model.

There are two design variables in N4SID, the *order* of the model (dimension of state vector) and an *auxiliary order* (=i block rows), used for the selection of state variables. For controller design purposes it is, for example, best to choose as low model order as possible, which still mimics the outputs reasonably well. That is, the outputs generated by the estimated model should only differ slightly from the true process outputs. The auxiliary order i is chosen to obtain minimum prediction error. A suitable default value is according to Matlab (MathWorks 1992) 1.2*ORDER+3.

In system identification a direct term, as in (6.2), is sometimes included

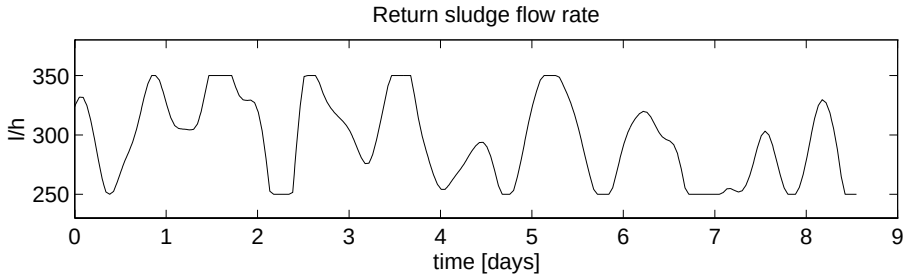

Figure 6.4: Return sludge flow.

in the model, i.e. (6.13) is modified to

$$y(t) = Cx(t) + D \begin{bmatrix} u(t) \\ d(t) \end{bmatrix} \tag{6.15}$$

This direct term is, however, not suitable for controller design, because an additional time delay then has to be introduced in the controller to make the design possible (otherwise $y(t)$ depends on $u(t)$, which depends on $y(t)$). To avoid the problem with a direct term, we try to estimate the best model without it, which is easily done in the N4SID algorithm in Matlab.

To obtain an accurate model, the mean values of all signals should be removed before the data is applied to the identification algorithm. This is common in system identification, see e.g. Söderström and Stoica (1989). The signals have also been slightly scaled. All flows are in the unit m^3/h, except for the external carbon flow rate which has the unit l/h.

The model is cross-validated on data which were not used for identification. Outputs, generated by the identified model are compared with the outputs from the true process. This is shown in Figure 6.6, where the first 3/4 of the data has been used to identify the model and the last 1/4 to validate the model. As seen the model simulates the outputs well. A simulation has also been done where all data was used for identification. This gave, however, no visible improvement when making the same comparison as in Figure 6.6.

The resulting model has order 4 and the auxiliary order in N4SID was chosen to 5.

$$F = \begin{bmatrix} 1.0356 & -0.0668 & -0.4454 & -0.0301 \\ -0.0013 & 0.9667 & -0.1066 & 0.5283 \\ 0.0802 & -0.0386 & 0.6120 & -0.0473 \\ 0.0110 & -0.0629 & 0.0069 & 0.5402 \end{bmatrix} \tag{6.16}$$

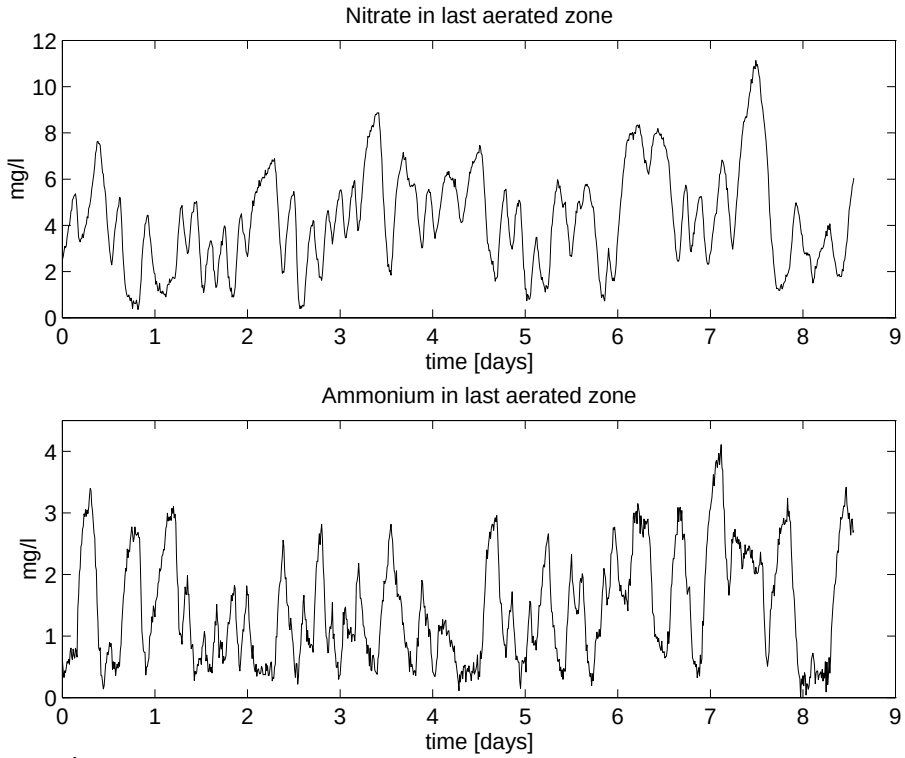

Figure 6.5: Nitrate and ammonium concentration in the last aerated zone. Generated with the input signals in Figure 6.2, 6.3 and 6.4.

$$G = \begin{bmatrix} -0.2920 & 0.2985 & -0.1922 \\ -0.2377 & 0.1682 & 0.1077 \\ -0.1155 & 0.1119 & 0.0705 \end{bmatrix} \tag{6.17}$$

$$G_d = \begin{bmatrix} -0.4531 & -0.0027 & -0.0066 \\ -1.7515 & 0.0051 & -0.0236 \\ -1.4949 & 0.0032 & -0.0352 \end{bmatrix} \tag{6.18}$$

$$C = \begin{bmatrix} 0.3081 & 0.1062 & 0.7712 & 0.1098 \\ -0.0222 & -0.3962 & -0.0508 & 0.8309 \end{bmatrix} \tag{6.19}$$

The poles (eigenvalues of F) of the estimated system are: 0.9291, 0.8728, 0.7128, and 0.6397. The slowest pole has a time constant around 4.5 h which seems reasonable, see e.g. Olsson and Jeppson (1994).

This model order 4 gave the best result. A higher model order did not reduce the difference between the outputs from the simulation and the outputs from true process, when using cross-validation. A linear time-invariant fourth order state-space model can hence model the activated

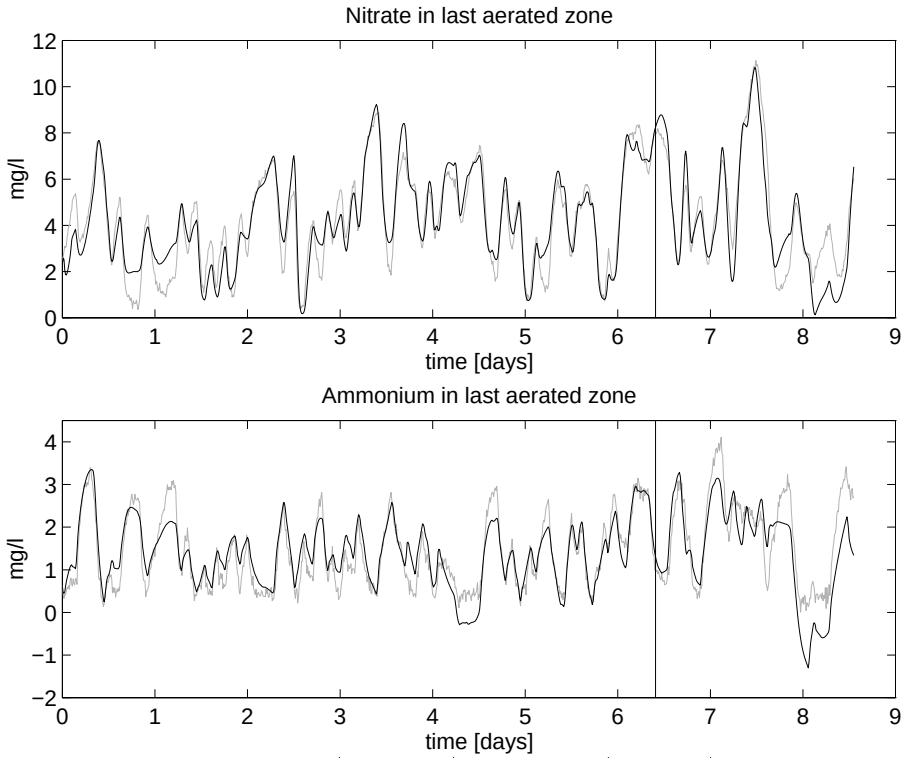

Figure 6.6: Simulated (black line) and "real" (grey line) nitrate and ammonium concentration. The last 25 % of the data (the vertical line indicates that point) was not used for identification.

sludge process reasonably well despite the rather large variations in influent flow, influent concentrations, internal recirculation, sludge recirculation, DO set-point and external carbon dosage.

The model used to generate the data (5 IAWQ models and the settler model) consists of around 100 coupled nonlinear differential equations. The identified fourth order model is hence a very much reduced order model which still manages to describe the activated sludge process well.

6.2 Control

The previously identified model is now used for controller design. The aim of the controller is to keep the ammonium and nitrate concentration in the last aerated zone as close as possible to the desired set-points by using the control signals (DO set-point, external carbon, and internal recirculation).

Feedforward from influent flow, influent carbon and influent ammonium is also applied. To make the controller able to remove stationary errors, integration is included.

It should be stressed that the most critical part in the controller design is to obtain a good model. A sufficiently good model may be estimated if the input signals are designed with care, like in the previous section.

6.2.1 Controller design

In Section 6.1.3 a state-space model (6.12) of the process was identified

$$x(t+1) = Fx(t) + Gu(t) + G_d d(t) \tag{6.20}$$
$$y(t) = Cx(t) \tag{6.21}$$

The state vector can be augmented with the measurable disturbances $d(t)$ as

$$\begin{bmatrix} x(t+1) \\ d(t+1) \end{bmatrix} = \begin{bmatrix} F & G_d \\ 0 & F_d \end{bmatrix} \begin{bmatrix} x(t) \\ d(t) \end{bmatrix} + \begin{bmatrix} G \\ 0 \end{bmatrix} u(t) + \begin{bmatrix} v_x(t) \\ v_d(t) \end{bmatrix} \tag{6.22}$$
$$y(t) = \begin{bmatrix} C & 0 \end{bmatrix} \begin{bmatrix} x(t) \\ d(t) \end{bmatrix} + e(t) \tag{6.23}$$

where the zeros are matrices of suitable size filled with zeros. By including $d(t)$ in the state vector, the feedforward design in the LQ controller will be convenient, see also Kwakernaak and Sivan (1972). To include $d(t)$ in the state vector, its dynamic has to be modeled, and therefore the matrix parameter F_d is included. It could e.g. be selected as $F_d = 0.99I$, which almost makes $d(t)$ a random walk process. To make the measurable disturbance $d(t)$ not be completely deterministic (which it of course is not), the noise $v_d(t)$ has been added. The noises $v_x(t)$, $v_d(t)$ and $e(t)$ are not used in the controller design, they are only included for completeness. In an observer design their variances could be used as design variables.

There exists different strategies to design an integrating controller. Two approaches will be studied. The first one is based on differentiating the system and deriving an incremental controller, see e.g. García *et al.* (1989). This approach is commonly used in Model Predictive Control (MPC). The second approach is to include additional integration states for each output, see e.g. Åström and Wittenmark (1990).

6.2.2 Controller design on differential form

The system is now differentiated and an incremental control signal is derived, see also e.g. García *et al.* (1989). We start by rewriting (6.22) and (6.23) to

$$\begin{aligned} x_n(t+1) &= F_n x_n(t) + G_n u(t) && (6.24)\\ y(t) &= C_n x_n(t) && (6.25) \end{aligned}$$

where the noise vectors have been excluded for simplicity. Besides that, (6.24) and (6.25) are identical to (6.22) and (6.23). Multiplying (6.24) and (6.25) with Δ gives

$$\begin{aligned} \Delta x_n(t+1) &= F_n \Delta x_n(t) + G_n \Delta u(t) && (6.26)\\ \Delta y(t) &= C_n \Delta x_n(t) && (6.27)\\ \Delta y(t+1) &= C_n \Delta x_n(t+1) = C_n(F_n \Delta x_n(t) + G_n \Delta u(t)) && (6.28)\\ y(t+1) &= y(t) + \Delta y(t+1) && (6.29)\\ \Delta &= 1 - q^{-1} && (6.30) \end{aligned}$$

Written in a new state-space form this becomes

$$\begin{aligned} \begin{bmatrix} \Delta x_n(t+1) \\ y(t+1) \end{bmatrix} &= \begin{bmatrix} F_n & 0 \\ C_n F_n & I \end{bmatrix} \begin{bmatrix} \Delta x_n(t) \\ y(t) \end{bmatrix} + \begin{bmatrix} G_n \\ C_n G_n \end{bmatrix} \Delta u(t) && (6.31)\\ y(t) &= \begin{bmatrix} 0 & I \end{bmatrix} \begin{bmatrix} \Delta x_n(t) \\ y(t) \end{bmatrix} && (6.32) \end{aligned}$$

The system (6.31) and (6.32) will be used to derive a steady-state feedforward feedback integrating LQ controller. The controller will contain feedforward since the state $x_n(t)$ contains the measurable disturbances $d(t)$, and integration since the system is differentiated. The control signal is determined by

$$u(t) = \begin{cases} u_{min} & u(t-1) + \Delta u(t) \le u_{min} \\ u(t-1) + \Delta u(t) & u_{min} < u(t-1) + \Delta u(t) < u_{max} \\ u_{max} & u(t-1) + \Delta u(t) \ge u_{max} \end{cases} \qquad (6.33)$$

where $\Delta u(t)$ is computed by

$$\Delta u(t) = -L \begin{bmatrix} \Delta x_n(t) \\ y(t) \end{bmatrix} + L_r r(t) = -\begin{bmatrix} L_x & L_d & L_y \end{bmatrix} \begin{bmatrix} \Delta x(t) \\ \Delta d(t) \\ y(t) \end{bmatrix} + L_r r(t) \qquad (6.34)$$

A suitable choice of L_r is

$$L_r = L_y \tag{6.35}$$

because the set-points $r(t)$ and outputs $y(t)$ are then amplified equally. Inserting (6.35) in (6.34) gives

$$\Delta u(t) = -[\ L_x \quad L_d\ ] \begin{bmatrix} \Delta x(t) \\ \Delta d(t) \end{bmatrix} + L_y(r(t) - y(t)) \tag{6.36}$$

The choice (6.35) gives in steady state ($\Delta u(t) = \Delta x(t) = \Delta d(t) = 0$) that $r(t) = y(t)$, which is natural.

The state feedback (and feedforward) L is found by minimizing

$$J = \lim_{N\to\infty} \sum_{t=0}^{N-1} \{ \begin{bmatrix} \Delta x_n(t) \\ y(t) \end{bmatrix}^T Q \begin{bmatrix} \Delta x_n(t) \\ y(t) \end{bmatrix} + \Delta u(t)^T R \Delta u(t) \} \tag{6.37}$$

The stationary solution ($N \to \infty$) is found by solving the Riccati equation

$$S = \Phi^T S \Phi + Q - \Phi^T S, [, {}^T S, \ + R]^{-1}, {}^T S \Phi \tag{6.38}$$

where Φ and , are given by

$$\Phi = \begin{bmatrix} F_n & 0 \\ C_n F_n & I \end{bmatrix} \qquad , = \begin{bmatrix} G_n \\ C_n G_n \end{bmatrix} \tag{6.39}$$

which are the system matrices in (6.31). The state feedback L is given by

$$L = [, {}^T S, \ + R]^{-1}, {}^T S \Phi \tag{6.40}$$

For solution of the algebraic Riccati equation, see Pappas *et al.* (1980).

Remark: The selected process has three inputs and two outputs which means that the controller has an additional degree of freedom. For the LQ design method, which is based on minimizing a criteria this may not be a problem. For design methods without a criterion it has to be decided what to do with the additional degree of freedom.

Observer design

As the state vector $[\ \Delta x(t) \quad \Delta d(t) \quad y(t)\ ]^T$ is not completely measurable, an observer is introduced:

$$\begin{aligned} \begin{bmatrix} \Delta\hat{x}(t+1) \\ \hat{y}(t+1) \end{bmatrix} &= \begin{bmatrix} F & 0 \\ CF & I \end{bmatrix} \begin{bmatrix} \Delta\hat{x}(t) \\ \hat{y}(t) \end{bmatrix} + \begin{bmatrix} G \\ CG \end{bmatrix} \Delta u(t) + \begin{bmatrix} G_d \\ CG_d \end{bmatrix} \Delta d(t) \\ &+ \begin{bmatrix} k_x \\ k_y \end{bmatrix} \left(y(t) - [\ 0 \quad I\ ] \begin{bmatrix} \Delta\hat{x}(t) \\ \hat{y}(t) \end{bmatrix} \right) \end{aligned} \tag{6.41}$$

The gain of the observer $[\ k_x \quad k_y\ ]^T$ is chosen by placing the observer poles slightly closer to the origin than the closed loop poles (0.9 times the closed loop poles). The solution which gives $[\ k_x \quad k_y\ ]^T$ is not unique, it is under-determined. The additional degrees of freedom are used to make the solution more robust. The sensitivity of the observer poles to perturbations in the system matrices is minimized, and the magnitude of the transient response is also minimized, see Kautsky *et al.* (1985) (the command *place* in Matlab's Control System Toolbox has this algorithm implemented).

An alternative to the observer pole placement design is the Kalman filter, but to derive that filter, the variances of the process noise and measurement noise are needed. Since these variances are unknown, we might as well use pole placement.

A problem when the state vector is not measurable is that the nice properties of the LQ controller (60^o phase margin and gain margin $]0.5, \infty[$) may be lost when the states have to be reconstructed. A solution to this problem may be to use Loop Transfer Recovery (LTR), see Doyle and Stein (1979), but this usually gives a very noise sensitive observer. This is another reason for using pole placement.

The final controller structure with observer, feedback and feedforward is illustrated in Figure 6.7.

Controller experiment

The controller will now be tried on the large model, presented in Section 2.3. In the controller design we chose the penalty matrix Q as

$$\begin{aligned} Q &= H^T H \\ H &= [\ 0 \quad I\ ] \end{aligned}$$

The control vector $u(t)$ consists of the following signals

$$u = [\ \Delta Q_{int} \quad \Delta DO_{ref} \quad \Delta Q_{Carbon}\ ]^T \tag{6.42}$$

and is penalized by the R-matrix which here is chosen to $R = 2I$. The choice of R may approximately be determined by the size of the control signals. A suitable choice may be obtained by using the following approximate relation

$$r_{ii} = 1/\tilde{u}_i^2 \tag{6.43}$$

where r_{ii} is the ii:th element in the R matrix for the i:th control signal, and $\tilde{u}_i$ is the maximally allowed value of u_i.

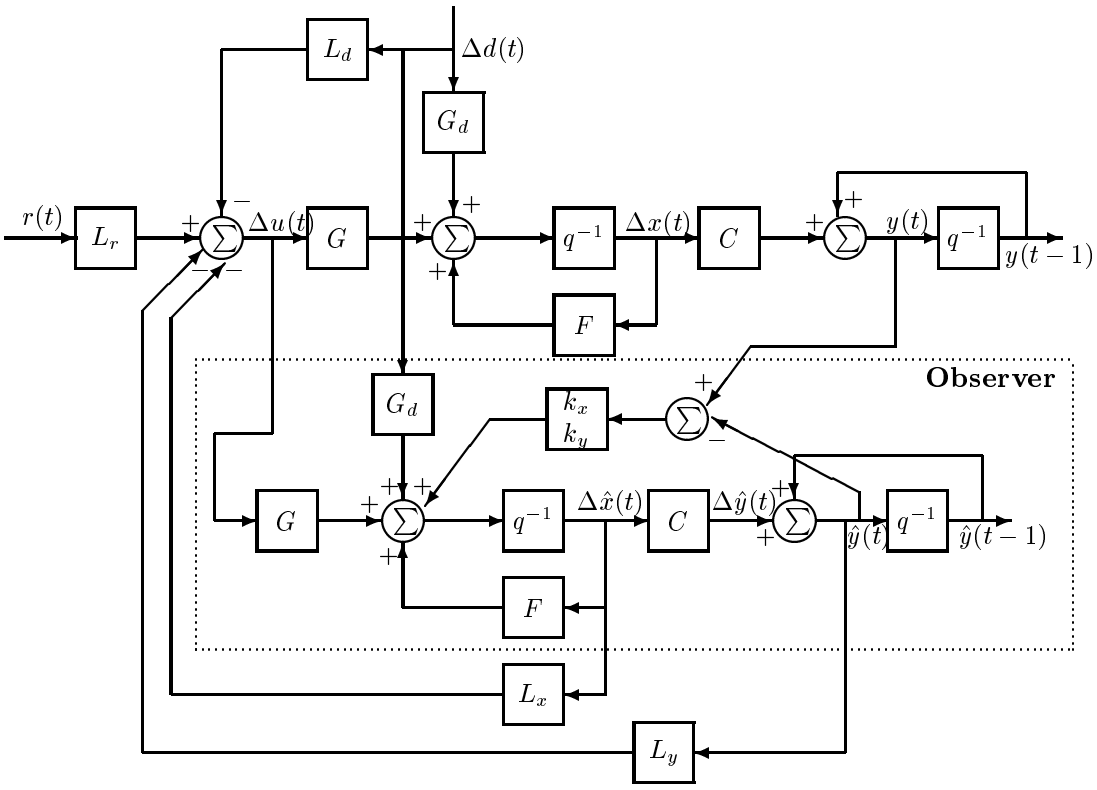

Figure 6.7: The controller structure with observer, feedback and feedforward.

A simulation using these matrices in the controller design and $F_d = 0.99I$ gives the result illustrated in Figure 6.8 where the control signals are also shown. As seen, the controller manage to reject the different disturbances well. In Figure 6.9 the disturbances in the influent water are presented.

A problem with this design is that there is not a unique combination of the control signals which can generate the outputs. This can make the control signals to drift. Since only the incremental control signal is penalized in the LQ criterion one control signal can take high values while another becomes almost zero. A possible solution could be to extend the state vector with the absolute value of the control signal to be able to penalize these too.

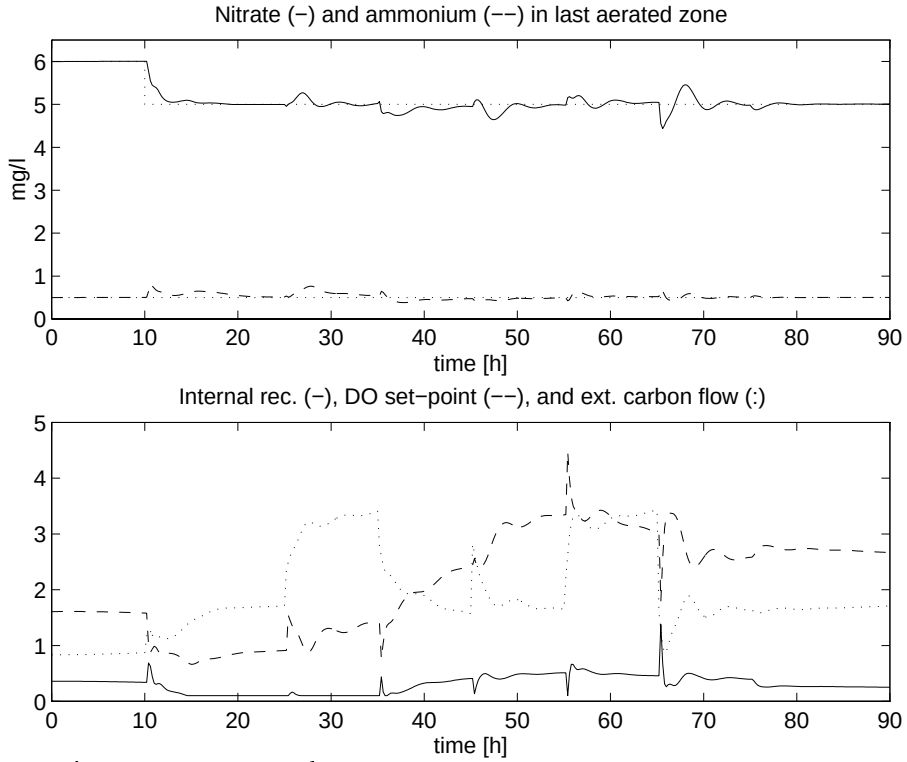

Figure 6.8: *Upper plot:* The outputs, nitrate and ammonium. The NO_3 set-point is changed from 6 to 5 after 10 hours. *Lower plot:* The control signals, DO set-point (mg/l), internal recirculation (m^3/h), and external carbon flow rate (l/h), with concentration 20000 mg/l COD.

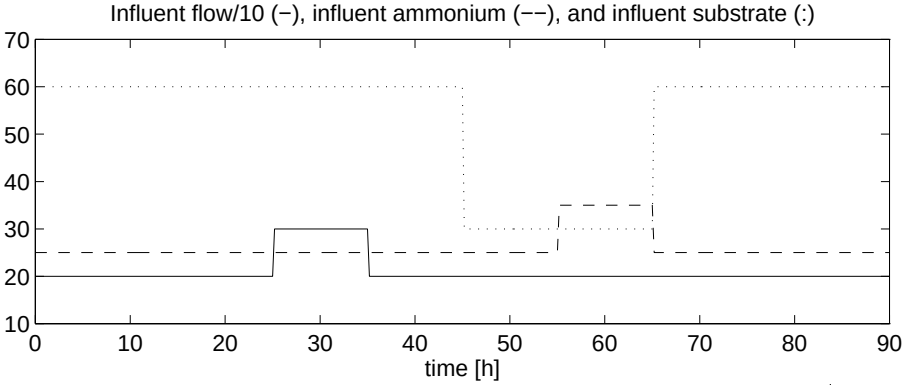

Figure 6.9: The measurable disturbances in the influent, flow/10 (l/h), ammonium (mg/l) and substrate (mg/l). The return sludge flow is 250 l/h, but at t =75h it is set to 400 l/h.

6.2.3 Controller design with integration states

An LQ controller where integration is included by using additional integration states $x_i(t)$ is derived in this section. The integration states are given by

$$x_i(t+1) = x_i(t) + r(t) - y(t) \tag{6.44}$$

see also Åström and Wittenmark (1990). In Figure 6.10 this is illustrated together with the feedback and the feedforward path.

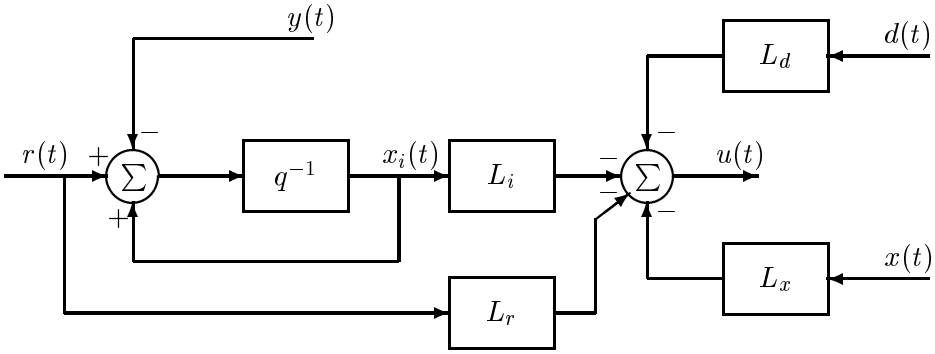

Figure 6.10: The LQ-controller with integration, feedforward and feedback.

The control signals are calculated by

$$u(t) = -\begin{bmatrix} L_x & L_i & L_d & L_r \end{bmatrix} \begin{bmatrix} x(t) \\ x_i(t) \\ d(t) \\ r(t) \end{bmatrix} = -LX(t) \tag{6.45}$$

To determine the L-vector the state vector in (6.22) has to be extended with two new types of states, the integration states $x_i(t)$ and the reference signals $r(t)$, as in (6.45).

$$\begin{bmatrix} x(t+1) \\ x_i(t+1) \\ d(t+1) \\ r(t+1) \end{bmatrix} = \begin{bmatrix} F & 0 & G_d & 0 \\ -C & I & 0 & I \\ 0 & 0 & F_d & 0 \\ 0 & 0 & 0 & F_r \end{bmatrix} \begin{bmatrix} x(t) \\ x_i(t) \\ d(t) \\ r(t) \end{bmatrix} + \begin{bmatrix} G \\ 0 \\ 0 \\ 0 \end{bmatrix} u(t) + \begin{bmatrix} v_x(t) \\ 0 \\ v_d(t) \\ v_r(t) \end{bmatrix}$$

$$y(t) = \begin{bmatrix} C & 0 & 0 & 0 \end{bmatrix} \begin{bmatrix} x(t) \\ x_i(t) \\ d(t) \\ r(t) \end{bmatrix} + e(t)$$

where F_d and F_r model the dynamics of the disturbances and the reference signals. A typical choice is $F_d = F_r = 0.99I$ (the size of the identity matrix

I is, however, different for F_d and F_r). The new system is now used for calculating the L-vector which is found by minimizing the LQ criterion

$$J = \sum_{t=0}^{\infty} X(t)^T Q X(t) + u(t)^T R u(t) \tag{6.46}$$

The minimum is found by solving the Riccati equation, see (6.38). Note that Φ and , are different here than in (6.38).

In (6.46), the Q and R matrices have to be selected. A suitable quantity to penalize with the Q matrix can be

$$r(t) - y(t) + \alpha x_i(t) \tag{6.47}$$

which means that the control error $(r - y)$ and a scaled part of the integration state x_i is penalized. The parameter α is a user parameter. Setting $\alpha = 0$ leaves out x_i which gives a controller without integration. Penalizing only x_i usually gives a controller with bad performance.

This particular penalty choice in (6.47) gives with $\alpha = 0.2$

$$\begin{aligned} Q &= H^T H \\ H &= [\ -C \quad 0.2I \quad 0 \quad I\ ] \end{aligned}$$

The control vector $u(t)$ which in this case consists of

$$u = [\ Q_{int} \quad DO_{ref} \quad Q_{Carbon}\ ]^T \tag{6.48}$$

is penalized in the LQ criterion by the R-matrix, which is chosen to

$$R = \begin{bmatrix} 0.5 & 0 & 0 \\ 0 & 0.5 & 0 \\ 0 & 0 & 2 \end{bmatrix} \tag{6.49}$$

Remark: Another idea to select the Q and R matrices could be to let these matrices in some way represent economical fees for effluent concentrations and prices of running pumps, external carbon dosing, etc. The LQ controller could then be based on the criterion $J = \sum_{t=0}^{\infty}[y(t)^T Q y(t) + u(t)^T R u(t)]$, where no integration is included. One could then hope that the LQ controller should find the optimal operating point. This did, however, not work well (the process was drifting around a lot) probably due to the criterion contains squared signals instead of linear signals.

Observer design

In this observer design it is only necessary to estimate $x(t)$. In the incremental design, outlined in Section 6.2.2, both $\Delta x(t)$ and $y(t)$ were estimated. Here $x(t)$ is estimated by

$$\hat{x}(t+1) = F\hat{x}(t) + Gu(t) + G_d d(t) + K(y(t) - C\hat{x}(t)) \tag{6.50}$$

The gain of the observer K is chosen by placing the observer poles slightly faster than closed loop poles (0.9 times the closed loop poles $F - GL_x$). The solution is under-determined and the additional degrees of freedom is used to make the observer more robust to perturbations in the system matrices, similar to the observer design in Section 6.2.2.

Antiwindup

To avoid integrator windup, where the integration states grow when a control signal has saturated, the integration states are not updated if a control signal has saturated. Hence

$$x_i(t+1) = \begin{cases} x_i(t) + r(t) - y(t) & \text{if no control signal has saturated} \\ x_i(t) & \text{when any control signal has saturated} \end{cases} \tag{6.51}$$

The control signal which saturates can now be limited without achieving an unacceptable performance. Note that the observer has to use the saturated control signals.

Controller experiment

In Figure 6.11 an application with the controller is illustrated. The disturbances are the same as in Figure 6.9. It is interesting to study how the controller trades off the different signals. Changing the NO_3 reference signal from 6 to 5, at $t = 10$h, causes the external carbon dosage and internal recirculation to increase, the DO set-point decrease and the ammonium becomes temporarily higher. An almost doubled return sludge flow at t=75h does hardly not affect the control, which is in agreement with the identification experiment, where it was found that using the return sludge flow as an input did not improve the estimated model.

The previous simulation was noise-free. The same simulation is now repeated, but with noise added on the output with standard deviation 0.1 on the ammonium sensor and 0.1 on the nitrate sensor. This is illustrated in Figure 6.12. As seen, the control signals becomes a bit noisy. A less

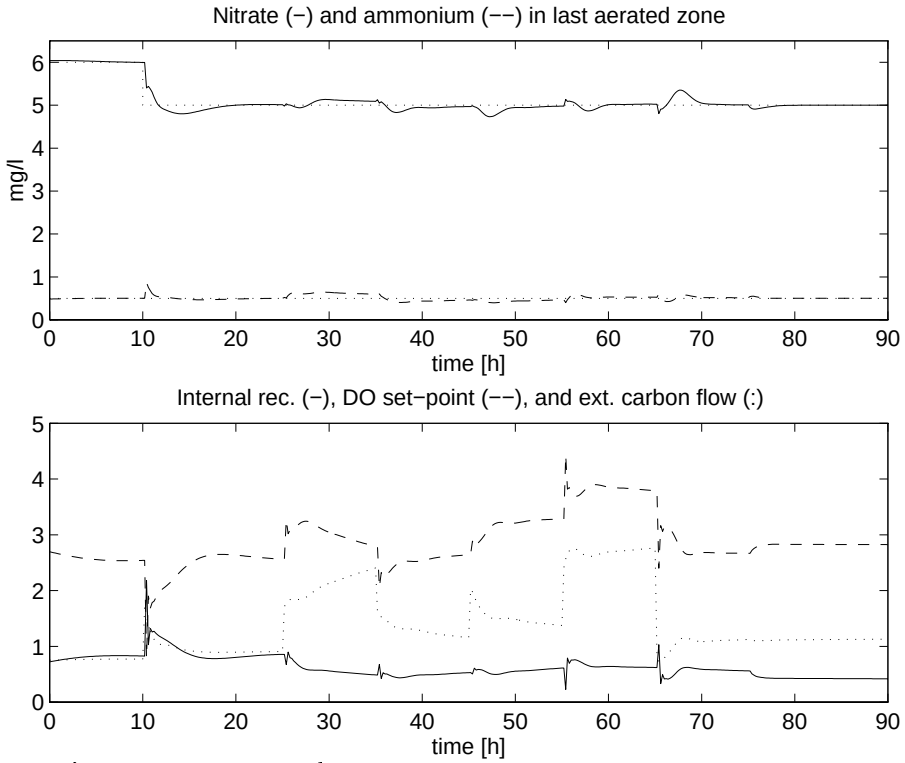

Figure 6.11: *Upper plot:* The outputs, nitrate and ammonium. The NO_3 set-point is changed from 6 to 5 after 10 hours. *Lower plot:* The control signals, DO set-point (mg/l), internal recirculation (m^3/h), and external carbon flow rate (l/h), with concentration 20000 mg/l COD.

noise sensitive controller can be achieved by designing a slower controller and a slower observer. A slower controller can be obtained by multiplying the previously used Q matrix with 0.5. The observer poles can be set equal to the closed loop poles, instead of scaling them by 0.9 as before.

6.2.4 Comparison between the two multivariable controllers

The two controllers gave similar performance despite the different design methods. The major differences are that the the controller on differential form penalize incremental states which makes it easier to obtain smooth control signals. A drawback with this method is that the size of the control signals are not penalized which makes it possible for the control signals to drift. This may happen if the control signals do not have a unique solution

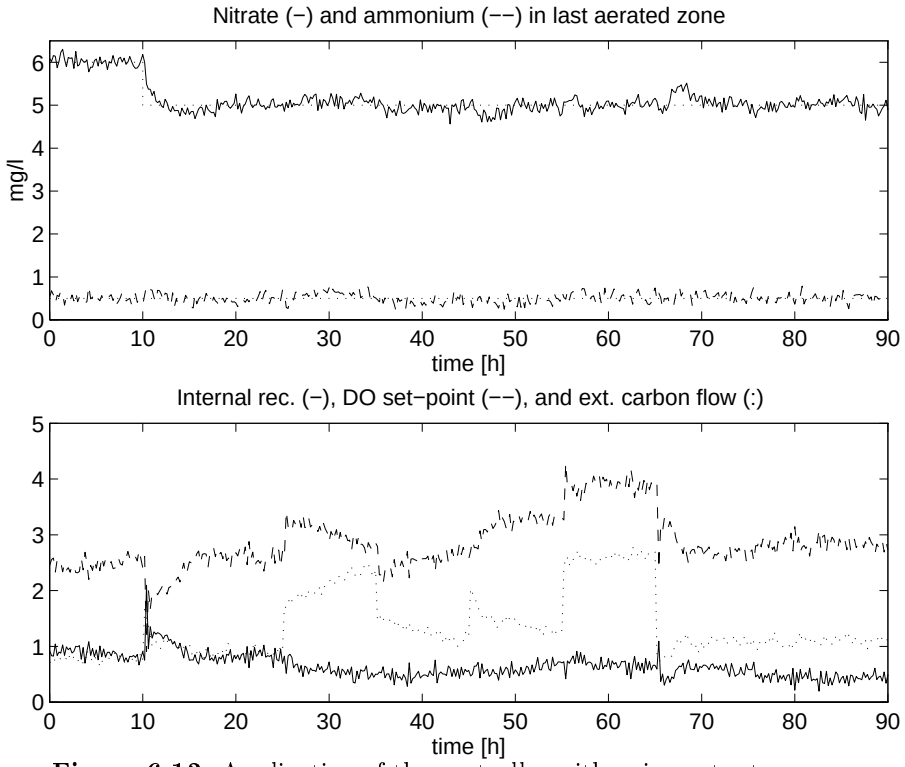

Figure 6.12: Application of the controller with noisy output sensors. *Upper plot:* The outputs, nitrate and ammonium. The NO_3 set-point is changed from 6 to 5 after 10 hours. *Lower plot:* The control signals, DO set-point (mg/l) and internal recirculation (m^3/h), and external carbon dosage (l/h, with concentration 20000 mg/l.

for a particular output, which is the case here. The controller with the additional integration states, on the other hand, penalizes the size of the control signals and it is then easier to reduce the drift, but the problem with the drift is not completely solved by this method either.

6.2.5 Comparison between SISO and MIMO control

Several single input single output (SISO) controllers could be used as an alternative to a multivariable controller. An approach consisting of three SISO controllers is presented here:

- Control of the ammonium concentration, as outlined in Section 5.5.

- Control of the nitrate concentration in the anoxic zone, as presented in Chapter 3.
- Control of the nitrate concentration in the last aerobic zone by using the internal recirculation flow rate as the control signal.

In this simulation, the adaptive model-based PI controller is used for control of the nitrate concentration in the anoxic zone. The other two controllers are PI controllers which are manually tuned. Since there are cross couplings in the process it is difficult to design fast SISO controllers. It is very easy to obtain an oscillating closed loop system.

In the comparison between the controllers, the reference signal for the nitrate concentration is changed from 6 to 5 mg/l. There are also variations in the influent wastewater, as illustrated in Figure 6.9, where both the influent flow rate, and influent wastewater composition are varied.

A simulation with the SISO controllers is illustrated in Figure 6.13. The SISO controllers manages reasonably well to reject the different disturbances. The nitrate concentration in the anoxic zone which is controlled by the external carbon flow rate is shown in Figure 6.14. This control works also well, the nitrate concentration in the anoxic zone is kept close to its set-point. An interesting question is, however, how to select the nitrate set-point in the anoxic zone. In the suggested MIMO controllers this choice does not exist.

The simulation with the MIMO controllers were shown in Figure 6.8 and 6.11. These controllers works even better than the SISO controller. The outputs ware kept very close to the desired set-points. It was also easier to tune these controller faster than the SISO controller, since the multivariable controllers are based on a multivariable model where all cross-couplings are known. A possible problem with this controller is that the controller signals are drifting, but on the other hand they are also drifting in the SISO case, so this may not be a particular problem for MIMO controllers.

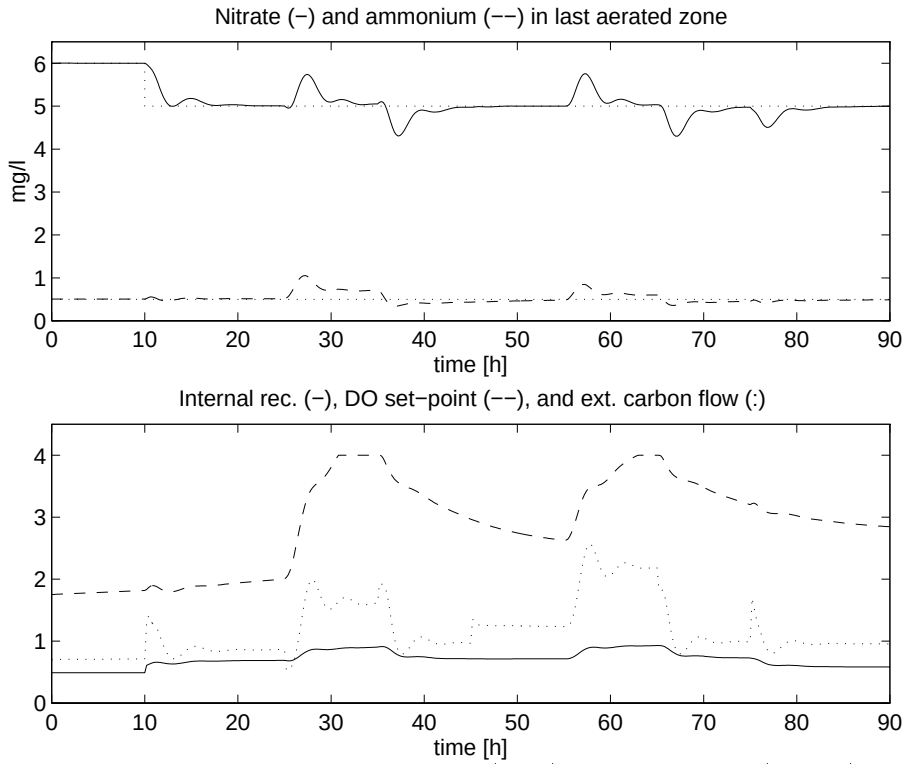

Figure 6.13: SISI control of nitrate (solid) and ammonium (dashed) concentrations (upper part), the reference values (dotted) are also shown. In the lower part, the control signals are shown, i.e. DO set-point (dashed), internal recirculation (solid), and external carbon dosage (dotted).

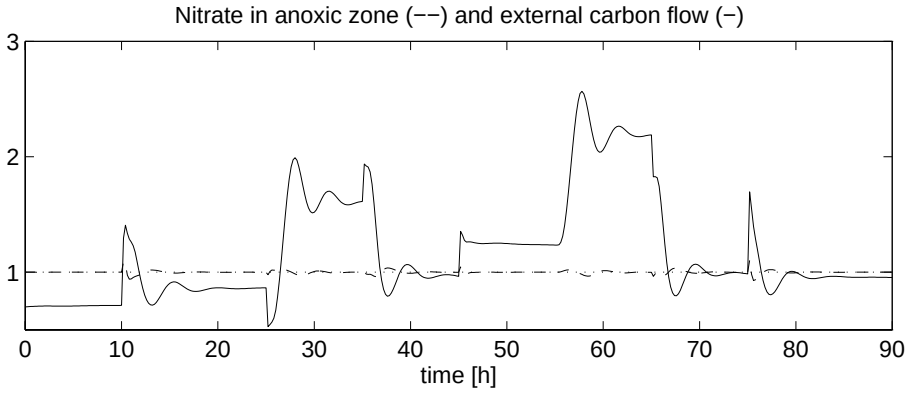

Figure 6.14: The nitrate concentration (dashed) in the anoxic zone, and the carbon flow rate (solid). The reference signal (dotted), is also shown.

6.3 Some remarks

Tuning the LQ-controllers are relatively simple (easier than tuning a PID controller). The elements in the R matrix (the Q matrix could also be used) are varied until the desired performance is obtained. To make the DO set-point, for example, smaller and less high frequent, the middle element in the R-matrix is increased.

The presented controllers do not use measurements of the nitrate concentration in the anoxic zone, and the air valve positions. It may hence be a good idea to extend the controller with these measurements, because of the following:

- If the nitrate concentration in the anoxic zone is close to zero, an increased dosage of external carbon is not very useful.
- If an air valve has saturated, it is no point increasing (decreasing) the DO set-point.

One may argue if it is a good strategy or not to maintain a set-point on the ammonium and nitrate concentration in the last aerated zone. It is likely that time-varying set-points are more optimal than constant ones. If a strategy for choosing the ammonium and nitrate set-points are derived, such a strategy may be applied to the multivariable controller.

A problem with the MIMO controllers is to find a good model of the process. Quite often a model is obtained which looks good in the validation from the identification, but when it is used in the controller design, the controller does not work well. The derived controller tries to use a negative internal recirculation rate. Before MIMO control can be applied reliably one has to find a method which can decide if an estimated model will work or not in a control design. One idea to solve this problem may be to study the step responses for the different input signals, and from this information decide if the model is suitable or not for controller design. Another problem is how to obtain a good model when you know the available model is not suitable. A possible solution could be to discard data used in the subspace identification, since this affects the estimated model. These problems are, however, topics for future research.

6.4 Conclusions

It has, by simulations, been shown that it is possible to estimate a linear time-invariant state-space model, which well can predict the ammonium

and nitrate concentration in the last aerated zone in a pre-denitrifying activated sludge process. The model uses the following six input signals: DO set-point, external carbon, internal recirculation, influent flow, influent carbon and influent ammonium.

Based on the estimated linear model, two multivariable linear quadratic (LQ) controller have been designed. The control strategy is based on maintaining the ammonium and the nitrate concentration in the last aerated zone close to specified set-points. The controllers use feedforward from measurable disturbances: influent flow, influent carbon and influent ammonium. The controllers were evaluated in a simulation study. The first one was based on differentiating the system and deriving an incremental controller. The second approach was to include additional integration states for each output. Both controllers showed high performance. It was, however, found that the modeling part is crucial for the control performance. A further study of this aspect is an important topic for future research.

Chapter 7

Conclusions and topics for future research

7.1 Conclusions

In this thesis some strategies to improve the control of wastewater treatment plants have been outlined. In particular control and estimation problems in a pre-denitrifying activated sludge process have been studied. By introducing more advanced control, the effluent concentrations of nitrate, ammonium, and oxygen consuming matter can be reduced. Less chemicals and energy are also needed, which give a significant economic incentive to use more advanced control strategies. The plant efficiency and capacity can hence be improved.

By adding an external carbon dosage, the effluent concentration of nitrate can be reduced. Four types of controllers for the external carbon dosage have been evaluated in a simulation study in Chapter 3. The control strategy was based on keeping the nitrate concentration in the anoxic zone at a constant low level. The four controllers were a PI-controller, a generalized minimum-variance adaptive controller, an adaptive LQ-controller, and a model-based adaptive PI controller. All controllers utilized feedforward. The PID-controller may be hard to tune and its control performance deteriorates when the process dynamic changes. The adaptive controllers were easier to tune, and they also worked well. A safety net was, however, required to avoid numerical problems with the adaptive controllers. The model-based adaptive PI controller showed high performance, and it uses physical knowledge of the process. The adaptive LQ-controller had also high performance. The direct adaptive controller adapted fast to changes

in the process and was easy to implement. A practical experiment with the direct adaptive controller has also been performed. It showed that the direct adaptive controller could keep the nitrate concentration in the anoxic zone tight to a desired set-point.

In Chapter 4, on-line methods for estimating the time-varying respiration rate and the nonlinear oxygen transfer function were presented. The estimator was based on a Kalman filter approach where measurements of the dissolved oxygen concentration and the airflow rate were used. Two different models of the nonlinear K_La function were suggested: an exponential model and a cubic spline model. Two models for modeling the time-varying respiration rate were also considered: a random walk model and an integrated random walk model. An approach to estimate the oxygen transfer function by differentiating the data was also briefly outlined. The estimation procedures were illustrated both in a simulation study and on real data from a pilot plant. The results were successful both in the simulation study and when applied to real data. In the practical experiment, the estimated respiration rate followed the measured respiration rate well.

The control of the dissolved oxygen in an activated sludge process was discussed in Chapter 5. The basic idea was to explicitly take the nonlinear oxygen transfer function into account in the control design. Two design approaches were then applied on the linearized process, pole-placement with a PI-regulator and linear quadratic control with feedforward. In a simulation study, the performance of a linear and a nonlinear controller was illustrated. It was shown that the nonlinear DO controller outperformed the linear controller. The results from the simulation study were also confirmed by experiments in a pilot plant. A set-point controller for the DO process was outlined. The basic idea was to control the DO set-point so that the ammonium concentration in the last aerobic zone was kept low. An experiment in the pilot plant showed that, by using this controller not only energy could be saved due to a lower DO set-point, but also the effluent nitrate concentration became significantly lower. A pressure controller was also evaluated in the pilot plant. The air pressure was controlled so that the most open valve was almost completely open.

In Chapter 6 it was shown, in simulations, that it was possible to estimate a linear time-invariant multivariable state-space model, which could predict the ammonium and nitrate concentration in the last aerated zone well. This model was then used for design of multivariable LQ controllers with feedforward. For the control, external carbon, internal recirculation rate, and DO set-point were considered as inputs. Ammonium and nitrate in the last aerated zone were outputs. The controllers used feedforward

from the measurable disturbances: influent flow rate, influent ammonium concentration and influent substrate. Two different controllers were evaluated in a simulation study. The first one was based on differentiating the system and deriving an incremental controller. The second approach was to include additional integration states for each output. Both controllers showed high performance. It was, however, found that the modeling part was crucial for the control performance.

7.2 Topics for future research

7.2.1 Spatial DO control

It is possible to extend the set-point controller presented in Chapter 5 in various respects, for example, to control the number of aerated zones. The order in which the aerated zones are switched off may be important. Changing the aerobic/anoxic ratio also affects the dynamic in the nitrification/denitrification processes. Ammonium and nitrate controllers may hence need different tuning for different number of aerated zones. Placement of sensors may be another practical problem when changing an aerobic zone to an anoxic.

7.2.2 Further studies of the effect of surfactants

The surfactants have large impact on some WWTP. For example, it reduces the K_La. When this happens the airflow rate have to be increased to maintain the oxygen concentration, which consumes energy. If it is possible to precipitate the surfactants this problem could be reduced. A control strategy for the surfactant could then be based on an estimated K_La.

Further studies are needed to determine if the surfactants deteriorate the sludge settling properties and sludge loss is obtained. If they do, it is another reason to either try to find a precipitation chemical or make the polluter reduce their use of surfactants.

7.2.3 Analyzing the information of the carbon dosage

Another topic for further research could be to analyze the additional information, as the variations in carbon flow rate may give. For example, the airflow rate gives some information about the organic load to the plant. The carbon flow rate could perhaps in a similar way be used to achieve information about the influent wastewater composition, the denitrification

rate, and/or to detect problems in the process.

7.2.4 Control of the sludge blanket and the biomass

Several control strategies have been suggested in this thesis, but how the sludge recirculation rate and excess sludge flow rate should be controlled have not been discussed. It would hence be interesting to design a controller where these important flow rates are controlled. Should the strategy be based on keeping the sludge blanket constant, or the food to biomass ratio constant. Is it possible to take the efficiency of the microorganisms into account and vary the different concentrations after the temperature for example. How this should be solved are challenging questions for a future research.

7.2.5 Plant-wide optimization

To optimize a whole plant, which is very complex, it is helpful to divide the plant into several smaller sub-processes, which are easier to control and optimize. The global optimum of the plant may then not be reached, but we may get close. The key idea is illustrated in Figure 7.1. In the lowest

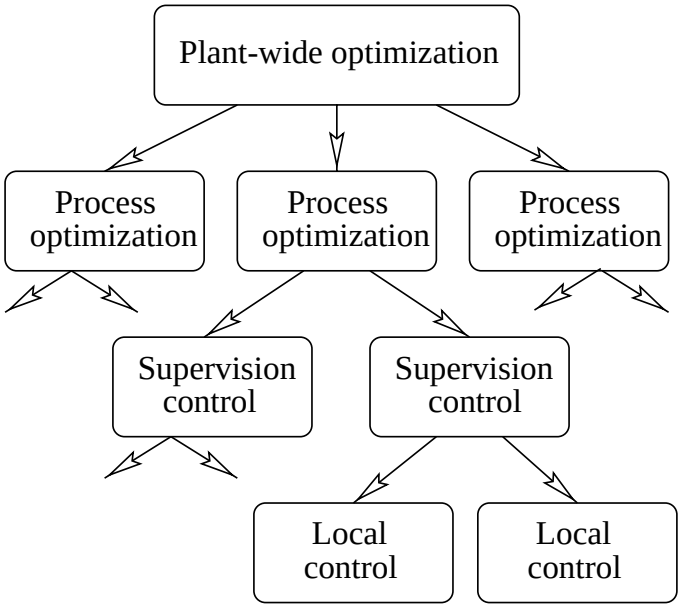

Figure 7.1: Different levels of control and optimization

layer there are simple control loops with relatively short time constants, like the DO controller, and the pressure controller which optimizes the

valve openings. In the next layer there are supervision controllers which controls the set-points of the controllers in the lower layer (cascade control). An example of this type of controller is the DO set-point controller. The multivariable controller could also fit into this category. In the second highest layer, set-points for the set-point controllers are derived in order to optimize the complete activated sludge process. Here cost functions may be a useful tool to find the most optimal operation of the process, see Section 7.2.6. The different disturbances in the influent are also considered. In the highest level, the complete wastewater treatment plant is optimized. That is, all processes at the WWTP are considered, i.e. sludge treatment, pre-sedimentation, the activated sludge process, etc. Also construction of new tanks could be considered. The long time planning is hence made at this level. How the optimization of the upper layers should be done is a topic for future research.

In the thesis, control algorithms which aims to optimize the complete WWTP have been started to be developed.

7.2.6 Cost functions

To find the optimal operation point for an activated sludge process a cost function may be used. By defining costs for effluent discharges and prices for running pumps, blowing air, dosing external carbon etc., the total cost for a specific operating condition can be calculated. Studies with these ideas have been made by Carstensen (1994) and Vanrolleghem *et al.* (1996).

Steady-state values for the outputs can be achieved for different combinations of the inputs by simulations. Using costs for the effluent discharges and prices of the inputs, the total cost can be determined at the different operating points. The minimum value of the cost function then gives the optimal operating point for that particular plant and influent. If the influent is changed (flow or composition) new simulations have to be made.

The cost function can not only be used to find the optimal operating point, the sensitivity for changes in the different control signals can also be studied. Plotting the cost function with respect to a control signal, a curve will appear. A narrow peak or a steep slope in the curve indicates that the process is sensitive to variations in the control signal. By applying a controller, much can be gained. A flat minimum on the other hand, means that not so much can be gained by controlling that signal. Running simulations for different influent compositions and flow rates, and then finding the optimal operating point for each inflow, gives an idea how the set-points should be varied when the inflow varies.

There are, however, some problems with this approach.

- To be able to apply the strategy to a real wastewater treatment plant, a well calibrated model of the activated sludge process is needed. This may be hard to obtain.
- The method is based on steady-state values, exactly how the method could be extended to be valid for a dynamic system is not clear. A simple idea could be to calculate the optimal steady-state operating points for the changing inflow, and then low pass filter these operating points.
- The way to compute the optimal controller signal is very computationally intense, if steady-state simulations should be used. Perhaps it is possible to find a less computationally intense method.

7.2.7 Extremum control

An alternative or modification of the previous outlined method could be to use extremum control. The extremum controller has similarities with the previous cost function approach, since it is also based on minimizing a cost function, but here real inputs and outputs will be used instead of simulated.

The idea is to define a cost function J_1 which is based on real costs of running the plant. Assume then that J_1 has an extremum point which, for example, can be modeled by

$$J_2 = U^T AU + B^T U + c$$

where U is the input vector which may consist of set-points, A is a coefficient matrix, B is a coefficient vector, and c a scalar. A, B, and c could be estimated by an identification method. The optimal control signal is then found by setting $dJ_2/dU = 0$, which gives

$$u = -\frac{1}{2} A^{-1} B$$

Exactly how this should work is a topic for future research, and there are some open issues, e.g.

- The contents of U is not obvious. Which inputs should be included (maybe the cost function in Section 7.2.6 could answer that) should time-lagged inputs be stored in the U vector.

- Could J_2 model the extremum point?
- Does there exist an extremum point.?
- How much excitation is needed to estimate A and B?

Appendix A

The generalized minimum-variance controller with feedforward

A.1 Derivation of the controller

The generalized minimum-variance controller, used to control the external carbon source in Chapter 3, is derived here.

Assume that the process to be controlled is described by the linear discrete-time model

$$A(q^{-1})y(t) = B(q^{-1})u(t-k) + D(q^{-1})w(t-d) + C(q^{-1})\frac{1}{\Delta(q^{-1})}e(t) \quad \text{(A.1)}$$

where $A(q^{-1})$, $B(q^{-1})$, $C(q^{-1})$ and $D(q^{-1})$ are polynomials in the backward shift operator q^{-1}, with degrees na, nb, nc, and nd. The polynomials $A(q^{-1})$ and $C(q^{-1})$ are monic, $y(t)$ is the output and $u(t)$ is the input. Furthermore, the time delays are denoted by k and d, and

$$\Delta(q^{-1}) = 1 - q^{-1} \quad \text{(A.2)}$$

The disturbance $w(t)$ is measurable and the disturbance $e(t)$ is unmeasurable zero mean white noise.

The controller has the following stucture

$$(R(q^{-1}) + \frac{\rho}{r_0}C(q^{-1}))\Delta u(t) = -S(q^{-1})y(t) - Q(q^{-1})\Delta w(t+k-d) \quad \text{(A.3)}$$

To determine the controller polynomials, a predictor for the system (A.1) has to be determined. First $y(t+k)$ is calculated from (A.1), it becomes

$$y(t+k) = q^{k-k}\frac{B}{A}u(t) + q^{k-d}\frac{D}{A}w(t) + \frac{C}{A\Delta}e(t+k) \tag{A.4}$$

The k-step predictor $\hat{y}(t+k|t)$ is found by predicting the future noise samples with their mean value, i.e. $e(t+i) = 0$, $i > 0$. It is hence desired to partition $\frac{C}{A\Delta}e(t+k)$ into two parts. One part which contains the future noise and one which contains the old noise. This can be done by

$$\frac{C}{A\Delta} = F + q^{-k}\frac{G}{A\Delta} \tag{A.5}$$

where F and G are polynomials determined by (A.5) with the degrees $\deg(F)=k-1$ and $\deg(G)=\max(\deg(\Delta A),\deg(C))-1$. F and G are determined by carrying out the polynomial division $\frac{C}{A\Delta}$.

Using (A.5) in (A.4) with the future noise equal to zero gives the predictor

$$\hat{y}(t+k|t) = \frac{B}{A}u(t) + q^{k-d}\frac{D}{A}w(t) + \frac{G}{A\Delta}e(t) \tag{A.6}$$

This predictor contains $e(t)$, which can be expressed in terms of $y(t)$, $u(t)$, and $w(t)$ by using (A.1). Inserting the expression of $e(t)$ in (A.6) gives the final predictor

$$\hat{y}(t+k|t) = q^{k-k}\frac{BF}{C}\Delta u(t) + q^{k-d}\frac{DF}{C}\Delta w(t) + \frac{G}{C}y(t) \tag{A.7}$$

The k-step predictor (A.7) can be found in e.g. Åström and Wittenmark (1990) except for the extra term $q^{k-d}DF/C\Delta w(t)$ which has been included to account for the measurable disturbance.

To find the control law which minimizes the criterion (see also Clarke and Gawthrop (1975))

$$J = \frac{1}{2}\mathrm{E}[y^2(t+k) + \rho(\Delta u(t))^2|Y_t] \tag{A.8}$$

we first notice that

$$y(t+k) = \hat{y}(t+k|t) + Fe(t+k) \tag{A.9}$$

The incremental control signal $\Delta u(t)$, which gives the minimum value of J is found by setting the derivative of J with respect to $\Delta u(t)$ to zero.

Combining (A.9) and (A.8) we obtain

$$J = \frac{1}{2}\mathrm{E}[(\hat{y}(t+k|t) + Fe(t+k))^2 + \rho(\Delta u(t))^2] \tag{A.10}$$

and thus

$$\begin{aligned} 0 &= \frac{\partial J}{\partial \Delta u(t)} = \hat{y}(t+k|t)\frac{\partial \hat{y}(t+k|t)}{\partial \Delta u(t)} + \rho \Delta u(t) \\ &= (\frac{BF}{C}\Delta u(t) + q^{k-d}\frac{DF}{C}\Delta w(t) + \frac{G}{C}y(t))b_0 + \rho \Delta u(t) \end{aligned} \tag{A.11}$$

The derivative of $\hat{y}(t+k|t)$ with respect to $\Delta u(t)$ is equal to b_0, since F and C are monic polynomials, and we only consider $\Delta u(t)$ terms with the time index t.

The controller is found by rearranging (A.11) to

$$(BF + \frac{\rho}{b_0}C)\Delta u(t) = -Gy(t) - DF\Delta w(t+k-d) \tag{A.12}$$

The generalized minimum-variance controller (A.3) is then obtained by identifying the polynomials in (A.3) and (A.12).

$$S = G \tag{A.13}$$
$$R = BF \tag{A.14}$$
$$Q = DF \tag{A.15}$$
$$r_0 = b_0 \tag{A.16}$$

Note that the F polynomial is monic. Using (A.14), this implies that $r_0 = b_0$.

This completes the derivation of the generalized minimum-variance controller with feedforward.

Appendix B

LQ-control with feedforward

The aim of linear quadratic (LQ) controller design is to find a controller which minimizes the sum of the variance of the output and the weighted variance of the input, see Åström and Wittenmark (1990).

When a measurable disturbance exists, a feedback controller can be complemented with disturbance measurement feedforward, see e.g. Sternad and Söderström (1988) and Grimble (1988). For a given degree of disturbance rejection, the high frequency gain of the feedback controller can then be reduced, which may increase the stability robustness, see Sternad (1991).

The LQ-controller derived here makes it possible to use separate penalties on the contributions to the control signal from measurable and unmeasurable disturbances. This makes it for example possible to use a controller with deadbeat feedforward in combination with a cautious feedback. The feedforward does not affect the closed-loop stability. It may therefore be useful to apply a smaller penalty on the control signal generated by the feedforward than on the feedback. Separate control penalties may also be fruitful, when the variance of the measurement noise on the feedforward sensor is different compared to the feedback sensor, see also e.g. Grimble (1988).

B.1 The LQ problem

Assume that the process to be controlled is described by the linear discrete-time model

$$A(q^{-1})y(t) = B(q^{-1})u(t-k) + D(q^{-1})w(t-d) + C(q^{-1})\frac{1}{\Delta(q^{-1})}e(t) \quad \text{(B.1)}$$

where $A(q^{-1})$, $B(q^{-1})$, $C(q^{-1})$ and $D(q^{-1})$ are polynomials in the backward shift operator q^{-1}, with degrees na, nb, nc, nd. The polynomials $A(q^{-1})$ and $C(q^{-1})$ are monic, $y(t)$ is the output and $u(t)$ is the input. Furthermore, the time delays are denoted by k and d, and

$$\Delta(q^{-1}) = 1 - q^{-1} \quad \text{(B.2)}$$

The disturbance $w(t)$ is measurable and the disturbance $e(t)$ is unmeasurable zero mean white noise. The measurable disturbance $w(t)$ is modelled by an ARMA process

$$w(t) = \frac{G(q^{-1})}{H(q^{-1})}v(t) \quad \text{(B.3)}$$

where $v(t)$ is zero mean white noise. The polynomials $G(q^{-1})$ and $C(q^{-1})$ are required to be stable polynomials[1]. A stable polynomial is defined as a polynomial which has all its zeros inside the the unit circle.

A frequently used criterion in LQ-design, see e.g. Åström and Wittenmark (1990) is

$$J = \lim_{N\to\infty} \frac{1}{N}\sum_{t=0}^{N}[\mathrm{E}y(t)^2 + \rho \mathrm{E}u(t)^2] \quad \text{(B.4)}$$

It is also common that, instead of penalizing the variance of the control signal $u(t)$ as in the criterion (B.4), the variance of

$$\Delta u(t) = u(t) - u(t-1) \quad \text{(B.5)}$$

is penalized instead. This allows the control signal to drift while the variations of the control signal are reduced. The choice of penalizing $\Delta u(t)$ instead of $u(t)$, is reasonable when there are drifting disturbances, since such disturbances require a drifting control signal, which forces the controller to contain integration[2]. The LQ controller to be derived here will

[1] If G or C are estimated, and zeros in $|z| \geq 1$ are obtained, these zeros then have to be projected into the stable region. Such a projection does not change the spectral density of $Gv(t)$ or $Ce(t)$.

[2] If the control signal is drifting, the problem of minimizing the criterion (B.4) would be unsolvable when penalizing $u(t)$ since the criterion grows to infinity for drifting signals.

therefore use Δu in the criterion. The obtained integrating controller is also advantageous for other reasons, e.g. it makes the controller less sensitive to low-frequency modelling errors.

To derive a LQ-controller where it is possible to use separate penalties on components of the control signal which originate from different disturbances, the control signal increment is partitioned as

$$\Delta u(t) = \Delta u_e(t) + \Delta u_v(t) \tag{B.6}$$

where $u_e(t)$ is the part of the control signal which is generated by the unmeasurable noise $e(t)$, and $u_v(t)$ is the part originating from the innovation sequence of the measurable disturbance $v(t)$. The new criterion with two penalty parameters is

$$J = \lim_{N\to\infty} \frac{1}{N} \sum_{t=0}^{N} [\mathrm{E}y(t)^2 + \mathrm{E}(\sqrt{\rho_e}\Delta u_e(t) + \sqrt{\rho_v}\Delta u_v(t))^2] \tag{B.7}$$

The q^{-1} argument is for simplicity skipped in most of the following polynomial equations. The polynomial $A(q^{-1})$, for example will only be denoted by A, and so on. Conjugated polynomials are also used. They are denoted by a * and defined as follows. If

$$B(q^{-1}) = b_0 + b_1 q^{-1} + b_2 q^{-2} + \dots \tag{B.8}$$

then

$$B^*(q) = b_0 + b_1 q + b_2 q^2 + \dots \tag{B.9}$$

If $B(q^{-1})$ is a stable polynomial, then $B^*(q)$ is unstable.

The controller minimizing the criterion (B.7) is presented in the following Theorem.

Theorem B.1 *Consider the system (B.1), and assume $A\Delta$ and B to have no common unstable factors. The controller which minimizes the criterion (B.7), where $v(t)$ and $e(t)$ are assumed to be uncorrelated, is then given by*

$$R(q^{-1})\Delta u(t) = -S(q^{-1})y(t) - \frac{Q(q^{-1})}{P(q^{-1})} w(t) \tag{B.10}$$

where $R(q^{-1})$, $S(q^{-1})$, $P(q^{-1})$ and $Q(q^{-1})$ are controller polynomials.

The feedback polynomials $R(q^{-1})$ and $S(q^{-1})$ are determined by the unique solution of the pole placement equation

$$\alpha \stackrel{\Delta}{=} AR\Delta + q^{-k}BS = \beta_e C \tag{B.11}$$

when $A\Delta$ and B have no common factors. If they have common factors, then see remark 2. In (B.11) r_e is a scalar and $\beta_e(q^{-1})$ is a stable monic polynomial derived from the spectral factorization

$$r_e\beta_e\beta_e^* = BB^* + \rho_e A\Delta\Delta^* A^* \tag{B.12}$$

The feedforward filter denominator $P(q^{-1})$ is determined by

$$P = G\beta_v \tag{B.13}$$

where $\beta_v(q^{-1})$ is a stable monic polynomial derived from the spectral factorization

$$r_v\beta_v\beta_v^* = BB^* + \rho_v A\Delta\Delta^* A^* \tag{B.14}$$

The feedforward polynomial $Q(q^{-1})$ is found as the unique solution of the linear polynomial equation

$$(RB^* - \rho_v\Delta^* A^* Sq^{-k})q^{-d+k}DG\Delta = r_v\beta_v^* Q + qL^*\alpha H \tag{B.15}$$

with respect to $Q(q^{-1})$ and $L^*(q^{-1})$.

Proof: The proof is given in Lindberg (1995).

Remark 1: As mentioned before, the control signal has been separated into two parts $u_e(t)$ and $u_v(t)$ which can be penalized separately. One should, however, be aware of the following property. Since $u_v(t)$ is derived from the measurable disturbance $v(t)$, a large value of ρ_v implies that $v(t)$ will not be rejected, not even by the feedback loop. The effect of the measurable disturbance $v(t)$ on the feedback signal will in such a case instead be (partly) cancelled by the feedforward control signal. In general one would like a slow feedback for stability reasons and a fast feedforward to reject measurable disturbances fast, then $\rho_e > \rho_v$ and this property does not occur.

Remark 2: When $A\Delta$ and B have common factors, the feedback polynomials $R(q^{-1})$ and $S(q^{-1})$ are determined by the unique solution to the coupled linear polynomial equations

$$\rho_e\Delta^* A^* C + q^{-k+1}BX^* = r_e\beta_e^* R \tag{B.16}$$

$$q^k CB^* - qA\Delta X^* = r_e\beta_e^* S \tag{B.17}$$

with respect to $R(q^{-1})$, $S(q^{-1})$ and $X^*(q)$.

Remark 3: When $\rho = \rho_e = \rho_v$, a special and simplified case is obtained, where the feedforward polynomials $P(q^{-1})$ and $Q(q^{-1})$ instead are

determined by the following equations:

$$P = G \tag{B.18}$$
$$q^{-d+1}DG\Delta X^* = r\beta^* Q + qL^* CH \tag{B.19}$$

where the $X^*(q^{-1})$ polynomial is obtained from either (B.16) or (B.17).

The degrees of the Q and L polynomials should here be chosen as

$$n_Q = \max(n_d + n_g + d + 1, n_c + n_h) - 1 \tag{B.20}$$
$$n_L = \max(0, k - d) + n_\beta - 1 \tag{B.21}$$

The feedback polynomials are not affected. When $\rho_e \neq \rho_v$ the degrees of the polynomials are derived as in Section B.1.1.

Remark 4: Typical selection of ρ_e and ρ_v. The most useful application of this controller is to design the feedforward loop faster than the feedback. Since the feedforward does not affect the closed-loop stability it is useful to apply a smaller penalty on the control signal generated by the feedforward (ρ_v) than on the feedback (ρ_e).

Remark 5: When the measurable disturbance $w(t)$ is drifting, i.e. when a factor Δ exists in the denominator of the model (B.3) of $w(t)$

$$w(t) = \frac{G}{\Delta H_1} v(t)$$
$$H = \Delta H_1$$

then (B.15) has to be slightly modified. Otherwise Δ becomes a common factor of both sides of the equation. To see this, we notice that Δ is a factor of the left-hand side of (B.15) and in one of the right-hand side terms (H). Then Δ must also be a factor of Q, if the equation is to have a solution. To avoid this problem, we explicitly introduce Δ as a factor in Q, as

$$Q = \Delta Q_1 \tag{B.22}$$

and cancel this factor everywhere in (B.15). Equation (B.15) is then reduced to

$$(RB^* - \rho_v \Delta^* A^* S z^{-k}) z^{-d+k} DG = r_v \beta_v^* Q_1 + z L^* \alpha H_1 \tag{B.23}$$

and can now be solved with respect to Q_1, defined in (B.22). As noted in Sternad (1991), the same type of modification must be applied to (B.19).

In Figure B.1 the process with the controller is illustrated. Note that $1/(R(q^{-1})\Delta(q^{-1}))$ is present in both the feedback and the feedforward loop.

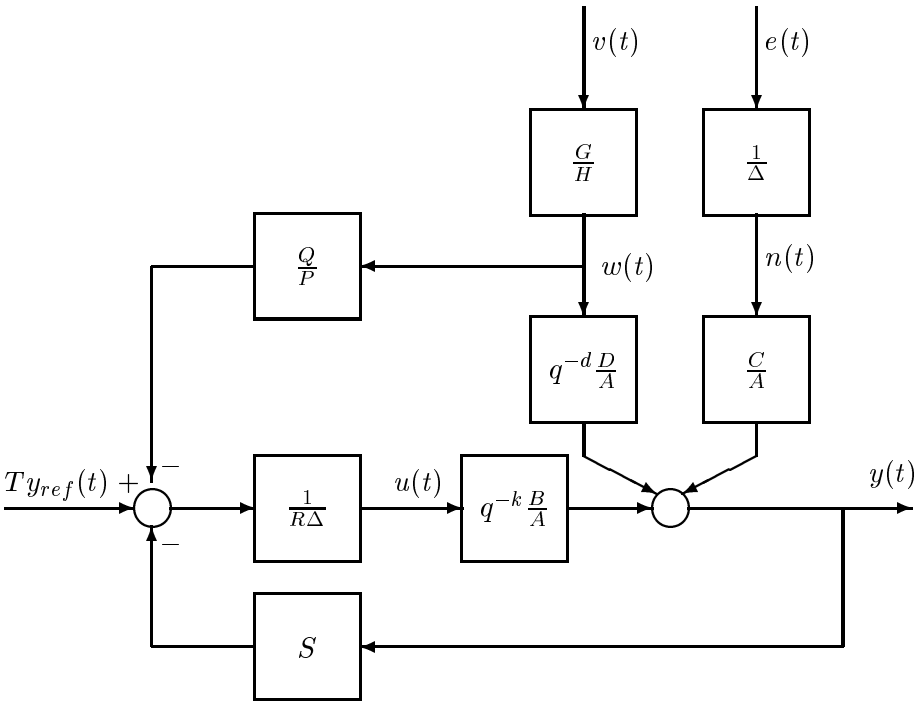

Figure B.1: The process with the controller

B.1.1 Choice of the degrees of the controller polynomials

To find the unique solution of the controller polynomials, their degrees have to be chosen properly. The degrees are defined so that the polynomials cover the maximal powers of q^{-1} and q in the equations.

Studying equation (B.16) gives

$$-\deg C \geq -\deg R \tag{B.24}$$

$$-k+1-\deg B \geq -\deg R \tag{B.25}$$

The minus signs appear because the polynomial argument is q^{-1}. Note that the * polynomials do not affect the maximal power of q^{-1}, since their leading coefficient is independent of q (e.g. $X^* = x_0 + x_1 q + \ldots$). Equation (B.24) and (B.25) can be simplified to

$$\deg R = \max(\deg B + k - 1,\ \deg C)$$

In the same way, the degrees of the other polynomials are determined (where the notation $n_x = \deg X$ is used)

$$n_{\beta_e} = \begin{cases} \max(n_a+1,\ n_b) & \text{if } \rho_e \neq 0 \\ n_b & \text{if } \rho_e = 0 \end{cases}$$

$$
\begin{aligned}
n_{\beta_v} &= \begin{cases} \max(n_a+1,\ n_b) & \text{if } \rho_v \neq 0 \\ n_b & \text{if } \rho_v = 0 \end{cases} \\
n_x &= n_{\beta_e} + k - 1 \\
n_r &= \begin{cases} \max(n_b+k-1,\ n_c) & \text{if } \rho_e \neq 0 \\ n_b+k-1 & \text{if } \rho_e = 0 \end{cases} \\
n_s &= \max(n_a,\ n_c-k) \\
n_q &= \begin{cases} \max(n_\alpha+n_h-1,\ d-k+n_d+n_g+1+\max(n_r,\ n_s+k)) & \text{if } \rho_v \neq 0 \\ \max(n_\alpha+n_h-1,\ d-k+n_d+n_g+1+n_r) & \text{if } \rho_v = 0 \end{cases} \\
n_l &= \begin{cases} \max(n_{\beta_v},\ k-d+\max(n_b,\ 1-d+n_a))-1 & \text{if } \rho_v \neq 0 \\ \max(n_{\beta_v},\ k-d+n_b)-1 & \text{if } \rho_v = 0 \end{cases}
\end{aligned}
$$

Appendix C

Cubic spline

A cubic spline polynomial may give a good approximation of many types of static nonlinearities. The spline function is (here) a piecewise third order polynomial with continuous first and second derivatives in its (grid) points, which do not need to be placed equidistant. It has an inherent smoothness which is natural from a physical point of view. In Figure C.1 a cubic spline is shown, together with some of the parameter definitions.

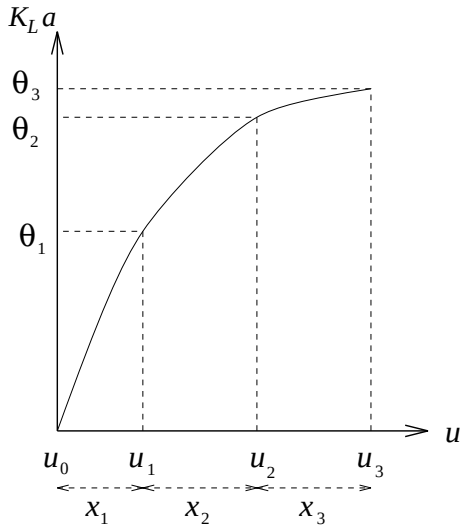

Figure C.1: A cubic spline function.

The common use of a cubic spline is for *interpolation*, see e.g. Dahlquist *et al.* (1974). For such a case θ, see Figure C.1, is known. Here the θ vector is unknown and will be estimated.

From Dahlquist *et al.* (1974) we have that a cubic spline polynomial can be written in the following form where u is in the interval $u_{i-1} \leq u < u_i$

$$\begin{aligned} K_L a(u)_i &= m_i\theta_i + (1-m_i)\theta_{i-1} \\ &+ x_i m_i(1-m_i)[(k_{i-1}-d_i)(1-m_i) - (k_i - d_i)m_i] \end{aligned} \quad \text{(C.1)}$$

where

$$x_i = u_i - u_{i-1} \quad \text{(C.2)}$$

$$d_i = \frac{\theta_i - \theta_{i-1}}{x_i} \quad \text{(C.3)}$$

$$m_i = \frac{u - u_{i-1}}{x_i}, \quad u \in [u_{i-1}, u_i] \quad \text{(C.4)}$$

$$i = 1, 2, \ldots, n \qquad n = \text{number of grid points} \quad \text{(C.5)}$$

The variables $k_0, k_1, ..., k_n$ are the derivatives of the spline at the grid points. Note that $K_L a(u_i)_i = \theta_i$.

The form (C.1) is not convenient for parameter estimation. Below a linear regression form for the model (C.1) will be outlined.

C.1 Derivation of the linear regression form

The purpuse of this derivation is to find an expression of $K_L a(u)$ in the following form.

$$K_L a(u)_i = \psi^T_{K_L a}\theta_{K_L a} \quad \text{(C.6)}$$

To find this expression we start by deriving the derivatives of the spline at the grid points, i.e. $k_0, k_1, ..., k_n$. The derivatives are determined from the condition that the second order derivative of the cubic spline, should be equal in the grid points, that is

$$K_L a''(u)_{i+1} = K_L a''(u)_i \quad \text{(C.7)}$$

This gives the linear system of equations

$$\begin{aligned} x_{i+1}k_{i-1} + 2(x_i + x_{i+1})k_i + x_i k_{i+1} &= 3(x_i d_{i+1} + x_{i+1}d_i) \\ i &= 1, 2, \ldots, n-1 \end{aligned} \quad \text{(C.8)}$$

Since (C.8) has $n+1$ unknowns, but only $n-1$ equations, two additional equations are needed to uniquely determine the spline function. These equations can be obtained by assuming that the spline function is a straight line outside the interval (Dahlquist *et al.* 1974). Hence

$$K_L a''(u_0)_1 = K_L a''(u_n)_n = 0 \quad \text{(C.9)}$$

which gives

$$2k_0 + k_1 = 3d_1 \tag{C.10}$$
$$k_{n-1} + 2k_n = 3d_n \tag{C.11}$$

The equations (C.8), (C.10) and (C.11) can be written in matrix form as

$$LK = 3D \tag{C.12}$$

where

$$K = [k_0 \dots k_n]^T$$

$$L = \begin{bmatrix} 2 & 1 & & & & \\ x_2 & 2(x_1+x_2) & x_1 & & & \\ & x_3 & 2(x_2+x_3) & x_2 & & \\ & & \ddots & \ddots & \ddots & \\ & & & x_{n-1} & 2(x_{n-2}+x_{n-1}) & x_{n-2} \\ & & & & 1 & 2 \end{bmatrix}$$

$$D = \begin{bmatrix} d_1 \\ x_1 d_2 + x_2 d_1 \\ x_2 d_3 + x_3 d_2 \\ \vdots \\ x_{n-1} d_n + x_n d_{n-1} \\ d_n \end{bmatrix}$$

The K-vector is thus obtained by solving

$$K = 3L^{-1}D \tag{C.13}$$

The L^{-1} consists only of terms involving the grid points (L^{-1} does not depends on the measurements) and can be expressed as

$$L^{-1} = \begin{bmatrix} r_{00} & r_{01} & \dots & r_{0n} \\ r_{10} & r_{11} & \dots & r_{1n} \\ \vdots & \vdots & & \vdots \\ r_{n0} & r_{n1} & \dots & r_{nn} \end{bmatrix} \tag{C.14}$$

Using (C.13), the i:th component can be written as

$$k_i = 3(r_{i0}D_0 + r_{i1}D_1 + \dots + r_{in}D_n) \tag{C.15}$$

where $D_0 \ \ldots \ D_n$ are the elements in the D-vector. Replacing the d_i elements in the D vector with the θ parameters as defined in (C.3), and writing k_i as a scalar product gives

$$k_i = 3\phi_i^T \theta_{K_L a} \tag{C.16}$$

$$\theta_{K_L a} = [\theta_0 \quad \ldots \quad \theta_n]^T \tag{C.17}$$

$$\phi_i = \begin{bmatrix} -r_{i0}\frac{1}{x_1} - r_{i1}\frac{x_2}{x_1} \\ r_{i0}\frac{1}{x_1} + r_{i1}(\frac{x_2}{x_1} - \frac{x_1}{x_2}) - r_{i2}\frac{x_3}{x_2} \\ \vdots \\ r_{i,m-1}\frac{x_{m-1}}{x_m} + r_{im}(\frac{x_{m+1}}{x_m} - \frac{x_m}{x_{m+1}}) - r_{i,m+1}\frac{x_{m+2}}{x_{m+1}} \\ \vdots \\ r_{i,n-2}\frac{x_{n-2}}{x_{n-1}} + r_{i,n-1}(\frac{x_n}{x_{n-1}} - \frac{x_{n-1}}{x_n}) - r_{in}\frac{1}{x_n} \\ r_{in}\frac{1}{x_n} + r_{i,n-1}\frac{x_{n-1}}{x_n} \end{bmatrix} \tag{C.18}$$

$$m = 2 \ldots n-2 \tag{C.19}$$

After straightforward algebraic manipulations, utilizing (C.1) and (C.16) – (C.18), we finally get

$$K_L a(u)_i = \psi_{K_L a}^T \theta_{K_L a} \tag{C.20}$$

$$\psi_{K_L a}^T = x_i m_i (1-m_i)[(1-m_i)3\phi_{i-1}^T - m_i 3\phi_i^T] + G \tag{C.21}$$

$$G = [0 \quad \ldots \quad 0 \quad \{1 + m_i^2(2m_i - 3)\}_{i-1} \quad \{m_i^2(3-2m_i)\}_i \quad 0 \quad \ldots 0] \tag{C.22}$$

where $\{\ldots\}_i$ stands for the i:th element in the array.

Appendix D

Estimation using an extended Kalman filter

An algorithm for estimating $K_L a$ and the respiration rate using an extended Kalman filter has been developed. The algorithm which also compensates for the sensor dynamics was derived in a Masters project (Nakajima 1996). It is as follows:

Consider a general nonlinear system

$$x(t+1) = f(t,x(t)) + g(t,x(t))v(t) \quad \text{(D.1)}$$
$$y_s(t) = h(t,x(t)) + e(t) \quad \text{(D.2)}$$

where $v(t)$ and $e(t)$ are independent white noise sequences. The extended Kalman filter (EKF) for the system (D.1) and (D.2), can for example, be found in Söderström (1994). The algorithm is as follows:

$$H(t) = \left.\frac{\partial h(t,x)}{\partial x}\right|_{x=\hat{x}(t|t-1)} \quad \text{(D.3)}$$
$$K(t) = P(t|t-1)H^T(t)[H(t)P(t|t-1)H^T(t) + R_2(t)]^{-1} \quad \text{(D.4)}$$
$$\hat{x}(t|t) = \hat{x}(t|t-1) + K(t)[y_s(t) - h(t,\hat{x}(t|t-1))] \quad \text{(D.5)}$$
$$P(t|t) = P(t|t-1) - K(t)H(t)P(t|t-1) \quad \text{(D.6)}$$
$$\hat{x}(t+1|t) = f(t,\hat{x}(t|t)) \quad \text{(D.7)}$$
$$F_E(t) = \left.\frac{\partial f(t,x)}{\partial x}\right|_{x=\hat{x}(t|t)} \quad \text{(D.8)}$$
$$G(t) = g(t,x)|_{x=\hat{x}(t|t)} \quad \text{(D.9)}$$
$$P(t+1|t) = F_E(t)P(t|t)F_E^T(t) + G(t)R_1G^T(t) \quad \text{(D.10)}$$

The EKF is now applied to estimate the respiration rate and K_La function utilizing a slow DO sensor. Let the linear DO sensor dynamics be given by the following system

$$\begin{aligned} x_s(t+1) &= A_s x_s(t) + B_s y(t) && \text{(D.11)} \\ y_s(t) &= C_s x_s(t) + e_s(t) && \text{(D.12)} \end{aligned}$$

where A_s, B_s, and C_s are found by converting the transfer function model in Section 4.4.3 to a state-space model. The noise $e_s(t)$ is white measurement noise. Note, however, that the time delays should be removed by time shifting the signal, this is important to improve the estimates.

The DO dynamics and the sensor dynamics can then be set together and described by

$$\begin{aligned} x(t) &= \begin{bmatrix} y(t) & \theta^T(t) & x_s(t) \end{bmatrix}^T && \text{(D.13)} \\ f(t,x(t)) &= \begin{bmatrix} f_1(x) \\ F\theta(t) \\ A_s x_s + B_s y(t) \end{bmatrix} && \text{(D.14)} \\ g(t,x(t)) &= 1 && \text{(D.15)} \\ h(t,x(t)) &= C_s x_s(t) && \text{(D.16)} \\ f_1(x) &= y(t) + h^*[\frac{Q(t)}{V}(y_{in}(t) - y(t)) \\ &+ K_L a(u(t))(y_{sat} - y(t)) - R(t)] && \text{(D.17)} \\ v(t) &= \begin{bmatrix} w(t) & e_\theta^T(t) & 0 \end{bmatrix}^T && \text{(D.18)} \\ e(t) &= e_s(t) && \text{(D.19)} \end{aligned}$$

where $w(t)$ was given in (4.9) and $e_\theta(t)$ in (4.27). The derivatives used in the EKF become

$$\begin{aligned} F_E(t) &= \left.\frac{\partial f(t,x)}{\partial x}\right|_{x=\hat{x}(t|t)} = \begin{bmatrix} \frac{\partial f_1}{\partial y} & \frac{\partial f_1}{\partial \theta} & 0 \\ 0 & F & 0 \\ B_s & 0 & A_s \end{bmatrix} && \text{(D.20)} \\ G(t) &= g(t,x)|_{x=\hat{x}(t|t)} = 1 && \text{(D.21)} \\ H(t) &= \left.\frac{\partial h(t,x)}{\partial x}\right|_{x=\hat{x}(t|t-1)} = \begin{bmatrix} 0 & 0 & C_s \end{bmatrix} && \text{(D.22)} \end{aligned}$$

Bibliography

Ahlén, A. and M. Sternad (1988). *Introduction to Adaptive control.* Systems and Control Group, Uppsala University. (In Swedish).

Ahlén, A. and M. Sternad (1989). Optimal deconvolution based on polynomial methods. *IEEE Trans. on Acoustics, Speech, and Signal Processing* **37**(2), 217 – 226.

Akaike, H. (1981). Modern development of statistical methods. In: *Trends and Progress in System Identification* (P. Eykhoff, Ed.). Pergamon Press.

Andersson, B., U. Nyberg and H. Aspegren (1995). Methanol and ethanol as external carbon sources for denitrification. Nordic Seminar: Espoo, Finland.

Andersson, C. and Y. Lundberg (1995). Addition of weighting agents for effectivisation of the activated sludge process. Master's thesis. Dep. of Water Resources Engineering, Royal Institute of Technology, Sweden. (In Swedish).

Andrews, J. F. (1994). Dynamic control of wastewater treatment plants. *Environ. Sci. Technol.* **28**(9), 434 – 440.

Aspegren, H., B. Andersson, U. Nyberg and J. la Cour Jansen (1992). Model and sensor based optimization of nitrogen removal at Klagshamn wastewater treatment plant. *Wat. Sci. Tech.* **26**(5–6), 1315 – 1323.

Åström, K. J. and B. Wittenmark (1989). *Adaptive Control.* Addison-Wesley, Reading, Massachusetts.

Åström, K. J. and B. Wittenmark (1990). *Computer-Controlled Systems.* Prentice-Hall International Editions, Inc. Englewood Cliffs.

Åström, K. J. and J. Nilsson (1994). Analysis of a scheme for iterated identification and control. SYSID 1994 Copenhagen, Denmark.

Åström, K. J. and T. Hägglund (1984). Automatic tuning of simple regulators with specifications on phase and amplitude margins. *Automatica* **20**(5), 645–651.

Balmér, P. and B. Hultman (1988). Control of phosphorus discharges: present situation and trends. *Hydrobiologia* **170**, 305–319.

Barnes, D. and P. J. Bliss (1983). *Biological Control of Nitrogen in Wastewater Treatment*. E. & F. N. Spon, London & New York.

Bastin, G. and D. Dochain (1990). *On-line Estimation and Adaptive Control of Bioreactors*. Elsevier, Amsterdam.

Behse, W. (1995). Nitrogen removal, process evaluation of the wtp in uppsala. Technical Report Mat.nr: 2447. Dept. of Water Resources Eng., Royal Institute of Technology. Stockholm, Sweden.

Bennett, G. F. (1980). Oxygen transfer rates, mechanisms, and applications in biological wastewater treatment. *Critical Rev. in Env. Control* pp. 301–391.

Bergh, S-G. (1996). Diagnosis problems in wastewater settling. Licentiate thesis. Lund Institute of Technology. Dept. of Industrial Electrical Eng. and Automation. CODEN:LUTEDX/(TEIE-1011)/1-118/(1996).

Bocken, S. M., M. Braae and P. L. Dold (1989). Dissolved oxygen control and oxygen utilization rate estimation: Extension of the holmberg/olsson method. *Wat. Sci. Tech.* **21**, 1197–1208.

Bradley, J. W., S. Kyosai, P. Matthews, K. Sato and M Webber (1992). Worldwide sludge management practices. In: *Municipal Sewage Sludge Management: Processing, Utilization and Disposal* (C. Lue-Hing, D. R. Zenz and R. Kuchenrither, Eds.). Technomic publishing company, Inc., Lancaster, USA.

Brenner, A. (1991). External carbon, additional reactor – To add or not to add?. Interactions of wastewater biomass and reactor configurations in biological treatment plants 21–23 August, Copenhagen, Denmark.

Carlsson, B. (1993). On-line estimation of the respiration rate in an activated sludge process. *Wat. Sci. Tech.* **28**(11–12), 427–434.

Carlsson, B. (1995). Automatic control in wastewater treatment plants. *Cirkulation* (6), –. (In Swedish).

Carlsson, B. (1997). The use of automatic control in wastewater treament plants. Nordisk konferens, kväverening och biologisk fosfor rening, Stockholm 20-30 Jan.

Carlsson, B. and C-F. Lindberg (1995). A control and supervision system for an activated sludge pilot plant. Ninth Forum for Applied Biotechnology, 27–29 Sept. pp 2491–2494.

Carlsson, B. and S. Hasselblad (1996). A process simulator for the activated sludge process. *Cirkulation* (5), –. (In Swedish).

Carlsson, B. and T. Wigren (1993). On-line identification of the dissolved oxygen dynamic in an activated sludge process. 12th World Congress of IFAC, Sydney, Australia, July 19-23.

Carlsson, B., C-F. Lindberg, S. Hasselblad and S. Xu (1994*a*). On-line estimation of the respiration rate and the oxygen transfer rate at Kungsängen wastewater plant in Uppsala. *Wat. Sci. Tech.* **30**(4), 255–263.

Carlsson, B., J. Latomaa and C-F. Lindberg (1994*b*). A control and supervision system for an activated sludge process (ett styr- och övervakningssytem för en aktivslamprocess. Reglermöte '94, 25–26 Oct. Västerås, Sweden.

Carlsson, B., S. Hasselblad, E. Plaza, S. Mårtensson and C-F. Lindberg (1997). Design and operation of a pilot-scale activated sludge plant. *Vatten* **53**(1), 27–32.

Carstensen, J. (1994). Identification of wastewater processes. PhD thesis. IMSOR & I. Krüger Systems AS, Lyngby, Denmark.

Clarke, D. W. and P. J. Gawthrop (1975). Self-tuning controller. *Proc. IEE* **122**, 929–934.

Cook, S. C. and P. W. Jowitt (1985). Investigation of dissolved oxygen dynamics in the activated sludge process. *IFAC Identification and System Parameter Estimation* pp. 241–248. York, UK.

Coury, B. G. (1996). Water level control for the toilet tank: A historical perspective. In: *The Control Handbook* (W. S. Levine, Ed.). CRC Press, Inc., Boca Raton, USA.

Dahlquist, G., Å Björck and N. Andersson (1974). *Numerical Methods.* Prentice-Hall.

Dochain, D. and M. Perrier (1993). Control design for nonlinear wastewater treatment processes. *Wat. Sci. Tech.* **28**(11–12), 283.

Doyle, J. C. and G. Stein (1979). Robustness with observers. *IEEE Trans. on Automatic Control* **AC–24**(4), 607–611.

Elmqvist, H., K. J. Åström and T. Schönthal (1986). *Simnon-User's Guide for MS-DOS Computers*. Dept. of Automatic Control, Lund Inst. of Techn., Sweden.

EPA (1989). *Fine Pore Aeration Systems*. United States Environmental Protection Agency, EPA/625/1-89/023.

Finnson, A. (1994). Computer simulations of full-scale activated sludge processes. Licentiate thesis. Royal Institute of Technology. Department of Water Resources Eng. TRITA-VAT 1941, Stockholm Sweden.

Flanagan, M.J., B.D. Bracken and J.F. Roesler (1977). Automatic dissolved oxygen control. *Journal of the Environmental Engineering Division* **EE4**, 707–722.

García, C. E., D. M. Prett and M. Morari (1989). Model predictive control: Theory and practice – a survey. *Automatica* **25**(3), 335–348.

Grijspeerdt, K., P. Vanrolleghem and W. Verstraete (1995). Selection of one-dimensional sedimentation models for on-line use. *Wat. Sci. Tech.* **31**(2), 193–204.

Grimble, M. J. (1988). Two-degrees of freedom feedback and feedforward optimal control of multivariable stochastic systems. *Automatica* **24**(6), 809–817.

Gustafsson, L-G., D. Lumley, C. Lindeborg and J. Haraldsson (1993). Integrating a catchment simulator into wastwater treatment plant operation. *Wat. Sci. Tech.* **28**(11–12), 45–54.

Gustafsson, T. (1988). *Regsim*. LUG Elektronik HB, Luleå, Sweden.

Hallin, S. and M. Pell (1996). Denitrification in activated sludge with external carbon sources – perspectives and consequences. *Vatten* **52**(3), 213–216. (In Swedish).

Hallin, S., C-F. Lindberg, M. Pell, E. Plaza and B. Carlsson (1996). Microbial adaptation, process performance and a suggested control strategy in a pre-dentrifying system with ethanol dosage. *Wat. Sci. Tech.* **34**(1–2), 91–99.

Harremoës, P., M. Henze, E. Arvin and E. Dahi (1994). *Teoretisk Vandhygiejne*. Polyteknisk Forlag, Lyngby, Denmark.

Hasselblad, S. and S. Hallin (1996). Intermittent dosage of ethanol in a predenitrifying activated sludge process. *Wat. Sci. Tech.* **34**(1–2), 387–389.

Hellström, B. G. and J. Bosander (1990). Styrstrategier av tillsats av extern kolkälla vid fördenitrifikation. SYVAB, Himmerfjärdsverket, Sweden.

Henze, M., C. P. L. Grady Jr., W. Gujer, G. v. R. Marais and T. Matsuo (1987). Activated sludge model no. 1. *Scientific and Technical Report No. 1.* IAWQ, London, Great Britain.

Henze, M., P. Harremoës, J. la Cour Jansen and E. Arvin (1995*a*). *Wastewater treatment, biological and chemical processes.* Springer-Verlag Berlin Heidelberg, Germany.

Henze, M., W. Gujer, T. Mino, T. Matsuo, M. C. Wentzel and G. v. R. Marais (1995*b*). Activated sludge model no. 2. *Scientific and Technical Report No. 3.* IAWQ, London, Great Britain.

Holmberg, A. (1981). Microprocessor-based estimation of oxygen utilization in the activated sludge wastewater treatment process. *Int. J. Systems Sci.* **12**(6), 703–718.

Holmberg, U. (1990). On the identifiability of dissolved oxygen concentration dynamics. IAWPRC's 25th Anniversary Conference and Exhibition, Kyoto, Japan.

Holmberg, U. and G. Olsson (1985). Simultaneous on-line estimation of the oxygen transfer rate and respiration rate. In: *Modelling and Control of Biotechnological Processes* (A. Johnson, Ed.). pp. 185–189. Pergamon Press, Oxford.

Holmberg, U., G. Olsson and B. Andersson (1989). Simultaneous DO control and respiration estimation. *Wat. Sci. Tech.* **21**, 1185–1195.

Hultman, B. (1992). The Baltic sea environment, session 9, water and wastewater management in the Baltic region. Royal Institute of Technology, Stockholm. ISBN 91-506-0905-X.

Hultman, B., B. Levin, P. Li, E. Plaza, J. Trela and S. Xu (1997). Evaluation of the effects of seeding of nitrification bacteria, addition of weighting agents and addition of organic material on the activated sludge process. In preparation.

Hultman, B., K. Jönsson and E. Plaza (1994). Combined nitrogen and phosphorus removal in a full-scale contiuous up-flow sand filter. *Wat. Sci. Tech.* **29**(10–11), 127–134.

Isaacs, S. H. and M. Henze (1995). Controlled carbon source addition to an alternating nitrification-denitrification wastewater treatment process including biological P removal. *Wat. Res.* **29**(1), 77–89.

Isaacs, S. H., M. Henze, H. Søeberg and M. Kümmel (1993). Activated sludge nutrient removal process control by carbon source addition. 12th IFAC Sydney.

Jeppsson, U. (1993). On the verifiability of the activated sludge system dynamics. Licentiate thesis. Lund Institute of Technology. Dept. of Industrial Electrical Eng. and Automation, Lund, Sweden.

Jeppsson, U. (1996). Modelling aspects of wastewater treatment processes. PhD thesis. Lund Institute of Technology. Dept. of Industrial Electrical Eng. and Automation, Lund, Sweden.

Ježek, J. and V. Kučera (1985). Efficient algorithm for matrix spectral factorization. *Automatica* **21**(6), 663–669.

Kautsky, J., N. K. Nichols and P. Van Dooren (1985). Robust pole assignment in linear state feedback. *Int. J. Control* **41**(5), 1129–1155.

Khalil, H. K. (1996). *Nonlinear systems*. Prentice Hall, Upper Saddle River, USA.

Klapwijk, A., H. Spanjers and H. Temmink (1993). Control of activated sludge plants based on measurements of respiration rates. *Journal A* **33**, 33–42.

Ko, K. Y., B. C. McInnis and G. C. Goodwin (1982). Adaptive control and identification of the dissolved oxygen process. *Automatica* **18**(6), 727–730.

Kommunförbundet (1988). *Avloppsteknik*. Tryckeri Balder AB. (In Swedish).

Kwakernaak, H. and R. Sivan (1972). *Linear Optimal Control Systems*. Wiley-Interscience.

Latomaa, J. (1994). A control and supervision system for an activated sludge pilot plant. Master's thesis. Systems and Control Group, Uppsala University. UPTEC 94077E.

Lindberg, C-F. (1995). Control of wastewater treatment plants. Licentiate thesis. Uppsala University. Systems and Control Group. UPTEC 95071R.

Lindberg, C-F. and B. Carlsson (1993). Evaluation of some methods for identifying the oxygen transfer rate and the respiration rate in an activated sludge process. Technical Report UPTEC 93032R. Systems and Control Group, Uppsala University. Uppsala, Sweden.

Lindberg, C-F. and B. Carlsson (1996*a*). Adaptive control of external carbon flow rate in an activated sludge process. *Wat. Sci. Tech.* **34**(3–4), 173–180.

Lindberg, C-F. and B. Carlsson (1996*b*). Efficient control of the DO in an activated sludge process. *Vatten* **52**(3), 209–212. (In Swedish).

Lindberg, C-F. and B. Carlsson (1996*c*). Estimation of the respiration rate and oxygen transfer function utilizing a slow DO sensor. *Wat. Sci. Tech.* **33**(1), 325–333.

Lindberg, C-F. and B. Carlsson (1996*d*). Nonlinear and set-point control of the dissolved oxygen dynamic in an activated sludge process. *Wat. Sci. Tech.* **34**(3–4), 135–142.

Lindbom, L. (1995). A Wiener filtering approach to the design of tracking algorithms. PhD thesis. Signal Processing Group, Uppsala University.

Linde, M. (1993). An approach to methanol dosage control in post-denitrification processes. Technical report. Dept. of Industrial Electrical Eng. and Automation, Lund Institute of Technology. Lund, Sweden.

Ljung, L. and S. Gunnarsson (1990). Adaptation and tracking in system identification – A survey. *Automatica* **26**(1), 7–21.

Ljung, L. and T. Söderström (1983). *Theory and Practice of Recursive Identification*. MIT Press, Cambridge, Mass.

Londong, J. (1992). Strategies for optimized nitrate reduction with primary denitrification. *Wat. Sci. Tech.* **26**(5–6), 1087–1096.

Lue-Hing, C., D. R. Zenz and R. Kuchenrither (1992). *Municipal Sewage Sludge Management: Processing, Utilization and Disposal*. Technomic publishing company, Inc., Lancaster, USA.

Lukasse, L.J.S., K.J. Keesman and G. van Straten (1996). Grey-box identification of dissolved oxygen dynamics in activated sludge processes. 13th World Congress of IFAC, San Francisco, USA, July.

Lundgren, L. J. (1994). Då torrdasset spolades. In: *Tankar om vatten* (A. Finnson, Ed.). Föreningen Vatten. Stockholm, Sweden (In Swedish).

Luttmer, J. (1995). Design of a simulator for an activated sludge process. Master's thesis. Systems and Control Group, Uppsala University. UPTEC 95149E.

Lynggaard-Jensen, A., N. H. Eisum, I. Rasmussen, H. Svanjær Jacobsen and T Stenstrøm (1996). Description and test of a new generation of nutrient sensors. *Wat. Sci. Tech.* **33**(1), 25–35.

MathWorks (1992). *Simulink, A program for simulating dynamic systems.* The Math Works, Inc., Natick, MA.

Mosca, E., G. Zappa and C. Manfredi (1984). Multistep horizon self-tuning controllers: the MUSMAR approach. IFAC 9th World Congress, Budapest, Hungary.

Nakajima, S. (1996). On-line estimation of the respiration rate and the oxygen transfer function using an extended kalman filter. Master's thesis. Department of Signals, Sensors and Systems: Royal Institute of Technology, Sweden.

Nielsen, M. K. and A. Lynggaard (1993). Superior tuning a reporting (STAR) – a new concept for on-line process control of wastewater treatment plants. *Wat. Sci. Tech.* **28**(11–12), 561–578.

Nielsen, M. K. and T. B. Önnerth (1995). Improvement of a recirculating plant by introducing STAR control. *Wat. Sci. Tech.* **31**(2), 171–180.

Nielsen, M. K., J. Carstensen and P. Harremoës (1996). Combined control of sewer and treatment plant during rainstorm. *Wat. Sci. Tech.* **34**(3–4), 181–187.

Nyberg, U., B. Andersson and H. Aspegren (1996). Real time control for minimizing effluent concentrations during storm water events. *Wat. Sci. Tech.* **34**(3–4), 127–134.

Nyberg, U., H. Aspegren and B. Andersson (1993). Integration of on-line instruments in the practical operation of the Klagshamn wastewater treatment plant. *Vatten* **49**(4), 235–244.

Olsson, G. (1993*a*). Advancing ICA technology by eliminating the constraints. *Wat. Sci. Tech.* **28**(11–12), 1–7.

Olsson, G. (1993*b*). Operator-Process Interactions is more than HCI. HCI'93, 5th International Conference on Human-Computer Interaction.

Olsson, G. and G. Piani (1992). *Computer Systems for Automation and Control*. Prentice Hall International, Hemel Hempstead, UK.

Olsson, G. and J. F. Andrews (1978). The dissolved oxygen profile – a valuable tool for control of the activated sludge process. *Water Research* **12**, 985–1004.

Olsson, G. and U. Jeppson (1994). Establishing cause-effect relationships in activated sludge plants - What can be controlled?. In: *Workshop Modelling, Monitoring and Control of Wastewater Treatment Plants*. pp. 2057–2070. Med. Fac. Landbouww. Univ. Gent.

Pappas, T., A. J. Laub and N. R. Sandell (1980). On the numerical solution of the discrete-time algebraic Riccati equation. *IEEE Trans. on Automatic Control* **AC–25**(4), 631–641.

Peterka, V. (1984). Predictor-based self-tuning control. *Automatica* **20**(1), 39–50.

Robinson, M. S. (1990). Operation experience of instrumentation, control and automation at Holdenhurst stw, Bournemouth. *J. Instn. Wat. and Envir. Mangt.*

Rundqwist, L. (1986). Self-tuning Control of the Dissolved Oxygen Concentration in an Activated Sludge Process. Licentiate thesis. Lund Institute of Technology. Department of Automatic Control, Lund, Sweden.

Ryckaert, V.G., J.E. Claes, C. Herremans, J.F. Van Impe, R. Gerards and L. Vriens (1995). Observer based estimation of oxygen uptake rate in cyclically operated biological wastewater treament plants. Ninth forum for applied biotechnology, Med. Fac. Landbouww. Univ. Gent, 60/4b, pp 2377–2384.

Söderström, T. (1994). *Discrete-Time Stochastic Systems*. Prentice Hall International, Hemel Hempstead, UK.

Söderström, T. (1996). The system identification competition of thermal performance in buildings – what happened? Reglermöte '96, 6–7 June, Luleå, Sweden (In Swedish).

Söderström, T. and P. Stoica (1989). *System Identification*. Prentice Hall International, Hemel Hempstead, UK.

Sorensen, J., D. E. Thornberg and M. K. Nielsen (1994). Optimization of a nitrogen-removing biological wastewater treatment plant using on-line measurements. *Water Environment Research* **66**(3), 236–242.

Spanjers, H. (1993). Respirometry in activated sludge. PhD thesis. Wageningen Agricultural University. Wageningen, the Netherlands.

Spanjers, H. and G. Olsson (1992). Modelling of the dissolved oxygen probe response in the improvement of the performance of a continuous respiration meter. *Wat. Res.* **26**, 945–954.

Spanjers, H., P. Vanrolleghem, G. Olsson and P. Dold (1996). Respirometry in control of the activated sludge process. *Wat. Sci. Tech.* **34**(3-4), 117–126.

Sternad, M. (1989). LQG feedforward regulator design for deterministic and stochastic disturbances. Technical Report UPTEC 89058R. Systems and Control Group, Uppsala University. Uppsala, Sweden.

Sternad, M. (1991). Use of disturbance measurement feedforward in LQG self-tuners. *Int. J. Control* **53**(3), 579–596.

Sternad, M. and T. Söderström (1988). LQG-optimal feedforward regulators. *Automatica* **24**(4), 557–561.

Takács, I., G. G. Patry and D. Nolasco (1991). A dynamic model of the clarification-thickening process. *Water Research* **25**(10), 1263–1271.

Tchobanoglous, G. and E. D. Schroeder (1985). *Water Quality*. Addison-Wesley Publishing Company.

Van Impe, J. F., J. Vandewalle, P. A. Vanrolleghem and W. Verstraete (1992). New trends in model-based monitoring and control of the activated sludge wastewater treatment process. *Journal A* **33**(3), 19–29.

Van Overschee, P. and B. De Moor (1996). *Subspace Identification for Linear Systems, Theory, Implementation, Applications*. Kluwer Academic Publishers.

Vanrolleghem, P. A. (1994). On-line modelling of activated sludge processes: Development of an adaptive sensor. PhD thesis. University of Gent. Gent, Belgium.

Vanrolleghem, P. A. and W. Verstraete (1993). On-line monitoring equipment for wastewater treatment processes: State of the art. In: *Proceedings TI-KVIV Studiedag Optimalisatie van Waterzuiveringsinstallaties door Proceskontrole en -sturing*. Gent, Belgium.

Vanrolleghem, P. A., L. K. Vermeersch, D. Dochain and G. C. Vansteenkiste (1993). Modelling of a nonlinear distributed parameter bioreactor: Optimisation of a nutrient removal process. In: *Modelling and Simulation* (A. Pavé, Ed.). pp. 563–567. SCS, San Diego.

Vanrolleghem, P. A., U. Jeppsson, J. Carstensen, B. Carlsson and G. Olsson (1996). Integration of wastewater treatment plant design and operation – A systematic approach using cost functions.. *Wat. Sci. Tech.* **34**(3–4), 159–171.

Viberg, M. (1994). Subspace methods in system identification. In: *Proceedings IFAC SYSID '94*. Copenhagen, Denmark.

Viberg, M., B. Wahlberg and B. Ottersten (1995). Anaysis of State Space System Identification methods based on instrumental variables and subspace fitting. Technical Report CTH-TE-34. Dept. of Applied Electronics, Chalmers University of Technology, Sweden.

Wagner, M. and H. J. Pöpel (1996). Surface active agents and their influence on oxygen transfer. *Wat. Sci. Tech.* **34**(3–4), 249–256.

Wells, C. H. (1979). Computer control of fully nitrifying activated sludge processes. *Instrumentation Technology* **4**, 32–36.

Wikström, A. (1993). Simnon models for activated sludge systems. Technical report. Dept. of Industrial Electrical Eng. and Automation, Lund Institute of Technology.

Wikström, A. (1994). Simulink models for activated sludge systems. Technical report. Dept. of Industrial Electrical Eng. and Automation, Lund Institute of Technology.

Youssef, C. B., G. Roux and B. Dahhou (1995). Multivariable adaptive predictive control of nonlinear systems: Application to a multistage wastewater treatment process. In: *Proc. of 3rd European Control Conference*. pp. 3585–3590. Rome, Italy.

Yuan, Z., H. Bogaert, P. Vanrolleghem, C. Thoeye, G. Vansteenkiste and W. Verstraete (1996). Carbon dosage control for predenitrification processes. In: *Proceedings Workshop Modelling, Monitoring and Control*

of Wastewater Treatment Plants. pp. 1733–1743. Med. Fac. Landbouww. Univ. Gent, 61/4a.